JOURNAL OF ASSOCIATED MEDICAL SCIENCES

JAMS

JOURNAL OF ASSOCIATED MEDICAL SCIENCES

THE OFFICIAL PEER-REVIEWED ONLINE JOURNAL

Volume 57 Number 2 May - August 2024 E-ISSN: 2539-6056

Journal of Associated Medical Sciences

Aims and scope

The Journal of Associated Medical Sciences belongs to Faculty of Associated Medical Sciences (AMS), Chiang Mai University, Thailand. The journal specifically aims to provide the platform for medical technologists, radiologic technologists, occupational therapists, physical therapists, speech-language pathologists and other related professionals to distribute, share, discuss their research findings, inventions, and innovations in the areas of:

1. Medical Technology
2. Radiologic Technology
3. Occupational Therapy
4. Physical Therapy
5. Communication Disorders
6. Other related fields

Submitted manuscripts within the scope of the journal will be processed strictly following the double-blinded peer review process of the journal. Therefore, the final decision can be completed in 1-3 months average, depending on the number of rounds of revision.

Objectives

The Journal of Associated Medical Sciences aims to publish integrating research papers in areas of Medical Technology, Physical Therapy, Occupational Therapy, Radiologic Technology, and related under peer-reviewed via double-blinded process by at least two internal and external reviewers.

Types of manuscript

Manuscripts may be submitted in the form of review articles, original articles, short communications, as an approximate guide to length:

- **Review articles** must not exceed 20 journal pages (not more than 5,000 words), including 6 tables/figures, and references (maximum 75, recent and relevant).
- **Original articles** must not exceed 15 journal pages (not more than 3,500 words), including 6 tables/figures, and 40 reference (maximum 40, recent and relevant).
- **Short communications** including technical reports, notes, and letters to the editor must not exceed 5 journal pages (not more than 1,500 words), including 2 tables/figures, and references (maximum 10, recent and relevant).

Peer review process

By submitting a manuscripts to Journal of Associated Medical Sciences, the authors agree to subject it to the confidential double-blinded peer-review process. Editors and reviewers are informed that the manuscripts must be considered confidential. After a manuscripts is received, it is assigned by a specific Associate Editor. The Associate Editor prepares a list of expert reviewers, which may include some suggested by the Editor-in-Chief. Authors can indicate specific individuals whom they would like to have excluded as reviewers. Generally, requests to exclude certain potential reviewers will be honored except in fields with a limited number of experts. All potential reviewers are contacted individually to determine availability. Manuscripts files are sent to at least two expert reviewers. Reviewers are asked to complete the review of the manuscripts within 2 weeks and to return a short review form. Based on the reviewers' comments, the Associate Editor recommends a course of action and communicates the reviews and recommendations to the Editor-in-Chief for a final decision.

The Associate Editor considers the comments made by the reviewers and the recommendation of the Editor-in-Chief, selects those comments to be shared with the authors, makes a final decision concerning the manuscripts, and prepares the decision letter for signature by the Editor-in-Chief. If revisions of the manuscripts are suggested, the Associate Editor also recommends who should review the revised paper when resubmitted. Authors are informed of the decision by e-mail; appropriate comments from reviewers and editors are appended.

Publication frequency

Journal of Associated Medical Sciences publishes 3 issues a year

Issue 1: January-April
Issue 2: May-August
Issue 3: September-December

Journal website
Homepage https://www.tci-thaijo.org/index.php/bulletinAMS/index

Journal E-ISSN:
2539-6056

Editorial Office
Faculty of Associated Medical Sciences, Chiang Mai University
110 Inthawaroros Road, Suthep, Muang, Chiang Mai, 50200
Phone 053 935072 Facsimile 053 936042

Journal of Associated Medical Sciences

Vol. 57 No. 2 : May 2024

Content

Content

Journal of Associated Medical Sciences 2024; 57(2): 1-8

JAMS
Journal of Associated Medical Sciences

Scopus Indexed & Thai-Journal Citation Index Centre (TCI)

Journal of Associated Medical Sciences

Journal homepage: https://www.tci-thaijo.org/index.php/bulletinAMS/index

Impacts of social media use on occupations of youths with hearing disability in a special education school in upper northern Thailand

Siriyanee Limthongchalearn Suchitporn Lersilp* Supawadee Putthinoi

Department of Occupational Therapy, Faculty of Associated Medical Sciences, Chiang Mai University, Thailand.

ARTICLE INFO

Article history:
Received 1 October 2023
Accepted as revised 14 December 2023
Available online 4 January 2024

Keywords:
Social media use, occupations, youths, hearing disability, special education school

ABSTRACT

Background: Social media have been used increasingly in the daily lives of the global population. Youths with hearing disability participate in many activities through social media, as do those in general. However, due to their hearing loss, they may experience different impacts, particularly in the special education context.

Objective: The purpose of this study was to investigate the impacts of social media use on occupations of youths with hearing disability, and the relationship of activity limitation and participation restriction in the special education school context.

Materials and methods: The participants comprised 92 youths with hearing disability, who were studying in a special education school. The research instrument was a questionnaire in two forms: paper-based and a sign language video clip. It was presented with acceptable content validity (IOC=0.60-1.00), good internal consistency reliability (α=0.88) and moderate stability reliability (ICC=0.70).

Results: Results showed that most of the participants had their own smart phone and used a hearing aid for access to social media. Frequency of social media use was daily for 1-3 hour(s) per day. Overall, most of the participants had no activity limitation or participation restriction in their occupations, but they showed a minimal level of limitation and restriction in education. In terms of social media use, most of the youths presented a positive impact on occupations, particularly in social participation. The overall results indicated the relationship between activity limitation and participation restriction and impacts of social media use on occupations (r= -0.293, *p*=0.005). When considering each type of occupation, the results indicated the relationships of education, work, and social participation significantly.

Conclusion: The findings of this study revealed the relationship between activity limitation and participation restriction and overall impacts of social media use on occupations. These findings were applied to social media use, particularly in parts of the text and virtual networks, as an optional channel for providing occupational therapy services and accessing meaningful occupations for youths with hearing disability.

Introduction

According to the Digital 2021 Global Overview Report, the number of social media users reached 4.2 billion people or 53.65% of the world's population.[1] Therefore, social media has a noticeable influence on the daily lives of people worldwide. In addition, the tendency in Thailand is to use social media continuously and quickly, as in the global society. This can be seen in a survey from the National Statistical Office, Ministry of Digital Economy and Society of Thailand.[2] It revealed that populations of all age groups tended to use the Internet in

* **Corresponding contributor.**
Author's Address: *Department of Occupational Therapy, Faculty of Associated Medical Sciences, Chiang Mai University, Thailand.*
E-mail address: suchitporn.l@cmu.ac.th
doi: 10.12982/JAMS.2024.021
E-ISSN: 2539-6056

various activities in their daily lives. People aged between 15 and 24 years were seen as the highest Internet users, and defined as 'Youth' by the United Nations. [3] Media from various channels play an important role in behavioral expression in the youth-age group, especially regarding social media. Social media are designed for easy access and convenience, and they can be a new communication channel that encourages learning exchange for youths beyond the classroom. On the other hand, youths might become addicted to social media through unsuitable or imbalanced time management, which has been found increasingly.[4]

Youths with hearing disability differ from those in general in terms of limited communication, due to their loss of hearing ability, which is an important component of learning a language in their communication skills. In Thailand, most of the students with hearing disability, especially those who are deaf or have moderate to profound hearing loss, study in special education schools. [5] Although studying through sign language in a special education school is in the context of an accessible communication environment, they might have limited access to meaningful activities when compared to youths without disability.[6,7] This limitation affects their daily life activities, especially when participating in social events. For this reason, social media were an alternative way for youths with hearing disability to access information, communicate, and participate in social activities.[8] However, the use of social media among youths who transformed into a digital society is an issue in which society realizes both positive and negative impacts. Previous studies indicated that social media interact more positively in the daily lives of youths with hearing disability, particularly in education and communication.[9-12] At the same time, social media might have negative effects due to misuse that leads to addiction, as in youths without disability.[13]

The International Classification of Functioning, Disability and Health (ICF) was developed by the World Health Organization, and it provides a framework to code information on health.[14] This framework is based on the concept of a Bio-Psycho-Social Model of Functioning, Disability and Health, which explains the relationship between pathological processes and perception of health, and the effects on health that lead to illness. The scope of the ICF covers health conditions, body functions, body structures, activities and participation, and environmental and personal factors at both individual and population levels. The components of functioning and disability of the ICF can be used to indicate both problematic and non-problematic aspects of health. Qualifiers are used to interpret the magnitude level of health in components of body function, body structure, activities and participation, and environmental factors. The qualifiers can be used to indicate difficulty and limitations in people performing activities. According to the ICF, social media can be an environmental factor in the form of products and technologies, as well as related services, systems, and policies. The qualifiers of social media in youths with disability can be either a facilitator or barrier.

From an occupational therapy perspective, occupations refer to everyday activities that individuals normally do as part of their personal lifestyle. Occupations cover activities people need to, want to, and are expected to do regarding their roles and contexts.[15] According to the Occupational Therapy Practice Framework: Domain and Process - Fourth Edition (OTPF-4), occupations are categorized as activity of daily living (ADLs), instrumental activity of daily living (IADLs), health management, rest and sleep, education, work, play, leisure, and social participation.[16] As mentioned above, social media use was related recently to occupations or everyday activities in the global population. However, although previous studies indicated the positive and negative effects of social media use on various aspects of physical and mental health, little literature explained how their use affected everyday activities.[17-19] Moreover, hardly any studies exist in the occupational therapy area regarding impacts of social media use on youths with hearing disability. Therefore, this study aimed to explore the impacts of social media use on occupations of youths with hearing disability, and the relationship of activity limitation and participation restriction in the special education school context. Consequently, this study leads to guidelines for occupational therapists, as healthcare providers, to promote health and health related contexts for the well-being of youths with hearing disability.

Materials and methods:

Ethical approval

This study was approved by the Research Ethics Committee of the Faculty of Associated Medical Sciences, Chiang Mai University, Thailand (AMSEC-65FB-006).

Participants

Only one special education school for students with hearing impairment was set up in Chiang Mai province in upper northern Thailand. The participants for this study were selected from the school by simple random sampling from a population of youth-age students with hearing disability. In addition, they had used social media continuously for at least 3 months. The participants comprised 92 students. Forty-eight of them were male (52.17%) and 44 female (47.83%). They were aged between 12 and 23 years (M = 15.63, SD = 2.43), with most of them deaf (81.52%) and studying in Grade 7 (18.48%). All of them used Thai sign language in school as their main form of communication.

Instrument

The research instrument in this study was a questionnaire on the impacts of social media use on occupations of youths with hearing disability. It was applied by the ICF, based on the Bio-Psycho-Social Model of Functioning, Disability and Health. In addition, it consisted of four parts, including demographic data, social media use, activity limitation and participation restriction in occupations, and impacts of social media use on occupations. The activity limitation and participation restriction part in occupations had a five-point rating scale

applied from the activity and participation qualifier of the ICF (0 = no problem, 1 = mild problem, 2 = moderate problem, 3 = severe problem, 4 = complete problem). Items with no opportunity to participate in activities were not calculated. The occupations were categorized by the OTPF-4, such as ADL, IADL, health management, rest and sleep, education, work, play, leisure, and social participation. Interpretation of this part was considered in each type of occupation at four levels as follows:

Mean	*Interpretation*
0.00 – 0.99	No activity limitation or participation restriction
1.00 – 1.99	Mild activity limitation and participation restriction
2.00 – 2.99	Moderate activity limitation and participation restriction
3.00 – 4.00	Severe activity limitation and participation restriction

The impacts part of social media use on occupations was applied from the activity and participation qualifier of the ICF by occupations, as in the third part. In addition, it had two directions, positive and negative impacts. Items were in a nine-point rating scale (0 = no impact, -1 = mild barrier, -2 = moderate barrier, -3 = severe barrier, -4 = complete barrier, 1 = mild facilitator, 2 = moderate facilitator, 3 = severe facilitator, 4 = complete facilitator). Items with no opportunity to participate in activities were not calculated. Interpretation of this part was considered at four levels in each direction as follows:

Positive impact	*Mean*	*Interpretation*
	0.00 - 0.99	No impact
	1.00 - 1.99	Low positive impact
	2.00 - 2.99	Moderate positive impact
	3.00 - 4.00	High positive impact

Negative impact	*Mean*	*Interpretation*
	0.00 - (-)0.99	No impact
	(-)1.00 - (-)1.99	Low negative impact
	(-)2.00 - (-)2.99	Moderate negative impact
	(-)3.00 - (-)4.00	High negative impact

Procedure

Phase 1: developing and testing psychometric properties of the research instrument

The steps of developing and testing psychometric properties of the research instrument are as follows:

1) Drafting the paper version of the questionnaire, based on the Bio-Psycho-Social Model, ICF, and OTPF-4.
2) Testing the content validity and correcting the questionnaire by considering the index of congruence (IOC) from five experts.
3) Forward translating the paper version to the first draft version of the Thai sign language by the first licensed Thai sign language interpreter. In this step, the instrument was in the form of a video clip.
4) Backward translating the first draft version of the Thai sign language to the paper version by another licensed Thai sign language interpreter. Confusing question items were corrected and improved by the interpreters and researchers.
5) After the final version of the Thai sign language instrument was developed, internal consistency reliability and stability reliability were examined in twelve youths with hearing disability. The internal consistency reliability was tested by the Cronbach's alpha coefficient. The stability reliability was tested by Intraclass Correlation Coefficient (ICC) from a test-retest-method.

Phase 2: exploring the impacts of social media use on occupations of youths with hearing disability in a special education school

In this phase, the researchers worked with a Thai sign language interpreter, who was informed regarding the responsibility of interpretation in each step of data collection. The participants, who signed the consent form and received the assent form from their parents or guardians, made an appointment for the interview. Before starting the interview, the participants were informed regarding the research objectives, and steps and length of the interview by the Thai sign language interpreter. Each question item was given through the video clip of the Thai sign language instrument. The participants marked their answers on the paper-version questionnaire while the video clip of each item was running.

Data analyses

In phase 1, the research instrument tested the psychometric properties. The content validity of the questionnaire was examined by the IOC. After that, internal consistency reliability was tested by the Cronbach's alpha coefficient (α). Stability reliability was tested by the ICC. In phase 2, demographic data, social media use, level of activity limitation and participation restriction, and impacts of social media use on occupations were analyzed by descriptive statistics, including frequency, percentage, mean and standard deviation. The relationship between activity limitation and participation restriction and impacts of social media use on occupations was analyzed by the Pearson correlation coefficient (r).

Results

Psychometric properties of the research instrument

The final version of the questionnaire consisted of 7 question items on social media use, 29 question items on activity limitation and participation restriction in occupations, and 34 question items on impact of social media use on occupations. Content validity of the questionnaire from the experts indicated an IOC of between 0.6 and 1.00. All of the question items were at the acceptable level. The Cronbach's alpha coefficient was

0.88, which indicated good internal consistency reliability. The ICC was 0.70, which indicated moderate stability reliability.

Social media use

Most of the participants (95.65%) used a smart phone as a communication device, and a hearing aid was usually used as an assistive device for accessing social media (59.78%). The majority of them used social media everyday (80.43%) for 1-3 hour(s) per day (78.26%) (as shown in Table 1).

Table 1. Social media use of the participants (n=92)

Social Media Use	Numbers (Percentage)
Communication device (multiple selection)	
Smart phone	88 (95.65)
Mobile phone without internet	1 (1.09)
Tablet	18 (19.57)
Desktop computer	62 (67.39)
Notebook computer	37 (40.22)
Thai Telecommunication Relay Service (TTRS)	34 (36.96)
Assistive device for accessing social media (multiple selection)	
Specific computer and software program	8 (8.70)
Cochlear implant	4 (4.35)
Hearing aid	55 (59.78)
Tracheoesophageal prosthesis	5 (5.43)
Not using any assistive device	27 (29.35)
Frequency of use	
3 days per month or less than	11 (11.96)
1-2 days per week	4 (4.35)
3-6 days per week	3 (3.26)
everyday	74 (80.43)
Duration of use each time	
Less than 1 hour	9 (9.78)
1-3 hour(s)	72 (78.26)
4-7 hours	7 (7.61)
8-11 hours	0 (0.00)
More than 11 hours	4 (4.35)

Activity limitation and participation restriction in occupations

Most of the participants had no activity limitation or participation restriction in their occupations (77.17 %). When considering each type of occupation, results indicated that most of the participants had no limitation or restriction in ADL, IADL, health management, rest and sleep, play, work, leisure, or social participation. However, most of them had a minimal level of activity limitation and participation restriction in education (as shown in Table 2).

Table 2 Level of activity limitation and participation restriction in occupations (n=92)

Occupations	Level of activity limitation and participation restriction			
	No limitation or restriction	Mild	Moderate	Severe
ADL	76 (82.61)	15 (16.30)	0 (0.00)	1 (1.09)
IADL	61 (66.30)	27 (29.35)	3 (3.26)	1 (1.09)
Health management	68 (73.91)	22 (23.91)	2 (2.17)	0 (0.00)
Rest and sleep	70 (76.09)	17 (18.48)	3 (3.26)	2 (2.17)
Education	33 (35.87)	**38 (41.30)**	16 (17.39)	5 (5.43)
Work	43 (46.74)	29 (31.52)	13 (14.13)	7 (7.61)
Play	61 (66.30)	24 (26.09)	4 (4.35)	3 (3.26)
Leisure	62 (67.39)	26 (28.26)	4 (4.35)	0 (0.00)
Social participation	64 (69.57)	22 (23.91)	3 (3.26)	3 (3.26)
Total	**71 (77.17)**	21 (22.83)	0 (0.00)	0 (0.00)

Impacts of social media use on occupations

In terms of overall impact, most of the participants (95.65%) presented a positive impact of social media use on their occupations, while some (4.35%) presented a negative one at the low to moderate level. When considering each type of occupation, results indicated that most of the participants presented a positive impact at the low level in all types of occupation. Moreover, social participation was an occupation in which most of the participants presented a positive impact, while play was presented by most as having a negative one (as shown in Table 3).

Table 3 Impacts of social media use on occupations of youths with hearing disability (n=92)

Occupations	Impacts								
	No impact	Positive				Negative			
		Low	Moderate	High	Total	Low	Moderate	High	Total
ADL	32 (34.78)	36 (39.13)	13 (14.13)	5 (5.43)	86 (93.47)	2 (2.17)	3 (3.26)	1 (1.09)	6 (6.53)
IADL	38 (41.30)	32 (34.78)	9 (9.78)	7 (7.61)	86 (93.47)	3 (3.26)	3 (3.26)	0 (0.00)	6 (6.53)
Health management	25 (27.17)	25 (27.17)	17 (18.48)	15 (16.30)	82 (89.13)	6 (6.52)	3 (3.26)	1 (1.09)	10 (10.87)
Rest and sleep	17 (18.48)	28 (30.43)	12 (13.04)	26 (28.26)	83 (90.22)	9 (9.78)	1 (1.09)	1 (1.09)	11 (11.96)
Education	20 (21.74)	17 (18.48)	33 (25.87)	11 (11.96)	81 (88.04)	9 (9.78)	1 (1.09)	1 (1.09)	11 (11.96)
Work	25 (27.17)	20 (21.74)	29 (31.52)	11 (11.96)	85 (92.39)	4 (4.35)	2 (2.17)	1 (1.09)	7 (7.61)
Play	18 (19.57)	16 (17.39)	25 (27.17)	21 (22.83)	80 (86.96)	6 (6.52)	4 (4.35)	2 (2.17)	**12 (13.04)**
Leisure	24 (26.09)	19 (20.65)	24 (26.09)	18 (19.57)	85 (92.39)	5 (5.43)	1 (1.09)	1 (1.09)	7 (7.61)
Social participation	29 (31.52)	23 (25.00)	26 (28.26)	12 (13.04)	**90 (97.83)**	1 (1.09)	1 (1.09)	0 (0.00)	2 (2.17)
Total	30 (32.61)	33 (35.87)	20 (21.74)	5 (5.43)	**88 (95.65)**	3 (3.26)	1 (1.09)	0 (0.00)	4 (4.35)

The relationship between activity limitation and participation restriction and impacts of social media use on occupations

The participants in this study presented the relationship between activity limitation and participation restriction and impacts of social media use on occupations (r = -.293, p = .005). When considering activity limitation and participation restriction in each type of occupation, the results indicated the relationship of education, work, and social participation (as shown in Table 4).

Table 4 Relationship between activity limitation and participation restriction and impacts of social media use on occupations

Occupations	Activity limitation and participation restriction		Impacts of social media use		*r*	*p-value*
	M	*SD*	*M*	*SD*		
ADL	.31	.58	1.01	1.28	–.002	.988
IADL	.83	.75	.89	1.29	–.204	.051
HM	.92	.80	1.18	1.59	–.078	.460
RS	.46	.71	1.48	1.63	–.168	.110
ED	1.14	1.05	1.26	1.55	–.255	**.014***
WK	1.22	.98	1.31	1.45	–.215	**.040***
PL	.95	1.17	1.36	1.79	–.105	.317
LE	.60	.63	1.38	1.53	–.114	.280
SC	.64	.76	1.47	1.27	–.216	**.039***
Total	.78	.47	1.18	1.19	–.293	**.005****

* *p*-value < .05 ** *p*-value < .01

ADL: activity of daily living, IADL: instrumental activity of daily living, HM: health management, RS: rest and sleep, ED: education, WK: work, PL: play, LE: leisure, SC: social participation

Discussion

This study was conducted in a special education school for students having hearing disability, with most of them being deaf or having severe to profound hearing loss. Those with some hearing ability may not have enough for communicating by listening and speaking, and thus resort to sign language as their main means of communication. This is a challenging situation for youths with hearing disability in Thailand.[20]

This study reflected the importance of accessing social media as well as assistive devices. The youths with hearing disability in this study mostly used a smart phone, the same as most people in general. Moreover, it was interesting that 36.96% of the participants reported communication methods through the Thai Telecommunication Relay Services (TTRS), which is assistive technology designed specifically for communication between people with and/or without hearing disability, and is located in special education schools for students with hearing disability in Thailand.[21] In terms of assistive devices for access to social media, most of the participants used hearing aids even though they were deaf or with severe to profound hearing loss, in which case using hearing aids was ineffective. Although hearing aids can be used by these people to hear general sounds, they would be unsuitable for communication purposes. Due to the need for hearing aids for people with hearing disability, their access to social media might be different from people without hearing disability.[22]

In terms of activity limitation and participation restriction in performing the occupations of youths with hearing disability, the overall result showed that most of the participants had no difficulty. When considering each type of occupation, it was found that most of the youths did not have difficulty in performing them, except for education, and this may be due to their hearing disability. Furthermore, hearing loss impacts their ability to communicate, thus leaving barriers to engage in activities that involve gatherings and exchange of information. Education is a crucial occupation, as the role of students requires communication and language-related skills for learning.

Overall results had a positive social media impact on the occupations of youths with hearing disability. These were the same results as those found in youths without disabilities, which showed the advantages of social media use in social behavior, with no obvious disadvantages for the disabled.[23] When considering the level of impact, results indicated that most of the youths had low positive impact. In addition, when considering each type of occupation, the results showed a positive impact on social participation by most of the youths. This means that the ICF was the social media used to facilitate occupations. This finding related to the study of Toofaninejad et al.,[10] who found that students with hearing disability often reported a positive impact of social media on their learning, in the form of increased interaction and motivation to learn, as well as personal support. In fact, the current situation regarding social media use also has evolved in youths with hearing disability. Descriptive text, images and clips now allow access to information for activities that are more convenient and easier. Social media use can help the youths to communicate quickly with not only people with hearing disability, but also those without disability.[8,24]

The results indicated the relationship between activity limitation and participation restriction and impacts of social media use on occupations. In addition, they indicated the relationships between impacts of social media use and activity limitation and participation restriction in education, work, and social participation. Negative coefficients were represented in the negative relationship. When activity limitation and participation restriction increase from hearing disability, the impacts of social media use on occupation tends to decrease, or vice versa. The reason for this is that youths with hearing disability in this study who have high level of limitation and restriction might meet a barrier in understanding written and spoken language. Social media use might not be preferred in communicating with peers or people without hearing disability in the school context. As a result, social media use might have less impact for youths with hearing disability and a high level of limitation and restriction. On the other hand, those with a low level of limitation and restriction will want to find new ways to communicate with others and gain more information on activities of education, work, and social participation. Youths usually choose social media because they provide extra means of communication, based primarily on text and images[9]. Social media use with hearing disability has grown typically with physical development, and so students with hearing disability are treated and encouraged to do their ADLs and IADLs by themselves, as youths in general do. In addition, this study was made in the special education school context that provided a health management service and performed rest and sleep, and leisure under the school rules. Moreover, youths that play might have less meaningful occupation at a young age. In other words, hearing loss development from childhood is a health condition associated with limited hearing and restriction of involvement in daily life.[14]

This study reflected that youths with hearing disability still presented activity limitation and participation restriction in many types of occupation. Most incidents indicated moderately positive impacts of social media use that helped to enable youths with hearing disability to have the same lifestyle activities as youths in general. They could perform occupations and occupy themselves in meaningful activities in the same way as people in general and reach quality in ADL and occupational activities independently.[25] As explained in the ICF, impairment and disability cause difficulties in performing personal daily life activities, with the environmental factor being both a barrier and facilitator.[26] Therefore, social media might be an environmental option that can support or facilitate youths. However, due to social media relying on the Internet and devices for access, support from public policy and services is necessary. Developing a policy that facilitates access to social media may be an option that

can reduce limitations in communication and activities related to it. However, an imbalance in time management regarding social media use usually impacts occupation in people in general, including youths with hearing disability. This is because although social media use can encourage the ability to learn, connect with other people in society, share viewpoints and relax, it usually involves physical inactivity, short attention span, and mental health problems.[23,27] Therefore, for occupational therapists to utilize social media as a means of supporting occupations and encouraging time-management skills that lead to an age-appropriate occupational balance is challenging. Social media in the form of individual and group virtual programs might be an effective tool for health promotion and intervention outreach.[28-29] They could be a channel for communicating and providing a service between occupational therapists and youths with hearing disability in order to build an understanding of proper healthcare and well-being.[30-31]

Limitation

The results of this study only give information for understanding behavior, limitations, and impact of social media use on occupations of adolescents with hearing impairment, according to the OTPF-4 classification. Therefore, they did not cover the impacts of social media use on youths with hearing disability in other dimensions. Furthermore, the study area was in the special education school context in upper northern Thailand, which may have limitations in generalizing in other contexts. Future research can be conducted in a wider area with a greater population. Finally, this study investigated behavior in social media use and its impact on occupations, but there is a lack of in-depth studies on patterns of social media use and impacts in terms of health and occupations. A qualitative research approach might be conducted to examine the in-depth impact from the perspective of youths, parents, teachers, or those involved in various contexts.

Conclusion

Social media use of the youths with hearing disability took a similar trend to that of youths in general, although the former was in the special education school context. However, despite their use of sign language in communication, most of the youths with hearing disability still used hearing aids as assistive technology to access social media. In addition, although most of them presented no activity limitation or participation restriction in occupations, they indicated mild limitation and restriction in education. In terms of impact of social media use on occupations, the youths with hearing disability presented positive impact, especially in social participation. Moreover, the findings of this study revealed the relationship between activity limitation and participation restriction and overall impacts of social media use on occupations. However, when considering each type of occupation, the results indicated the relationships of education, work and social participation, despite activity limitation and participation restriction mostly having no relationship with the impacts of social media use. These findings were applied to social media use as the option of a channel crucial for providing occupational therapy services for youths with hearing disability.

Conflict of interest

The author(s) declared no potential conflicts of interest with respect to the research, authorship, and/or publication of this article.

References

[1] Digital 2021 Global Overview Report. Global Overview Report 2021. 2021 [cited 2022 Mar 18]. Available from: https://datareportal.com/reports/digital-2021-global-overview-report.

[2] Ministry of Digital Economy and Society of Thailand. Survey report on internet usage behaviors in Thailand 2021. 2021 [cited 2022 Mar 18]. Available from: https://www.etda.or.th/th/Useful-Resource/publications/iub2021.aspx.

[3] United Nations. Sustainable Development Goals. 2015 [cited 2023 Apr 1]. Available from: https://www.un.org/sustainabledevelopment/sustainable-development-goals/.

[4] Kolkijkovin V, Wisitpongaree C, Techakasem P, Pornnoppadol C, Supawattanabodee B. Computer game addiction: Risk and protective factors in students in Dusit district, Bangkok. Vajira J. 2015; 59(3): 1-30 (in Thai).

[5] Lersilp S, Putthinoi S, Lersilp T. Facilitators and barriers of assistive technology and learning environment for children with special needs. Occup Ther Int. 2018; 4: 1-9. doi: 10.1155/2018/3705946.

[6] Scherer N, Smythe T, Hussein R, Wapling L, Hameed S, Eaton J, Kabaja N, Kakuma R, Polack S. Communication, inclusion and psychological wellbeing among deaf and hard of hearing children: A qualitative study in the Gaza Strip. PLOS Glob Public Health. 2023; 3(6): e0001635. doi: 10.1371/journal.pgph.0001635.

[7] Engel-Yeger B, Hamed-Daher S. Comparing participation in out of school activities between children with visual impairments, children with hearing impairments and typical peers. Research in Developmental Disabilities. 2013; 34(10): 3124-3132. doi:10.1016/j.ridd.2013.05.049.

[8] Tayseer M, Zoghieb F, Alcheikh I, Awadallah MN. Social network: academic and social impact on college students. In: ASEE 2014 Zone I Conference; 2014. p. 3-5.

[9] Azy B, Yael S. Internet use and personal empowerment of hearing-impaired adolescents, Comput Hum Behav. 2008; 24(5): 1802-1815. doi:10.1016/j.chb.2008.02.007.

[10] Toofaninejad E, Zaraii Zavaraki E, Dawson S, Poquet O, Sharifi Daramadi P. Social media use for deaf and hard of hearing students in educational settings: a systematic review of literature. Deaf Educ Int. 2017; 19(3-4): 144-161.

[11] Muhingi WN, Mutavi T, Kokonya D, Kuria M. Social networks and students' performance in secondary schools: lessons from an open learning centre, Kenya. J Educ Pract. 2015; 6(21): 15-30.
[12] Saunders GH, Frederick MT, Silverman S, Papesh M. Application of the health belief model: Development of the hearing beliefs questionnaire (HBQ) and its associations with hearing health behaviors. Int J Audiol. 2013; 52(8): 558-567. doi:10.3109/14992027.2013.803237.
[13] Schäfer K, Miles F. Social media use and mental health in deaf or hard-of-hearing adults - results of an online survey. Front Commun. 2023; 17(8): 1175461. doi:10.3389/fcomm.2023/1175461.
[14] World Health Organization. International Classification of Functioning, Disability and Health. Geneva: World Health Organization; 2001.
[15] World Federation of Occupational Therapists. About occupational therapy. 2012 [cited 2022 Mar 22]. Available from: http://www.wfot.org/about-occupational-therapy.
[16] American Occupational Therapy Association. Occupational therapy practice framework: Domain and process. Am J Occup Ther. 2020; 74(2): 74124 10010. doi:10.5014/ajot.2020.74S200.
[17] Eckberg ZS, Erler K, Nakamura W, Kennell B. Social media as occupation: Implications for occupational therapy practice. Open J Occup Ther. 2020; 8(2): 1-6. doi:10.15453/2168-6408.1670.
[18] Shensa A, Sidani JE, Dew MA, Escobar-Viera CG, Primack BA. Social media use and depression and anxiety symptoms: A cluster analysis. Am J Health Behav. 2018; 42(2): 116-128. doi:10.5993/ajhb.42.2.11.
[19] Uhls YT, Ellison NB, Subrahmanyam K. Benefits and costs of social media in adolescence. Pediatrics. 2017; 140(2): 67-70.
[20] Office of the Education Council. Thailand's Education Development Guidelines for the 21st Century [Research Report]. Bangkok: Office of the Education Council; 2017.
[21] Thai Telecommunication Relay Services. Getting to know the TTRS number. 2021. Available from: https://cmu.to/FcZ29.
[22] Choudhury M, Dinger Z, Fichera E. The utilization of social media in the hearing aid community. Am J Audiol. 2017; 26(1): 1-9. doi:10.1044/2016_AJA-16-0044.
[23] Al-Sharqui L, Hashima H, Kutbi I. Perceptions of social media impact on students' social behavior: A comparison between arts and science students. Int J Educ Soc Sci. 2015; 2(4): 1-15. doi:10.11648/j.ijsedu.20150204.11.
[24] Yeampayung P, Sawangmek S. Study of socioscientific issue approach with reflection of using social media to enhance socioscientific decision making about human and environment for 12th grade students. J Educ Naresuan Univ. 2021;23(1):237-251.
[25] Ahn SN. Effectiveness of occupation-based interventions on performance quality for hemiparetic stroke in community-dwelling: A randomized clinical trial study. NeuroRehabilitation. 2019; 44(2): 275-282. doi:10.3233/NRE-182631.
[26] World Health Organization. Adolescent pregnancy. [Internet]. 2020 [cited 2023 Apr 15]. Available from: https://www.who.int/news-room/fact-sheets/detail/adolescent-pregnancy.
[27] Gok T. The effects of social networking sites on students' studying habits. Int J Res Educ Sci. 2016; 2(1): 85-93.
[28] Crowson MG, Tucci DL, Kaylie D. Hearing loss on social media: Who is winning hearts and minds? Laryngoscope. 2018; 128(6): 1453-1461. doi:10.1002/lary.26902.
[29] Kožuh I, Debevc M. The utilization of social media among users with hearing loss: An analysis of Facebook communities. Univ Access Inf Soc. 2020; 19(3): 541-555.
[30] Al-Dmour H, Masa'deh RE, Salman A, Abuhashesh M, Al-Dmour R. Influence of social media platforms on public health protection against the COVID-19 pandemic via the mediating effects of public health awareness and behavioral changes: integrated model. J Med Internet Res. 2020; 22(8): e19996. doi:10.2196/19996.
[31] Beyens I, Pouwels JL, van Driel II, Keijsers L, Valkenburg PM. The effect of social media on well-being differs from adolescent to adolescent. Sci Rep. 2020; 10(1): 10763.

Journal of Associated Medical Sciences 2024; 57(2): 9-19

JAMS
Journal of Associated Medical Sciences

Scopus Indexed & Thai-Journal Citation Index Centre (TCI)

Journal of Associated Medical Sciences

Journal homepage: https://www.tci-thaijo.org/index.php/bulletinAMS/index

The development of a cylindrical phantom for nanoDot™ calibration with multiple beam angles

Sumalee Yabsantia[1*] Siwapon Munsing[2] Thunyarat Chusin[1] Chatrawut Pattaweerakul[2] Nuntawat Udee[1] Titipong Keawlek[1] Kamonchanok Nobphuek[2]

[1]Department of RadiologicalTechnology, Faculty of Allied Health Sciences, Naresuan University, Phitsanulok Province, Thailand.
[2]Department of Radiology, Faculty of Medicine, Naresuan University, Phitsanulok Province, Thailand.

ARTICLE INFO

Article history:
Received 27 October 2023
Accepted as revised 22 December 2023
Available online 10 January 2024

Keywords:
Calibration factor, calibration phantom, nanoDot™, OSLD calibration

ABSTRACT

Background: The nanoDot™ dosimeter, an optically stimulated luminescent dosimeter (OSLD), is compact and precise, ideal for various applications like radiation dosimetry. The nanoDot™ requires calibration before use with the detector alignment perpendicular to the central beam axis. It exhibits angular dependence that may impact the calibration factor, requiring the fabrication of a specific cylindrical phantom for the calibration procedure.

Objective: This study aimed to develop a cylindrical phantom for nanoDot™ calibration to facilitate dose measurements in composite fields with various beam angles and to evaluate the nanoDot™ calibration factors for different plans.

Materials and methods: The cylindrical phantom was constructed using cast nylon material to accommodate the nanoDot™ or a cylindrical ionization chamber (IC). The novel phantom underwent validation for physical characteristics, including dimensions, density, and uniformity. Validation for the calibration factor, using cylindrical phantom (CF_{cylin}) under standard conditions with a 10x10 cm^2 field size at 10 cm depth was conducted with 6 MV X-rays, comparing it with calibration factor using slab solid water phantoms (CF_{solid}). The CF_{cylin} for different numbers of beams were determined and validated against a reference IC in various planning conditions. Furthermore, angular correction factors were determined for their application in the single-beam calibration factor.

Results: The cylindrical phantom had dimensions of 20 cm in diameter and 30 cm in length, a density of 1.145 g/cm^3 and good uniformity. As a result of single beam, the $CF_{cylin,}$ agreed well with CF_{solid}, showing a difference of -0.069%. The CF_{cylin} increased with the number of beams, ranging between 1.179 and 1.242. Additionally, the angular correction factor increased as the number of beams increased, peaking at 1.058 with 9 beams. When comparing the results to the IC, it was observed that with an increase in the number of beams to 4 beams, the single-beam calibration factor exhibited a variation of more than 2%. However, when applying the CF_{cylin} specific to the number of beams or correcting for the angular correction factor, the dose differences between nanoDot™ and IC measurements were within 2%.

Conclusion: The developed cylindrical phantom is suitable for nanoDot™ calibration under single beam angle and in composite fields with various beam angles. The new calibration factors for specific numbers of beams allow for accurate dose measurements using nanoDot™, thus reducing the dose difference from the IC to acceptable levels. Further studies should investigate its application in clinical situations.

∗**Corresponding contributor.**
Author's Address: *Department of Radiological Technology, Faculty of Allied Health Sciences, Naresuan University, Phitsanulok Province, Thailand.*
E-mail address: sumaleey@nu.ac.th
doi: 10.12982/JAMS.2024.022
E-ISSN: 2539-6056

Introduction

The nanoDot™ (Landauer Inc., Glenwood, IL, USA) is a type of optically stimulated luminescent dosimeter (OSLD) commonly utilized in point dosimetry for radiation

therapy applications.[1–6] It is employed for in vivo dosimetry to determine organ doses during irradiation, such as for the skin[7–10] and eye lens.[11] The nanoDot™ offers several advantages, including its small size and repeatable readout, making it a preferred choice for in vivo dosimetry.[11,12] However, being a passive dosimeter, it requires calibration before use.

Calibrating the nanoDot™ to determine the calibration factor before using it for measurements is essential. This factor is necessary for converting the measured signals into accurate radiation doses. The calibration factor for the luminescence dosimeters should be established through a cross calibration with a calibrated ion chamber, ideally under reference conditions, to ensure traceability.[13] Therefore, this calibration is conducted under reference conditions by comparing the nanoDot™ reading (the value obtained after reading the nanoDot™ with the reader) to an ionization chamber (IC) measurement taken at the central axis with a gantry angle of 0 degrees, using a standard solid water phantom. However, this calibration factor may not be suitable when there is gantry angle variation, as in Intensity-modulated radiation therapy (IMRT) techniques, due to the angular dependence of the nanoDot™, which can affect the measured signal. Previous research discovered that the nanoDot™ exhibited significant angular sensitivity when exposed to photon beams. Specifically, when subjected to incident photon beams parallel to the dosimeter's plane, the nanoDot™ response was 4% lower at 6 MV and 3% lower at 18 MV compared to the response observed when exposed to incident beams perpendicular to the dosimeter's plane.[14]

In a preliminary study, the calibration factor for the nanoDot™ was determined using a standard method (single beam angle, perpendicular to detector) with solid water phantom (CF_{solid}).[15] This process involved comparing the nanoDot™ reading obtained from the reader with an ionization chamber (IC) measurement taken at the central axis, with a gantry angle of 0 degrees and a source-to-axis distance (SAD) of 100 cm, using slab solid water phantoms. Subsequently, these factors were applied to nanoDot™ measurements to determine the dose in the eye lens and thyroid in a phantom for an IMRT plan in head and neck cancer. The results indicated that the dose variation between the nanoDot™ and the treatment planning system (TPS) exceeded 6%. This discrepancy may be attributed to the angular dependence of the nanoDot™. Therefore, calibrating the nanoDot™ in composite fields, a treatment technique where multiple radiation beams or fields are combined to deliver a dose to a target volume (isocenter), may increase the accuracy of dose measurements in multiple beams techniques.

To the best of our knowledge, a phantom for nanoDot™ calibration has not been established, and the calibration factor for different beam angles has not been studied. Therefore, the objective of this study was to develop a cylindrical phantom for nanoDot™ calibration in composite fields with various beam angles. This phantom is designed to accommodate both OSLD nanoDot™ and ionization chamber devices for calibration under the same conditions. The calibration factors for the nanoDot™, determined using the developed cylindrical phantom (CF_{cylin}), were validated through dose measurements against an ionization chamber.

Materials and methods

Phantom fabrication

The calibration phantom was designed with the concept of maintaining a constant depth for all angles, which led to the selection of a cylindrical phantom. The detector, either the nanoDot™ or the PTW 30010 Farmer ionization chamber (PTW, Freiburg, Germany) with a 0.6 cm^3 volume, can be precisely inserted into the center of the phantom at the intended 10 cm depth by changing the detector holder rod. Cast nylon, with a density of 1.14 g/cm^3, was selected as the material for constructing the phantom due to its ease of construction and cost-effectiveness. [16]

The cylindrical rod for embedding the detector, with a 3 cm diameter and a length of 30 cm, was designed to accommodate both types of detectors. During use, it is inserted into the center of the cylindrical phantom.

The phantom was fabricated from cast nylon 6 with a density of 1.14 g/cm^3. The material composition of cast nylon 6 typically includes polyamide 6 (nylon 6), additives (such as plasticizers, stabilizers, lubricants, and pigments), and fillers, depending on the application and desired properties. The specific formulation can vary among manufacturers. In the fabrication of the phantom, the raw material of cast nylon 6, formed through the casting process with dimensions large enough to lathe the phantom to 20 cm in diameter and 30 cm in length, was shaped using CNC (Computer Numerical Control) technology to create a cylindrical phantom. Subsequently, the central hole of the cylindrical phantom was drilled using a Radial Drilling machine. The cylindrical rod of detector holder for nanoDot™ and IC was also fabricated using a similar process.

Phantom characteristics

Dimensions and density were determined, with density calculated using Equation 1. Subsequently, CT numbers and the uniformity of the phantom were evaluated using computed tomography images obtained from the Philips CT simulator Brilliance Big Bore (Philips Medical Systems, Bothell, Washington, United States).

$$\text{density } (g/cm^3) = \frac{\text{mass (g)}}{\text{volume } (cm^3)} \quad (1)$$

Uniformity was assessed by measuring the Hounsfield units (HU) in 5 regions of interest (ROI) at both a central and four peripheral positions within a transverse CT phantom image. Appropriate uniformity should exhibit a difference of no more than 5 HU between these positions[17] this work is currently focused on quality assurance (QA).

Determination of nanoDot™ sensitivity correction factor

The sensitivity correction factor for the nanoDot™ accounts for corrections needed due to non-uniformity in

readings among detectors within the same batch. Ideally, all detectors should yield identical dose measurements, but individual detectors may exhibit sensitivity differences. Consequently, these variations in sensitivity are corrected using a factor known as the "sensitivity correction factor" ($k_{sensitivity}$).

For each individual nanoDot™, this correction factor was calculated by determining the ratio of the average reading from all detectors (M_{avg} in cGy) in the same batch to its own reading (M in cGy), as shown in Equation 2.

$$k_{sensitivity} = \frac{M_{avg}}{M} \quad (2)$$

For sensitivity correction factor determination, 100 nanoDot™ detectors were irradiated with a 1 Gy dose of 6MV X-ray beam at a source-to-axis distance (SAD) of 100 cm, a depth of 10 cm, and a field size (FS) of 20x20 cm^2. The Clinac 2100 (Varian Medical Systems, Palo Alto, CA, USA) was employed in this study. Subsequently, the sensitivity correction factor for each nanoDot™ was determined using Equation 2. Any nanoDot™ with a sensitivity correction factor exceeding ±5% was excluded, and only detectors with sensitivities close to 1 were utilized in the next experiment.

Evaluation of phantom

The evaluation of the developed phantom for nanoDot™ calibration involved comparing the calibration factors of nanoDot™ OSLDs obtained using a custom-made cylindrical phantom (CF_{cylin}) to those obtained through calibration with a Solid Water™ phantom (Gammex RMI, Middleton, WI, USA) - CF_{solid}. The comparison was conducted under reference conditions, involving a single beam of 10x10 cm^2, 100 cm SAD, and 10 cm depth, as illustrated in Figure 1.

This study utilized nanoDot™ dosimeters in conjunction with the microStar OSL reader (Landauer, Inc., Glenwood, IL, USA). The dosimeter, based on aluminum oxide doped with carbon (Al_2O_3:C), features a disk-shaped active volume measuring 4 mm in diameter and 0.3 mm in thickness. It is enclosed within a light-tight plastic cassette with dimensions of 10 mm × 10 mm × 2 mm.

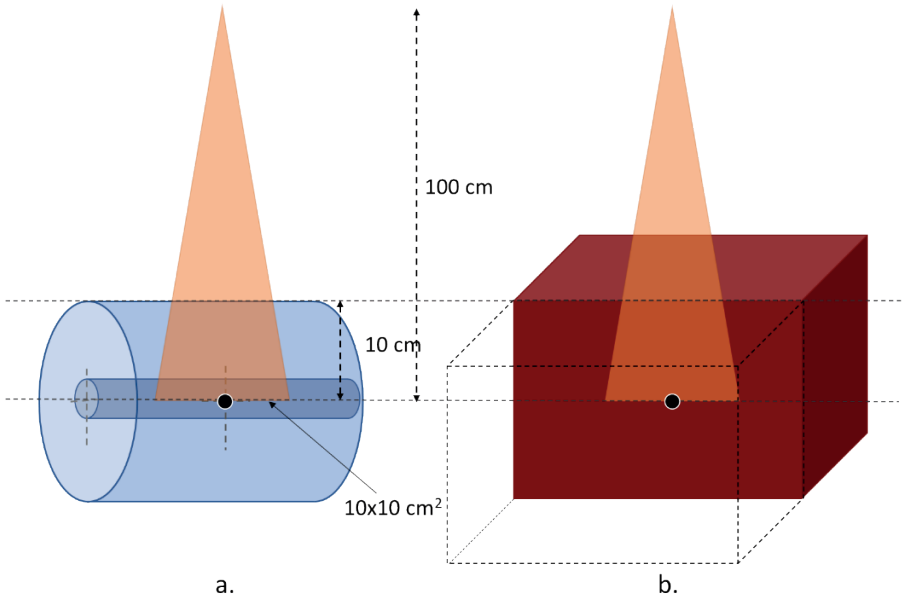

Figure 1. *Comparison of the setup geometry for calibration factor determination between (a) a developed cylindrical phantom, and (b) a standard solid water phantom.*

The effect of angular variation on calibration factor

Determination of calibration factor (CF_{clin})

The determination of the CF_{clin} was carried out using a cylindrical phantom with a single beam at gantry 0 degrees, perpendicular to the dosimeter. Additionally, multiple beams, specifically 5, 7, and 9 beams, were employed for this purpose. In the configuration with multiple beams, the radiation beams were adjusted at equal-angle intervals, starting from 0 degrees, as depicted in Figure 2.

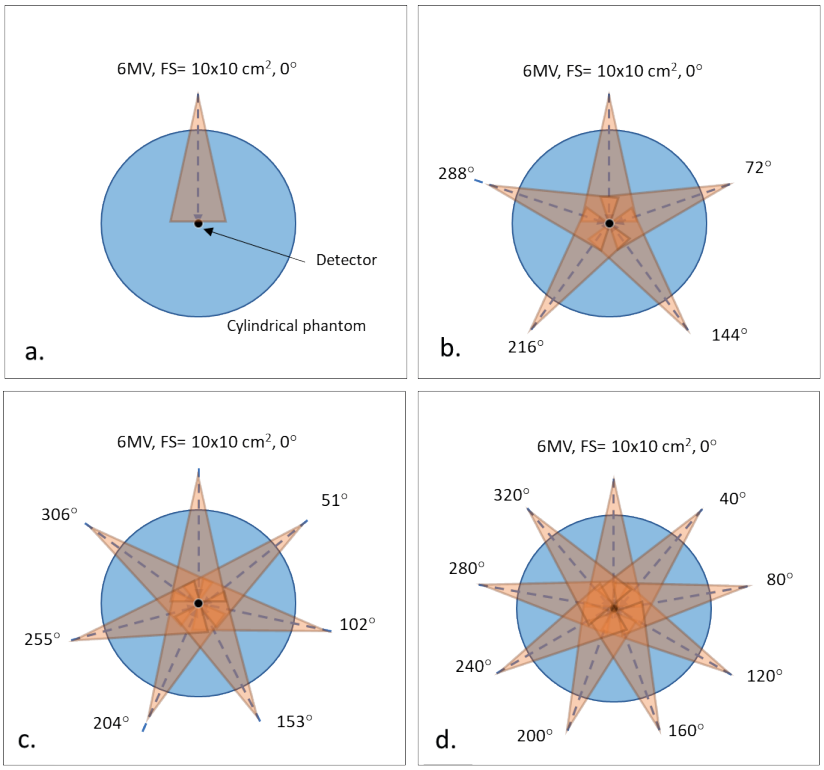

Figure 2. *Illustration of the arrangement of radiation beams for a single beam (a), 5 beams (b), 7 beams (c), and 9 beams (d).*

All of these beams were irradiated with field size of 10x10 cm^2, and the measurement depth was set at SAD of 100 cm with a depth of 10 cm, delivering 1 Gy of 6 MV x-ray radiation at the isocenter. The center of each detector was positioned at the isocenter, as depicted in Figure 3a. The nanoDot™ measurements were repeated three times, using one detector each time, for each beam condition to assess experimental variation.

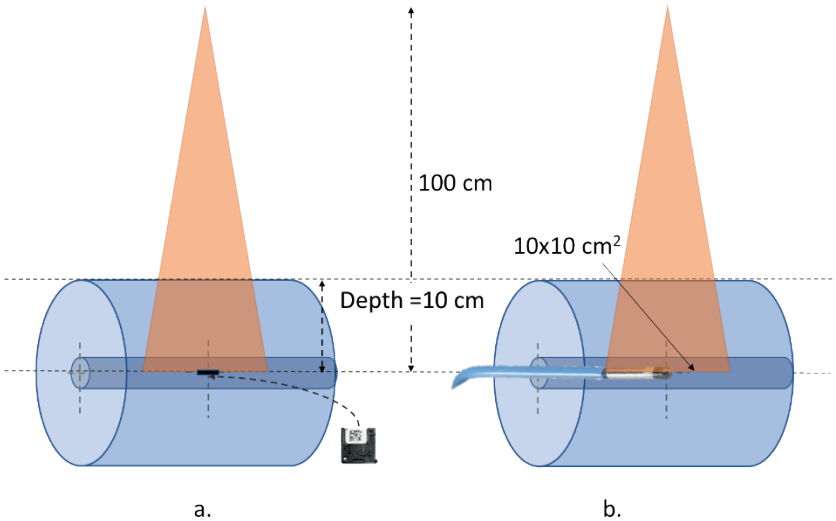

Figure 3. *Illustration of setup geometry of nanoDot™ and ionization chamber for calibration factor (CF_{cylin}) determination*

The reference dose was measured using a 0.6 cm^3 ionization chamber following the TRS 398 protocol [18] under the same conditions as the nanoDot™, with a dose of 1 Gy of 6 MV x-ray, as shown in Figure 3b.

After irradiation, the nanoDot™ readings were analyzed using the MicroStar reader. The readings were repeated three times to calculate the average for each detector. Subsequently, the averages of the three measurements were used to determine the calibration factor, as calculated by Equation 3.

$$\text{Calibration factor} = \frac{D_{IC}}{M_{OSLD}} \quad (3)$$

where D_{IC} is the absorbed dose measured by ionization chamber (cGy) and M_{OSLD} is the nanoDot™ reading with sensitivity correction (cGy).

Because the nanoDot™ exhibits angular dependence, the calibration factor also depends on the orientation of the nanoDot™ relative to the beam angle. As illustrated in Figure 2, the number of beams is associated with beam angles in different directions. As the number of beams increases, the beam angles vary. Correcting each beam angle individually may be complex in practical implementation, so employing the concept of the number of beams could assist in manual correction for this purpose. Therefore, in this study, the angular correction factors, denoted as 'k_{angle}', were determined and related to the number of beams. The was calculated as the ratio of the calibration factor for any number of beams ($CF_{cylin,angle}$) to the calibration factor at a single beam with gantry angle 0 degrees ($CF_{cylin,1beam}$), as shown in Equation 4. This factor accounts for variations in the number of beams.

$$k_{angle} = \frac{CF_{cylin,\,angle}}{CF_{cylin,\,1beam}} \quad (4)$$

For the implementation of to correct changes in the number of beams, the equation to calculate the dose from nanoDot™ was formulated by multiplying the single-beam calibration factor with k_{angle}.

Validation of calibration factor (CF_{cylin}) of nanoDot™

To validate the calibration factor of the nanoDot™, dose measurements were conducted in various conditions (as shown in Table 1), comparing the results obtained with the nanoDot™ and an ionization chamber. These conditions included open fields of 5x5 cm^2 and 15x15 cm^2 at a depth of 8 cm using a 30x30x30 cm^3 solid water phantom. Additionally, validation was performed for two parallel opposing beams and four fields in a 5x5 cm^2 configuration, using a cylindrical phantom at a depth of 10 cm. In all cases, a 1 Gy dose was delivered to the isocenter.

Table 1. Plan parameters for the validation of calibration factors (CF_{cylin}).

Plan	Phantom	Planning		
A	Solid water	Depth 8 cm, SAD 100 cm, Gantry 0 degrees	1 beam	FS 5x5 cm^2
B	Solid water		1 beam	FS 15x15 cm^2
C	Cylindrical	AP and PA parallel opposing, SAD 100 cm	2 beams	FS 5x5 cm^2, depth 10 cm, SAD 100 cm
D	Cylindrical	4 field box, SAD 100 cm	4 beams	FS 5x5 cm^2, depth 10 cm, SAD 100 cm

Note: FS: field size

The nanoDot™ measurements were repeated three times, utilizing one detector each time, for each beam condition. Each nanoDot™ reading was individually multiplied by the sensitivity correction factor and then averaged across all repeated measurements. The nanoDot™ readings were analyzed by the reader under the same conditions, as described in Section 4.2. The doses measured with the nanoDot™ (D_{OSLD} in cGy) were calculated using Equation 5.

$$D_{OSLD} = M_{OSLD} \times CF \quad (5)$$

where M_{OSLD} (cGy) represents the nanoDot™ reading multiplied by the sensitivity correction factor ($M \times k_{sensitivity}$) and averaged for all repeated measurements, CF is the nanoDot™ calibration factor. The calibration factors for both single and multiple beams were applied to calculate the dose using Equation 5. Additionally, the doses measured with the nanoDot™ were also calculated by implementing the k_{angle} to the calibration factor in the single beam ($CF_{cylin,1beam}$), as shown in Equation 6.

$$D_{OSLD} = M_{OSLD} \times CF_{cylin,\,1beam} \times k_{angle} \quad (6)$$

Subsequently, the dose measured with the nanoDot™ was compared to the measurement obtained by the 0.6 cm^3 ionization chamber following the TRS 398 protocol, calculating the percentage difference using Equation 7.

$$\%\text{difference} = \frac{(D_{OSLD}-D_{IC})}{D_{IC}} \times 100 \quad (7)$$

where D_{OSLD} represents the dose determined by the nanoDot™ (cGy), while D_{IC} represents the dose determined by the ionization chamber (cGy). A percentage difference within 2% is considered acceptable according to the TRS 430 recommendation.[19]

Statistical analysis

Mean and standard deviation (SD) were employed to describe the data. The %difference was used to compare the dose between nanoDot™ and IC measurements.

Results

Developed phantom

The cylindrical cast nylon phantom, with dimensions of 20 cm in diameter and 30 cm in length, incorporates a cylindrical plug measuring 3 cm in diameter and 30 cm in length for embedding the detectors (nanoDot™ and 0.6 cm^3 ionization chamber), as shown in Figure 4.

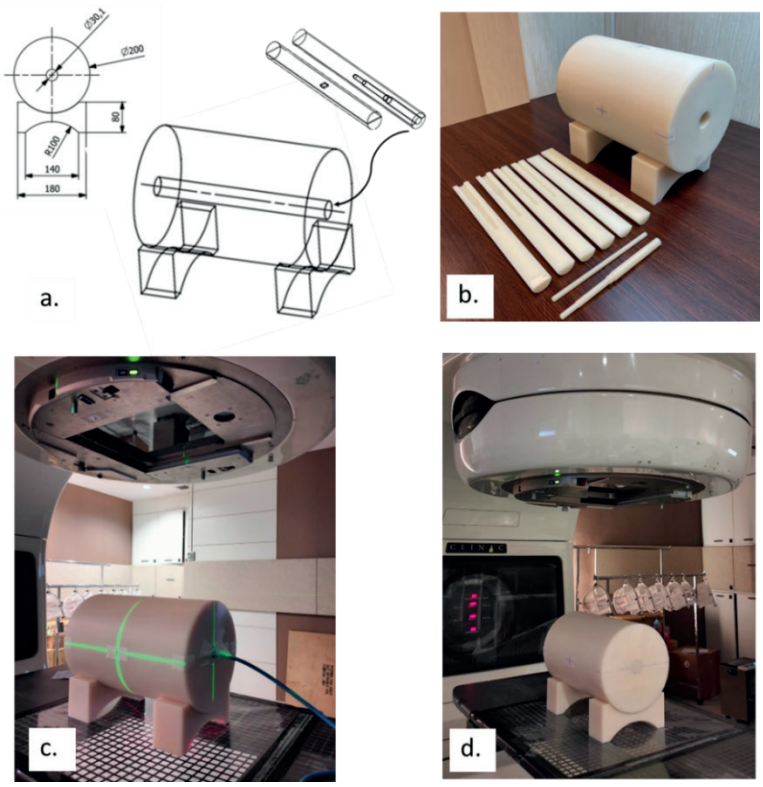

Figure 4. *The novel cylindrical phantom for nanoDot™ calibration factor determination: (a) Phantom drawing, (b) fabricated phantom with a different detector plug, (c) a phantom with an 0.6 cm^3 IC, and (d) a phantom with nanoDot™ embedded.*

Physical characteristics of phantom

The exact dimensions were 20 cm in diameter and 30 cm in length, with a weight of 10.8 kg and a volume of 9,420 cm^3. The calculated density was 1.145 g/cm^3. The HU at the center were 100.4 ± 4.6, and at the periphery, they were 102.2±4.5, 100.8±4.5, 102.7±4.5, and 102.0±4.1 HU, as shown in Figure 5. The results demonstrated good uniformity in HU values throughout the phantom, with differences not exceeding ±5 HU, in accordance with IAEA HHS No. 19 guidelines.[17] For comparison with the HU value of the solid water phantom, the mean HU value of the cylindrical phantom with cast nylon material was 101.62±0.98 HU, while the solid water phantom provided a value of 27.26±0.09 HU. The difference in HU between the two materials, attributed to the density of nylon, was higher than that of the solid water phantom (1.03 g/cm^3).[20]

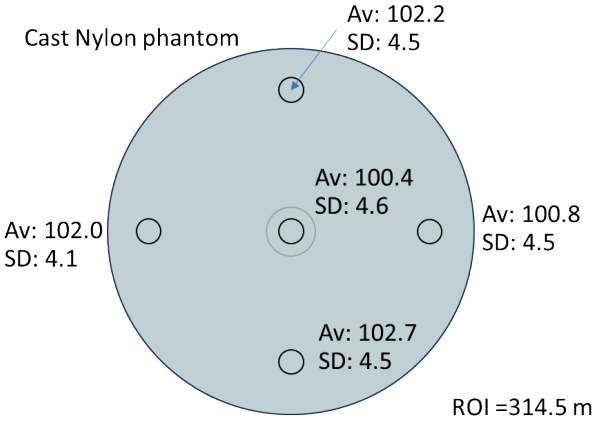

Figure 5. *The image of a cylindrical phantom showing the location of the region of interest (ROI) used to determine HU values.*

Sensitivity correction factor of nanoDot™

Figure 6 illustrates sensitivity correction factors for 100 nanoDot™ detectors. The mean and SD of sensitivity correction factors of all detectors was 1.00±0.023, with a coefficient of variance of 2.26%. The sensitivity correction factor of each nanoDot™ detector was applied to correct the dose determination. The nanoDot™ detectors with a correction factor greater than ±5% were excluded from this study.

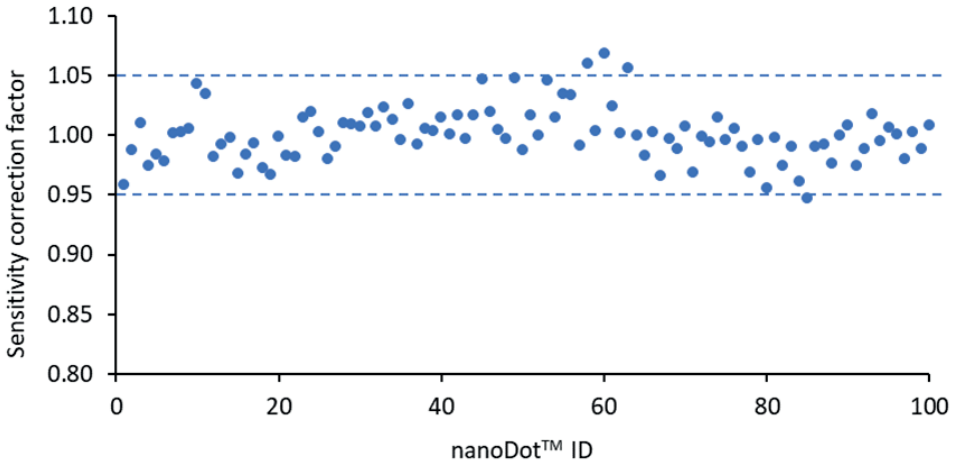

Figure 6. *Sensitivity correction factors of 100 nanoDot™ detectors.*

Evaluation of cylindrical phantom

The calibration factor of the developed phantom (CF_{cylin}) was 1.1785, and the calibration factor of the solid water phantom (CF_{solid}) was 1.1793, as shown in Table 2. The results demonstrate good agreement, with a difference of -0.069%. Therefore, the cylindrical phantom is suitable for the nanoDot™ calibration factor.

Table 2. Calibration factors of nanoDot™ from solid water phantom (CF_{solid}) and the newly developed (CF_{cylin}).

Phantom	Dose of IC (cGy)	nanoDot™ reading (cGy)[a]	Calibration factor	Difference
Solid water	100.20	84.96	1. 1793	-0.069 %
Cylindrical phantom	100.32	85.12	1.1785	

Note: IC: ionization chamber, [a]averaged from 3 nanoDot™ detectors

The effect of angular variation on calibration factor (CF_{cylin})

Calibration factor (CF_{cylin})

The average nanoDot™ readings from the single and multiple beams (new method) compared to the dose from the ionization chamber are illustrated in Figure 7. As the number of beams increased, the nanoDot™ readings decreased. Therefore, the CF_{cylin} values were adjusted according to the number of beams.

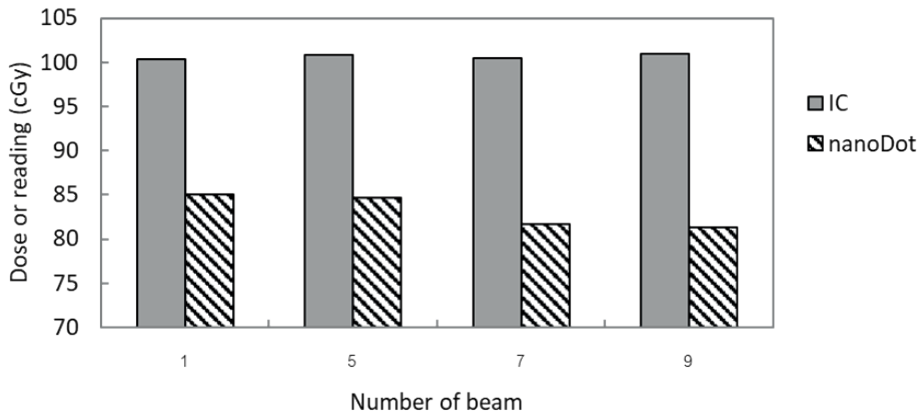

Figure 7. *Comparison of doses from the ionization chamber (IC) and the average reading of nanoDot™ for different numbers of beams using the cylindrical phantom.*

The calibration factors determined from the cylindrical phantom for single and multiple beams are shown in Figure 8. The results indicate that the calibration factor increased as the number of beams increased, ranging within a calibration factor from 1.179 to 1.242. The relationship between the calibration factors and the number of beams follows the polynomial equation (Equation 8) with an R^2 value of 0.9287.

$$CF = 0.0008x^2 + 0.0005x + 1.1759 \quad (8)$$

where CF is the calibration factor, and x is the number of beams.

The angular correction factors, influenced by the number of beams, are depicted in Figure 9. These values can be applied to nanoDot™ measurements, as shown in Equation 6.

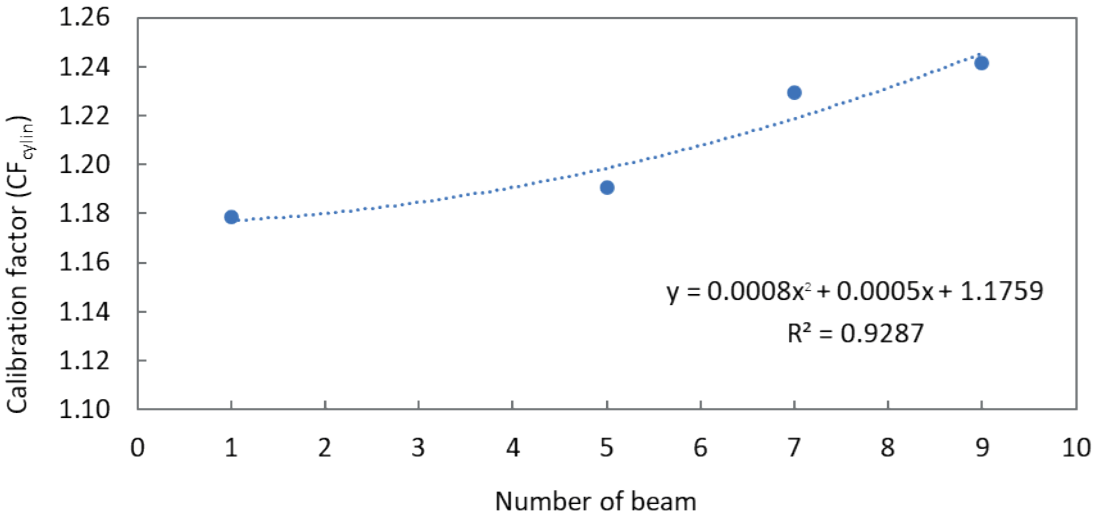

Figure 8. *The relationship between calibration factors determined using the cylindrical phantom (CF_{cylin}) and the number of beams (second-order polynomial equation).*

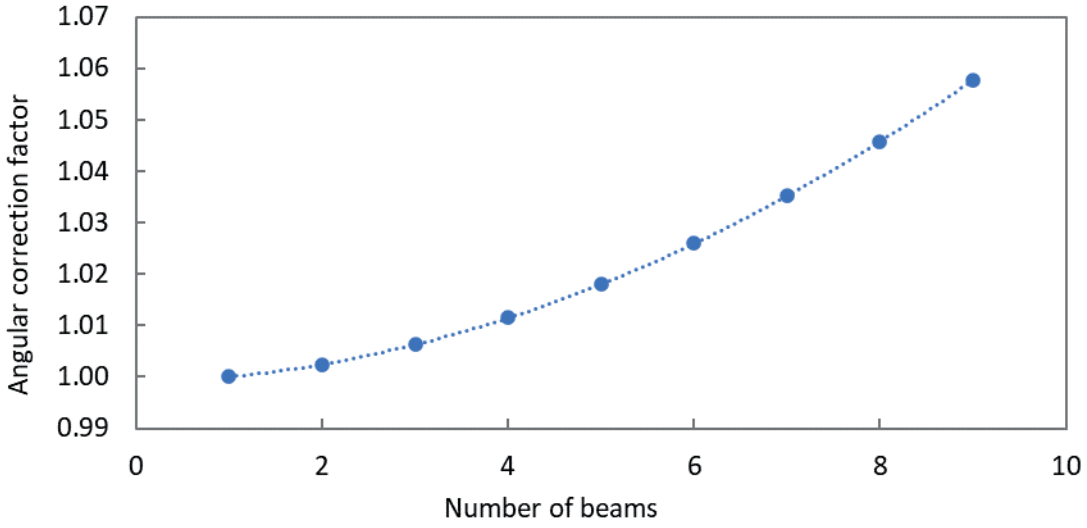

Figure 9. *The relationship between the angular correction factor and the number of beams (Second-order Polynomial Equation) using the cylindrical phantom.*

Validation of calibration factor of nanoDot™

The results showed that the nanoDot™ measurements for the 4-field plan (Plan D) exhibited the largest deviation from the IC when compared to the single-beam and 2-beam plans (Plan A, B, and C). The difference in Plan D slightly exceeded 2%, while the differences in the other plans remained within 2% (as shown in Table 3).

Table 3. The comparison involves doses determined from the calibration factor determined using cylindrical phantom, including the single-beam calibration factor (), new calibration factors using the fitting equation (CF_{poly}), and that of correction for angular correction factor, against those measured by the ionization chamber.

Plan	Dose (cGy)				%difference		
	Ionization chamber	nanoDot™			nanoDot™ vs Ionization chamber		
		CF_{1beam}	CF_{poly}	$CF_{1beam} \times k_{angle}$	CF_{1beam}	CF_{poly}	$CF_{1beam} \times k_{angle}$
A	100.60	99.37	99.37	99.37	-1.23	-1.23	-1.23
B	100.76	100.74	100.74	100.74	-0.02	-0.02	-0.02
C	100.40	99.85	99.98	100.10	-0.54	-0.42	-0.30
D	100.37	98.34	99.38	99.47	-2.02	-0.98	-0.90

CF_{1beam} : single-beam calibration factor with 0 degrees gantry angle, CF_{poly} : calibration factor from polynomial equation, $CF = 0.0008x^2 + 0.0005x + 1.1759$ (x= number of beams), : single-beam calibration factor multiplied by angular correction factor.

When applying the calibration factor based on the number of beams, the percentage difference in Plans C and D decreased. There was no notable difference between applying the calibration factor from the polynomial equation (Equation 8) and correcting for the number of beams ($CF_{1beam} \times k_{angle}$). Therefore, the angular correction factor (k_{angle}) can be utilized for clinical applications in various situations, as determined in this study. However, by incorporating the k_{angle} value from this study, the nanoDot™ calibration factor of single beam should still be determined specifically at the user institute.

Discussion

This study utilized cast nylon to create the phantom. Previous research also employed cast nylon for CT dosimetry phantoms, demonstrating its viability as an alternative for CTDI measurement. [16] Intang A *et al*. demonstrated the suitability of cast nylon phantoms for SRS end-to-end testing using an alanine dosimeter.[21] The cylindrical nylon phantom in this study had a density of 1.145 g/cm³, comparable to the work of Sookpeng S *et al*[16]. Despite its density being higher than that of water (1 g/cm³) and solid water phantom (1.03 g/cm³), it did not affect the determination of the calibration factor. The calibration factor for the developed phantom (CF_{cylin}) closely matched that of solid water phantom (CF_{solid}), with a percentage difference of -0.069%.

A cylindrical cast nylon phantom proved beneficial for multiple beam determinations, for which the slab water phantom was found unsuitable. Consequently, this study designed the phantom with a cylindrical shape. However, the cylindrical shape was hard to set up due to its easy rotation. Hence, improvements in the design of the alignment marker were necessary for practical application. Another advantage of the cylindrical nylon phantom designed in our study is the reproducibility of the nanoDot™ setup. This is attributed to the cylindrical plug designed for embedding the detector, specifically designed to match the dimensions of the nanoDot™, with the center of the sensitive volume of the nanoDot™ aligned with the center of the cylindrical phantom. This feature facilitates an easier, more accurate, and more reproducible setup compared to using a slab solid water phantom.

Typically, calibration factors of nanoDot™ were determined using a solid water phantom at a reference depth, such as 10 cm, with the nanoDot™ oriented perpendicularly to the beam in reference condition, and then compared with IC measurements. For practical applications, this calibration factor was utilized for dose measurements with nanoDot™. However, clinical irradiation often involves beams coming from non-perpendicular directions, as previous studies have demonstrated that nanoDot™ responses are highly dependent on the angular of the incident beam.[14] This angular effect leads to a reduction in measurement signals. Therefore, our study aimed to investigate this effect when applying nanoDot™ for dose measurements in plans with multiple beam angles. The calibration factor required adjustment to account for the angular aspect, and an angular correction factor was applied to the single-beam calibration factor, as illustrated in Equation 6. This study did not provide the calibration factor specifically for individual gantry angles because it is challenging to correct in practice. Instead, we adapted the calibration factor for the composite field with multiple beam angles, as used in IMRT. For future studies, exploring the calibration factor for arc therapy configurations, such as VMAT, may be useful. The results showed that adjusting the calibration factor for specific numbers of beams improved dose measurements with nanoDot™, reducing the percentage difference from 2.02% to less than 1% (Table 3).

It's worth noting that the calibration factor is also influenced by the beam quality and the reader system of the detector. The calibration factors derived from this study are specific to our setup and not be directly applied in other hospitals or with different reader systems. To extend these findings to other institutions, the values

were determined. Calculations using Equation 6, along with the calibration factor obtained from the standard method with single beam under reference condition, can be employed to determine doses with the nanoDot™. With values, there is no need to determine the calibration factor for different numbers of beams. This approach may be particularly useful for institutions lacking access to a cylindrical phantom and can reduce the time needed for calibration factor determination.

For future research, we recommend investigating the application of nanoDot™ in clinical settings, such as in intensity-modulated radiation therapy (IMRT) and volumetric modulated arc therapy (VMAT) techniques. Additionally, exploring organ doses outside the irradiation beam should be a subject of further investigation.

Limitation

The limitation of this study is the lack of investigation in clinical applications. While the validation of the new calibration was performed for single, two and four-field plans, higher numbers of beams and modulated beams have not been investigated.

Conclusion

The new cylindrical phantom is suitable for determining the nanoDot™ calibration factor, obtaining a calibration factor comparable to the standard solid water phantom. Another implication of the cylindrical phantom is its suitability for multiple-beam measurements, which is appropriate for angular-dependent studies. The calibration factors are dependent on the number of beams. The calibration factor specific to the number of beams or the angular correction factor improves dose measurements using the nanoDot™ and aligns with ionization chamber measurements, showing a difference of less than 2%.

Conflict of interest:

None

Funding

The research was funded by the Faculty of Allied Health Science, Naresuan University, for the Budget Year 2023, under Contract Number AH-66-01-002.

Acknowledgements

We sincerely thank our undergraduate students for analyzing the nanoDot™ reading.

References

[1] Yukihara EG, Yoshimura EM, Lindstrom TD, Ahmad S, Taylor KK, Mardirossian G. High-precision dosimetry for radiotherapy using the optically stimulated luminescence technique and thin Al2O3:C dosimeters. Phys Med Biol [Internet]. 2005; 50(23): 5619-28. doi.org/10.1088/0031-9155/50/23/014.

[2] Jursinic PA. Characterization of optically stimulated luminescent dosimeters, OSLDs, for clinical dosimetric measurements. Med Phys. 2007; 34(12): 4594-604. doi: 10.1118/1.2804555

[3] Dunn L, Lye J, Kenny J, Lehmann J, Williams I, Kron T. Commissioning of optically stimulated luminescence dosimeters for use in radiotherapy. Radiat Meas. 2013; 51-52: 31-9. doi: 10.1016/j.radmeas.2013.01.012.

[4] Viamonte A, Da Rosa LAR, Buckley LA, Cherpak A, Cygler JE. Radiotherapy dosimetry using a commercial OSL system. Med Phys. 2008; 35(4): 1261-6. doi: 10.1118/1.2841940.

[5] Alvarez P, Kry SF, Stingo F, Followill D. TLD and OSLD dosimetry systems for remote audits of radiotherapy external beam calibration. Radiat Meas [Internet]. 2017; 106: 412-5. doi.org/10.1016/j.radmeas.2017.01.005.

[6] Mrčela I, Bokulić T, Izewska J, Budanec M, Fröbe A, Kusić Z. Optically stimulated luminescence in vivo dosimetry for radiotherapy: Physical characterization and clinical measurements in 60Co beams. Phys Med Biol. 2011; 56(18): 6065-82. doi: 10.1088/0031-9155/56/18/018.

[7] Yusof FH, Ung NM, Wong JHD, Jong WL, Ath V, Phua VCE, *et al*. On the use of optically stimulated luminescent dosimeter for surface dose measurement during radiotherapy. PLoS One. 2015; 10(6): 1-15. doi: 10.1371/journal.pone.0128544.

[8] Zhuang AH, Olch AJ. Validation of OSLD and a treatment planning system for surface dose determination in IMRT treatments. Med Phys. 2014; 41(8): 081720. doi: 10.1118/1.4890795.

[9] Wake JR, Chen FQ, Ashworth S, Byth K, Wang W, Stuart KE. Verification using in vivo optically stimulated luminescent dosimetry of the predicted skin surface dose in patients receiving postmastectomy radiotherapy. Med Dosim. 2021; 46(2): e1-6. doi: 10.1016/j.meddos.2020.10.001.

[10] Butson M, Chen T, Alzaidi S, Pope D, Butson E, Gorjiara T, *et al*. Extrapolated skin dose assessment with optically stimulated luminescent dosimeters. Biomed Phys Eng Express. 2016; 2(4): 047001. doi: 10.1088/2057-1976/2/4/047001.

[11] Raj LJS, Pearlin B, Peace BST, Isiah R, Singh IRR. Characterisation and use of OSLD for in vivo dosimetry in head and neck intensity-modulated radiation therapy. J Radiother Pract. 2021; 20(4): 448-54. doi: 10.1017/S146039692000062X.

[12] Ponmalar R, Manickam R, Ganesh KM, Saminathan S, Raman A, Godson HF. Dosimetric characterization of optically stimulated luminescence dosimeter with therapeutic photon beams for use in clinical radiotherapy measurements. J Cancer Res Ther. 2017; 13(2): 304-12. doi: 10.4103/0973-1482.199432.

[13] Kry SF, Alvarez P, Cygler JE, DeWerd LA, Howell RM, Meeks S, *et al*. AAPM TG 191: Clinical use of luminescent dosimeters: TLDs and OSLDs. Med Phys. 2020; 47(2): e19-51. doi: 10.1002/mp.13839.

[14] Kerns JR, Kry SF, Sahoo N, Followill DS, Ibbott GS. Angular dependence of the nanoDot OSL dosimeter. Med Phys. 2011; 38(7): 3955-62. doi: 10.1118/1.3596533

[15] Yabung K, Khunnarong P, Wongsurija S. The application of OSLD for in vivo dosimetry in head and neck intensity-modulated radiation therapy: A phantom study [Thesis]. Faculty of Allied Health Sciences: Naresuan University; 2022 [in Thai].

[16] Sookpeng S, Cheebsumon P, Pengpan T, Martin C. Comparison of computed tomography dose index in polymethyl methacrylate and nylon dosimetry phantoms. J Med Phys. 2016; 41(1): 45-51. doi: 10.4103/0971-6203.177287

[17] International Atomic Energy Agency. Quality Assurance for Computed Tomography - Diagnostic and Therapy Applications [HHS No.19]. Vienna: IAEA; 2012.

[18] International Atomic Energy Agency. Absorbed Dose Determination in External Beam Radiotherapy [TRS398]. Vienna: IAEA; 2001.

[19] International Atomic Energy Agency. Commissioning and Quality Assurance of Computerized Planning Systems for Radiation Treatment of Cancer (TRS 430). Vienna: IAEA; 2004.

[20] International Atomic Energy Agency. Dosimetry of Small Static Fields used in External Beam Radiotherapy: An IAEA–AAPM International Code of Practice for Reference and Relative Dose Determination [TRS 483]. Vienna: IAEA; 2017.

[21] Intang A, Oonsiri P, Kingkaew S, Chatchumnan N, Oonsiri S. Validation of the fabricated cast nylon head phantom for stereotactic radiosurgery end-to-end test using alanine dosimeter. J Med Phys. 2023; 48(1): 74-9. doi: 10.4103/jmp.jmp_98_22.

Journal of Associated Medical Sciences 2024; 57(2): 20-30

JAMS
Journal of Associated Medical Sciences

Scopus Indexed & Thai-Journal Citation Index Centre (TCI)

Journal of Associated Medical Sciences

Journal homepage: https://www.tci-thaijo.org/index.php/bulletinAMS/index

Activity Card Sort's existence and execute in various languages and versions: A scoping review

Jayachandran Vetrayan[1] Supaporn Chinchai[1] Peeraya Munkhetvit[1] Prathap Suganthirababu[2] Jananya P. Dhippayom[1*]

[1]Department of Occupational Therapy, Faculty of Associated Medical Sciences, Chiang Mai University, Chiang Mai Province, Thailand.
[2]Saveetha College of Physiotherapy, Saveetha Institute of Medical and Technical Sciences, Saveetha University, India.

ARTICLE INFO

Article history:
Received 25 October 2023
Accepted as revised 22 December 2023
Available online 15 January 2024

Keywords:
Activity Card Sort (ACS), reliability, validity, psychometric properties

ABSTRACT

Background: Activity Card Sort (ACS) measures patient activity participation, especially in older adults. It was developed to evaluate instrumental, social, and leisure activities of low and high demand in various populations. Transferring an ACS tool between diverse settings is challenging due to significant socio-economic, linguistic, and environmental impacts. Hence, to tailor ACS tools to a specific society's socio-cultural context, comprehension of the accessible validated ACS tools and their psychometric attributes is essential.

Objective: This scoping review was conducted to explore the availability of the ACS tool and to summarize the psychometric properties, such as the reliability and validity, of different languages and versions of ACS available worldwide.

Materials and methods: A search was performed in PubMed, PsycNET, Cochrane, and Embase. Two independent reviewers conducted the screening process and extracted the data. The total sample included 370 articles, of which 26 studies met the inclusion criteria, providing information on psychometric properties. English and non-English versions (Arabic, Dutch, and Spanish) in different populations were included.

Results: Among the 26 studies in this review, most ACS studies used the English version (62.5%). All the reported studies revealed "good" internal consistency, in which the Cronbach's alpha (α) ranges between 0.61 and 0.91. Test-retest reliability was measured using ICC values ranging from 0.78 to 0.98 for numeric data and Kappa statistics for binary data. Two studies used Kappa statistics to test the reliability, which ranged from 0.48 to 0.85 for all domains, indicating moderate to good reliability. Measures of content validation, face validity, concurrent, convergent, and discriminative validity were also reported.

Conclusion: Good psychometric properties were reported. No study is available on the Indian population using the ACS tool. Hence, developing and validating an ACS tool for the Tamil Nadu population is needed.

Introduction

The Activity Card Sort (ACS) is a useful occupational therapy tool used to measure the impact of health conditions on participation in activities.[1] The ACS is a robust and consistent measure of involvement for older people and children.[2] It can be used to gather information on a patient's activity patterns, which can assist in establishing routines and encouraging participation in meaningful activities. The ACS has shown increased engagement in instrumental, social, and leisure activities in patients following a stroke when occupational therapy interventions based on occupations were used with specific

* **Corresponding contributor.**
Author's Address: *Department of Occupational Therapy, Faculty of Associated Medical Sciences, Chiang Mai University, Thailand.*
E-mail address: jananya.p@cmu.ac.th
doi: 10.12982/JAMS.2024.023
E-ISSN: 2539-6056

task training.[1] The ACS is a newly established tool that serves as a standardized evaluation tool to measure the quantity and quality of physical activity and the degree of participation in various activities.[3] The domains of ACS include instrumental activities of daily living (IADL) which are essential to preserve self and property, social activities (SC), and both high-demand leisure activities (HDL) that require physical strength, and low-demand leisure activities (LDL).[2]

Adapting an ACS tool from one setting to another, particularly when the settings are vastly different, poses significant challenges. The influence of socio-economic, linguistic, and environmental factors on specific life dimensions is considerable. Consequently, it is imperative to tailor the activities of ACS tools to the socio-cultural context of a specific society. The importance of understanding participation in social activities cannot be overstated, given their direct impact on physical and mental health, as well as well-being perception.[4] India, a developing country, is in the process of analyzing the psychometric properties of this ACS tool. Language serves as a crucial parameter for homogeneity within a population group. Tamil Nadu, the tenth-largest Indian state by area and the sixth-largest by population is predominantly Tamil-speaking.[5] The state is renowned for its rich traditional culture, including the Bharatanatyam dance style, cultural festivals like Pongal and Jallikattu, and unique attire such as dhoti and saree. The participation in daily activities in Tamil Nadu is likely to differ from that in Western populations due to its distinct culture and language. The current scoping review aims to investigate the availability of validated ACS tools for adults in the Tamil Nadu population and summarize the key aspects, including the psychometric properties (reliability and validity) of different languages and versions of ACS available globally. This understanding will facilitate the development of a new ACS for specific conditions in the Tamil Nadu population.

Methods

Study design

This scoping review is reported according to the Preferred Reporting Items for Systematic Reviews and Meta-Analyses Extension for Scoping Reviews (PRISMA-ScR).[6]

Information sources and search strategy

The search strategy was constructed following the recommendations of the peer review of the Electronic Search Strategies 2015 guidelines.[6] This scoping review included all the published articles on the development of ACS under different conditions and in different cultures. The articles were retrieved from the following electronic databases: MEDLINE/PubMed, Cochrane, Embase, and PsycNET (Includes PsycINFO, PsycBOOKS, PsycARTICLES, PsycTESTS, and PsycTherapy video library). The keywords used in the search included "activity card sort" [Mesh Terms], "activity card sort" [All Fields], "activity card sort" [Title/Abstract], "activity card sort" [All Fields], or "activity card sort" [Title/Abstract].

The articles were then screened for their titles, abstracts, and index terms. A medical librarian (Mr. P) was involved in finding the most appropriate Medical Subject Headings terms for the search and modifying them for the databases used. Based on this exploratory scoping phase, the search strings for each database were finalized. A total of 370 articles were retrieved from all databases. Finally, all retrieved articles from each database were imported into reference management software.

Eligibility criteria

The following inclusion and exclusion criteria were established to focus our review on the availability of validated ACS tools.

Inclusion criteria

1. Studies reporting reliability and validity of Activity Card Sort
2. Articles published from 2003 to through June 30th, 2023
3. All original research studies were included.

Exclusion criteria

Multiple studies of the same version of the ACS tool were excluded.

Study selection

A team of two independent reviewers (JC and XX) consolidated the search results on the different databases. Reviewers screened the titles and abstracts of the articles to exclude those that did not meet the eligibility criteria. At this stage, the divergences were resolved by consensus between the two reviewers. In case of doubt, the study was selected for further evaluation. The full-text article was retrieved for those articles included under level 1 screening. Three categories (yes, no, and maybe) were used to select the full text for inclusion. Consequently, conflicts were resolved by a third reviewer (JS). The final decision to include articles for the data extraction process proceeded only after majority agreement across the team.

Data collection and charting

Data were extracted based on a consistent format for each study. For each article, two reviewers extracted information regarding author details, year of publication, language version, country of study, measurement properties, and ACS version. The extracted data was charted in Microsoft Excel. Discrepancies in the data extracted were negotiated until a consensus was reached. In addition, information on the demography of the study population and age group was also extracted. Based on the data extraction model, the reviewers independently extracted and plotted the data for each article.

Synthesis of results

Each article was analyzed and summarized based on study objectives and outcomes (measurement properties) in a table format.

Result

The research examining psychometric properties has disclosed cross-cultural adaptations, inter- and intra-examiner agreement analysis, internal consistency, reliability, and validity.

Figure 1 shows the results of this scoping review study's search and screening process. A total of 208 records after the removal of duplicates were screened for level 1 (title/abstract) screening. A full-text review (level 2 screening) was completed for 75 articles, of which only 26 met this study's inclusion criteria. The remaining 49 articles were excluded as they did not fall under inclusion criteria, and the same version of ACS was used in multiple studies.

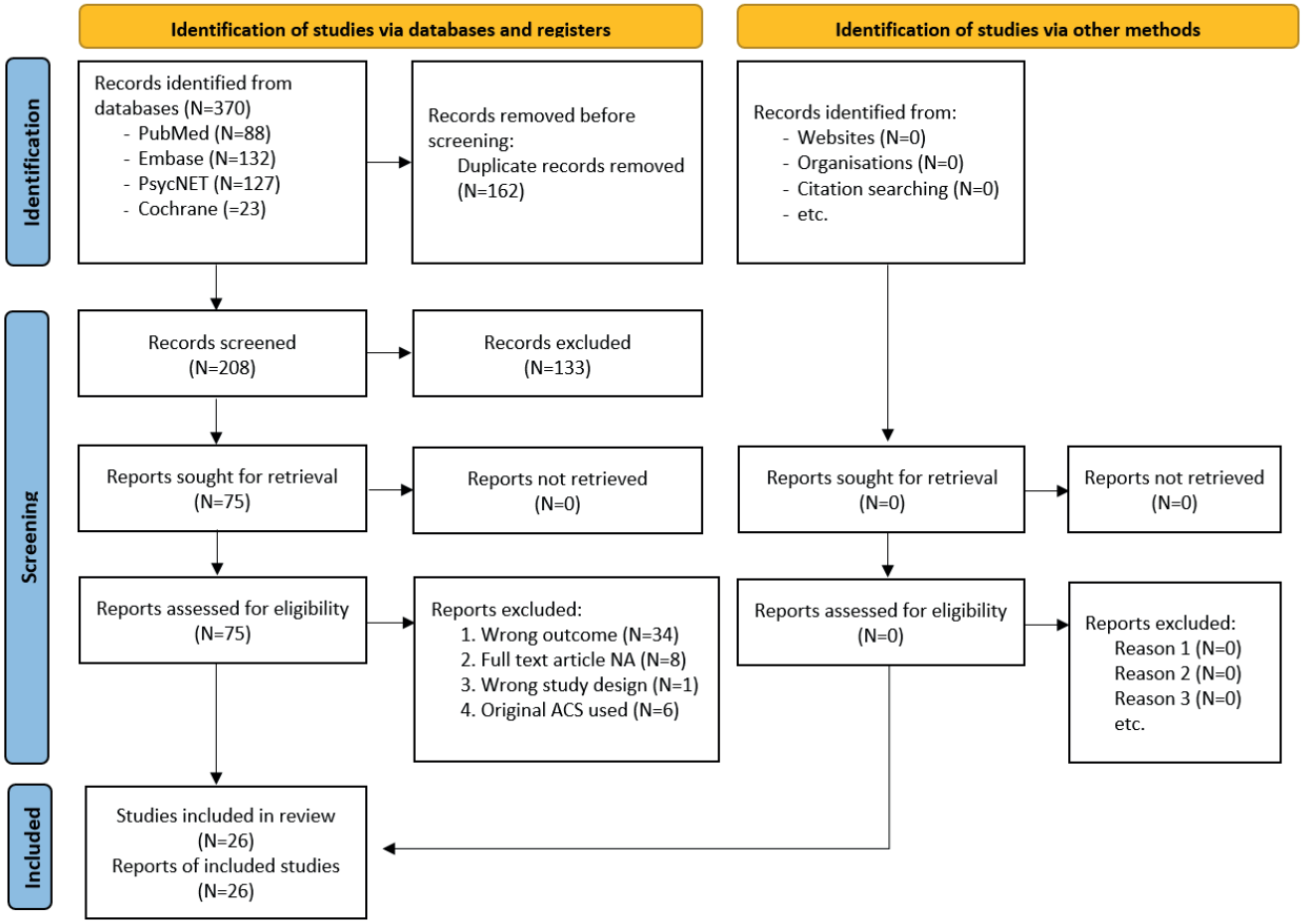

Figure 1. *Flow chart of article selection process.*

Characteristics of the selected study

According to this scoping review, seven distinct variations of the ACS version have been identified, each available in a different language: English, Spanish, Arabic, Puerto Rican Spanish, Dutch, Chinese (Hong Kong), and Israeli. The availability of these versions in different locations is documented in Table 1. While the ACS is predominantly accessible in English, it has also been implemented in several countries, reflecting cultural diversity. These countries include the United States of America (USA), Australia, Lebanon, the Netherlands, the United Kingdom (UK). The ACS has been most extensively studied and utilized in the USA. Studies have yet to be conducted in regional languages within India.

Table 1. Summary of location, language, and version of ACS among included studies.

Location study	Language -Version						
	Israeli	**Chinese HK**	**English**	**Spanish**	**Arabic**	**Puerto Rican Spanish**	**Dutch**
Israel Katz *et al*.[7]	Israeli-adapted ACS						
Hong Kong Chan *et al*.[11]		ACS-HK					
US Berg *et al*.[14] Stoffel *et al*.[20] Orellano *et al*.[8] Gronski *et al*.[27] Berg *et al*.[12] Mc Collum *et al*.[13] Hoyt *et al*.[17] Tyminski *et al*.[18] Hoyt CR *et al*.[10] Boone AE *et al*.[24]			PACS PACS AYA-ACS AYA-ACS ITACS ACS-AIP ITACS ACS3 Electronic version	PACS		PR-ACS	
Australia Doney *et al.*[19] Tse,T *et al*.[9] Gustafsson *et al*.[29] Gustafsson *et al*.[30]			ACS-Aus ACS-Aus ACS-Aus ACS-App				
Lebanon Lyons *et al*.[25]			m-ACS				
Netherland Jong *et al*.[26] Poerbodipoero *et al*.[22] Leenders *et al*.[31]							ACS-NL ACS- NL ACS- NL
UK Laver-Fawcett *et al*.[2] Laver-Fawcett *et al*.[28]			ACS-UK ACS-UK				
Jordan Hamed *et al*.[15] Hamed *et al*.[21] Malkawi *et al*.[16] Malkawi *et al*.[23]					A-ACS A-ACS Arab-PACS Arab-PACS		

Note: ACS: Activity Card Sort, ACS-HK: Activity Card Sort Hong-Kong Version, PACS: Pre-school Activity Card Sort, AYA-ACS: Adolescent and Young Adult Activity Card Sort, ITACS: Infant Toddler Activity Card Sort, ACS-AIP: Activity Card Sort: Advancing Inclusive Participation, ACS 3 electronic version: Activity Card Sort Electronic Version, ACS-Aus: Australian Activity Card Sort, ACS-AAP: Activity Card Sort with Adelaide Activity Profile, PR-ACS: Activity Card Sort Peurto-Rican Spanish Version, mACS: Activity Card Sort (modified), A-ACS: Arab heritage Activity Card Sort, ACS-NL: Dutch Activity Card Sort Institutional Version, ACS-UK: Activity Card Sort United Kingdom, Arab-PACS: Arabic Pre-school Activity Card Sort, Israeli-adapted ACS: Israeli-adapted Activity Card Sort.

Study population

Based on the data presented in Table 2, it can be observed that a significant proportion of the research incorporated a sample of individuals aged 60 years and older, commonly referred to as the geriatric population. The study included individuals from various age groups, including young, middle-aged, and elderly residents. The involvement of parents of preschool children (ages 3-6) and caregivers responsible for children aged 0-3 was observed in specific research investigations. One study was conducted on special populations, specifically homeless individuals, and rehabilitation inpatients. The study also considered individuals afflicted with various medical conditions, such as multiple sclerosis, neuromuscular illness, stroke, or those undergoing stem cell transplantation. A study was conducted on a diverse group, including healthy adults, caretakers, and patients with various diseases. The study included diverse participants, such as children diagnosed with autism spectrum disorder (ASD), pre-schoolers with disabilities, those experiencing developmental delays, and typically developing children.

Measurement properties

Twenty-six studies investigated reliability (test-retest reliability, interrater reliability, or internal consistency) along with its construct, convergent, content, face, and discriminative validity. The summary of measurement property data extracted for each study is shown in Table 2.

Table 2. Summary of psychometric properties of ACS among different age group and population.

S.NO	Author	Age group	Study population	Internal consistency (Cronbach's alpha)	Test reliability (ICC/KAPPA)	Validity measures
1	Katz *et al*.[7]	Average age between 47 to 75 years in various groups	Mixed population (Adults, caregivers, diseased)	Ranging from 0.61 to 0.82	NR*	NR*
2	Chan *et al.*[11]	65 years or older	Stroke patients	0.89: Good internal consistency	ICC; (α=0.98)	NR*
3	Berg *et al.*[14]	3 to 6 years	Preschoolers with disabilities	NR *	NR *	Content validity (To establish content validity, 10 nationally recognized pediatric occupational therapists reviewed the photograph)
4	Doney *et al*.[19]	60 to 95 years	Community-dwelling geriatric population	NR*	NR*	Moderate concurrent validity (*r*=0.434), Moderate convergent construct validity (*r*=0.354), and strong discriminative validity (*p*=0.000)
5	Stoffel *et al*.[20]	children between 3 to 6 years	Parents of preschool children	NR*	NR*	Moderate concurrent validity in self-care domains and low concurrent validity for mobility and social domains
6	Lyons *et al*.[25]	54 years	Patients scheduled to undergo Stem Cell Transplantation-Bone marrow	NR*	ICC (α= 0.86 to 0.96)	NR*
7	Hamed *et al*.[15]	Young and older adults	Jordanians from different age groups and socioeconomic classes	NR*	NR*	Two rounds of content validity (Ranking and reranking)
8	Orellano *et al*.[8]	Diseased: 50 years and above Normal: 60 years and older	Multiple Sclerosis patients and Well older adults - both Puerto Rican origin	0.91: high internal consistency	ICC; (0.82), good test-retest reliability	Good concurrent and construct validity
9	Jong *et al*.[26]	Median age: 77.5 Minimum age: 60 years	Special population (older rehabilitation)	NR*	ICC; inter-rater agreement (0.78 and 0.87) ICC; intra-rater agreement (0.79 and 0.89).	NR*

Table 2. Summary of psychometric properties of ACS among different age group and population (continued).

S.NO	Author	Age group	Study population	Internal consistency (Cronbach's alpha)	Test reliability (ICC/KAPPA)	Validity measures
10	Laver-Fawcett *et al.*[2]	65 years and older	Community-dwelling geriatric population	NR*	NR*	Content validity
11	Hamed *et al.*[21]	Younger: 20 to 60 years Older adults: 61+ years	Multiple Sclerosis patients	ICC; (α= 0.90), excellent internal consistency	ICC; (0.80), good test-retest reliability.	Moderate concurrent, convergent and discriminative validity
12	Gronski *et al.*[27]	3 to 6 years	Preschoolers with and without disability	NR*	ICC=0.93 for test-retest reliability and ICC=0.91 for inter-rater reliability	Internal validity with reliability coefficient (0.85-0.97)
13	Berg *et al.*[12]	17 to 25 years	Young adults	NR*	Moderate test-retest reliability with Kappa; (0.48-0.85) for all domains	Content validity and face validity was assessed
14	Malkawi *et al.*[16]	3 to 6 years	Parents of preschool children	NR*	NR*	Content validation performed using Delphi method
15	Poerbodipoero *et al.*[22]	42 to 87 years	Parkinson's disease (PD)	NR*	ICC; of USER-P (0.84) for the satisfaction scale	Good discriminative validity and poor convergent validity
16	Laver-Fawcett *et al.*[28]	>65 years	Community dwelling older adults	NR*	NR *	Good face validity and content validity were assessed
17	Tse,T *et al.*[9]		Stroke cohort	excellent internal consistency score for total retained participation (α=0.91) at 3 months and (α=0.89) at 12 months	NR*	Moderate to good concurrent and convergent validity (p<0.001) at 3 months and 12 months
18	Mc Collum *et al.* [13]	Young adults (18-25) and caring adults	Diagnosed with ASD	NR*	Excellent test-retest reliability (chores Kappa =0.74, social Kappa=0.72, education Kappa=0.85, And moderate agreement for health Kappa=0.48, leisure Kappa=0.48, and work Kappa=0.53) There was poor agreement for parenting Kappa=0.15	NR*
19	Malkawi *et al.*[23]	3 to 6 years.	Preschool children	ICC; (α=0.85), excellent overall internal consistency	ICC= 0.97, Good test-retest reliability	Moderate Construct and concurrent validity
20	Gustafsson *et al.*[29]	18 to 64 years	Adults	0.83: acceptable internal consistency	ICC;(0.92) acceptable parallel-form reliability	NR*

Table 2. Summary of psychometric properties of ACS among different age group and population (continued).

S.NO	Author	Age group	Study population	Internal consistency (Cronbach's alpha)	Test reliability (ICC/KAPPA)	Validity measures
21	Gustafsson *et al*.[30]	18 to 64 years	Community dwelling adults	NR*	ICC; (0.75), high test-retest reliability for overall retained activity	NR*
22	Hoyt *et al*.[17]	Caregivers of children 0-3 years	Caregivers	NR*	NR*	Content validation
23	Tyminski *et al*.[18]	20 to 70 years	Special population (homeless population)	NR*	NR*	Content validation and face validation
24	Hoyt *et al*.[10]	Caregivers of children's (0-3 years)	Caregivers of Children who were typically developing (TD) or had a developmental delay (DD)	High initial internal consistency (α=0.77 to 0.85)	Moderate test–retest reliability for total sample (ICC=0.73) and TD (ICC=0.73). Low test-retest reliability in DD cohort (ICC=0.62)	Moderate concurrent validity
25	Boone *et al*.[24]	Middle aged and older adults (mean=57.5)	General population	NR*	NR*	Good concurrent validity
26	Leenders *et al*.[31]	18-64 years	Patients diagnosed with neuromuscular disease	NR*	Excellent reliability (ICC=0.95) average total day score	NR*

**NR: not reported*

Internal consistency and test-retest reliability

Various versions of ACS have been used to investigate its internal consistency using Cronbach's alpha and test reliability using ICC for numeric data and KAPPA statistics for binary data. Considering the internal consistency, among the 26 studies, only seven have reported Cronbach's alpha. All the reported studies revealed "good" internal consistency in which the Cronbach's alpha (α) ranged between 0.61 and 0.91.[7,8,9] Among the 26 studies, 12 revealed test reliability using ICC and were good to excellent overall. The moderate test-retest reliability was noted in the study by Hoyt in 2021 for the total sample (ICC=0.73) and typically developed (TD) (ICC=0.73), with low test-retest reliability in the developmental delay (DD) cohort (ICC=0.62).[10] A study by Chan *et al*. in 2006 showed the highest test reliability (ICC=0.98).[11] Two studies used Kappa statistics to test the reliability, which ranged from 0.48 to 0.85 for all domains, indicating moderate to good reliability.[12,13]

Content validity and face validity:

Eight studies have performed content validation with or without face validation (Table 3). To establish content validity, Berg *et al*. engaged ten nationally recognized pediatric occupational therapists to review a set of photographs.[14] These were also given to parents, who were asked to identify the most frequent activities after collecting 73 images. Content experts accepted 57 photos, and the parents accepted 58. The content validation for the A-ACS was conducted by a two-round process (Round 1: ranking and Round 2: re-ranking) with a cut-off score of mean 2, and 88 activities were selected.[15] Laver-Fawcett *et al*. conducted a content validity study to generate and select culturally relevant activity items for inclusion in the ACS-UK.[2] This was done through a two-round survey (Round 1: activity participation questionnaire, Round 2: review of round 1) with a cut-off score of <2. This process selected 73 activities in round 1 and 107 in round 2.

In another study, the participants were administered the 70 items of the AYA-ACS. Half of this group in this study were shown photographs, while the other half responded to line drawings. Content validation was measured by chi-square, and face validity was measured based on a score of 2 (some do it) and above, which is considered good face validity.[12] Content validation was performed using the Delphi method for validating the A-PACS and ITACS. A cut-off score of a mean of 1.75 was set to select 95 activities. The content validation index was set at 80 percent agreement among the experts in validating the photos. Forty-one items were finalized, respectively.[16,17] In a study by Tyminski *et al.* participants were presented with each card without a written caption and were asked to name the activity depicted.[18] After each response, the participant was verbally given the caption and asked whether they thought it depicted the activity. After the review, 76 validated line drawings were used. It was clear that the occupations occurring in this card sort were not available in other ACS.

Table 3. Summary of internal consistency, reliability, and validity measures among ACS.

Parameter	Number	Percentage (%)
Internal consistency (Cronbach's alpha)		
Not reported	18	69.20
Ranging from 0.61 to 0.82	1	3.85
0.89: good internal consistency	1	3.85
0.91: high internal consistency	1	3.85
0.83: acceptable internal consistency	1	3.85
High initial internal consistency (α=0.77 to 0.85)	1	3.85
ICC; (α= 0.85), excellent overall internal consistency	1	3.85
ICC; (α= 0.90), excellent internal consistency	1	3.85
excellent internal consistency score for total retained participation (α=0.91) at 3 months and (α=0.89) at 12 months	1	3.85
Test Reliability (ICC/KAPPA)		
ICC (α= 0.86 to 0.96)	1	3.85
ICC=0.93 for test-retest reliability and ICC=0.91 for inter-rater reliability	1	3.85
ICC; (0.82), good test-retest reliability	1	3.85
ICC; (α=0.98)	1	3.85
ICC; (0.80), good test-retest reliability	1	3.85
ICC; inter-rater agreement (0.78 and 0.87)	1	3.85
ICC; intra-rater agreement (0.79 and 0.89)	1	3.85
Kappa; (0.48-0.85) for all domains, moderate test-retest reliability	1	3.85
ICC; of USER-P (0.84) for the satisfaction scale	1	3.85
Kappa; (0.48-0.85) for all domains, excellent test-retest reliability	1	3.85
ICC=0.97, good test-retest reliability	1	3.85
ICC; (0.92) acceptable parallel-form reliability	1	3.85
ICC; (0.75), high test-retest reliability for overall retained activity	1	3.85
ICC; (α=0.73), moderate test-retest reliability for total sample	1	3.85
ICC; (α=0.95), excellent reliability average total day score	1	3.85
Not reported	11	42.25
Validity measures*		
Content validity	8	29.63
Face validity	3	11.11
Concurrent validity	8	29.63
Convergent validity	4	14.82
Internal validity	1	3.70
Discriminative validity	3	11.11
Not reported	8	30.77

**some studies reported multiple types of validity.*

Concurrent and convergent validity

Eight out of 26 studies have demonstrated concurrent validity. The results ranged from good to moderate (Table 3). Concurrent validity testing demonstrated a significant but moderate *(r*=0.43) correlation between the ACS-Aus and the Adelaide Activity Profile (APP), an Australian Assessment of Activities.[19] Stoffel *et al*. showed moderate concurrent validity in self-care domains (*r*=0.73) and low concurrent validity for mobility (*r*=0.28) and social domains (*r*=0.51) in the Pediatric Evaluation of Disability Inventory (PEDI) compared to PACS total activity score.[20] The PR-ACS Spanish version demonstrated good concurrent and construct validity with health-related quality of life (*r*=0.66).[8] The ACS-NL in the overall sample showed weak cross-sectional correlations with the Canadian Occupational Performance Measure (COPM) performance score (*r*=0.19).[22] The ACS-Aus demonstrated moderate to good concurrent and convergent validity with the Stroke Impact Scale (SIS) participation score and modified ranking score (*r*=0.61).[9] In a study about concurrent validity, significant correlations were found between the A-PACS and the Vineland Adaptive Behavior Scale (VABS) in the communication domain (*r*=0.62), social domain *(r*=0.57), and motor domain (*r*=0.69).[23] ITACS demonstrated moderate concurrent validity with the Pediatric Evaluation of Disability Inventory-Computer Adaptive Test (PEDI-CAT) in the domain of mobility in the Developmental Delay (DD) group (*r*=0.34) and the domain of daily activities (*r*=0.27). However, there was no significant correlation among children in the typically developing (TD) group

(range=−0.012 to 012), indicating weak concurrent validity for the TD group.[10] In a study comparing the electronic version of the ACS (ACS3) with the original ACS, high correlations (Spearman's p values) were found across each of the four domains, including IADL, low-demand leisure activities, high-demand leisure activities, and social activities (r=0.83). A high correlation was also found for the total current activities score (r=0.86) between the ACS and ACS3 among middle-aged and older adults.[24]

The Personal Well-being Index (PWI), an Australian measure of subjective well-being (ASWB), was utilized to examine convergent construct validity, which resulted in moderate convergent validity (r=0.35).[19] The A-ACS showed a moderate correlation with the total scores of the Mayo-Portland Adaptability Inventory (MPAI) (r=0.45) and the total score on the Arabic version of the self-report Performance Assessment of Self-care Skills (A-PASS) (r=0.58).[21] The assessment and domains that were correlated with ACS are listed in Table 4.

Table 4. Correlation of ACS with other assessments and domains.

S.No	Activity Card Sort	Correlation with other assessments and domains
1	ACS-Aus[19]	Adelaide Activity profile (APP) Australian Assessment of Activities Personal Well-being Index (PWI) Australian Measure of Subjective Well-being (ASWB)
2	PACS[20]	Self-care, social, and mobility domains of the Paediatric Evaluation of Disability Inventory (PEDI)
3	PR-ACS[8]	Health-related Quality of Life
4	A-ACS[21]	Participation Index of Mayo-Portland Adaptability Inventory (MPAI) Arabic Version of the Self-report Performance Assessment of Self-care Skills (A-PASS)
5	ACS-NL[22]	Canadian Occupational Performance Measure (COPM)
6	ACS-AUS[9]	Stroke Impact Scale (SIS)
7	A-PACS[23]	Vineland Adaptive Behavior Scale (VABS)
8	ITACS[10]	Pediatric Evaluation of Disability Inventory-Computer Adaptive Test (PEDI-CAT) in the mobility domain and domain of daily activities
9	ACS-3[24]	Original ACS with domains of IADL, low-demand leisure activities, high-demand leisure activities, and social activities

Note: PACS : Pre-school Activity Card Sort, ITACS : Infant Toddler Activity Card Sort, ACS 3 Electronic Version : Activity Card Sort Electronic Version, ACS-Aus : Australian Activity Card Sort, PR-ACS : Activity Card Sort Peurto-Rican Spanish Version, ACS-NL : Dutch Activity Card Sort Institutional Version, Arab-PACS : Arabic Pre-school Activity Card Sort, A-ACS : Arab Heritage Activity Card Sort.

Discriminative validity

The most substantial evidence for the validity of the ACS-Aus was demonstrated through discriminative construct validity (p=0.000), as determined by an independent T-test analysis compared to existing measures of activity participation and quality of life.[19] The A-ACS could discriminate between patients and healthy participants based on current and retained levels of participation (F=5.09, p<0.0; F=6.01, p<0.02, respectively).[21] ACS-NL exhibited good discriminative validity.[22]

Discussion

In this scoping review, the psychometric measures of the ACS tool were critically reviewed and evaluated. The tool has been utilized across various populations and in different languages; the review aimed to explore the availability of a language-specific ACS. In the process, some key characteristics of existing ACS tools were summarized, including language, location of use, and the nature of the population studied. The review also attempted to summarize the instruments' internal consistency, reliability, and validity.

According to the review findings, English is the most common language version available. Other non-English language versions used included Arabic, Dutch, and Israeli. Most studies have been contributed by the USA and Australia, followed by Jordan, Puerto Rico, Spain, and the Netherlands. The study's key findings indicated that, in most cases, attempts were made to use the local language version of the tool, with a few exceptions. For instance, in one study by Stoffel *et al.* although the study was conducted in the USA, the authors used the Spanish version of the tool because the participants were Spanish-speaking.[20] Only in one study by Lyons *et al.* was the English language version used on a Lebanese population.[25] This indicates a strong inclination among scientists to prefer the local language version of ACS over the generic English version. Observing the instrument's internal consistency (the degree to which a test measures a single construct) and test-retest reliability (the degree to which the tool yields the same result on repeated tests) have provided us with an objective basis for preferring the local language version of the ACS. If the reported reliability parameters are poor in language-discordant

studies compared to language-concordant studies, we may conclude that language concordance increases the scientific quality of ACS. However, the study by Lyons *et al*. reported high internal consistency (α=0.86 to 0.96).[25] Since there is only one study on the discordance between the instrument's language and the native language, no meaningful conclusions can be drawn.

Three studies have used the Delphi method to report on content validation, the degree to which a test is model-based, and the involvement of experts in test design.[12,14,16] Studies have shown good to moderate concurrent validity, which is the extent to which the test measures a theoretical construct, with other instruments such as the Vineland Adaptive Behavior Scale (VABS),[23] ITACS with the Pediatric Evaluation of Disability Inventory-Computer Adaptive Test (PEDI-CAT),[10] and ACS-Aus with the Adelaide Activity Profile (AAP).[19] A few studies have also focused on how socioeconomic factors and cultural context affect the content validity of ACS leading to the deletion of some activities in the P-ACS study.[14,15] In this study discussed how activities varied according to the Spanish culture population compared to English-speaking people, based on differences in contexts and environments. Also, socioeconomic factors were clearly examined since they can create bias, leading to the elimination of some activities.[14] In another study, the A-ACS selected 19 activities specific to their cultures and socioeconomic status to determine the content validity of ACS. Some culturally irrelevant activities, such as gambling and betting, were removed from the A-ACS, and some activities in the leisure domains of A-ACS were modified. A few other ACS, such as ACS-HK and ACS-UK were also developed based on their respective cultures and languages.[2,11]

The scoping review also highlighted the versatility of the ACS tool for diverse population groups. The age range of population studies included preschool children, adolescents, community-dwelling adults, older adults, and the elderly without any specific health condition. The utility of the ACS instrument in special population groups, such as the homeless population and rehabilitation inpatients, highlighted the broader utility of ACS. The ACS instrument was primarily used for the disease conditions were chronic and degenerative conditions affecting the elderly and older adults. Stroke was the only acute condition with prolonged disability in which ACS was used. Another critical group study was caregivers of various conditions, such as those caring for pre-schoolers' and children aged 0-3 years.

Strengths and limitations

This study represents the first attempt to summarize the critical dimensions of all the available versions of the ACS tool, highlighting the gaps and setting an agenda for future research. The study's primary limitation was excluding non-English-language versions of the literature. As a result, a few other language versions of the tools may have been missed.

Recommendations

Given the potential for poor internal consistency and reliability, applying an English or non-native language version of the ACS could be better. Therefore, there is a need to develop and implement a local language version of the tool, and the different cultural contexts also impact the use of ACS in other cultures. Since we could not find any versions of the tool for the Tamil Nadu population in our comprehensive literature review, developing an ACS for this population is crucial. Additionally, it is essential to consider the composition of the target population and attempt to develop disease- or population-specific versions of the ACS.

Conclusion

Most of the studies indicated that the ACS had good psychometric properties. It was found that using ACS with different groups of people depends on their culture, and different versions of ACS were made for different medical conditions. Based on this identified gap, there is a need to conduct a study on the Indian population with specific population conditions.

Conflict of Interest

No conflict of interest to declare.

Acknowledgements

We acknowledge the technical support in data entry, analysis, and manuscript editing by Evidencian Research Associates.

References

[1] Bernardo LD, Pontes TB, Souza KID, Ferreira RG, Deodoro TMS, Almeida PHTQD. Activity Card Sort e o repertório ocupacional de idosos: uma revisão integrativa da literatura. Cad Bras Ter Ocupacional. 2021; 29: e2130. doi: 10.1177/07334648211015458.

[2] Laver-Fawcett A, Mallinson S. Development of the Activity Card Sort-United Kingdom Version (ACS-UK). OTJR Occup Particip Health. 2013; 33(3): 134-45. doi: 10.3928/15394492-20130614-02

[3] Sachs D, Josman N. The Activity Card Sort: A factor analysis. OTJR Occup Particip Health. 2003; 23(4): 165-74. doi:10.1177/153944920302300404

[4] Neri AL, Vieira LAM. Envolvimento social e suporte social percebido na velhice. Rev Bras Geriatr E Gerontol. 2013; 16(3): 419-32. doi.org/10.1590/S1809-98232013000300002

[5] Tamil Nadu. In: Wikipedia [Internet]. 2023 [cited 2023 Aug 10]. Available from: https://en.wikipedia.org/w/index.php?title=Tamil_Nadu&oldid=1167832165#cite_ref-FOOTNOTECensus_of_Tamil_Nadu2001_94-0

[6] Tricco AC, Lillie E, Zarin W, O'Brien KK, Colquhoun H, Levac D, *et al*. PRISMA Extension for scoping reviews (PRISMA-ScR): Checklist and explanation. Ann Intern Med. 2018; 169(7): 467-73. doi: 10.7326/M18-0850

[7] Katz N, Karpin H, Lak A, Furman T, Hartman-Maeir A. Participation in occupational performance: Reliability and validity of the Activity Card Sort. OTJR Occup Part

Health. 2003;23(1):10-7. doi.org/10.1177/1539449 2030230010

[8] Orellano EM, Ito M, Dorne R, Irizarry D, Dávila R. Occupational participation of older adults: Reliability and validity of the Activity Card Sort-Puerto Rican Version. OTJR Occup Part Health. 2012; 32(1): 266-72. doi.org/10.3928/15394492-20110708-01

[9] Tse T, Carey LM. The Activity Card Sort-Australia: Validation and reliability in an Australian stroke cohort. Cerebrovasc Dis. 2016; 42: 112. doi: 10.1177/ 1539449216681277

[10] Hoyt CR, Chuck AC, Varughese TE, Fisher LC, Manis HE, KE O, *et al*. Psychometric properties of the Infant Toddler Activity Card Sort. OTJR Occup Particip Health. 2021; 41(4): 259-67. doi.org/10.1177/15394 492211012657

[11] Chan VWK, Chung JCC, Packer TL. Validity and reliability of the Activity Card Sort-Hong Kong Version. OTJR Occup Part Health. 2006; 26(4): 152-8. doi: 10.5014/ajot.2010.09033

[12] Berg C, McCollum M, Cho E, Jason D. Development of the Adolescent and Young Adult Activity Card Sort. OTJR Occup Particip Health. 2015; 35(4):221-31. doi: 10.5014/ajot.2010.09033

[13] McCollum M, LaVesser P, Berg C. Participation in daily activities of young adults with high functioning autism spectrum disorder. J Autism Dev Disord. 2016; 46(3): 987-97. doi: 10.1007/s10803-015-2642-z

[14] Berg C, LaVesser P. The Preschool Activity Card Sort. OTJR Occup Part Health. 2006; 26(4): 143-51. doi.org/ 10.1037/t56111-000

[15] Hamed R, Alheresh R, Dahab SA, Collins B, Fryer J, Holm MB. Development of the Arab Heritage Activity Card Sort. Int J Rehabil Res Int Z Rehabil Rev Int Rech Readaptation. 2011; 34(4): 299-306. doi: 10.1097/ MRR.0b013e32834afc58

[16] Malkawi SH, Hamed RT, Abu-Dahab SM, AlHeresh RA, Holm MB. Development of the Arabic Version of the Preschool Activity Card Sort (A-PACS). Child Care Health Dev. 2015; 41(4): 559-68. doi: 10.1111/ cch.12209

[17] Hoyt CR, Fernandez JD, Varughese TE, Grandgeorge E, Manis HE, O'Connor KE, *et al*. The Infant Toddler Activity Card Sort: A caregiver report measure of children's occupational engagement in family activities and routines. OTJR Occup Particip Health. 2020; 40(1): 36-41. doi.org/10.1177/1539449219852030

[18] Tyminski QP, Drummond RR, Heisey CF, Evans SK, Hendrix A, Jaegers LA, *et al*. Initial development of the Activity Card Sort-advancing inclusive participation from a homeless population perspective. Occup Ther Int. 2020; 2020: 9083082. doi: 10.1155/ 2020/9083082

[19] Doney RM, Packer TL. Measuring changes in activity participation of older Australians: Validation of the Activity Card Sort-Australia. Australas J Ageing. 2008; 27(1): 33-7. doi: 10.1111/j.1741-6612.2007.00265.x

[20] Stoffel A, Berg C. Spanish translation and validation of the Preschool Activity Card Sort. Phys Occup Ther Pediatr. 2008; 28(2): 171-89. doi: 10.1080/0194263 0802031859

[21] Hamed R, Holm MB. Psychometric properties of the Arab Heritage Activity Card Sort. Occup Ther Int. 2013; 20(1): 23-34. doi: 10.1002/oti.1335

[22] Poerbodipoero SJ, Sturkenboom IH, van Hartingsveldt MJ, Nijhuis-van der Sanden MW, Graff MJ. The construct validity of the Dutch Version of the Activity Card Sort. Disabil Rehabil. 2016; 38(19): 1943-51. doi: 10.3109/09638288.2015.1107779

[23] Malkawi SH, Abu-Dahab SMN, Amro AF, Almasri NA. The psychometric properties of the Arabic Preschool Activity Card Sort. Occup Ther Int. 2017; 2017: 5180382. doi: 10.1155/2017/5180382

[24] Boone AE, Wolf TJ, Baum CM. Development and initial testing of the Electronic Activity Card Sort (ACS3) among community-dwelling adults. Am J Occup Ther Off Publ Am Occup Ther Assoc [Internet]. 2022 May;76(3). Available from: https://pubmed.ncbi.nlm.nih.gov/35671503/ doi: 10.5014/ajot.2022.047522

[25] Lyons KD, Li Z, Tosteson TD, Meehan K, Ahles TA. Consistency and construct validity of the Activity Card Sort (modified) in measuring activity resumption after stem cell transplantation. Am J Occup Ther Off Publ Am Occup Ther Assoc. 2010; 64(4): 562-9. doi: 10.5014/ajot.2010.09033

[26] Jong AM, van Nes FA, Lindeboom R. The Dutch Activity Card Sort institutional version was reproducible, but biased against women. Disabil Rehabil. 2012; 34(18): 1550-5. doi: 10.3109/09638288.2011.647232

[27] Gronski MP, Niemann A, Berg C. Participation patterns of urban preschoolers attending head start. OTJR Occup Part Health. 2013; 33(2): 68-75. doi.org/ 10.3928/15394492-20121026-01

[28] Laver-Fawcett A, Brain L, Brodie C, Cardy L, Manaton L. The face validity and clinical utility of the Activity Card Sort-United Kingdom (ACS-UK). Br J Occup Ther. 2016; 79(8): 492-504. doi.org/10.1177/0308022616 629167

[29] Gustafsson L, Hung IHM, Liddle J. Test-retest reliability and internal consistency of the Activity Card Sort-Australia (18-64). OTJR Occup Part Health. 2017; 37(1): 50-6. doi: 10.1177/1539449216681277

[30] Gustafsson L, Martin A, Buijsman L, Poerbodipoero S, Liddle J, Ireland D. Parallel-forms reliability and clinical utility of an application version of the Activity Card Sort Australia (18-64). Am J Occup Ther Off Publ Am Occup Ther Assoc. 2018; 72(6): 7206205070 p1-8. doi: 10.5014/ajot.2018.028688

[31] Leenders JMP, Geurts ACH, Steultjens EMJ, Packer TL, Cup EHC. Test-retest reliability of three life balance measures in people with neuromuscular disease: the Activity Card Sort-NL, the activity calculator, and the occupational balance questionnaire. Disabil Rehabil. 2023; 1-7. doi: 10.1080/09638288.2023.2213482

Journal of Associated Medical Sciences 2024; 57(2): 31-40

JAMS
Journal of Associated Medical Sciences

Scopus Indexed & Thai-Journal Citation Index Centre (TCI)

Journal of Associated Medical Sciences

Journal homepage: https://www.tci-thaijo.org/index.php/bulletinAMS/index

Speech services by speech volunteers for children with cleft lip and palate in professional lacking area: Pilot study

Benjamas Prathanee[1] Ampika Rattanapitak[2] Tanyaratch Sampanthawong[3] Kalyanee Makarabhirom[4*]

[1]Department of Otorhinolaryngology, Faculty of Medicine, Khon Kaen University, Khon Kaen Province, Thailand.
[2]Eastern Languages Department, Faculty of Humanities, Chiang Mai University, Chiang Mai Province, Thailand.
[3]Northern Women's Development Foundation, YMCA, Chiang Rai Building, Chiang Rai Province, Thailand.
[4]Department of Communication Sciences and Disorders, Faculty of Medicine, Ramathibodi Hospital, Mahidol University, Bangkok, Thailand.

ARTICLE INFO

Article history:
Received 27 August 2023
Accepted as revised 2 February 2024
Available online 7 February 2024

Keywords:
Articulation disorder, cleft palate, speech therapy, volunteer

ABSTRACT

Background: Cleft lip and cleft palate are the most common birth defects. Children with cleft lip with or without cleft palate (CP±L) face a vary of challenges, depending on the type and severity of the cleft including speech difficulty, dental problems, feeding difficulty, ear infections and hearing loss. Articulation error is the most common residual defect in children with cleft palate with or without cleft lip.

Objective: To compare the numbers of pre- and post- articulation errors after using the Model of Speech Therapy by Volunteers (STV) for children with CP±L**.**

Materials and methods: 9 children, aged range 6; 4-14; 2 years old, were included in this study and completely participated in the study. Pre- and post-articulation tests by Myanmar Articulation, Resonation, Nasal Emission and Nasal Turbulence Test were assessed at Mahamuni Monastery, and Thiriyadana Guha Pone Htoon Shan Monastery, Tachileik, Myanmar. STV is composed of a 3-day speech camp (1st month), 3 times 1-day site visits for complicated cases (2nd, 6th, and 10th months) and 3 times of 1-day follow-up speech camps (4th, 8th, and 12th months), Phonological approaches, traditional strategies, and specific techniques for speech correction in children with CP±L were taught to speech volunteers (SVs) and caregivers. Homework was assigned to SVs and caregivers. SVs provided a session of 45-minute speech correction every week. Caregivers practiced 5 sessions of 30 minutes in speech exercises /weeks at home.

Results: STV revealed significant reductions in the numbers of articulation errors including articulation screening test [median difference: MD=6 (95% confident interval: CI=5.2-9.2)]**,** and Myanmar articulation standard test at both word and sentence levels; [MD=8 (95% CI=6.5-10.8) and MD=5 (95% CI=4.2-8.3), respectively].

Conclusion: STV significantly decreased a number of articulation errors in children with CP±L of Myanmar, a professional lacking area, and could be applied in any area that has a similar situation. The result was a primary study, the further research should enroll more participants for generalization.

Introduction

Primary repair was conducted within the first 6 months of life in children with cleft palate with or without cleft lip (CP±L).[1] Most children with CP±L generally performed cheiloplasty or lip repair at 3 months old and palatoplasty at 1 year.[2] For children with CP±L in lower-income and lower-middle-income countries (LMIC), palatoplasty is often performed around the age of 1 year.[3] Primary surgery was conducted within the first 6 months of life in Myanmar.[1]

∗ **Corresponding contributor.**
Author's Address: *Department of Communication Sciences and Disorders, Faculty of Medicine, Ramathibodi Hospital, Mahidol University, Bangkok, Thailand.*
E-mail address: kalyanee.mak@cmu.ac.th
doi: 10.12982/JAMS.2024.024
E-ISSN: 2539-6056

For Myanmar, prevalence of CP±L was found to be 1-1.3/1,000 live births.[4] The residual abnormalities after repair or after primary palatoplasty were commonly articulation disorders (71.2-88.6%), hypernasality (43.3-69 %) especially from velopharyngeal insufficiency (VPI), voice disorders (19.1), and delayed speech and language development (16.3%).[5-8] Compensatory articulation disorders (CAD)(Abnormal articulation placement due to abnormal structure) are very common and require prolonged periods of speech intervention in children with CP±L.[6,7,9,10]

Normal speech is the goal for treatment in children with non-syndromic CP±L. The limited access to intervention and guidance for parents on comprehensive care in speech intervention is a major challenge in developing countries.[11,12] particularly in LMIC. Different models and strategies were implemented to solve the lack of speech services, for example: speech summer camp, phonologic-based intervention and articulatory or phonetic-based intervention, and naturalistic intervention in Mexico[11,14,15] and paraprofessional training in Lao People's Democratic Republic *(*LPDR*).*[16] as well as training for speech assistants, community-based speech model and speech camps in Thailand.[17-21]

In Myanmar, surgical treatment and speech therapy services are limited. Similar to LPDR, speech services are in a shortage or none because of a lack of speech and language pathologists (SLPs). There was only SLP who worked in private hospitals and no speech service was available in general hospitals. The purpose of this paper was to investigate the effectiveness of Speech Therapy by Volunteers (STV) for Children with CP±L to reduce the numbers of articulation errors.

Materials and methods

Design**:** A prospective one-group pre-post study

Setting**:** Mahamuni Monastery, and Thiriyadana Guha Pone Htoon Shan Monastery, Tachileik, Myanmar.

Participants

Inclusion criteria: children with CP±L, who had already lip and palate repair, aged ranged 4-15 years old, lived in Eastern Shan State, Myanmar.

Exclusion criteria: children with CP±L who had any condition as follows: 1) no articulation errors based on pre-articulation tests; 2) syndromic CP±L; 3) hearing loss problems (>40 dB both ears); 4) learning disorders; 5) other cognitive disorders or global delayed development.

There were 12 children with CP±L. Two of them were excluded because of no articulation defects after pre-assessment. 10 children with CP±L, ages ranged 6 years 4 months-14 years 2 months old, were enrolled in this study. They understood Burmese which the official language is used in school. None of them had received previous speech therapy. A boy (C07) withdrew from the study because he moved to continue his education in another city at the 2nd follow-up speech camp. 9 children along with their caregivers were enrolled in the complete study.

Seven speech volunteers (SVs), who had Burmese literacy and were non-paraprofessionals (a company employee, 5 teachers, and a 4th-year university student, who worked in a community nearby children's home) and they were speech assistants. SVs committed to join the project. Each SV was assigned to practice 1-2 children based on geographics.

Five research assistants (RAs) who fluently spoke and wrote both Thai and Burmese were interpreters.

Procedures

Study design

This study was a prospective one-group pre-post study, the design outline was shown in Figure 1.

Assessment:

The study included 2 tests that cover speech characteristics of cleft types (characterized by hypernasality and compensatory articulations) based on universal reporting systems[22-24] as follows:

1. Myanmar Articulation Screening Test with pictures: composed of 4 connected sentences that cover all sounds in Burmese and focus articulation on connected contexts,
2. Myanmar Articulation, Resonation, Nasal Emission, and Nasal Turbulence Standard Test with pictures

Tests included all the Burmese phonetic sounds composed of 32 initial consonants and 7 basic vowels 3 tones. Each test is composed of 2 versions:

a) Myanmar version with pictures for testing. This version was Burmese language so that SVs, Ras, and caregivers could understand the meaning.
b) Myanmar-Thai version with pictures (composed of both Myanmar and Thai reading pronunciation, as well as translation of the meaning to Thai) for Thai speech and language pathologists (TSLPs) to understand the meaning and identify articulation errors.

Tests gave information on parameters of articulation, resonance, voice, understandability, acceptability, nasal emission and turbulence, and facial grimace.

1. Myanmar Articulation Exercises included 2 versions composed of 2 versions: 3.1) Myanmar Version 3.2) Myanmar-Thai version.[25]
2. Daily home record for speech correction. This was recorded by SVs and caregivers to monitor speech correction.[26]
3. Language tests: The Burmese Early Language Screening Test (adapted and translated from Thai Early Language Milestones)[27] and Utah test[28] for language screening.

Examination, pre- and post-perceptual assessments were performed as follows:

- Speech and language pathologist (SLP) performed an oral examination for detection of the anatomical defects.
- A short conversation between the child and SLP was carried on to elicit understandability and acceptability of speech.

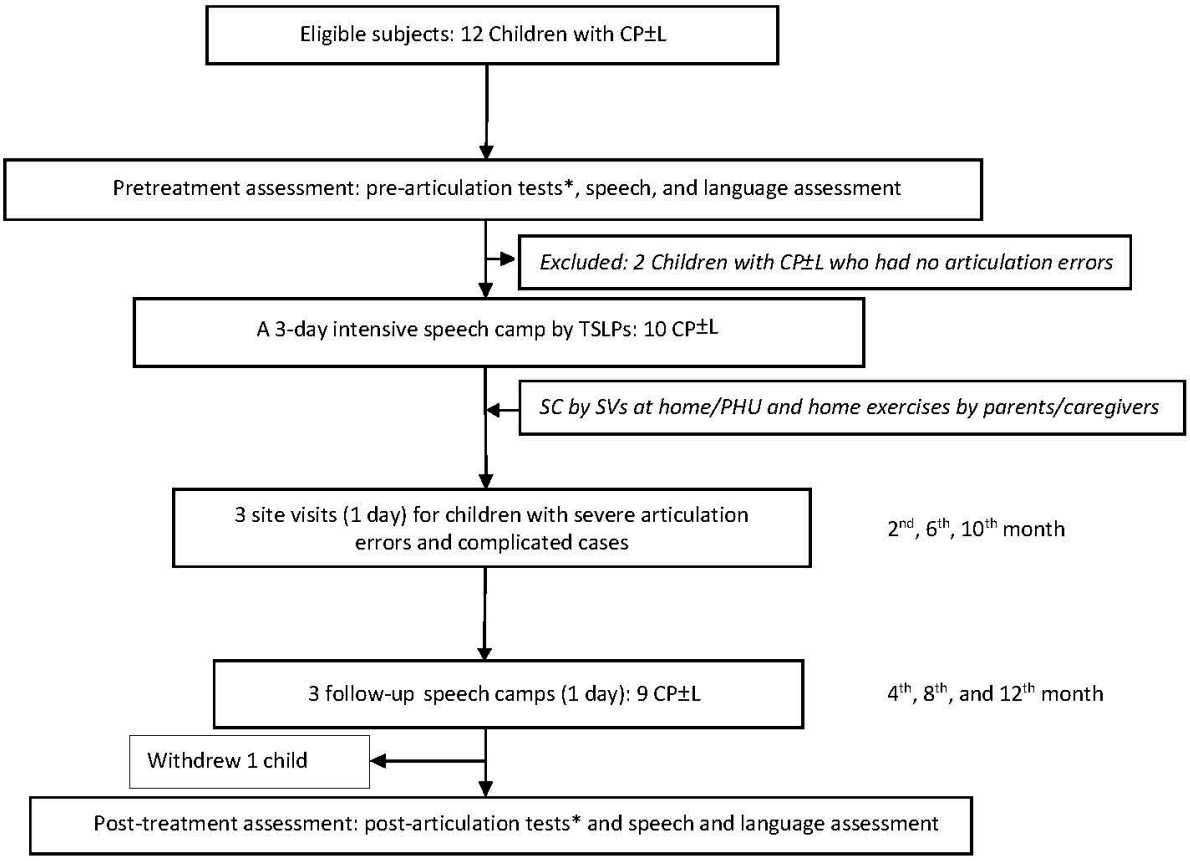

Figure 1. *Design outline. 1: Myanmar Articulation Screening Test, 2: Myanmar Articulation, Resonation, Nasal Emission and Nasal Turbulence Test, CP±L: Cleft palate with or without cleft lip, TSLPs: Thai speech and language pathologists; PHU: Primary Health Care Unit, SVs: Speech volunteers, SC: Speech correction by speech volunteers.*

- Pre- and post-articulation tests with perceptual assessment using 1) the Myanmar Articulation Screening test which is composed of 4 connected speech and 2) Myanmar Universal Parameters of Speech Outcomes for People with Cleft Palate that were used for articulation assessment.[29] Outcomes were summarized by consensus among investigators and teams. Speech characteristics were assessed as articulation, resonance, nasal emission or turbulence, voice, speech understandability, and acceptability.
- Speech and language screening test by UTAH test of language development.[28] This test is a language screening evaluation that composed of both expressive and receptive languages based on children's age. A child who passes every item of the UTAH test was interpreted that his/her language skill was normal. If a child cannot pass any item, language skill is interpreted as delayed.

Outcomes were summarized by consensus among investigators and teams including: 1) 2 TSLPs who had >30 years' experience in investigation; 2) a Thai-Burmese linguistic, 3) a Burmese research assistant who had a literacy of both Burmese and Thai and graduated with bachelor's degree in Thai program from Mae Fah Luang University, Chiang Rai Province.

Speech therapy: the process of STV was summarized in Table 1.

Table 1. Timeline of speech therapy.

Time	Name	Duration	Activities	Note
1st month	An intensive speech camp	3 days	Day 1: introduction to speech camp, workshop of basic knowledge about Myanmar phonetics and an exercise manual for SVs and caregivers Day 2: Oral examination and assessments Day 3: 6 sessions of 45-minute of speech therapy	Each child was provided 6 sessions of 45-minute speech therapies per day.
2th, 6th, 10th months	Three site visits of speech therapy	1 day	A session of 60 minutes of speech therapy via teaching on services was provided by TSLPs with RAs for 5 children with CP±L (No. C01, C02, C03, C04, C06), who had severe articulation errors with/without complicated cases	- Severe articulation errors: ≥ 5 articulation errors - Complicated cases: less cooperation of home exercise practices, needed special help for training, a teenager with a shyness
4th, 8th, 12th months	Three follow-up speech camps	1 day	Six sessions of 45-minute speech therapy	Each child was provided 6 sessions of 45-minute speech therapies per day.

Training speech correction for SVs:

Criteria for recruited speech volunteers: People or non-paraprofessionals who have literate Burmese and lived or worked in a community or area near children with CP±L's home. They needed commitment to do the project for 1 year. Research assistants directly contacted speech volunteers or communicated via health care providers.

TSLPs taught and demonstrated speech correction of each articulation error for individuals with CP±L via demonstration, teaching on service, and training for being speech volunteers in every speech therapy session. Then, speech volunteers displayed speech correction. TSLPs gave comments and suggestions. TSLPs did a demonstration of teaching on service again until speech volunteers understood and did correct speech correction. In case of speech volunteers or caregivers could not speak or understand research assistant explained it in Burmese language. Speech volunteers had to fill in daily home records every time that they did speech correction. In case of SVs had any problems with speech correction or training, they can contact TSLPs by phone at any time.

Encouragement and commitment were provided for speech correction (SC) at children's homes or schools or primary health care units (PHC) near their home (a session of 45 minutes /week) to SVs and homework practice (5 sessions of 30 minutes/week) to caregivers. The project gave compensation for traveling SVs' expenses. Children's daily home records of speech corrections by speech volunteers and homework exercises by caregivers were tallied by RAs and selected SVs who gave the most consistent speech correction to be the best speech volunteers and the best caregivers. The winner got an award on the closing day of the project. The project provided souvenirs for every SV.

Phonological approach, traditional strategy, and specific technique for remedy cleft type characteristics (e.g., glottal substitution, nasal for oral sounds, pharyngeal fricative for oral fricatives, etc.) in speech correction were demonstrated by TSLPs via interpreters based on teaching on services (demonstration, practicing, supervision, monitoring, and checking) during 3 days of a speech camp until they could do independently.

If there was any phonological pattern, a phonological approach would be applied for speech therapy. Traditional strategy was a secondary step, then specific techniques were used if the traditional strategy was not effective. After that SVs were assigned to do speech correction in individual sound errors for 1-2 children and continually did speech correction for their children once a week for 1 year depending on geographic matching and administrative convenience. These exercises were done within the target context of the Myanmar Articulation Exercise.

Statistical Analysis

Assessment scales of speech characteristics including articulation, resonance (hypernasality, hyponasality, nasal emission, and nasal turbulence), voice, understandability, acceptability, and facial grimace were evaluated based on criteria of universal parameters for reporting speech outcomes in individuals with cleft palate.[23,24]

The main outcomes of this study were the number of pre- and post-articulation errors. Wilcoxon Signed-Rank Test was used to demonstrate the effectiveness of STV for children with CP±L by comparing the numbers of pre- and post-articulation errors in children with CP±L.

Results

Nine students with CP±L, aged range 6 years 4 months-14 years 2 months old (mean = 7.67 years; median = 8 years 3 months), were recruited to the project. No children had received previous speech therapy. Characteristics of children with CP±L were displayed in Table 2. Participants used 4 native languages or mother tongue languages (Lahu, Shan, Mandarin, Burmese),

understood Burmese (the formal language or language in the school), and received the language screening test. The average session that SVs did in the project was 1.1-2.7 sessions/week depending on the available time that they had. Speech characteristics by Myanmar Articulation, Resonation, Nasal Emission, and Nasal Turbulence Standard Test for People with Cleft Palate were shown in Table 3.

Table 2. Children with CP±L's general characteristics.

No.	Gender	Age Year; Month	Language	Diagnosis	Distance to reach child's home[$] (km)	Number of sessions of SCs[&]
C01	Male	11; 3	Shan	Bilat. CLP	2	2
C02	Male	7; 6	Shan	CP	10	2
C03	Female	14; 2	Lahu	CP	25	2.1
C04	Female	7; 1	Burmese	Lt. CLP	0	2.7
C05	Male	6; 9	Lahu	Rt. CLP	10	2.7
C06	Male	11; 6	Shan	Bilat. CLP	5	1.7
C08	Male	8; 3	Mandarin	Rt. CLP	5	1.9
C09	Female	6; 4	Burmese	Lt. CLP	5	1.1
C10	Female	10; 5	Burmese	Rt. CLP	8	1.7

Note: Bilat. CLP: Bilateral cleft lip and palate, CP: Cleft palate, Rt. CLP: Right cleft lip and palate, Lt. CLP: Left cleft lip and palate, [$]: Distance from speech volunteer' s home to child's home (kilometers), [&]: Average number of sessions of speech correction by speech volunteers per week.

Table 3. Speech characteristics by perceptual assessment in children with CP±L.

No.	Hypernasality				Audible nasal air emission /nasal turbulence				Voice**		Understandability*		Acceptability**		Facial grimace	
	Pre	Post	Pre	Post	Pre	Post	Pre	Post	Pre	Post	Pre	Post	Pre	Post	Pre	Post
C01	1	1	1	1	1	1	1	1	1	0	0	0	1	0	0	0
C02	2	2	2	2	1	3	1	3	1	0	1	0	2	0	0	1
C03	2	1	2	1	1	1	1	1	1	1	0	0	1	0	0	0
C04	3	3	3	3	2	2	3	2	3	0	2	0	3	0	0	2
C05	1	1	1	1	1	1	1	1	1	0	0	0	1	0	N/A	0
C06	1	1	1	1	1	1	1	1	N/A	0	N/A	0	N/A	0	N/A	0
C08	1	1	1	1	1	1	1	1	1	0	0	0	1	0	2	0
C09	1	2	1	2	2	1	2	2	2	0	0	0	2	0	1	0
C10	1	2	1	2	1	1	1	1	1	0	0	0	1	0	0	2

*Note: *assessment from conversational speech,** assessment from whole speech sample, N/A: not available, Hypernasality: 1=normal, 2=mild, 3=moderate, 4=severe, Audible nasal air emission/nasal: 1=within normal limits/None, 2=intermittent or variable, 3=frequent or pervasive, Voice: 0=normal, 1=abnormal, Understandability: 0=speech is always easy to understand, 1=speech is occasionally hard to understand, 2=speech is often hard to understand, 3=speech is hard to understand most or all of the time, Acceptability: 0=within normal limits: Speech is normal; 1=speech deviates from normal to a mild degree, 2=speech deviates from normal to a moderate degree, 3=speech deviates from normal to a severe, Facial Grimace: 0=none, 1=Ala, 2=nasal bridge, 3=forehead.*

Individual pre- and post-articulation patterns were quantified and presented in Table 4. Table 5 displayed the overall percentage of pre- and post-articulation patterns. Pre- and post-articulation numbers of all children with CP±L were shown in Table 6.

Table 4. Individual pre- and post- articulation pattern.

No.	Words		Sentences		Screening	
	Pre-	Post-	Pre-	Post-	Pre-	Post-
C01	/p/ for /b/, /s/ for /z/, /m/ for /hm/, n/ for /hn/, /ŋ/ for /hŋ/, /w/ for /hw/, /l/ for /hl/, /j/ for /hj/	-	/p/ for /b/, /s/ for /z/, /m/ for /hm/, /n/ for /hn/, /ŋ/ for /hŋ/, /w/ for /hw/, /l/ for /hl/, /j/ for /hj/	-	/s/ for /z/	-
C02	/p/ for /b/, /t/ for /θ/, /t/ for /d/, /c/ for /j/, /k/ for /g/, /s/ for /sh/, /s/ for /z/, /m/ for /hm/, /n/ for /hn/, /ŋ/ for /hŋ/, /ŋ/ for /hj/, /w/ for /hw/, /l/ for /hl/,	NAE(z)	/p/ for /b/, /t/ for /d/, /c/ for /j/, /k/ for /g/, /s/ for /ch/, /s/ for /sh/, /s/ for /z/, /m/ for /hm/, /n/ for /hn/, /ŋ/ for /hŋ/, /l/ for /hl/, /j/ for /hj/, /-yo/ for /ɛ/,	NAE(z,s,hs	/k/ for /g/, /c/ for /j/, /s/ for /ch/, /s/ for /sh/, /s/ for /z/, /m/ for /hm/, /n/ for /hn/, /ŋ/ for /hŋ/, /l/ for /hl/,	/s/ for /sh/, /s/ for /ch/, NAE(z)(2)
C03	/m/ for /hm/, /n/ for /hn/, /ŋ/ for /hŋ/, /w/ for /hw/, /l/ for /hl/,	-	/m/ for /hm/, /n/ for /hn/, /ŋ/ for /hŋ/, /w/ for /hw/, /l/ for /hl/,	-	/n/ for /hn/, /ŋ/ for /hŋ/, /ɲ/ for /hɲ/, /l/ for /hl/	-
C04	/p/ for /b/, /t/ for /s/, /ʔ/ for /th/, /ʔd/ for /d/, /ʔNE/ for /kh/, /ʔ/ for /hs/, /n/ for /hl/, /n/ for /l/, /ŋ/ for /k/, /ŋ/ for /g/, /j/ for /c/, /j/ for /ch/, /j/ for /sh/, /jNE/ for /j/, /jNE/ for /z/, NE for /ph/	/c/ for /j/, /kʔ/ for /g/	/t, /ʔc/ for /s/, /t/, /ʔNE/ for /th/, /c/, /ʔ/ for /ch/, /ʔ/ for /hs/, /ʔt/ for /θ/, /ʔd/ for /d/, /ʔc, /j/ for /sh/, /ʔw/ for /hw/, /n/ for /hl/, /n/ for /l/, /ŋ/ for /k/, /ŋ/ for /kh/, /ŋ/ for /g/, /j/ for /c/, /j/ for /z/, NE for /ph/	/c/ for /j/, Dental lisping, N(h), /kʔ/ for /g/	dental lisplisping, /t/ for /sh/, /ʔ/ for /t/, /ʔ/ for /d/, /ʔ/ for /n/, /ʔt/ for /s/, /h/ for /th/, /m/ for /hm/, /n/for /d/, /n/ for /hl/, /ŋ/ for /d/, /ŋ/ for /k/, /ɲ/ for /z/, /ɲ/ for /sh/, /ɲ/ for /c/, /ɲ/ for /ch/, /y/ for /d/, /y/ for /ch/,	WPC(c,th), N(c), /s/ for /z/, (1)
C05	/ʔg/ for /g/, /l/ for /hl/	-	/ʔg/ for /g/, /ch/ for /hs/, /s/ for /sh/, /m/ for /hm/, /ŋ/ for /hŋ/, /l/ for /hl/	-	/t/ for /θ/, /chs/ for /s/, /s/ for /z/, /m/ for /hm/, /mɣ/ for /ɲ/, /n/ for /hn/, /ŋ/ for /hŋ/, /ɲ/ for /hɲ/, /l/ for /y/, /l/ for /hl/,	-

Table 4. Individual pre- and post- articulation pattern (continued).

No.	Words		Sentences		Screening	
	Pre-	Post-	Pre-	Post-	Pre-	Post-
C06	/t/ for /θ/, /t/ for /d/, /c/ for /j/, /ch/ for /sh/, /s/ for /hs/, /s/ for /z/, /m/ for /hm/, /n/ for /hn/, /ŋ/ for /hŋ/, /ŋ/ for /hj/, /w/ for /hw/, /l/ for /hl/	-	/th/ for /d/, /c/ for /j/, /ch/ for /sh/, /k/ for /g/, /s/ for /z/, /m/ for /hm/, /n/ for /hn/, /ŋ/ for /hŋ/, /ŋ/ for /hj/, /w/ for /hw/, /l/ for /hl/	/ch/ for /sh/	/k/ for /g/, /m/ for /hm/, /n/ for /hn/, /ŋ/ for /hŋ/, /ɲ/ for /hɲ/, /l/ for /hl/, /y/ for /ɲ/	-
C08	/p/ for /b/, /t/ for /d/, /t/ for /θ/, /n/ for /hn/, /w/ for /hw/, /l/ for /hl/	-	/p/ for /b/, /t/ for /d/, /t/ for /θ/, /s/ for /z/, /m/ for /hm/, /ŋ/ for /hŋ/, /w/ for /hw/,	-	/s/ for /z/, /n/ for /hn/	-
C09	/p/ for /b/, /t/ for /θ/, /t/ for /d/, /l/ for /hl/, NT for /hs/, NT for /z/	-	/p/ for /b/, /t/ for /θ/, /t/ for /d/, /ch/ for /sh/, /s/, NT for /z/, /n/ for /hn/, /ŋ/ for /hŋ/, /l/ for /hl/, NT for /s/, NT for /hs/	NAE(hs)	/s/ for /z/, /m/ for /hm/, /n/ for /hn/, /ŋ/ for /hŋ/, /l/ for /hl/,	NAE(z)
C10	/t/ for /θ/, /L/ for /ch/, /L/ for /hs/	-	/t/ for /θ/, L for /ch/, L for /hs/	N(c)	/sh/ for /ch/	-

Note: NAE: nasal air emission, N: nasalization, NT: nasal turbulence.

Table 5. Overall percentage of pre- and post-articulation patterns*

Pattern		Word level				Sentence level				Screening/connected speech			
		Pre		Post		Pre		Post		Pre		Post	
		No.	%	No.	%	No.	%	No.	%	No.	%	No.	%
Normal		-	-	8	88.9	-	-	**7**	**77.**8	-	-	**7**	**77.**8
Pharyngeal		1	2.1	-	-	-	-	-	-	-	-	-	-
Glottal		1	2.1	-	-	1	2.1	-	-	1	2.1	-	-
Mid-dorsum palatal		1	2.1	-	-	2	22.2	-	-	-	-	-	-
Nasalization		-	-	-	-	-		2	22.2	-	-	1	2.1
Nasal consonant for oral pressure consonant		1	2.1	-	-	1	2.1			-	-	1	2.1
Phonological error	V/VL	8	88.9	-	-	8	88.89			6	66.67	-	-
	VL/V	5	55.6			6	66.7			2	22.2	1	2.1
Functional/other oral misarticulation		8	88.9	1	2.1	9	100	1	2.1	4	44.4	2	22.2
Dental lisping		2	22.2	-	-	2	22.2	1	2.1	-	-	-	-
Coarticulation		2	22.2	1	2.1	2	22.2	1	2.1	2	22.2	-	-
Lateralization		1	2.1	-	-	1	2.1	-	-	-	-	-	-
Weak pressure consonant		-	-	-	-	-	-	-	-	-	-	1	2.1

*Note: V/VL: voice substitute voiceless, *: overall articulation pattern in all participants.*

Table 6. Number of pre- and post-articulation errors.

No.	Word		Sentence		Screening	
	Pre	Post	Pre	Post	Pre	Post
C01	8	0	8	0	1	0
C02	13	0	13	0	9	2
C03	5	0	5	0	4	0
C04	15	2	17	2	24	1
C05	2	0	6	0	10	0
C06	12	0	11	1	7	0
C08	6	0	7	0	2	0
C09	3	0	8	0	5	0
C10	3	0	3	0	1	0

** Number of articulation errors in each child*

In this study, common articulation substitution was voiceless substituted for voice such as /p/ for /b/, /t/ for /d/. C04, C02, and C6 had orderly the most severe articulation errors at the pre-articulation period.

Phonological errors and functional articulation errors were common the pattern in children with CP±L in this study at both pre-articulation and post-articulation tests.

C01, C03, C05, C08. C09 and C10 had normal articulation at all levels of tests (word, sentence, and screening or connected speech level) at the end of a project.

The medians of numbers of articulation errors between pre- and post-articulation tests were analyzed by the Wilcoxon signed-rank test. Results showed significant reductions in the number of articulation errors after running the model for 1 year (Table 7).

Table 7 Median difference of pre- and post-articulation disorders.

(N=9)	Median		Min, Max		Median difference	95% CI	*p* value
	Pre	Post	Pre	Post			
Screening/connected speech	6	0	1-24	0-2	6	5.2-9.2	<0.001
Word	8	0	2-15	0-2	8	6.4-10.8	<0.001
Sentence	5	0	3-17	0-2	5	4.2-8.3	<0.001

Note: 95% CI: 95 % Confident interval, # : comparison of the number pre- and post- articulation errors

Discussion

Rates of speech defects in Table 3 support the prevalence of speech disorders.[5-7, 9, 20] After 1 year of treatment, these speech characteristics had significant improvement (Table 3-6) except hypernasality and audible nasal emission because this project focused on speech correction for CAD.

The most error patterns of articulation were nasal voice substitution for voicelessness (e.g., /m/for /hm/, /n/ for /hn/, /ŋ/ for /hŋ/) and these were very common in Burmese articulation patterns because most sounds of Burmese are nasalized, and it wasn't a common cleft speech characteristic. Correct placement and articulation resulted in a reduction of nasal resonance in some children; this was a similar result to a previous study that provided 6 hours of individualized speech therapy in 3 or 4 days and resulted in progression of nasalance values and/or articulation.[30] Some children had more severe hypernasality (C09 and C10) after speech therapy while they had significant improvement in the number of articulation errors or some children had no residual articulation defects in all of the standard tests in word, sentence levels, and screening/ connected speech tests. Regarding more hypernasality, it is possible that speech therapy focuses on placement correction that changes the articulation valve and proportion of acoustic energy of the oral and nasal cavity such as when corrected /ʔ/ to /b/, placement changed from vocal cord to bilabial that makes high-pressure acoustic energy from vocal cord passed velopharyngeal valve to be a bilabial valve. It has more opportunity to leak into the nasal cavity resulting in more hypernasality.

Regarding articulation patterns, the summation of articulation patterns in each child and displayed as percentages. Articulation patterns presented that phonological errors were the most common patterns (Table 5). Similar to previous studies found that phonological error was one of the common patterns in children with CP±L[31] because they had delayed phonological development. On the other hand, the errors of retraction/backing of alveolar target consonants to a velar place of articulation occurred frequently, these were supported by previous studies.[5,20,32,33] Phonological and traditional approaches including placement and manner of articulation techniques might solve these errors in this study. After applying STV for children with CP±L, 77.78-88.88% had normal articulation patterns (Table 5). Only 1 or 2 children still had 1-2 error patterns in phonological errors and functional articulation disorders. Table 4 indicated that they had more severe articulation errors (C02, C04, C06) and might need a longer period of speech training. Patterns of articulation errors had improved. Pharyngeal (e.g., /h/ for /tʰ/; /h/ for /n/), glottal (e.g., /ʔ/ for /tʰ/; /ʔ/

for /n/), mid-dorsum palatal (e.g., /j/ for /c/ ;/j/ for /hŋ/) substitutions, nasalization, nasal consonant for oral reassure consonant (e.g., /ɲ/ for /c/; /ɲ/ for /sh,z/), and phonological errors were reduced. Most glottal and coarticulation with glottal substitution, (e.g., /ʔ/ for /tʰ/, /ʔd/ for /d/, /ʤ/ for /c/, /ʔt// for /θ/, /t,ʔ for /tʰ/), were corrected to be the right placement in oral sounds (e.g., /t/, /d/, /c/, /θ/) after 1-year of speech therapy. However, Table 3 presented that there was increasing of nasalization in sentence level from post-tests of standard and screening tests. This indicated that after correction placement, it might affect to manner of articulation from coarticulation of speech organs (combination of articulators below velopharyngeal valve and oral sounds) to be oral or correct sounds (e.g., correction of /ʔd/ to be /d/ and /ʔc/ to be /c/), it could be higher oral pressure and easier leak to nasal cavity to be nasalization. Because the sound pressure of placement below the velopharyngeal valve (/ʔ/) disappeared from the correction placement of /d/ and /c/. It made acoustic energy of /d/ and /c/ directly flow to the oral via the VP valve and leak from the nasal cavity to the oral cavity. Therefore, it was possible to have increasing of the more nasalization and hypernasality after therapy.

The number of articulation errors decreased in most of the speech characteristics (Table 3-6). Comparison of the numbers of pre-and post-articulation errors by the Wilcoxon Signed-Rank Test that presented medians of the post-articulation numbers significantly less than pre-articulation numbers (Table 7). Similar to previous models,[10,14,18,21,34,35] these findings supported that there were several models or methods of solving problems about limitations of SLPs and speech services.

STV is similar to the speech therapy model for patients with cleft palate in Lao People's Democratic Republic: lack of speech services but speech volunteers were not health care providers and performed speech correction at home or primary health care unit.[16] This STV presented that local non-healthcare providers or speech volunteers could facilitate speech correction under the monitoring of SLPs. In summary, STV presented the speech intervention via facilitation from speech volunteers and local non-government organization (NGO) networking and support as an effective way to improve speech defects in children with CP±L in Myanmar, a developing country lacking speech service.

Limitations of study

A limitation of the study was the small sample size. This study recruited all children with CP±L in Tachileik and the surrounding area who received lip and/or palate repair. The result was a primary study in which future research should enroll more participants for generalization.

Conclusion

The STV significantly decreased the number of articulation errors or CAD and improved other speech defects in Myanmar children with CP±L, who lack speech therapy service.

Conflict of interest

There are no potential conflicts of interest to declare.

Ethic approval

According to the Helsinki Declaration (HE601372), the Ethics Committee for Human Research, Khon Kaen University reviewed and approved (Oct 24, 2018) the protocols.

Acknowledgements

This study was supported funding from the cooperation of the Northern Women's Development Foundation and Transforming Faces (Contract signed between Transforming Faces and Northern Women's Development Foundation: Extension of Network for Comprehensive Cleft Care in Myanmar - Phase 1: 1st January 2018 - 31st December 2020). The authors thank the children with CP±L and their families for their cooperation and for providing valuable data and gave acknowledgement to Professor James A Will, for editing the manuscript via the publication clinic, KKU, Thailand.

References

[1] Uemura T, Preeyanont P, Udnoon S. Humanitarian cleft lip/palate surgeries in buddhist Thailand and neighboring countries. J Craniofac Surg. 2015; 26(4): 1112-5. doi: 10.1097/SCS.0000000000001620.

[2] Prado DZA, Ambrosio ECP, Jorge PK, Sforza C, De Menezes M, Soares S, *et al*. Evaluation of cheiloplasty and palatoplasty on palate surface area in children with oral clefts: longitudinal study. Br J Oral Maxillofac Surg. 2022; 60(4): 437-42. doi: 10.1016/j.bjoms.2021.07.011.

[3] Bluher AE, Cunningham TD, Reeves TD. Effect of cleft palate repair timing on inpatient complication Rate: Review of a national database. J Craniofac Surg. 2021; 32(2): 466-8. doi: 10.1097/SCS.0000000000007069.

[4] Thant YM, editor Title Mission in New Look New Life (The Sun Rise). 36th Myanmar Dental Conference: meeting the challenges to provide quality dental care; 2016 26-30 January; Yangon: University of Dental Medicine,.

[5] Prathanee B, Thanawirattananit P, Thanaviratananich S. Speech, language, voice, resonance and hearing disorders in patients with cleft lip and palate. J Med Assoc Thai. 2013; 96 Suppl 4:71-80.

[6] Albustanji YM, Albustanji MM, Hegazi MM, Amayreh MM. Prevalence and types of articulation errors in Saudi Arabic-speaking children with repaired cleft lip and palate. Int J Pediatr Otorhinolaryngol. 2014; 78(10): 1707-15. doi: 10.1016/j.ijporl.2014.07.025.

[7] Rezaei P, Poorjavad M, Abdali H. Speech outcomes after palatal closure in 3-7-year-old children. Braz J Otorhinolaryngol. 2022; 88(4): 594-601. doi: 10.1016/j.bjorl.2020.08.005.

[8] Balasubramaniyan S, Raghunathan V, Rajashekhar B, Sathiyasekaran BWC, Nagarajan R. Planning community-based intervention for speech for children with

cleft lip and palate from rural South India: A needs assessment. Indian J Plast Surg. 2017; 50(3): 295-301. doi: 10.4103/ijps.IJPS_174_17.

[9] Prandini EL, Pegoraro-Krook MI, Dutka Jde C, Marino VC. Occurrence of consonant production errors in liquid phonemes in children with operated cleft lip and palate. J Appl Oral Sci. 2011; 19(6): 579-85. doi: 10.1590/s1678-77572011000600007.

[10] Pamplona C, Ysunza A, Patiño C, Ramírez E, Drucker M, Mazón JJ. Speech summer camp for treating articulation disorders in cleft palate patients. Int J Pediatr Otorhinolaryngol. 2005; 69(3): 351-9. doi: 10.1016/j.ijporl.2004.10.012.

[11] Subramaniyan B, Nagarajan R, Vaidyanathan R, Rajashekhar B, Sathiyasekaran BWC. Caregivers' perception of speech and language status and related needs in children with cleft lip and palate. Int J Pediatr Otorhinolaryngol. 2018; 108: 22-5. doi: 10.1016/j.ijporl.2018.02.027.

[12] Mossey P, Little J. Addressing the challenges of cleft lip and palate research in India. Indian J Plast Surg. 2009; 42 Suppl(Suppl): 9-18. doi: 10.4103/0970-0358.57182.

[13] Pamplona MC, Ysunza A, Espinosa J. A comparative trial of two modalities of speech intervention for compensatory articulation in cleft palate children, phonologic approach versus articulatory approach. Int J Pediatr Otorhinolaryngol. 1999; 49(1): 21-6. doi: 10.1016/s0165-5876(99)00040-3.

[14] Pamplona MC, Ysunza A, Ramirez P. Naturalistic intervention in cleft palate children. Int J Pediatr Otorhinolaryngol. 2004; 68(1): 75-81. doi: 10.1016/j.ijporl.2003.09.007.

[15] Prathanee B, Pumnum T, Yoodee P, Makarabhirom K. Speech therapy model for patients with cleft palate in Lao People's Democratic Republic: Lack of speech services. Int J Pediatr Otorhinolaryngol. 2020; 138: 110366. doi: 10.1016/j.ijporl.2020.110366.

[16] Makarabhirom K, Prathanee B, Suphawatjariyakul R, Yoodee P. Speech therapy for children with cleft lip and palate using a community-based speech therapy model with Speech Assistants. J Med Assoc Thai. 2015; 98 Suppl 7: 140-50.

[17] Prathanee B. Cost effectiveness of speech camps for children with cleft palate in Thailand. J Med Assoc Thai. 2011; 94 Suppl 6: 33-9.

[18] Prathanee B, Chowchuen B. Community-based network system and interdisciplinary management for children with cleft-lip/palate. J Med Assoc Thai. 2010; 93 Suppl 4: 63-70.

[19] Prathanee B, Makarabhirom K, Jaiyong P, Pradubwong S. Khon Kaen: a community-based speech therapy model for an area lacking in speech services for clefts. Southeast Asian J Trop Med Public Health. 2014; 45(5): 1182-95.

[20] Suphawatjariyakul R, Lorwatanapongsa P, Makarabhirom K, Prathanee B, Manochiopinig S, Wattanawongsawang W. Speech camp: community-based speech therapy model for Thai children with cleft lip/palate in Amnatchareon Province. Saraburi Hosp Med J. 2007; 33(2): 118-25.

[21] Makarabhirom K, Rattanapitak A, Prathanee B. Myanmar articulation, resonation, nasal emission and nasal turbulence test: Preliminary study. Arch Plast Surg. 2023; 50 (5): 468-77. doi: 10.1055/s-0043-1771522.

[22] Henningsson G, Kuehn DP, Sell D, Sweeney T, Trost-Cardamone JE, Whitehill TL. Universal parameters for reporting speech outcomes in individuals with cleft palate. Cleft Palate Craniofac J. 2008; 45(1): 1-17. doi: 10.1597/06-086.1.

[23] Prathanee B, Lorwatanapongsa P, Anantapong D, Buakanok N. Thai speech parameters for patients with cleft palate in a universal reporting system. Asia Pac J Speech Lang Hear. 2011; 14(1): 31-49.

[24] Prathanee B, Rattanapitak A, Makarabhirom K. Myanmar articulation exercises. Chieng Rai: Northern Woman Development Foundation; 2018.

[25] Prathanee B. Record book of speech therapy for children with cleft lip and palate. Khon Kaen: Klangnanawittaya Press; 2010.

[26] Lorwatanapongsa P, Isarasena Na Adhuya P, Ahsiravej P, Prathanee B. Adapted Thai early language milestone. Khon Kaen: Department of Otorhilaryngology, Khon Kaen University; 2011.

[27] Mecham MJ, Jones JD. UTAH test of language development. Salt Lake City, Utah: Jones Communication Research Associates; 1967.

[28] Makarabhirom K, Rattanapitak A, Prathanee B. Myanmar Articulation, resonation, nasal emission and nasal turbulence test. Chiang Rai: Northern Women's Developmnet Foundation; 2018.

[29] Luyten A, Bettens K, D'Haeseleer E, Hodges A, Galiwango G, Vermeersch H, *et al*. Short-term effect of short, intensive speech therapy on articulation and resonance in Ugandan patients with cleft (lip and) palate. J Commun Disord. 2016; 61: 71-82. doi: 10.1016/j.jcomdis.2016.03.006.

[30] Powers GR, Dunn C, Erickson CB. Speech analyses of four children with repaired cleft palates. J Speech Hear Disord. 1990; 55(3): 542-9. doi: 10.1044/jshd.5503.542.

[31] Prathanee B, Seephuaham C, Pumnum T. Articulation disorders and patterns in patients with cleft. Asian Biomed. 2014; 8(6): 699-706. doi: 10.5372/1905-7415.0806.347.

[32] Willadsen E, Poulsen M. A restricted test of single-word intelligibility in 3-year-old children with and without cleft palate. Cleft Palate Craniofac J. 2012; 49(3): e6-e16. doi: 10.1597/10-141.

[33] Prathanee B, Lorwatanapongsa P, Makarabhirom K, Suphawatjariyakul R, Wattanawongsawang W, Prohmtong S, *et al*. Speech camp for children with cleft lip and/or palate in Thailand. Asian Biomed. 2011; 5(1): 111-8. doi: 10.5372/1905-7415.0501.013.

[34] Pamplona MDC, Ysunza PA. Speech pathology telepractice for children with cleft palate in the times of COVID-19 pandemic. Int J Pediatr Otorhinolaryngol. 2020; 138: 110318. doi: 10.1016/j.ijporl.2020.110318.

Journal of Associated Medical Sciences 2024; 57(2): 41-48

JAMS
Journal of Associated Medical Sciences

Scopus Indexed & Thai-Journal Citation Index Centre (TCI)

Journal of Associated Medical Sciences

Journal homepage: https://www.tci-thaijo.org/index.php/bulletinAMS/index

Does mild chronic obstructive pulmonary disease need a standard pulmonary rehabilitation program? A case report

Nimit Kosura[1,2] Aung Aung Nwe[1,2] Worawat Chumpangern[3] Kongrit Sriya[4] Chatchai Phimphasak[1,2*] Chulee Ubolsakka-Jones[1,2]

[1]School of Physical Therapy, Faculty of Associated Medical Sciences, Khon Kaen University, Khon Kaen Province, Thailand.
[2]Innovation to Improve Cardiopulmonary and Physical Performance (IICP), Khon Kaen University, Khon Kaen Province, Thailand
[3]Department of Medicine Faculty of Medicine, Khon Kaen University, Khon Kaen Province, Thailand.
[4]Senior Family Medicine, Namphong Hospital, Khon Kaen Province, Thailand.

ARTICLE INFO

Article history:
Received 29 August 2023
Accepted as revised 6 February 2024
Available online 12 February 2024

Keywords:
COPD, rehabilitation, clinical practice guideline, exercise test.

ABSTRACT

Background: Patients with mild chronic obstructive pulmonary disease (COPD) are usually not recommended for a standard pulmonary rehabilitation (PR)program based on the GOLD guideline in mild COPD GOLD A classification. Especially, the scientific evidence on exercise capacity that can be identified for recruitment in PR programs has been less reported. Thus, a preliminary case study to identify the exercise capacity under cardiopulmonary responses by aerobic exercise testing among patients in mild COPD GOLD A classification was the aim of this study.

Objective: To evaluate the cardiopulmonary responses from exercise capacity testing in individual COPD patients with mild COPD GOLD A Classification.

Materials and methods: Four participants with mild COPD GOLD A performed an exercise endurance capacity test at home using Spot Marching Exercise Test (SMT), marching on the spot with high hip and arm raising. The load of SMT was indicated by a controlled stepping rate at 70, 80, 90, 100, and 110 steps/min. Every participant performed Incremental SMT (ISMT) with every 3 min incremental load, and the Constant SMT (CSMT) at the peak load. Both exercise tests were terminated at symptom limit. Resting time between ISMT and CSMT was at least 30 minutes. Cardiopulmonary exercise responses, Borg perceived breathlessness (RPB) and exertion (RPE) were monitored every minute during the exercise test. The duration of exercises was recorded.

Results: Peak exercise capacity using ISMT was low with the end exercise load at 70, 80, 80, and 90 steps/min which is equivalent to moderate to high intensity at 81%, 62%, 65% and 93% of age-predicted maximum heart rate (HRmax). The exercise test was stopped by breathlessness at RPB 7, 8, 6, and 5. Respiratory rates (RR) were 36, 26, 38, and 38 breaths/min. With CSMT, the results showed very short exercise duration 1.78, 4.60, 2.15, and 2.47 mins with RPB 7, 8, 5, and 5 and RR of 33, 27, 34, and 41 breaths/min respectively.

Conclusion: This preliminary report reveals that all four mild COPD GOLD A show low exercise capacity and very poor exercise endurance that should identify the appropriated standard PR program in the future.

Introduction

COPD is a progressive lung disease characterized by persistent airflow limitation. Patients with COPD exhibit chronic respiratory symptoms, including dyspnea, cough, sputum, and exacerbations.[1] The prevalence of COPD is increasing globally due to factors like increased exposure to inhaled particles and a rising ageing population.[2]

The airflow limitation is one of the factors that relate to exercise capacity although it is weakly correlated.[3]

∗ **Corresponding contributor.**
Author's Address: *School of Physical Therapy, Faculty of Associated Medical Sciences, Khon Kaen University, Khon Kaen Province, Thailand.*
E-mail address: chatphi@kku.ac.th
doi: 10.12982/JAMS.2024.025
E-ISSN: 2539-6056

However, it is important to consider that even mild COPD (%FEV1≥80) who has mild airflow limitation has already established pathophysiological changes.[4,5] Previous studies reported that exertional dyspnea and dynamic hyperinflation of lungs even occur in mild COPD[4] There are various factors that can influence the individual's exercise capacity such as musculoskeletal system, cardiovascular system etc.[6]

The pulmonary rehabilitation (PR) guidelines recommend the PR should be provided in chronic respiratory diseases, especially in symptomatic patients.[7-11] Meta-analysis of PR trials in COPD demonstrated that the benefits of PR could improve health status, exercise capacity, dyspnea, quality of life and particularly rate of re-hospitalizations in both stable and post exacerbated patients.[12]

The COPD GOLD guidelines 2023-recommend promoting physical activity for every individual with COPD.[1] However, the recruitment of a standard PR program is based on symptom/risk assessment. According to this guideline, the symptom/risk assessment used two questionnaires: modified medical research council dyspnea scale (mMRC) and COPD assessment test (CAT) as well as previous 1-year history of exacerbation or hospitalization into three groups: GOLD A (low symptoms and 0-1 moderate exacerbation), GOLD B (moderate-severe symptoms and 0-1 moderate exacerbation), and GOLD E (whichever severity of symptoms and ≥2 moderate exacerbation or hospitalization. PR is recommended to only GOLD B and GOLD E but not for GOLD A.

This recommendation is not based on the actual exercise capacity but only symptom/risk assessment.[1,13] Therefore, there is an ambiguity, as to whether missing out on the mild COPD GOLD A from the standard PR program is good practice for this group. It is difficult to include every patient with COPD into standard PR because referring COPD patients to PR is limited by Thai COPD clinical practice guideline that follow GOLD guideline.[1] However, it is also important that patients who have low exercise capacity should not lose the benefit of attending standard PR programs.[14] Therefore, this study aimed to evaluate exercise capacity and cardiopulmonary responses in patients with mild COPD GOLD A. This preliminary study would inform the way of clinical practice in PR that should be based on pre-exercise testing and include patients who need it.

Materials and methods:

Study design and participants

This study was a descriptive study. The participant's recruitment was done from Nam-Phong Hospital and Srinagarind Hospital, Khon Kaen Province, Thailand between December 2022 to March 2023. This study included mild COPD (FEV1% predicted > 80%), aged between 40 to 80 years, with good communication, cooperation, and cognition as well as 0-1 moderate exacerbation or hospitalization prior to 1 year, and mMRC 0-1. In addition, participants who had exacerbation within 4 weeks before the study were also excluded. Before the enrollment, every participant signed an informed consent. This study was approved by Center for Ethics in Human Research, Khon Kaen University (HE641234).

Procedure

After recruitment, the participants were interviewed with CAT, mMRC scores, exacerbation history from the previous year, current medications, and assessed the vital signs (Nihon Kohden, Vismo PVM-4763). The participants then were assessed the lung function by the spirometry Vyntus™ PC SPIRO by a certified investigator (Thoracic Society of Thailand under Royal Patronage) following the American Thoracic Society (ATS)/European Respiratory Society (ERS) guideline for spirometry (2019) with the Thai predicted reference value. (2000).[15,16]

Before the exercise test, the participants were instructed as following: resting for a minimum of two hours, refraining from vigorous exercise for at least 24 hrs prior, avoiding caffeine on the day of the test, and refraining from smoking for at least 8 hours. Moreover, every participant was requested to wear comfortable clothing and shoes that are appropriate for exercise.[17] They were also taught how to score of their dyspnea and exertion sensation using Borg's CR-10 (zero as no symptoms, three as moderate, five as severe, seven as very severe, and ten as maximum) until they could express clearly. Exercise testing procedure, consisted of three phases: resting (5 min in comfortable sitting and 1 min standing), testing phase, and recovery phase (at least 5 min). Electrocardiogram, heart rate (HR), oxygen saturation (SpO2), blood pressure (BP), respiratory rate (RR), and end-tidal carbon dioxide (End-tidal CO2) were monitored at the end of every phase.

Exercise testing

Spot Marching Exercise testing, a new field exercise test was used. To define exercise capacity, there were 2 steps of exercise test; (1) Incremental Spot Marching Test (ISMT) to determine peak exercise load, and (2) Constant Spot Marching Test (CSMT) to determine exercise endurance capacity Symptom-limited exercise test was used according to the American Association of Cardiovascular and Pulmonary Rehabilitation guidelines and the European Respiratory Society statement on standardization of cardiopulmonary exercise testing in chronic lung diseases.[8,15] Patients who had any contraindications for exercise testing were excluded from this study. The participants completed the ISMT first. They rested for at least 30 minutes before starting CSMT. Details of both tests were as follow:

Incremental Spot Marching Exercise Testing (ISMT)

ISMT is the incremental exercise test to define peak exercise load. This test involves participants' marching on the spot with alternate knees raising (hip flex 45-70 degrees) and arm raising above shoulder height (shoulder flex >90 degrees). The intensity or load of SMT is stepping rate. There was a good correlation of stepping rate and oxygen consumption (VO_2) in COPD patients (r0.709), therefore increasing stepping rate could result in increasing exercise intensity.[18,20] The starting stepping

rate was 70 steps/min then incrementally 10 steps/min for every 3 minutes. The stepping rates were controlled by using a metronome. The arms and legs range of motions was controlled via visual feedback (individualized tape markings of the height of arm and leg raising were placed on the wall in front of them). Moreover, verbal feedback was also given to encourage and control their consistency of step rates and range of motion. Parameters of uncoordinated step rate within ±5% were allowed. However, if an uncoordinated step rate >±5% occurred and verbal instruction was unable to correct this, the exercise test was terminated. The participants performed exercise testing until their symptoms ceased. The peak step rates and duration of the exercise test were recorded.

Constant Spot Marching Exercise Testing (CSMT)

The procedure of CSMT was the same as ISMT except using peak step rates achieved in ISMT as a constant load. Peak step rate of ISMT has been found to be submaximal exercise intensity based on VO_2 response of this exercise testing in a previous study.[18] The duration of exercise test was recorded.

Outcome measurement

Cardiopulmonary responses during exercise testing

- Heart rate (HR) was monitored with electrocardiogram (ECG) every minute.
- Blood pressure (BP) was measured with arm cuff sphygmomanometer every 2 minutes.
- Oxygen saturation (SpO_2) was measured with finger pulse oximeter every minute.
- Respiratory rate (RR) was derived from capnography.
- Maximum heart rate (%HRmax) was calculated using 206.9-0.69 * age.[21]

Rate of perceived breathlessness and exertion

- Borg's CR-10 was used to assess the severity of exercise-induced dyspnea and physical exertion.
- These outcomes were monitored in resting, exercise, and recovery phases.

Data Analysis

Demographic characteristics and the outcomes were reported with descriptive statistics using median and interquartile range (IQR).

Results

The demographic and clinical characteristics of four mild COPD patients are presented in Table 1. All participants were old age (68-80 years old), long-term smokers with a smoking history were 23.50 (21.25, 32.50) pack-years. Additionally, there were no reports of exacerbation in the previous year for all participants.

Table 1 Demographic and clinical characteristics of 4 participants.

Variable	No.1	No.2	No.3	No.4	Median
Age: years old	80	68	75	77	76 (69, 79)
Weight: kg	50	79	46	49	49 (46, 72)
Hight: cm	155	171	160	162	161 (156, 168)
BMI: kg/m^2	20.8	27.2	18.0	18.7	19.74 (18.14, 25.59)
Smoking Status					
Ex-smoker: pack-years	25	35	21	22	23.50 (21.50, 30.00)
Dyspnea Questionnaires					
CAT score	4	4	4	4	4 (4, 4)
mMRC	1	1	1	1	1 (1,1)
Exacerbation in previous 1 yrs.	0	0	0	0	
Symptoms/Risk Classification	A	A	A	A	
Pulmonary Function					
FVC: L	2.09	3.18	2.54	2.75	2.65 (2.20, 3.07)
FVC: %pred	95.87	99	100	110	99.50 (96.65, 107.50)
FEV_1: L	1.43	2.03	1.54	1.56	1.55 (1.46, 1.91)
FEV_1: %pred	85	84	80	83	83.50 (80.75, 84.75)
FEV_1/FVC	62.37	63.95	69.46	56.67	63.16 (58.09, 68.08)
Medication	S FL	B FO TI	S FL	S FL	
Comorbidity	HT	HT	No	HT	

Note: *Data represent as median (IQR), BMI: body mass index, FVC: force vital capacity, FVC%pred: percent predicted of force vital capacity, FEV1: force expiratory volume in 1 second, FEV1%pred: percent predicted force expiratory volume in 1 second, FEV1/FVC%: percent ratio of force expiratory volume in 1 second by force vital capacity. Medication S: salmeterol, FL: fluticasone, B: budesonide, FO: formoterol, TI: tiotropium. Comorbidity HT: hypertension.*

All participants followed the protocol of ISMT and CSMT. No adverse events occurred during the tests. The individualized and median (IQR) data of RR, SpO2, ETCO2, BP, HR, %HRMax, %HRR, RPB, RPE, step rates and exercise duration of ISMT and CSMT, were shown in Table 2 and Table 3 respectively. All participants reached the peak exercise load with severe symptoms of breathlessness and RR in 2.8-8 minutes of low load at 70-90 step/min. The end exercise HR were 63-93 % HRmax as shown in Table 1.

The time course of changes in HR, RR, RPB and RPE during CSMT was presented in Figure 1. Participants stopped exercise in 2-5 minutes with RR of 26-41 breath/min at the RPB of 5-8 and RPE of 3-9.

Table 2 Cardiopulmonary and exercise responses of 4 participants at the end of the Incremental Spot Marching Exercise Test (ISMT).

Responses	No.1		No.2		No.3		No.4	
	Resting	End exercise	Resting	End exercise	Resting	End exercise	Resting	End exercise
Intensity and Duration								
Symptoms limited Intensity (step/min)	NA	80	NA	90	NA	70	NA	80
Duration: min	NA	5	NA	8	NA	2.8	NA	5.95
Cardiovascular system								
HR (beat/min)	85	123	76	100	61	102	91	144
HRMax (%)	56	81.1	47	62.5	39	65.7	59	93.6
HRR (%)	0	56.7	0	28.2	0	43.2	0	84.3
SBP (mmHg)	120	144	114	145	116	141	125	142
DBP (mmHg)	55	78	74	76	77	83	73	105
Pulmonary System								
RR (breath/min)	19	36	17	26	12	38	12	38
SpO_2 (%)	97	97	98	96	97	95	100	96

Note: *RR: respiratory rate, HR: heart rate, HRMax%: percentage of maximal heart rate, HRR%: percentage of heart reserve, %SpO_2: percentage of oxygen saturation, SBP: systolic blood pressure, DBP: diastolic blood pressure, MAP: mean arterial pressure, RPB: rate perceives of breathlessness, RPE: rate perceives of exertion.*

Table 3 Cardiopulmonary and exercise responses of 4 participants at the end of exercise endurance test using Constant Spot Marching Exercise Test (CSMT).

Responses	No.1		No.2		No.3		No.4	
	Resting	End exercise	Resting	End exercise	Resting	End exercise	Resting	End exercise
Intensity and Duration								
Symptoms limited Intensity (step/min)	NA	80	NA	90	NA	70	NA	80
Duration: min	NA	1.78	NA	4.60	NA	2.15	NA	2.47
Cardiovascular system								
HR (beat/min)	89	123	76	98	63	75	88	150
HRMax (%)	59	81	47	61	40	48	57	97
HRR (%)	NA	53	NA	25	NA	13	NA	94
SBP (mmHg)	112	141	107	123	107	108	125	124
DBP (mmHg)	63	81	73	84	71	91	74	81
Pulmonary System								
RR (breath/min)	24	33	14	27	13	34	14	41
SpO_2 (%)	95	97	96	96	96	97	99	96

Note: *RR: respiratory rate, HR: heart rate, HRMax%: percentage of maximal heart rate, HRR%: percentage of heart reserve, %SpO_2: percentage of oxygen saturation, SBP: systolic blood pressure, DBP: diastolic blood pressure, MAP: mean arterial pressure, RPB: rate perceives of breathlessness, RPE: rate perceives of exertion.*

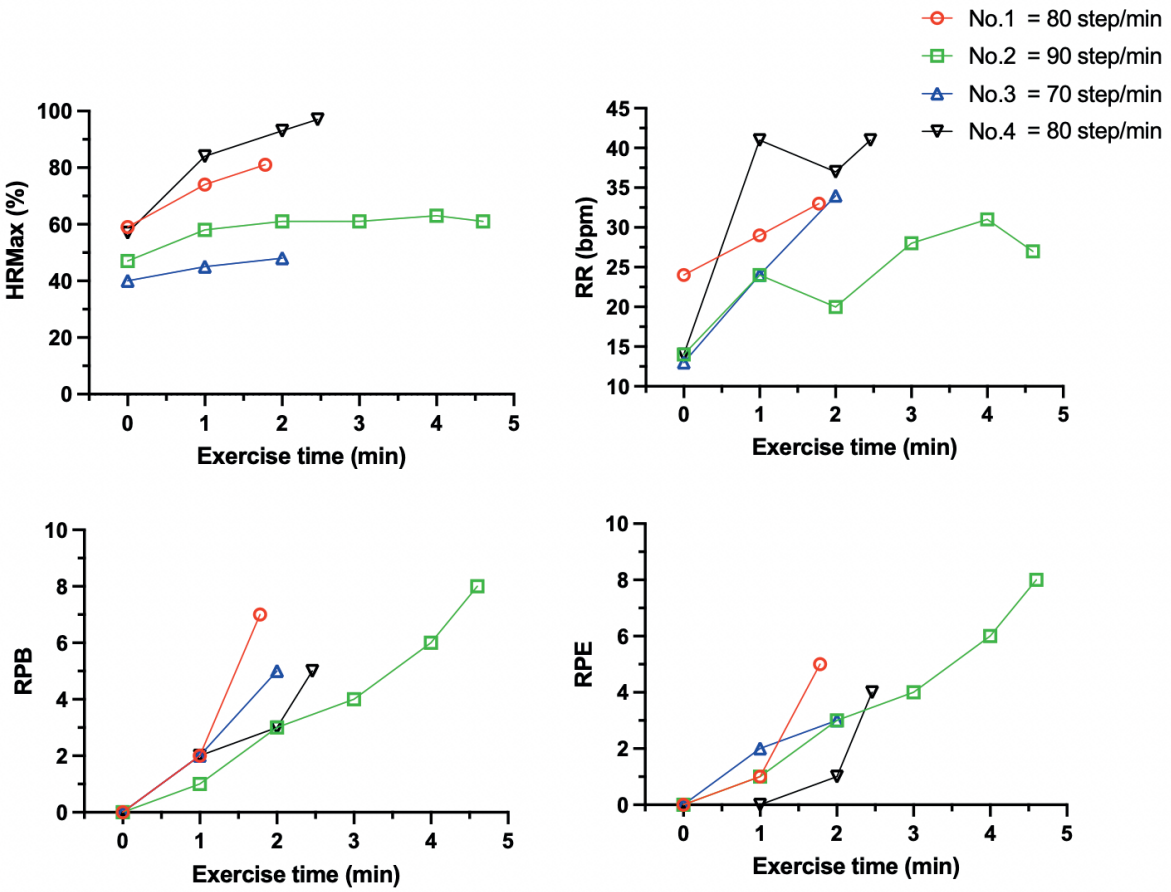

Figure 1 *Cardiopulmonary and Borg's perceived breathlessness and exertion responses during Constant Spot Marching Exercise Test.*
HRmax%: percentage of maximal heart rate, RR: respiratory rate,
RPB: rate perceived of breathlessness, RPE: rate perceived of exertion.

Discussion

This study reveals surprisingly low exercise capacity in mild COPD GOLD A during incremental and constant load of exercise with the Spot Marching Exercise test (SMT). All participants had low peak exercise capacity and poor exercise endurance as seen with very short exercise duration at submaximal exercise intensity. Exercise endurance was early terminated because of severe breathlessness. However, there were different cardiac responses to the exercise test at the same load.

There are several field tests and laboratory tests such as the 6-minute walk test, shuttle walk test, and treadmill test cycle ergometry, that have been used in previous studies of COPD.[22-24] The present study used SMT, a form of simple field test of moderate intensity based on criteria of oxygen consumption.[18] This exercise test was chosen because of the functioning pattern, minimum space and devices needed and easy to do at home. It is also suitable for people with lung dysfunction. This new exercise testing protocol has been used in moderate to severe COPD patients.[18,19,25-27]

Although participants No.1 and 4 exercised with a low stepping rate of 80 steps/min but this contributed to high stress of cardiopulmonary functions in just about 2 minutes of exercise. The exercise heart rate reached a high percentage of HRmax and severe breathlessness (Table 2, 3, Figure 1). This indicates poor exercise capacity and exercise endurance as the previous reports.[18,28]

Participant No 3 showed different responses of cardiac function from others with mild intensity less than 50 % HRmax at low load (70 steps/min). Even at this low intensity, this participant also presented early exercise termination of less than 3 minutes. Again, severe breathlessness was the limiting factor.

The exercise capacity and endurance of participant No 2 were better than the others with the longer exercise time of 5 minutes at moderate intensity of 60%HRmax. However, the breathless score reached a severe level in a short time as well.

This phenomenon of poor exercise capacity and endurance is usually seen in COPD especially in moderate to severe COPD due to dynamic hyperinflation (DH). Some previous studies showed that COPD has the main characteristic of airflow limitation that is usually associated with DH and so dyspnea, reduced exercise capacity, and restrictions in activities.[29,30] Moreover, it has been proved that individuals with mild COPD have a wide range of lung structure abnormalities such as vessels, lung compliance,

and trapping of the air.[31,32] Therefore, DH could occur even in mild COPD regardless of static hyperinflation.[29] Furthermore, the increased effort/displacement ratio which is usually high in DH strongly correlates with dyspnea due to neuro-ventilatory mismatching.[33,34] Therefore, the present study hypothesized that although mild COPD has minimal symptoms, there might be an increasing ventilatory limitation during exertion because of DH and so reduced exercise tolerance.

The low exercise capacity and poor endurance found in this study could possibly be not only due to DH but also the amount of working muscles including respiratory muscles during the exercise and the age of all participants. SMT is a whole-body exercise that requires whole-body muscle work. The exercise involves both upper and lower limb movement together with body stabilization. Typically, this exercise places more constraints on the weak respiratory muscles as a result of the arm raising over 90 degrees.[35,36] Khaweephab *et al*. 2016 compared CSMT (self-pacing) and 6 MWT in COPD patients and found that the CSMT stress greater lung function than 6MWT with similar cardiovascular loading.[25] Therefore, the limiting exercise factors would be due to more muscle work and overload on the respiratory system. This effect is seen in high RR at the relatively lower intensity based on the percentage of %HRmax.

Aging lung would be another exercise limiting factor. Since all participants in the present study were old with declining lung capacity. The previous studies by Chaw Su Win *et al*. evaluated cardiopulmonary responses of ISMT in older adults with age 65±4 years 60-70 years.[28] They found that the majority of the older adults stopped exercise at a load of 100 steps/min with a duration of 9.26±3.74 minutes (95%CI 7.97-10.10.54 minutes). Most of the participants terminated exercise in their study due to leg fatigue. In contrast, every participant in the current study terminated the test in both ISMT and CSMT due to the reason of severe dyspnea as a result of added-on lung pathology. However, one of our participants aged 68 years old terminated ISMT at the load of 90 steps/min with a duration of 8 minutes which is slightly lower than the previous study. This participant would be the ideal mild COPD GOLD A.

Limitation

The limitation of the current study is a very small sample size.

Conclusion

Mild COPD GOLD A shows unexpectedly low exercise capacity and endurance. This led to the answer that this group of COPD should be reconsidered by being enrolled in exercise training in a standard PR program. Every participant with COPD should be assessed for their exercise capacity with the whole-body exercise test to detect their exercise limitation before being excluded from the PR program.

Conflict of interest

There are no conflicts of interest in this study.

Funding

We also appreciated funding support by "Research Fund for Supporting Lecturer to Admit High Potential Student to Study and Research on His Expert Program Year 2020, Graduated School, Khon Kaen University", "National Science Research and Innovation Fund (NSRF): Research Grant for New Scholar year 2022", and "Faculty of Associated Medical Sciences, Khon Kaen University".

Acknowledgements

We want to express our sincere gratitude to the participants of this study for their valuable contributions. We also appreciate the medical professionals and experts who generously shared their knowledge and insights.

References

[1] Agustí A, Celli BR, Criner GJ, Halpin D, Anzueto A, Barnes P, *et al*. Global initiative for chronic obstructive lung disease 2023 report: GOLD executive summary. Am J Respir Crit. 2023; 207(7): 819-37. doi: 10.1183/13993003.00239-2023.

[2] Mathers CD, Loncar D. Projections of global mortality and burden of disease from 2002 to 2030. PLoS medicine. 2006; 3(11): e442. doi: 10.1371/journal.pmed.0030442.

[3] Calverley P, Koulouris N. Flow limitation and dynamic hyperinflation: key concepts in modern respiratory physiology. Eur Respir J. 2005; 25(1):186-99. doi: 10.1183/09031936.04.00113204.

[4] Ofir D, Laveneziana P, Webb KA, Lam Y-M, O'Donnell DE. Mechanisms of dyspnea during cycle exercise in symptomatic patients with GOLD stage I chronic obstructive pulmonary disease. Am J Respir Crit. 2008; 177(6):622-9. doi: 10.1164/rccm.200707-1064OC.

[5] O'donnell DE, Laveneziana P, Ora J, Webb KA, Lam YM, Ofir D. Evaluation of acute bronchodilator reversibility in patients with symptoms of GOLD stage I COPD. Thorax. 2009; 64(3):216-23. doi: 10.1136/thx.2008.103598.

[6] Franssen FME, Rochester CL. Comorbidities in patients with COPD and pulmonary rehabilitation: do they matter? Eur Respir Rev. 2014; 23(131):131-41. doi: 10.1183/09059180.00007613.

[7] Rochester CL, Alison JA, Carlin B, Jenkins AR, Cox NS, Bauldoff G, *et al*. Pulmonary rehabilitation for adults with chronic respiratory disease: an official American thoracic society clinical practice guideline. Am J Respir Crit. 2023; 208(4): e7-e26. doi: 10.1164/rccm.202306-1066ST.

[8] American Association of Cardiovascular and Pulmonary Rehabilitation (AACVPR) Guidelines for pulmonary rehabilitation programs: Human Kinetics; 2011.

[9] Bolton CE, Bevan-Smith EF, Blakey JD, Crowe P, Elkin SL, Garrod R, *et al*. British Thoracic Society guideline on pulmonary rehabilitation in adults: accredited by NICE. Thorax. 2013; 68(Suppl 2): ii1-ii30. doi: 10.1136/thoraxjnl-2013-203808.

[10] Man W, Chaplin E, Daynes E, Drummond A, Evans RA, Greening NJ, *et al*. British Thoracic Society Clinical

Statement on pulmonary rehabilitation. Thorax. 2023; 78(Suppl 4): s2-s15. doi: 0.1136/thorax- 2023-220439.

[11] Spruit MA, Singh SJ, Garvey C, ZuWallack R, Nici L, Rochester C, *et al*. An official American Thoracic Society/European Respiratory Society statement: key concepts and advances in pulmonary rehabilitation. Am J Respir Crit. 2013; 188(8): e13-64. doi: 10.1164/rccm.201309-1634ST.

[12] McCarthy B, Casey D, Devane D, Murphy K, Murphy E, Lacasse Y. Pulmonary rehabilitation for chronic obstructive pulmonary disease. Cochrane Database Syst Rev. 2015; 2015(2): CD003793. doi: 10.1002/14651858.CD003793.pub3.

[13] Hanania NA, O'Donnell DE. Activity-related dyspnea in chronic obstructive pulmonary disease: physical and psychological consequences, unmet needs, and future directions. Int J Chron Obstruct Pulmon Dis. 2019; 14: 1127. doi: 10.2147/COPD.S188141.

[14] Jácome C, Marques A. Pulmonary rehabilitation for mild COPD: a systematic review. Respir Care. 2014; 59(4): 588-94. doi: 10.4187/respcare.02742.

[15] Dejsomritrutai W, Nana A, Maranetra KN, Chuaychoo B, Maneechotesuwan K, Wongsurakiat P, *et al*. Reference spirometric values for healthy lifetime nonsmokers in Thailand. J Med Assoc Thai. 2000; 83(5): 457-66.

[16] Graham BL, Steenbruggen I, Miller MR, Barjaktarevic IZ, Cooper BG, Hall GL, *et al*. Standardization of spirometry 2019 update. An official American thoracic society and European respiratory society technical statement. Am J Respir Crit. 2019; 200(8): e70-e88. doi: 10.1164/rccm.201908-1590ST.

[17] Radtke T, Crook S, Kaltsakas G, Louvaris Z, Berton D, Urquhart DS, *et al*. ERS statement on standardisation of cardiopulmonary exercise testing in chronic lung diseases. Eur Respir Rev. 2019; 28(154): 180101-25. doi: 10.1183/16000617.0101-2018.

[18] Limphatcharaporn Jirawat, Chidnok Weerapong, Suntrapiwat Kajorn, Jones Chulee. A new cardiopulmonary exercise testing with the Incremental Spot Marching Exercise Test in patients with chronic obstructive pulmonary disease: a pilot study. Thai J Phys Ther. 2020; 42(2): 69-82.

[19] Ubolsakka-Jones C, Jones DA, Pukdeechat M, Boonsawat W, Kritsanapan W, Phimphasak C. Effect of a Conical-PEP Mask on Exercise in Subjects With COPD. Respir Care. 2023; 69(2): 191-201 doi: 10.4187/respcare.11016.

[20] Naosang S, Wannachit N, Jones C. A new endurance exercise test "Spot Brisk Marching": Lung capacity. Poster session presented at The 8th National Physical Therapy Conferrence. 2016: 20-3.

[21] Gellish RL, Goslin BR, Olson RE, McDonald A, Russi GD, Moudgil VK. Longitudinal modeling of the relationship between age and maximal heart rate. Med Sci Sports Exerc. 2007; 39(5): 822-9. doi: 10.1097/mss.0b013e31803349c6.

[22] Puente-Maestu L, Palange P, Casaburi R, Laveneziana P, Maltais F, Neder JA, *et al*. Use of exercise testing in the evaluation of interventional efficacy: an official ERS statement. Eur Respir J. 2016; 47(2): 429-60. doi: 10.1183/13993003.00745-2015.

[23] Society AT. ATS statement: guidelines for the six-minute walk test. Am J Respir Crit Care Med. 2002; 166: 111-7. doi: 10.1164/ajrccm.166.1.at1102.

[24] Fotheringham I, Meakin G, Punekar YS, Riley JH, Cockle SM, Singh SJ. Comparison of laboratory-and field-based exercise tests for COPD: a systematic review. Int J Chron Obstruct Pulmon Dis. 2015; 10(1): 625-43. doi: 10.2147/COPD.S70518.

[25] Khaweephab V, Jones C, Phimphasak C, Jones D. Comparison of cardiopulmonary responses between a new spot marching test and six minute walk test in mild to moderate COPD patients. Eur Respiratory Soc; 2016; 48(60): 1592. doi: 10.1183/13993003.congress-2016.PA1592.

[26] Jones C, Phimphasak C, Pukdeechat M, Jones D. Spot Marching Exercise for home-based pulmonary rehabilitation in COPD: physical performance and quality of life. Eur Respiratory Soc; 2018; 52: 3651. doi: 10.1183/13993003.congress-2018.PA3651.

[27] Chidnok W. The suitability of self-paced spot marching exercise as a field endurance test for COPD Chest. 2019; 155(4): 281A. doi.org/10.1016/j.chest.2019.02.271.

[28] Chaw Su Win CJ, Nantinee Nualnim. Cardiopulmonary responses to incremental spot marching exercise test as functional capacity measurement in older adults. International Physical Therapy Research Symposium 2023 (IPTRS 2023); June 8-9, 2023; Khon Kaen University2023. p. 1-11.

[29] O'Donnell DE, Gebke KB. Activity restriction in mild COPD: a challenging clinical problem. Int J Chron Obstruct Pulmon Dis. 2014; 9: 577-88. doi: 10.2147/COPD.S62766.

[30] James MD, Milne KM, Phillips DB, Neder JA, O'Donnell DE. Dyspnea and exercise limitation in mild COPD: the value of CPET. Front Med. 2020; 7: 442. doi: 10.3389/fmed.2020.00442.

[31] Matsuoka S, Washko GR, Dransfield MT, Yamashiro T, Estepar RSJ, Diaz A, *et al*. Quantitative CT measurement of cross-sectional area of small pulmonary vessel in COPD: correlations with emphysema and airflow limitation. Acad Radiol. 2010; 17(1):93-9. doi: 10.1016/j.acra.2009.07.022.

[32] Rambod M, Porszasz J, Make BJ, Crapo JD, Casaburi R, Investigators COPDGene. Six-minute walk distance predictors, including CT scan measures, in the COPD Gene cohort. Chest. 2012; 141(4): 867-75. doi: 10.1378/chest.11-0870.

[33] O'Donnell DE, Bertley JC, Chau LK, Webb KA. Qualitative aspects of exertional breathlessness in chronic airflow limitation: pathophysiologic mechanisms. Am J Respir Crit. 1997; 155(1): 109-15. doi: 10.1164/ajrccm.155.1.9001298.

[34] O'Donnell DE. Ventilatory limitations in chronic obstructive pulmonary disease. Med Sci Sports Exerc. 2001; 33(7): S647-55. doi: 10.1097/00005768-200107001-00002.

[35] McKeough ZJ, Alison JA, Bye PT. Arm positioning alters lung volumes in subjects with COPD and healthy subjects. Aust J Physiother. 2003; 49(2): 133-7. doi: 10.1016/s0004-9514(14)60129-x.

[36] Laoakka T, Jones C, Khrisanapant W. Inspiratory muscle training increases elevated arm exercise endurance but not 6 minutes walk distance in the elderly. Eur Respir J. 2006; 28(50): 284.

Journal of Associated Medical Sciences 2024; 57(2): 49-55

JAMS
Journal of Associated Medical Sciences

Scopus Indexed & Thai-Journal Citation Index Centre (TCI)

Journal of Associated Medical Sciences

Journal homepage: https://www.tci-thaijo.org/index.php/bulletinAMS/index

Comparative analysis of deep learning techniques for accurate stroke detection

Titipong Kaewlek[1,2*] Ketmanee Sitinwan[1] Kunaporn Lueangaroon[1] Wasita Sansuriyawong[1]

[1]Department of Radiological Technology, Faculty of Allied Health Sciences, Naresuan University, Phitsanulok Province, Thailand.
[2]Interdisciplinary Health and Data Sciences Research Unit, Faculty of Allied Health Sciences, Naresuan University, Phitsanulok Province, Thailand.

ARTICLE INFO

Article history:
Received 20 November 2023
Accepted as revised 9 February 2024
Available online 12 February 2024

Keywords:
Brain CT image, computed tomography image, deep learning, stroke, VGG-16

ABSTRACT

Background: The traditional diagnosis of strokes through computed tomography (CT) heavily relies on radiologists' expertise for accurate interpretation. However, the increasing demand for this critical task exceeds the available radiologist workforce, necessitating innovative solutions. This research addresses this challenge by introducing deep learning techniques to enhance the initial screening of stroke cases, thereby augmenting radiologists' diagnostic capabilities.

Objective: This study aims to compare four techniques for classifying stroke lesions in CT images.

Materials and methods: Four distinct models-CNN-2-Model, LeNet, GoogleNet, and VGG-16-were trained using a dataset comprising 1,636 CT images, including 1,111 normal brain images and 525 stroke images. Seventy percent of the images were used to train the most effective deep learning model, and subsequently, these images were utilized to evaluate the performance of each model. The evaluation involved assessing accuracy, precision, sensitivity, specificity, F1 score, false positive rate, and AUC.

Results: The evaluation process included a comprehensive statistical analysis of the models' prediction results. The findings revealed that VGG-16 emerged as the top-performing deep learning model, achieving an impressive accuracy of 0.969, precision of 0.952, sensitivity of 0.952, specificity of 0.978, F1 score of 0.952, false positive rate of 0.022, and AUC of 0.965.

Conclusion: In conclusion, deep learning techniques, particularly the VGG-16 model, demonstrate significant promise in enhancing the accuracy of stroke lesion classification in CT images. These findings underscore the potential of leveraging advanced technologies to address the growing challenges in stroke diagnosis and pave the way for more efficient and accessible healthcare solutions.

Introduction

A stroke occurs when there is a sudden disruption in the blood supply to the brain, leading to an immediate impairment of brain function. It manifests in two primary forms: ischemic stroke and hemorrhagic stroke.[1] The World Health Organization (WHO) report on World Stroke Day in 2022, observed on October 29, emphasizes stroke as the primary cause of global disability and the second leading cause of death.[2] According to the 2022 Global Stroke Factsheet, strokes contribute to five million annual fatalities worldwide. In Thailand, data from the Ministry of Public Health for 2022 reports 37,802 cases, translating to 58.0 patients per 100,000 individuals in the Thai population. This underscores a rising incidence of stroke cases, aligning with global trends, and notably, stroke

* **Corresponding contributor.**
Author's Address: *Department of Radiological Technology, Faculty of Allied Health Sciences, Naresuan University, Phitsanulok Province, Thailand.*
E-mail address: titipongk@nu.ac.th
doi: 10.12982JAMS.2024.026
E-ISSN: 2539-6056

ranks as the second leading cause of death among the elderly in Thailand.[3]

The traditional diagnostic approach for stroke involves a thorough examination, encompassing medical history assessments, physical examinations, and imaging studies such as CT scans and MRIs.[4,5] Gathering medical history entails obtaining information about the patient's background, including risk factors like hypertension, diabetes, smoking, and prior strokes. Physical examination assesses neurological symptoms, covering aspects such as strength, coordination, reflexes, and sensory function.

Imaging studies, crucial to the diagnostic process, include CT scans (Computed Tomography) and MRI (Magnetic Resonance Imaging).[4,5] CT scans are frequently employed for the swift determination of whether a stroke is ischemic or hemorrhagic. Furthermore, they aid in pinpointing the location and extent of the damage. MRI, offering more detailed images compared to CT scans, is particularly valuable for detecting ischemic strokes. The advent of artificial intelligence (AI) in medical imaging has opened avenues for improving the accuracy and efficiency of stroke detection. AI algorithms trained on extensive datasets of medical images, possess the capacity to autonomously analyze intricate patterns, potentially revolutionizing the diagnostic process.[6,7]

In recent studies for stroke classification, Ammar *et al*. compared five deep learning models (ReNet50, VGG-16, Xception, InceptionV3, and InceptionResNetV2), with VGG-16 demonstrating the highest performance accuracy at 96.0% for intracranial hemorrhage.[8] Worachotsueptrakun compared four deep learning models (AlexNet, VGG-16, GoogleNet, and ResNet), with GoogleNet exhibiting the best performance, achieving accuracy, precision, recall, and F1-score of 92.00%, 94.00%, 83.96%, and 88.70%, respectively.[9] Additionally, Vamsi *et al*. achieved an accuracy of 97.81 % using VGG-16 and random forest. [10]

This study aims to compare the efficacy of stroke classification among four models using brain CT images. Specifically, the research seeks to assess the performance of four conventional neural networks-CNN-2-Model, LeNet, GoogleNet, and VGG-16-utilizing deep learning techniques for stroke classification.

Materials and methods

Data collection

The 1,636 CT images were collected from Kaggle. [11,12] This dataset included 1,111 normal brain images and 525 stroke images. Inclusion criteria comprised axial CT image plane, non-ionic contrast media images, and indicated labels for stroke and normal. Exclusion criteria encompassed multi-lesion brain images, unidentified results, and images of the base of the skull region. For image preparation, the dataset was divided into three groups: 70% for training, 20% for validation, and 10% for testing. A total of 328 images were selected for training the brain segmentation.

Stoke classification technique

The stroke detection process in this study has two parts: brain segmentation and stroke classification, as shown in Figure 1. For brain segmentation, we use the U-net architecture to separate the brain tissue from the skull bone in CT images.[13] Subsequently, the brain-segmented images were trained using four convolutional neural network models (CNN-2-Model, LeNet, GoogleNet, and VGG-16), and their performance in stroke classification was compared.

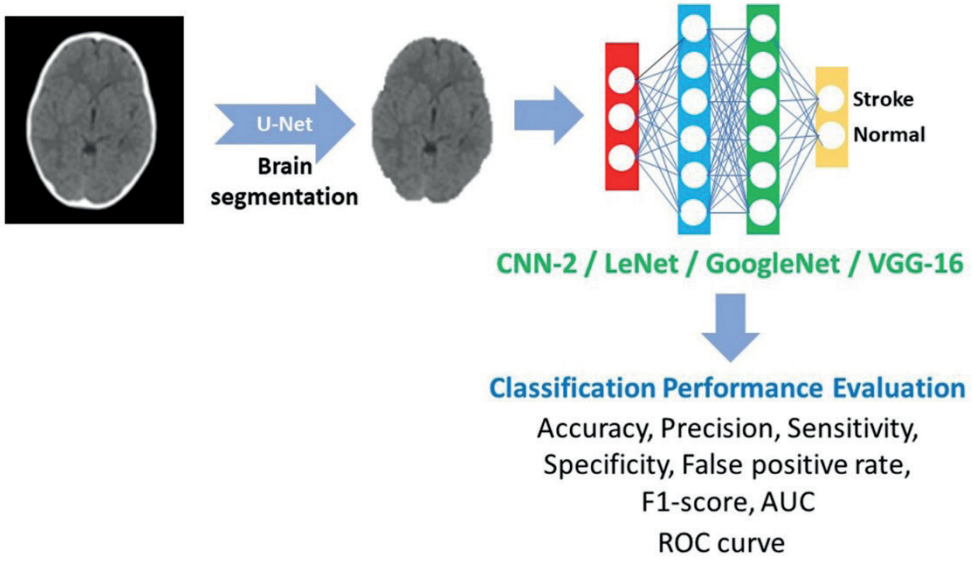

Figure 1. *Flowchart of stoke detection.*

Brain segmentation

In brain segmentation, we apply the U-net architecture modified from Kairess's model as shown in Table 1.[13] The input consists of 328 images (256x256x1 pixels). The contracting path follows the typical architecture of a convolutional network, with the repeated application of 3x3 convolutions, each followed by a rectified linear unit (ReLU), and a 2x2 max-pooling operation with a stride of 2 for down sampling. Every step in the expansive path consists of upsampling the feature map followed by a 3x3 convolution that halves the number of feature channels, a concatenation with the correspondingly cropped feature map from the contracting path, and each followed by a sigmoid. The 32x32x128 dense layer was connected to the down-up sampling. At the final layer, 256x256x64 pixels, with a 3x3 convolution and a 1x1 convolution, is followed by a sigmoid. The model was trained using a learning rate of 0.000001. The network training was set to a batch size of 32 for 80 epochs. The Dice similarity coefficient (DSC), Dice loss, and Weighted bce Dice loss were used to evaluate the performance of brain segmentation.

Table 1. U-net architecture parameters.

Layer (type)	Output Shape	Parameter
input_1 (InputLayer)	(None, 256, 256, 1)	0
conv2d (Conv2D)	(None, 256, 256, 32)	320
max_pooling2d (MaxPooling2D)	(None, 128, 128, 32)	0
conv2d_1 (Conv2D)	(None, 128, 128, 64)	18496
max_pooling2d_1 (MaxPooling2D)	(None, 64, 64, 64)	0
conv2d_2 (Conv2D)	(None, 64, 64, 128)	73856
max_pooling2d_2 (MaxPooling2D)	(None, 32, 32, 128)	0
dense (Dense)	(None, 32, 32, 128)	16512
up_sampling2d (UpSampling2D)	(None, 64, 64, 128)	0
conv2d_3 (Conv2D)	(None, 64, 64, 128)	147584
up_sampling2d_1 (UpSampling2D)	(None, 128, 128, 128)	0
conv2d_4 (Conv2D)	(None, 128, 128, 64)	73792
up_sampling2d_2 (UpSampling2D)	(None, 256, 256, 64)	0
conv2d_5 (Conv2D)	(None, 256, 256, 1)	577
Total parameters: 331,137, Trainable parameters: 331,137, non-trainable parameters: 0		

Comparative analysis for stroke detection

The 1,636 CT images were collected from Kaggle.[11,12] This dataset included 1,111 normal brain images and 525 stroke images. For image preparation, 70 % of the images were used for training, 20% for validation, and 10% for testing. The brain segmentation images were trained, validated, and tested using four model techniques (CNN-2-Model, LeNet, GoogleNet, and VGG-16). The optimizer used was the Adam method, and the loss function employed was cross-entropy. The structure of the four models is shown in Table 2. The models were trained on Google Colab with Tesla T4.

Table 2. The structure of four models.

Model	CNN2-model	LeNet	GoogleNet	VGG-16
Input layer	256×256×1	256×256×1	256×256×1	256×256×1
1st Blocks	1. A Conv 2. Relu 3. a MaxPooling	1. A Conv 2. Relu 3. a MaxPooling	1. A Conv 2. Relu 3. a MaxPooling	1. Two Conv 2. Relu 3. a MaxPooling
2nd Block	1. A Conv 2. Relu 3. a MaxPooling	1. A Conv 2. Relu	1. Two Conv 2. Relu 3. a MaxPooling	1. Two Conv 2. Relu 3. a MaxPooling
3rd Block	-	-	1. Two inceptions 2. MaxPooling	1. Three Conv 2. Relu 3. a MaxPooling
4th Block	-	-	1. Five inceptions 2. MaxPooling	1. Three Conv 2. Relu 3. a MaxPooling
5th Block	-	-	1. Two inceptions 2. AvePooling (0.4 dropout)	1. Three Conv 2. Relu 3. a MaxPooling
Output layer	1. A flattened layer 2. Two dense layers 3. Softmax (2 class)	1. A flattened layer 2. Two dense layers 3. Softmax (2 class)	1. A flattened layer 2. Two dense layers 3. Softmax (2 class)	1. A flattened layer 2. Two dense layers 3. Softmax (2 class)

Note: *Conv: convolutional, Relu: rectified linear unit*

Statistical evaluation

Table 3 represents the confusion matrix for evaluating the efficiency of the four models in classifying stroke and normal brain images on CT images where:

True Positives (TP): The model correctly detects and classifies strokes.

True Negatives (TN): The model correctly identifies normal images without detecting a stroke.

False Positives (FP): The model incorrectly detects a stroke on a normal image or an incorrect lesion.

False Negatives (FN): The model fails to detect a stroke on an actual stroke image.

Table 3. Confusion matrix of stoke detection.

Model	Pathology		Total
	Stroke	Normal	
Stroke (positive)	TP	FP	TP+FP
Normal (negative)	FN	TN	FN+TN
Total	TP+FN	FP+TN	TP+FP+FN+TN

The performance of the model was analyzed. The accuracy, positive predictive value (precision), sensitivity (recall), specificity, F-1 score, and false positive rate were calculated using Equations (1) to (6). The receiver operating characteristic curve (ROC) and area under the curve (AUC) were also evaluated.

$$\text{Accuracy} = \frac{TP+TN}{TP+FP+TN+FN} \quad (1)$$

$$\text{Precision} = \frac{TP}{TP+FP} \quad (2)$$

$$\text{Sensitivity (Recall)} = \frac{TP}{TP+FN} \quad (3)$$

$$\text{Specificity} = \frac{TN}{TN+FP} \quad (4)$$

$$\text{F1-score} = 2* \frac{Precision*Sensitivity}{Presision+Sensitivity} \quad (5)$$

$$\text{False Posotive Rate} = 1\text{-Specificity} \quad (6)$$

Results

All brain CT images were segmented, as demonstrated in Figure 2, showing the result that the U-net deep learning model can segment the brain CT images in this study. The predicted area indicates a higher performance of brain segmentation. The average Dice similarity coefficient (DSC) is 0.963, with a Dice loss of 0.037 and a Weighted BCE Dice loss of 0.185.

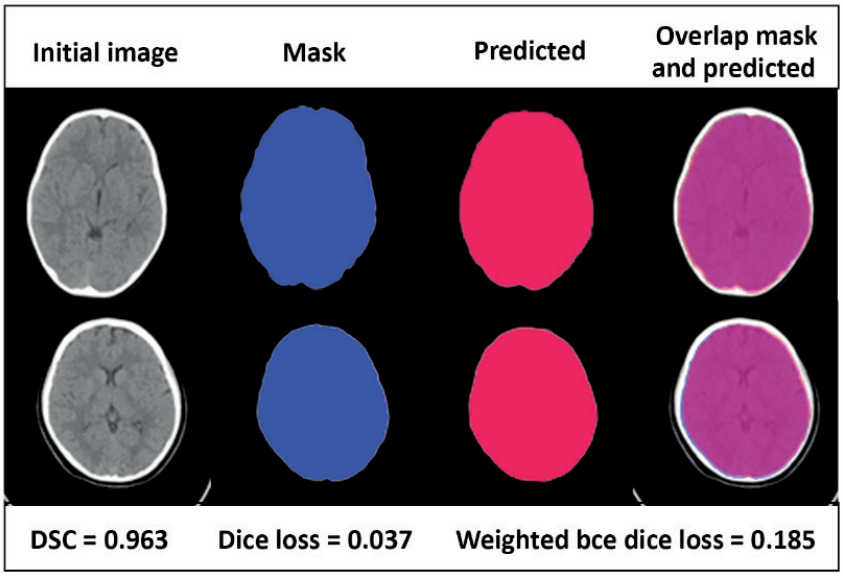

Figure 2. *Segmented brain CT image.*

Table 4 presents the results of evaluating the four models for detecting stroke lesions in CT images. The highest accuracy was achieved by VGG-16 (0.969), while the best precision was observed with GoogleNet (0.976), with VGG-16 as the second-best (0.952). VGG-16 (0.952) also demonstrated the highest sensitivity, whereas GoogleNet had the lowest sensitivity. The specificity of VGG-19 (0.978) was slightly lower than that of GoogleNet (0.988). The F1-score of VGG-16 (0.952) was higher than that of GoogleNet (0.901), CNN-2 model (0.886), and LeNet (0.886). Additionally, the false positive rate of VGG-16 (0.022) was lower than that of the CNN-2 model (0.074) and LeNet (0.074), and comparable to GoogleNet (0.012).

Table 4. The performance of four models

Model	Accuracy	Precision	Sensitivity	Specificity	F-1 score	False positive Rate
CNN-2-model	0.932	0.833	0.946	0.926	0.886	0.074
LeNet	0.932	0.833	0.946	0.926	0.886	0.074
GoogleNet	0.932	0.976	0.837	0.988	0.901	0.012
VGG-16	0.969	0.952	0.952	0.978	0.952	0.022

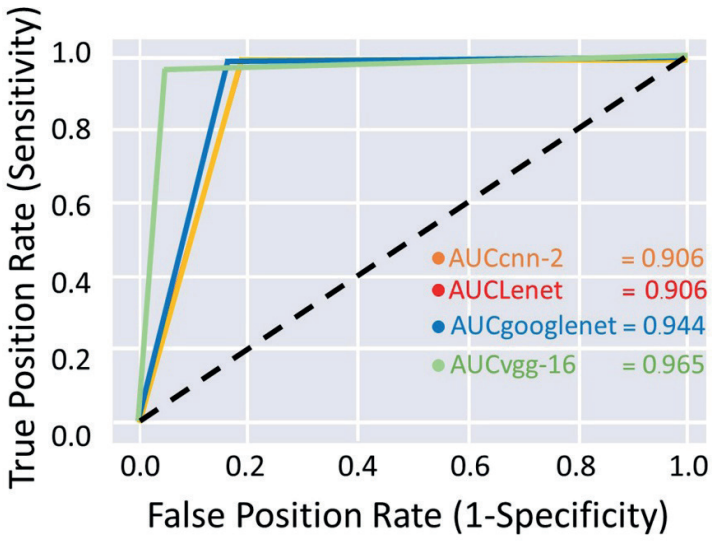

Figure 3. *The receiver operating characteristic curves and areas under the curve of the CNN-2, LeNet, GoogleNet, and VGG-16 models.*
ROC curve and AUC of the VGG-16 (Green Line) model, presented in Figure 3, confirm the highest performance in the detection of strokes in brain CT images. The second-best performance is observed in GoogleNet (Blue Line). The ROC curve and AUC of the CNN-2 (Yellow Line) model are equal to those of LeNet (Red Line), and they exhibit the lowest performance.

Discussion

The primary goal of this study was to address the challenges in stroke diagnosis by introducing and comparing four deep learning techniques for classifying stroke lesions in CT images. The overarching objective was to enhance the diagnostic capabilities of radiologists and contribute to the development of innovative solutions to meet the increasing demand for accurate stroke interpretation. Our evaluation process involved training and assessing four distinct models-CNN-2-Model, LeNet, GoogleNet, and VGG-16-using a dataset comprising 1,636 CT images. Notably, the dataset included a balanced representation of 1,111 normal brain images and 525 stroke images, providing a comprehensive basis for model training and evaluation.

Our study revealed that among the evaluated models, VGG-16 emerged as the top-performing deep learning model. With an accuracy of 0.969, an F-1 score of 0.952, and an AUC of 0.965, VGG-16 demonstrated superior capabilities in accurately classifying stroke lesions in CT images. The robust performance of VGG-16 can be attributed to its deep architecture and its ability to capture intricate patterns within the image data. The model's capacity to learn hierarchical features is particularly advantageous in the nuanced task of stroke lesion classification, contributing to its superior performance compared to other models.

In previous studies, Ammar *et al*. compared five deep learning models (ReNet50, VGG-16, Xception, InceptionV3, and InceptionResNetV2), with VGG-16 demonstrating the highest accuracy performance at 96.0 % for intracranial hemorrhage.[8] Worachotsueptrakun compared four deep learning models (AlexNet, VGG-16, GoogleNet, and ResNet), with GoogleNet exhibiting the best performance, achieving accuracy, precision, recall, and F1-score of 92.00%, 94.00%, 83.96%, and 88.70%, respectively.[9]

Chen *et al*. studied four methods (CNN-2, VGG-16, ResNet-50, and ResNet-50 without dropout) and varied the batch size of training models to 8, 16, 32, 64, and 128, respectively.[14] The best performance was observed in CNN-2 and ResNet-50 without dropout, using a batch size of 128 (98.72% accuracy), followed by CNN-2 with a batch size of 32. Chen's work indicates the effect of batch size on the accuracy of training model performance. Additionally, hybrid algorithms have shown high performance. Ozaltin *et al*.[15] used the hybrid technique of OzNet (Deep Learning combined with Decision tree (Machine learning)) and achieved 98.42% accuracy, compared with only OzNet, where the accuracy of the hybrid method surpassed that of the sole deep learning method (87.74% accuracy). Vamsi *et al*. achieved an accuracy of 97.81% using VGG-16 and random forest, representing another successful hybrid approach.[10]

Implications and future directions

The success of VGG-16 in this study underscores the potential of leveraging deep learning techniques to enhance the accuracy and efficiency of stroke diagnosis. The application of such models in the initial screening of stroke cases holds promise for reducing the burden on radiologists and addressing workforce shortages. However, it is crucial to acknowledge certain limitations in our study, such as the reliance on a specific dataset and the need for further validation on diverse datasets to ensure the generalizability of the findings. Additionally, the interpretability of deep learning models remains an ongoing challenge, and efforts to enhance model explainability are essential for fostering trust in clinical applications.

Conclusion

In conclusion, our research provides valuable insights into the comparative analysis of deep learning techniques for stroke lesion classification in CT images. The superior performance of VGG-16 highlights its potential as a valuable tool in the initial screening of stroke cases. As technology continues to advance, further research and collaboration between clinicians and technologists will be essential to harness the full potential of deep learning in improving stroke diagnosis and patient outcomes.

Conflict of interest

None

Funding

This study received support from the Faculty of Allied Health Sciences, with a grant for general researchers (Grant No. AH-66-01-005) and a research grant for the development of students into researchers in 2023, both provided by the Faculty of Allied Health Sciences, Naresuan University.

Ethical approval

This study was approved by the Ethics Committee of Naresuan University, Thailand (IRB No. P1-0165/2565).

References

[1] Amarenco P, Bogousslavsky J, Caplan LR, Donnan GA, Hennerici MG. Classification of Stroke Subtypes. Cerebrovasc Dis. 2009; 27 (5): 493-501. doi.org/10.1159/000210432

[2] World Health Organization (WHO). World stroke day 2022 [cited 2022 November 17]. Available from: https://www.who.int/srilanka/news/detail/29-10-2022-world-stroke-day-2022

[3] The Ministry of Public Health of Thailand, Public Health Statistics A.D. 2022. [cited 2022 May 14]. Available from: https://spd.moph.go.th/wp-content/uploads/2023/11/Hstatistic65.pdf

[4] González RG. Current State of Acute Stroke Imaging. Stroke. 2013; 44(11): 3260-4. doi.org/10.1161/STROKEAHA.113.003229

[5] Birenbaum D, Bancroft LW, Felsberg GJ. Imaging in Acute Stroke. West J Emerg Med. 2011; 12(1): 67-76. https://www.ncbi.nlm.nih.gov/pmc/articles/PMC3088377/

[6] Raghavendra U, Gudigar A, Paul Aritra, Goutham TS, Inamdar MA, Hegde A, *et al*. Brain tumor detection and screening using artificial intelligence techniques: Current trends and future perspectives. Comput Biol Med. 2023; 163: 107063. doi.org/10.1016/j.compbiomed.2023.107063

[7] Yousaf F, Iqbal S, Fatima N, Kousar T, Rahim MSM. Multi-class disease detection using deep learning and human brain medical imaging. Biomed Signal Process Control. 2023; 85: 104875. doi.org/10.1016/j.bspc.2023.104875

[8] Ammar M, Lamria MA, Mahmoudib S, Laidia A. Deep Learning Models for Intracranial Hemorrhage Recognition: A comparative study. Procedia Comput Sci. 2022; 196: 418-25. doi.org/10.1016/j.procs.2021.12.031

[9] Worachotsueptrakun C. A comparison of 3D Convolutional neural network for brain stroke classification with CT scan images. Chulalongkorn University theses and dissertations. 2022. https://digital.car.chula.ac.th/chulaetd/6664

[10] Vamsi B, Bhattacharyya D, Midhunchakkravarthy D, Kim JY. Early Detection of Hemorrhagic Stroke Using a Lightweight Deep Learning Neural Network Model. Trait du signal. 2021; 38(6): 1727-36. doi.org/10.18280/ts.380616

[11] Tasnia N. brain-stroke-prediction-ct-scan-image-dataset. [cited 2022 May 1]. Available from: https://www.kaggle.com/datasets/noshintasnia/brain-stroke-prediction-ct-scan-image-dataset

[12] Vbookshelf. Brain CT Images with Intracranial Hemorrhage Masks. [cited 2022 May 1]. Available from: https://www.kaggle.com/datasets/vbookshelf/computed-tomography-ct-images

[13] Pandey N. Lung segmentation from Chest X-Ray dataset. Kaggle Inc [cited 2022 April 28]. Available from: https://www.kaggle.com/code/nikhilpandey360/lung-segmentation-from-chest-x-ray-dataset/notebook

[14] Chen YT, Chen YL, Chen YY, Huang YT, Wong HF, Yan

JL, Wang JJ. Deep Learning–Based Brain Computed Tomography Image Classification with Hyperparameter Optimization through Transfer Learning for Stroke. Diagnostics 2022; 12, 807. doi.org/10.3390/diagnostics12040807

[15] Ozaltin O, Coskun O, Yeniay O, Subasi A. A Deep Learning Approach for Detecting Stroke from Brain CT Images Using OzNet. Bioeng. 2022; 9(12): 783. doi.org/10.3390/bioengineering9120783

Journal of Associated Medical Sciences 2024; 57(2): 56-66

JAMS
Journal of Associated Medical Sciences

Scopus Indexed & Thai-Journal Citation Index Centre (TCI)

Journal of Associated Medical Sciences

Journal homepage: https://www.tci-thaijo.org/index.php/bulletinAMS/index

Cognitive intervention using Montessori and DementiAbility for people with mild cognitive impairment

Chadchom Ratsameemonthon[1*] Teppagone Pittayapinune[2] Arbtip Petchsakul[3] Sasithorn Kemsen[4]

[1]Faculty of Education and Liberal Arts, Hatyai University, Songkla Province, Thailand.
[2]Thai Wisdom Institute for Research and Development, Songkla Province, Thailand.
[3]Hatyai City Municipality Office, Songkla Province, Thailand.
[4]Songkhla Rajanagarindra Phychiatric Hospital, Songkla Province, Thailand.

ARTICLE INFO

Article history:
Received 24 September 2023
Accepted as revised 5 February 2024
Available online 22 February 2024

Keywords:
Mild cognitive impairment, Montessori, dementiAbility, cognitive program ability

ABSTRACT

Background: Age-related illnesses are more prevalent with advancing age, with seniors facing more chronic diseases and disabilities. Chronic diseases that mostly older adults deal with are caused by high blood pressure, diabetes, and high cholesterol-also called noncommunicable diseases (NCDs). NCDs can cause severe chronic diseases such as heart disease, kidney failure, and cerebrovascular disease, and these can result in a high risk of Mild Cognitive Impairment (MCI). Together, brain cells shrink around 2,000 million cells when getting older, causing difficulty recalling names or words, decreased attention span, or a decreased ability to handle many tasks simultaneously. Therefore, protecting senior citizens with MCI needs to be seriously consideration.

Objectives: This quasi-experimental research aimed to study the effects of a program to reduce brain deterioration in older people with Mild Cognitive Impairment (MCI).

Materials and methods: The samples consisted of senior males and females requiring service at Songkhla Rajanagarindra Psychiatric Hospital, Songkhla, Thailand. A sample group was selected using an equivalent group design. The researcher utilized inclusion and exclusion criteria to gather 32 older adults and employed a simple random selection into experimental and control groups. For three months, the experimental group engaged in a seven-care-kit program based on Montessori's philosophy and DementiAbility methods to help protect against brain deterioration. Mann-Whitney U test and Wilcoxon Value were used to analyze the result of the program's effectiveness, which assessed cognitive ability by MoCA.

Results: The attention span domain showed a significant statistical difference at (p=0.03) after post-tests comparing the experimental and control groups. A comparison of the pre-test and post-test of the experimental group found four domains-total cognitive domain, attention span domain, delayed recall domain, and visuospatial perception domain were significant with a statistical difference of (p=0.001, p=0.002, p=0.003, and p=0.004 respectively). Moreover, two domains- the delayed recall domain and the total cognitive domain in the control group showed a significant statistically increasing difference at (p=0.001 and p=0.005, respectively).

Conclusion: The senior citizens' active daily activities may help protect against dementia in older adults with MCI. The Home-Based Protection of Brain Deterioration Program demonstrated a satisfactory program that enhanced the attention span, visuospatial domain, and delayed recall of older people with mild cognitive impairment. Hence, the program as a dementia prevention program for older adults with MCI.

* **Corresponding contributor.**
Author's Address: *Faculty of Education and Liberal Arts, Hatyai University, Songkla Province, Thailand.*
E-mail address: leelie@hu.ac.th
doi: 10.12982/JAMS.2024.027
E-ISSN: 2539-6056

Introduction

In 2022, the world's population aged 60 and over was 779 million. This condition is because the aging population is living longer. Seniors are reaching their sixties and beyond. Thus, there is no doubt that by 2050, the number of seniors aged 60 years will double (2.1 billion), and seniors aged 80 and beyond will be 426 million. Thailand will be an aged society soon because the number of older adults has been increasing dramatically since 2018, increasing to 16.06%, 2019 up to 16.73%, and in 2020 increasing to 17.57% of the population.[1] If any country has older adults reporting 20% or above of the population, that country is called an aging society.

Age-related illnesses are more prevalent with advancing age, with seniors facing more chronic diseases and disabilities.[2] Chronic diseases that mostly older adults deal with are caused by high blood pressure, diabetes, and high cholesterol-also called noncommunicable diseases (NCDs). NCDs can cause severe chronic diseases such as heart disease, kidney failure, and cerebrovascular disease, and these can result in a high risk of Mild Cognitive Impairment (MCI).[3] Together, brain cells shrink around 2,000 million cells when getting older, causing difficulty recalling names or words, decreased attention span, or a decreased ability to handle many tasks simultaneously.[4] Farias *et al.* mentioned that a person diagnosed with MCI will have a higher risk of having dementia, around 10-15%, compared with ordinary people.[5] Therefore, protecting senior citizens with MCI needs to be seriously consideration.

Previous research found that people who stay active and have regular social interaction will have a lower risk of dementia.[6] However, during the Covid-19 pandemic, most older adults stayed at home to prevent the spread of the virus. Consequently, many older adults lost mobility and less frequently engaged in social activities. Pellecchia *et al*. found that Physical Functional Impairment (PFI) played an intermediary role in the relationship between Post-Traumatic Stress Disorder (PTSD) and Mild Cognitive Impairment (MCI).[7] The researchers mentioned that PFI may be the first sign of MCI in people with PTSD. Less physical movement increases the chances of diseases, disability, hospitalization, poorer quality of life, and death. It could imply that people with MCI stayed active in their physical, cognitive, social, and spiritual activities, their deteriorating cognition condition could be reduced, and cognition could return to normal depending on the level of engagement.[8]

In Thailand, previous research promoting cognition exercise in older adults with MCI found various results, e.g., Samael, Thaniwattananon, and Kong-In reported that attention span was reduced when reducing the number of cognition exercise appointments.[9] Jeeraya *et al*. revealed no significant difference in the cognition level, but there was a higher level of self-competency in the experimental group compared with the control group.[10] Lastly, Apichonkit *et al.* employed multi-activities to develop different domains of cognition and showed positive results in all parts of understanding except language and delayed recall.[11] The researchers claimed that these two domains are the most challenging in improving people's awareness of MCI.

Previous research implied that activities for improving aging people's cognition with MCI are needed, and various activities to improve different cognitive domains and consistency of engaging in activities played significant roles in designing a stimulating cognitive program. As a result, this research utilized the Montessori philosophy and DementiAbility to develop a cognition exercise program. Both theoretical concepts are derived from a person-centered concept. For example, Montessori focuses on systematic activity presentation to help a person achieve in activity, resulting in increased self-value. DementiAbilty designs activities based on people's needs, interests, and experiences relevant to each culture and religion; therefore, it helps people engage in activities consistently by enhancing their abilities. Moreover, activities are designed to help older people participate at home to prevent the spread of COVID-19. Hence, it could assist older adults in learning even during the lockdown during the COVID pandemic or even due to their physical functioning limitations.

Materials and methods

This research was conducted as a quasi-experimental design to study the effect of intervention activities on participants' cognitions. The Montreal Cognitive Assessment (MoCA) assessed it, consisting of visuospatial/executive, naming three kinds of animal, memory, attention span, language, abstraction, delayed recall, and orientation domains. A simple random sampling and an equivalent group design were employed to select a sample group with no different abilities into an experimental group and a control group equally. Ethical approval was obtained from the Suan Saranrom Psychiatric Hospital (DMH.IRB 004/2564). Procedures were explained to get informed consent before participants joined the research. All participants signed an informed consent form after reading it and agreeing to join the study.

Participants

Purposive sampling was applied to select participants for this research. The participants were those using a service at the Songkhla Rajanagarindra Psychiatric Hospital, Thailand, specializing in neurological disorders. The sample was (N=32) aged between 60 and 70 years with MCI identified by a Thai version of the MoCA and with an assessment range between ≥17 to ≤24. Thirty-two people were randomly distributed into an experimental group and a control group. Both experimental and control groups reported spending life typically and could read, understand, and write in Thai. Interviews were conducted to gather personal data on physical health, motivation, ability, daily routine, fears, worries, and needs to design activities matching their interests and abilities. People who were diagnosed as clinically depressed were excluded from the research samples. The experimental group participated in a program protecting against the deterioration of cognitive impairment, which designed

activities based on Montessori and DementiAbility and focused on individual needs, abilities, and interests. Seven home care kits were sent to the experimental group's homes. A video presentation and Line, a messaging application, were utilized to follow up on the activity's participation. There was no extra activity from researchers for the control group. They spent their daily routine typically.

Measurement

Two measurements were used for the exclusion and inclusion of participants participating in the research, which were TGDS-15 and MoCA. Moreover, the MoCA was employed to be an outcome measurement. The detail was described as follows:

1) The Thai Geriatric Depression Scale, TGDS-15-Short version created by Shiekh, Yesavage[12] translated into Thai version by Wongpakaran, Wongpakaran, Reekum.[13] Each question is scored as 0 or 1 point; the maximum score is 15. A score above five is used as the cut-off point for detecting depression and has a sensitivity of 86.0% and specificity of 91.0%. The measurement presented good reliability, as shown by the score of Cronbach's alpha at 0.85.
2) Nasreddine *et al*. created the Montreal Cognitive Assessment Thai-version (MoCA). The MoCA Thai version was translated and tested for the reliability in 2007.[14] Eleven questions testing capability comprised Visuospatial, Naming, Attention Span, Language, Delayed recall, Orientation, and Total cognitive ability. The questionnaire took about 10 minutes to complete. A total score of 30 points and a score of more than or equal to 17 and less than or similar to 24 indicated that the subject had mild cognitive impairment. The measurement presented good reliability, shown by a Cronbach's alpha score of 0.80.[15] MoCA was utilized to measure outcomes by assessing before and after implementing the treatment program. MoCA assessor was two persons. One person was a psychologist who gained certification as an administrator from MoCA Test Inc., and one was a nurse with experience using MoCA for more than ten years at a psychiatric hospital.

The process of samples' inclusion and exclusion and outcome assessment is illustrated in Figure 1.

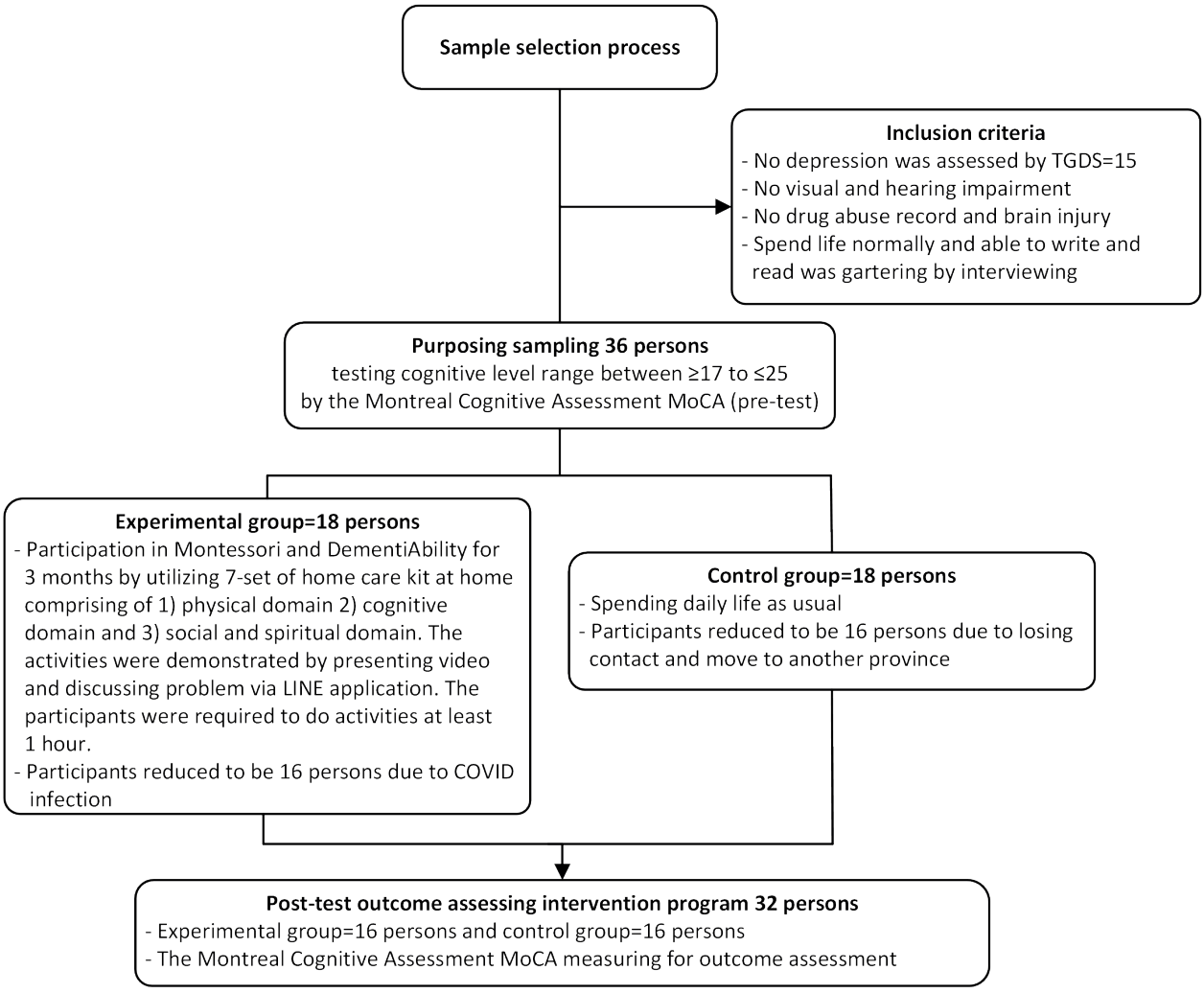

Figure 1 *Diagram of samples' inclusion and exclusion and outcome assessment.*

Procedure

The participant screening was from November to December 2021 at Songkhla Rajanagarindra Psychiatric Hospital. Participants were the older adults who gained a MoCA assessment ranking of more than or equal to 17 and less than or equal to 24 and had no diagnosis of depression, brain injury, or drug addiction. Almost all participants could read, write, work, and financially help their families. Thirty-two people were randomly assigned into two groups: 16 for the experiment and 16 for the control groups. The treatment program for the experimental group was conducted from January to March 2022. As this research was conducted during the COVID pandemic, the intervention program or a seven-set home care kits was a treatment program sent to the participants' homes for three months. The seven-set home care kits were comprised of 3 domains: 1) physical domain emphasizing physical exercise activities such as left-right brain exercise using hand and fingers and 9-square-table aerobic exercise 2) cognitive domain enhancing attention, stimulating cognition such as brain teaser exercise, e.g., mathematics and languages, and eye-hand coordination activities, and 3) social and spiritual domain nurturing social connection such as writing cards and enhancing spiritual belief such as coloring mandala arts and praying relevant to individual respectfulness.

Before launching the intervention, a pilot test was applied to three elderly people with MCI who had similar backgrounds to the research participants but lived in different places. The pilot group participated in the program for two weeks. After that, they were interviewed about program satisfaction and practicality. The researcher adjusted the program based on the pilot group's suggestions. Finally, the program has been approved by three experts: a psychiatrist and two nurses with more than five years of experience with people having dementia and MCI.

At the first day of the intervention, the instruction was demonstrated by video presentations. In addition, the Line application was used to communicate and follow up regarding the activities' difficulty level and designed activities to match participants' interests and abilities. The participants were asked to engage in activities for at least one hour per day, e.g.,1) physical activities spending time for 20 minutes or more per day, 2) cognitive activities using time for 20 minutes or more per day, e.g., brain tease exercise, and 3) social and spiritual activities utilizing time for 20 minutes per day or more, e.g., coloring or praying. Each week, participants reported levels of activities engagement to evaluate the effectiveness of each activity. After completing the treatment program, the experimental and control groups did a post-test of the MoCA and were interviewed to gather more information.

Statistical analysis

Demographic data and activity satisfaction were analyzed and illustrated using mean and percentages. The Median Wilcoxon Value was employed to identify the cognition differences in the post-test of the two groups. Mann-Whitney U was employed to examine the differences between pre-test and post-tests scores of each group. Interview data was analyzed for satisfaction with the activities.

Results

Most of the participants were between the age of 60-65 (56.25%), predominantly female (78.12%), and mostly completed primary school six years of schooling (59.38%). Most participants were gardeners (34.38%), chronic illness (87.50%). No difference existed between the group before the intervention, indicated by the median experimental group, 21.00, and the control group, 20.50. After the intervention, Mild cognitive impairment was evident by a median of MoCA's score for the experimental group of pre-test 21.00 and post-test 25.00 and for a control group of pre-test 20.50 and post-test 23.00. All values are present. Demographic information is shown in Table 1

Table 1 Baseline of demographic characteristics of participants.

Details	Experimental group	Control group	Percentage (range)
Age (60-65 years)	9 (56.25%)	9 (56.25%)	18 (56.25%)
Gender (female)	13 (81.25%)	12 (75.00%)	25 (78.12%)
Education (primary level)	9 (56.25%)	10 (62.50%)	19 (59.38%)
Occupation (gardener)	5 (31.25%)	6 (37.50%)	11 (34.38%)
A chronic illness	15 (93.75%)	13 (81.25%)	28 (87.50 %)
Mild cognitive impairment (Montreal cognitive assessment Thai version (MoCA))			
Pre-test	21.00 (median)	20.50 (median)	Min=17 Max=24
Post-test	25.00 (median)	23.00 (median)	Min=18 Max=28

Intervention program and cognitive level

The Mann-Whitney U Test was applied to compare the effect of intervention between the experiment group and the control group before and after the experiment. Before the experiment period, there was no significant difference between the experiment group and the control group, as shown in Table 2. After the investigation, the results found a statistically significant difference between the experimental and control groups regarding the attention span domain (p=0.03). There were four domains that the experimental group showed a higher medium score than the control group: visuospatial perception (experimental group M=3.50 and control group M=3.00), attention span (experimental group M=5.00, control group M=4.50), language use (experimental group M=2.00, and control group M=1.00), and abstract thinking (experimental group M=1.00, control group M=0.50). The two domains, naming three kinds of animals and delayed recall, showed the same medium score between groups. The orientation domain of the control group presented a higher medium score than the experimental group (experimental group M=5.00 and control group M=6.00), which is illustrated in Table 3.

Table 2 Comparison cognitive score of mean, median, and Mann-Whitney U test before intervention of experimental group and control group separated in each domain.

Cognitive domain	N	Median	Mean	Mean rank	Sum of rank	Mann-Whitney U	
						Value	Prob
Visuospatial							
Experimental group	16	3.00	3.13	15.41	246.50	110.5	0.51
Control group	16	3.50	3.38	17.59	281.50		
Total	32	3.00	3.25				
Naming							
Experimental group	16	3.00	2.87	16.56	265.00	127.0	0.99
Control group	16	3.00	2.81	16.44	263.00		
Total	32	3.00	2.84				
Attention span							
Experimental group	16	4.00	4.13	16.88	270.00	122.0	0.84
Control group	16	4.00	3.94	16.13	258.00		
Total	32	4.00	4.03				
Language							
Experimental group	16	1.00	1.38	16.63	266.00	126.0	0.96
Control group	16	1.00	1.38	16.38	262.00		
Total	32	1.00	1.38				
Abstraction							
Experimental group	16	1.00	0.94	17.72	283.50	108.5	0.47
Control group	16	1.00	0.75	15.28	244.50		
Total	32	1.00	0.84				
Delayed recall							
Experimental group	16	2.00	1.94	16.00	256.00	120.0	0.78
Control group	16	2.50	2.06	17.00	272.00		
Total	32	2.00	2.00				
Orientation							
Experimental group	16	6.00	6.00	17.00	272.00	120.0	0.78
Control group	16	6.00	5.94	16.00	256.00		
Total	32	6.00	5.97				
Total cognitive ability							
Experimental group	16	21.00	20.75	16.88	270.00	122.0	0.84
Control group	16	20.50	20.56	16.13	258.00		
Total	32	21.00	20.66				

Table 3 Comparison cognitive score of mean, median, and Mann-Whitney U test after intervention of experimental group and control group separated in each domain.

Cognitive domain	N	Median	Mean	Mean rank	Sum of rank	Mann-Whitney U	
						Value	Prob
Visuospatial							
Experimental group	16	3.50	3.75	18.16	290.50	101.5	0.32
Control group	16	3.00	3.31	14.84	237.50		
Total	32	3.00	3.53				
Naming							
Experimental group	16	3.00	2.94	17.03	272.50	119.0	0.75
Control group	16	3.00	2.81	15.97	255.50		
Total	32	3.00	2.87				
Attention span							
Experimental group	16	5.00	5.25	20.09	321.50	70.50	0.03**
Control group	16	4.50	4.31	12.91	206.50		
Total	32	5.00	4.79				
Language							
Experimental group	16	2.00	1.44	16.69	267.00	125.0	0.93
Control group	16	1.00	1.44	16.31	261.00		
Total	32	1.50	1.44				
Abstraction							
Experimental group	16	1.00	1.19	18.41	294.50	97.5	0.25
Control group	16	0.50	0.88	14.59	233.50		
Total	32	1.00	1.03				
Delayed recall							
Experimental group	16	4.00	3.81	15.50	248.00	112.0	0.56
Control group	16	4.00	4.19	17.50	280.00		
Total	32	4.00	4.00				
Orientation							
Experimental group	16	5.00	5.88	15.50	248.00	112.0	0.56
Control group	16	6.00	6.00	17.50	280.00		
Total	32	6.00	5.97				
Total cognitive ability							
Experimental group	16	25.00	24.75	19.00	304.00	88.0	0.14
Control group	16	23.50	23.19	14.00	224.00		
Total	32	24.00	23.19				

The experiment group (before and after the experiment period)

The Wilcoxon Value was employed to compare cognition scores before and after joining the intervention program of the experimental group. The result showed that four domains showed a statistically significant difference, e.g., total cognition ability (p=0.001), attention span (p=0.002), delayed recall (p=0.003), and visual-spatial perception (p=0.004). Moreover, the median score of all cognitive domains in the experimental group after the intervention period reported a higher score than before the intervention period, except naming, abstraction, and orientation, which reported the same score, which is shown in Table 4.

Table 4 Comparison cognitive score of mean, median, and The Wilcoxon Value test after intervention of experimental group separated in each domain.

Cognitive domain	N	Median	Mean	SD	Wilcoxon value	Wilcoxon prob
Visuospatial						
Post-intervention	16	3.50	3.73	1.29	2.673	0.004**
Pre-intervention	16	3.00	3.13	1.09		
Naming						
Post-intervention	16	3.00	2.94	0.25	1.000	0.158
Pre-intervention	16	3.00	2.87	0.34		
Attention span						
Post-intervention	16	5.00	5.25	0.78	2.951	0.002**
Pre-intervention	16	4.00	4.13	1.15		
Language						
Post-intervention	16	2.00	1.44	0.89	0.159	0.437
Pre-intervention	16	1.00	0.89	0.81		
Abstraction						
Post-intervention	16	1.00	1.19	0.66	1.265	0.103
Pre-intervention	16	1.00	0.94	0.68		
Delayed recall						
Post-intervention	16	4.00	3.81	1.33	2.783	0.003**
Pre-intervention	16	2.00	1.94	1.61		
Orientation						
Post-intervention	16	6.00	5.88	0.34	1.414	0.079
Pre-intervention	16	6.00	6.00	0.00		
Total cognitive ability						
Post-intervention	16	25.00	24.75	2.15	3.360	0.001**
Pre-intervention	16	21.00	20.75	2.05		

The control group (before and after the experiment period)

The results showed a statistical difference in the total cognition ability (p=0.005) and delayed recall (p=0.001). After the experimental period, three parts-total cognition ability, delayed recall, and attention span-showed a higher medium score. Three domains-language, naming three kinds of animals, and time and place orientation-showed the same medium score. Visual-spatial perception and abstract thinking showed a lower medium score when compared before and during the intervention periods, presented in Table 5.

Table 5 Comparison cognitive score of mean, median, and The Wilcoxon Value test after intervention of control group separated in each domain.

Cognitive domain	N	Median	Mean	SD	Wilcoxon value	Wilcoxon prob
Visuospatial						
Post-intervention	16	3.00	3.31	1.14	0.183	0.427
Pre-intervention	16	3.50	3.38	1.59		
Naming						
Post-intervention	16	3.00	2.81	0.54	0.000	0.500
Pre-intervention	16	3.00	2.81	0.54		
Attention span						
Post-intervention	16	4.50	4.31	1.20	1.103	0.135
Pre-intervention	16	4.00	3.94	1.19		
Language						
Post-intervention	16	1.00	1.44	1.03	0.183	0.428
Pre-intervention	16	1.00	1.38	1.09		
Abstraction						
Post-intervention	16	0.50	0.88	1.025	0.302	0.381
Pre-intervention	16	1.00	0.75	0.78		
Delayed recall						
Post-intervention	16	4.00	4.19	0.83	3.443	0.001**
Pre-intervention	16	2.50	2.06	1.44		
Orientation						
Post-intervention	16	6.00	6.00	0.00	1.000	0.159
Pre-intervention	16	6.00	5.94	0.25		
Total cognitive ability						
Post-intervention	16	23.00	23.19	2.99	2.584	0.005**
Pre-intervention	16	20.50	20.56	2.16		

Discussion and implication

Over ten weeks, a seven-set home care kit was delivered to the experimental group's homes every 12 weeks. A stimulating daily program schedule has been set to develop three domains: the physical, cognitive, and social domains, including spiritual domains. Furthermore, MoCA was used as an outcome measurement to identify the treatment program's effectiveness. The results showed that the post-test comparison between the experimental and control groups was significantly different in the attention span domain at p=0.03 (experimental group, M=5.00 and control group, M=4.50). Using the Wilcoxon Value, the results showed that pre- and post-test scores of the experimental group were significantly different in 4 domains: total cognition ability p=0.001, (pre-test, M=21.00 and post-test M=25.00), attention span p=0.002, (pre-test, M=4.00 and post-test M=5.00), delayed recall p=0.003, (pre-test, M=2.00 and post-test M=4.00) and visuospatial perception ability p=0.004, (pre-test, M=3.00 and post-test M=3.50). For control group, there were two domains that showed significant different between pre- and post-test: delayed recall p=0.001 (pre-test, M=2.50 and post-test, M=4.00) and total cognition ability p=0.005 (pre-test, M=20.50 and post-test, M=23.00).

According to these research findings, the attention span domain significantly differed between the experimental and control groups. This finding may be due to using Montessori's pedagogy and the multidisciplinary research integrated throughout the DementiAbility Methods. Montessori was primarily focused on the attention domain. She mentioned that attention helps a person concentrate and derives from an internal passion, resulting in repetitive and consistently engaging activities. The DementiAbility Methods expand on Montessori's work and with current research that includes both forms (procedural and declarative/explicit and implicit) and types (working, short-term, and long-term) of memory to help explain enhanced functioning in each of the three personhood domains (cognitive, physical, and social/spiritual). Neuropsychologists have discovered that success related to achieving tasks and activities is based on what is known about supporting memory loss and understanding spared abilities and learned associations.[16,17] When memory is supported, individuals can circumvent the deficits associated with cognitive decline (according to the type of damage, location of injury, and extent of damage at the brain level).

Attention, visual-spatial perception, working memory, and cognition ability

Attention plays a significant role in storing visuospatial information, particularly related to new items entering perception, attention-helping encoding, maintenance, and retrieval.[18] Two areas of attention and working memory (WM) function harmoniously. First, attention helps to keep the information in mind and protects irrelevant stimuli or wandering thoughts from interfering.[19] Attention also helps with removing irrelevant information from working memory in an attempt to remain focused.[20] Second, working memory is necessary when carrying out a new task that was just learned or being learned.[21] Working memory operates on the further action inconsistent with a previously learned one and when it switches from one study to another. WM plays a crucial role in controlling attention and action automatically in response to changing to a new one.[22] Regarding visual-spatial ability, older adults' cognition deterioration and gaze behavior require working memory to apply different encoding strategies to interpret spatial relationships. For example, Meiran found that older adults prefer to use landmark strategies (such as windows or doors) as the categorical representations of location concerning the environment.[22] They found this was due to difficulties in formulating precise space relations, which differs from young adults who focus on the local arrangement of objects.[23] Therefore, the impact of external irrelevant stimuli must be more clearly understood when creating interventions and environments (e.g., eliminating unnecessary external markings on activities, flooring, and table tops) and applied to interventions and environments for those with MCI. It may imply that when older adults face uninformative landmarks, they are more likely to have difficulty extracting helpful information from the tasks. Then, they must control their attention to encode data into categorical relationships to facilitate decision-making precision. As a result, people with MCI who are challenged by WM deficits need more understanding when new tasks involve complicated processes. When the limitations of WM and the need to control and focus on attention are considered, interventions can be developed to enhance performance and quality outcomes, such as understanding new tasks, including protection against the risk of falling.[23]

The DementiAbility Methods embed these concepts of working memory into its pedagogy. Research related to all forms of memory is integrated into all parts of the DementiAbility Methods, including assessment tools, activities, environments, and resources for individuals. All forms of memory need to be clearly understood and integrated into understanding and addressing the needs and abilities of individuals to achieve successful outcomes. It is a critical component of successful programming, as older adults adopt mastery avoidance goals, and, overall, they do not want to fail or showcase that their ability or comprehension has diminished.[25] When older adults understand a task and complete it, they are more likely to engage with a sense of achievement, mastery, and joy, thereby prolonging engagement and successful outcomes.

Research on the neuroplastic brain, also known as neural plasticity of the brain, has grown in recent years.[26-28] This research suggests that even if the brain's physical structures deteriorate, learning ability is flexible, and the brain can reorganize its structures and functions, thus creating the ability to learn new activities. This research can be used to re-teach people what they previously knew and teach older adults to learn and do new things.[29] When applying their past experiences to learn and understand new tasks, a systematic approach of visual-spatial perception helps them spend less time trying to understand how to perform activities.[22] Nilakantan *et al*. found that learning occurs in sequence, discovering that moving from simple to complex activities and tasks is best.[22] Montessori and DementiAbility integrate this concept into their programming. When these concepts are implemented, older adults enjoy a sense of achievement, thus creating successful outcomes when engaged in activities that match their abilities. Also, attention plays a crucial role in restoring visual-spatial perception related to sensation perception and the environment, leading to formulating plans and conceptual thinking.[30] Enhanced self-esteem and well-being goals can be more readily achieved When activities enhance their confidence to set and initiate their daily schedules and engage them successfully while adding purpose in life. Wells and Dawson have found that a lot of the decline witnessed in dementia is due to disuse rather than due to neurological abnormalities.[31] Owen, Berry, and Brown found that when activities are meaningful, stimulating, and purposeful, behavioral concerns are addressed, and quality of life is enhanced for the person with dementia and their care providers.[32] Sutin *et al.* also found that older adults engaging in intervention with a strong sense of purpose could reduce the risk of dementia by 30%.[33] Therefore, enabling abilities based on a clear understanding of the function of memory (working memory, declarative, and procedural memory) can impact outcomes when considered with multi-modal interventions (including activity programming). However, due to the short intervention duration, the participants may remember content in the MoCA as utilizing only the outcome assessment.

In conclusion, research on memory, learning, and perceptual deficits play a crucial role in creating successful, engaging activities and environments for older adults, and most importantly, an understanding of memory impacts outcomes when activities are matched to interests, skills, and abilities. Programs such as Montessori for dementia and DementiAbility not only take these critical components of memory into account as they relate to MCI, but they also focus on the whole person's needs, taking the physical domain, cognitive domain, and the social and spiritual domain into account. It, in turn, enhances the attention domains and promotes working on visual-spatial perception and delayed recall in working memory in older adults with MCI. The results of this paper provide evidence that current research on memory when integrated into activity programming, enhances abilities and may help protect against dementia in older adults with MCI.

Conflict of interest

The authors declare no conflict of interest.

Funding

This study was supported by The office of the Ministry of Higher Education, Science, Research, and Innovation.

Acknowledgements

We thank Elliot Gail (DementiAbility Enterprises Inc.) for the education, supporting tools, and materials. Her mentorship helped create person-focused activity kits.

References

[1] Department of Older People. National Senior Citizen of the Year 2020: Amarin Printing and Publishing Public Company Limited, Bangkok, Thailand; 2020.

[2] Franceschi C, Garagnani P, Morsiani C, Conte M, Santoro A, Grignolio A, *et al*. The continuum of aging and age-related diseases: Common mechanisms but different rates. Front Med (Lausanne). 2018; 12 (5). doi: 10.3389/fmed.2018.00061. PMID: 29662881; PMCID: PMC5890129.

[3] Nukred B. Ageing Nursing. Bangkok: Yuttarin Printing Co; 2007.

[4] Chasirikarn S, Janvetsaman P. Exercise brain manual. 2nd Ed. Bangkok: We print; 2008.

[5] Farias ST, Cahn-Weiner D, Harvey D, Reed B, Mungas D, Kramer JH, Chui H. Longitudinal changes in memory and executive functioning are associated with longitudinal change in instrumental activities of daily living in older adults. Clin Neuropsychol. 2009; 23: 446-61.

[6] Sommerlad A, Sabia S, Singh-Manoux A, Lewis G, Livingston G. Association of social contact with dementia and cognition: 28-year follow-up of the Whitehall II cohort study. PLoS Med. 2019; 16(8): e1002862. doi: 10.1371/journal.pmed.1002862.

[7] Pellecchia A, Kritikos M, Guralnik J, Ahuvia I, Santiago-Michels S, Carr M, Kotov R, Bromet EJ, Clouston SAP, Luft BJ. Physical functional impairment and the risk of incident Mild Cognitive Impairment in an observational study of World Trade Center responders. Neurol Clin Pract. 2022; 12(6): 162-171. doi:10.1212/CPJ.0000000000200089.

[8] Stieger M, Lachman ME. Increases in cognitive activity reduce aging-related declines in executive functioning. Front Psychiatry. 2021; 12: 708974. doi:10.3389/fpsyt.2021.708974.

[9] Samael L, Thaniwattananon P, Kong-in W. The Effect of Muslim-Specific Montessori-Based Brain-Training Program on Promoting Cognition in Muslim Elderly at Risk of Dementia. Princes of Naradthiwas University Journal. 2016; 8: 16-21.

[10] Jeeraya S, Hengudomsub P, Vatanasin D, Pratoomsri, W. Effects of cognitive stimulation program on perceived memory self-efficacy among older adults with mild cognitive impairment. JFONUBUU 2018; 26(2): 30-9.

[11] Apichonkit S, Narenpitak A, Mudkong U, Awayra P, Pholprasert P, Pichaipusit A. Effectiveness of a cognitive function's improvement program in elderly MCI patients of primary care unit network of Udonthani Hospital. Udonthani 2019; 27(2): 138-49. (in Thai).

[12] Sheikh JI, Yesavage JA. Geriatric Depression Scale (GDS): Recent evidence and development of a shorter version. Clin Gerontol. 1986; 5(1-2): 165-73. doi:10.1300/J018v05n01_09.

[13] Wongpakaran N, Wongpakaran T, Van Reekum R. The Use of GDS-15 in Detecting MDD: A Comparison Between Residents in a Thai Long-Term Care Home and Geriatric Outpatients. J Clin Med Res. 2013; 5(2): 101-11. doi:10.4021/jocmr1239w

[14] Nasreddine ZS, Phillips NA, Bedirian V, Charbonnean S, Whitehead V, Collin I, Cummings JL, Chertkow H. The Montreal Cognitive Assessment, MoCA: A brief screening tool for Mild Cognitive Impairment. J Am Geriatr Soc. 2005; 53(4): 695-9.

[15] Hemrungrojn S. MoCA Thai version 2007. In: MoCA Montreal - Cognitive Assessment. 2011.

[16] Tulving E. Memory and consciousness. Can Psychol. 1985; 26(1): 1-12. doi:10.1037/h0080017.

[17] Tulving E. Concepts of memory. In: Tulving E, Craik FIM, editors. The Oxford Handbook of Memory. Oxford: Oxford University Press; 2000. p. 33-43.

[18] Jonides J, Lewis RL, Nee DE, Lustig CA, Berman MG, Moore KS. The mind and brain of short-term memory. Annu Rev Psychol. 2008; 59: 193-224. doi:10.1146/annurev.psych.59.103006.093615.

[19] Postle BR. Working memory as an emergent property of the mind and brain. Neuroscience. 2006; 139(1): 23-38. doi:10.1016/j.neuroscience.2005.06.005.

[20] Oberauer K. Working Memory and Attention: A Conceptual Analysis and Review. J Cogn. 2019; 8(2): 3-23. doi:10.5334/joc.58.

[21] Oberauer K, Souza AS, Druey M, Gade M. Analogous mechanisms of selection and updating in declarative and procedural working memory: experiments and a computational model. Cogn Psychol. 2013; 66: 157-211. doi: 10.1016/j.cogpsych.2012.11.001

[22] Meiran N, Liefooghe B, De Houwer J. Powerful instructions: Automaticity without practice. Curr Dir Psychol Sci. 2017; 26(6): 509-14. doi:10.1177/0963721417711638.

[23] Nilakantan AS, Bridge DJ, VanHaerents S, Voss JL. Distinguishing the precision of spatial recollection from its success: Evidence from healthy aging and unilateral mesial temporal lobe resection. Neuropsychologia. 2018; 119: 101-6. doi:10.1016/j.neuropsychologia.2018.07.035.

[24] Montero-Odasso M, Muir SW, Speechley M. Dual-task complexity affects gait in people with mild cognitive impairment: the interplay between gait variability, dual tasking, and risk of falls. Arch Phys Med Rehabil. 2012; 93: 293-9.

[25] Bong M. Age-Related differences in achievement goal differentiation. J Educ Psychol. 2009; 101(4): 879-96.

[26] Diamond M. C. An optimistic view of the aging brain. GENERATIONS. 1993; 17 (1): 31-3.

[27] Demarin V, Morović S. Neuroplasticity. Periodicum Biologorum. 2014; 116, (2): 209-11.
[28] Fuchs E, Flügge G. Adult neuroplasticity: More than 40 years of research. Neural plast. 2014; 541870. doi.org/10.1155/2014/541870.
[29] Vance D, Camp C, Kabacoff M, Greenwalt L. Montessori methods: Innovative interventions for adults with Alzheimer's disease. Montessori Life. 1996; 8: 10-2.
[30] Presmeg N. Research on visualization in learning and teaching mathematics. In: Gutiérrez A, Boero P, editors. Handbook of research on the psychology of mathematics education: Past, Present and Future. Rotterdam: Sense; 2006. p. 205-236.
[31] Wells DL, Dawson P. Description of retained abilities in older persons with dementia. Res Nurs Health. 2000; 23(2): 158-66.
[32] Owen R, Berry K, Brown LJ. Enhancing older adults' well-being and quality of life through purposeful activity: A systematic review of intervention studies. Gerontologist. 2022; 62: e317-e32.
[33] Sutin AR, Aschwanden D, Luchetti M, Stephan Y, Terracciano A. Sense of purpose in life is associated with lower risk of incident dementia: A Meta-Analysis. J Alzheimers Dis. 2021; 83(1): 249-58. doi:10.3233/JAD-210364.

Journal of Associated Medical Sciences 2024; 57(2): 67-75

JAMS
Journal of Associated Medical Sciences

Scopus Indexed & Thai-Journal Citation Index Centre (TCI)

Journal of Associated Medical Sciences

Journal homepage: https://www.tci-thaijo.org/index.php/bulletinAMS/index

Effect of mangiferin isolated from *Mangifera indica* leaves on *in vitro* blood coagulation and cell migration activities

Isaya Janwitayanuchit[1*] Suwanna Semsri[1] Wicharn Janwitayanuchit[2] Kiattawee Choowongkomon[3]

[1]Faculty of Medical Technology, Huachiew Chalermprakiet University, Samutprakarn Province, Thailand.
[2]Faculty of Pharmaceutical Sciences, Huachiew Chalermprakiet University, Samutprakarn Province, Thailand.
[3]Center for Advanced Studies in Nanotechnology for Chemical, Food and Agricultural Industries, KU Institute Advanced Studies, Kasetsart University, Bangkok, Thailand.

ARTICLE INFO

Article history:
Received 3 December 2023
Accepted as revised 19 February 2024
Available online 23 February 2024

Keywords:
Anticoagulation, antiplatelet aggregration, anticancer, cell migration, mangiferin

ABSTRACT

Background: Mangiferin, a natural compound has been reported to possess a variety of biological activities such as anticancer, anti-diabetic, antimicrobial, antioxidant, cardioprotective activities, etc. Screening on blood coagulation activity effects of mangiferin might be helpful for further activities investigation.

Objective: This study aimed to isolate mangiferin from mango leaves and evaluate its blood coagulation and anticancer activities against human lung cancer cell lines (A549 cells).

Materials and methods: Mangiferin was extracted from mango leaves and characterized by IR, NMR, and mass spectroscopic techniques. It was determined *in vitro* activities as follows: blood clotting time, platelet aggregation, activated partial thromboplastin time (aPTT), prothrombin time (PT), clot lysis, fibrinolysis, and cell migration assay.

Results: It was found that mangiferin had a significantly slower effect on inducing blood clots than the control group, with the coagulation value of 13.09±2.97 minutes and decreasing platelet aggregation at an inhibition percentage value of 14.1±1.2. There was significant (p<0.05) prolongation of PT and aPTT activities tested with the mangiferin at the value of 12.4±1.2 and 29.9±3.1 seconds, respectively. However, mangiferin was unable to cause fibrin clot dissolution on fibrinolysis test. Mangiferin also showed anticancer activity against A549 cells by inhibition of cell migration assay.

Conclusion: Mangiferin showed antiplatelet aggregation activity and prolongation of prothrombin time (PT) and activated partial thromboplastin time (aPTT) assay without fibrinolysis activity. In addition, mangiferin showed anticancer activity against A549 cells by inhibiting cell migration.

Introduction

Blood coagulation, also known as blood clotting, is a necessary process that helps block a bleeding when a blood vessel is injured. Nevertheless, blood clot formation in the vessel without any apparent injury can cause several complications in the human body. The undesired blood clot interferes with the free flow of blood, resulting in several life-threatening diseases. Meanwhile, thrombolytic activity is the process of breaking down the blood clot, which helps improving the blood flow.[1] In fact, platelet dysfunction and coagulation defects are becoming more associated with the onset and progression of several cardiovascular diseases, including atherosclerosis, thrombosis, peripheral artery disease, myocardial infarction, and ischemic stroke.

∗ **Corresponding contributor.**
Author's Address: *Faculty of Medical Technology, Huachiew Chalermprakiet University, Samutprakarn Province, Thailand.*
E-mail address: isaya@hcu.ac.th
doi: 10.12982/JAMS.2024.028
E-ISSN: 2539-6056

Several anticoagulant agents used in clinical practices to prevent or reduce coagulation of blood consist of heparins, vitamin K-antagonists, coumarin derivatives, and factor Xa inhibitors. Thrombolytic agents used for dissolving blood clots are streptokinase, urokinase, recombinant tissue plasminogen activators, etc.[2] Some drugs have limitations of use and unwanted effects; novel potential drugs still need to be discovered and developed.[3] Natural products continue to be the focus of drug discovery research, and several drugs have been derived from plants. Nowadays, active constituents and crude extracts from plants have been widely screened for various biological activities.[4] Mangiferin, the major constituent obtained at significant level from leaves and barks of *Mangifera indica*, is a xanthone C-glucoside having a glucose substituent at position 2 of xanthone skeleton. Mangiferin has been reported to have numerous biological activities[5,6] such as anticancer,[7,8] antidiabetic,[9-13] antioxidant,[14] anti-inflammatory,[15] antiviral,[16] antibacterial,[17,18] cardiovascular protection[19] and hepatoprotective activities.[20] Due to its low toxicity, mangiferin has been widely used in nutritional supplement.[21] Furthermore, many mangiferin analogues have been synthesized and evaluated for their biological activities.[22] Interestingly, several studies have reported that mangiferin exerts markedly antineoplastic effects toward many types of cancer such as prostate cancer,[23] colon cancer,[24] leukemia,[25] and lung cancer.[26]

The present study aimed to investigate the potential effects of mangiferin on *in vitro* blood coagulation and anticancer activities.

Materials and methods

Reagent kits for prothrombin time (PT) and activated partial thromboplastin time (aPTT) (Siemens, Germany), 100 U/mL penicillin and 100 µg/mL of streptomycin (Invitrogen, USA), Dulbecco's modified Eagle's medium (DMEM) (Invitrogen, USA), fetal bovine serum (FBS) (Invitrogen, USA) and other analytical grade chemicals were purchased from commercial vendors. Nuclear magnetic resonance (NMR) spectra were recorded using a 500-MHz Jeol NMR spectrometer. The infrared (IR) spectra were taken on a Perkinelmer Spectrum 100 FTIR spectrometer. Mass analysis was performed using a Joel JMS-S3000 mass spectrometer.

Extraction and purification of mangiferin

Several methods of mangiferin extraction have been reported.[27,28] The extraction and isolation of mangiferin herein was carried out following modified methods from Jutiviboonsuk *et al*.[29] and Shindea *et al*.[30] The leaves of 'Nam Dok Mai' mango cultivar collected from Samut Prakarn province were extracted with methanol (Merck, Germany) in a soxhlet apparatus for 48 hrs. The extract solvent was concentrated under reduced pressure to yield semisolid mass which was chromatographed over silica gel column eluted with dichloromethane (Merck, Germany): methanol (1:1) which gave amorphous mangiferin powder. Then, crystallization with 70% ethanol gave the needle-shaped crystals of mangiferin which were characterized by melting point, IR, NMR, and mass spectroscopy compared with mangiferin standard.

Blood sample preparation

Blood samples were collected from 60 healthy volunteers with no nonsteroidal anti-inflammatory drugs (NSAIDs). Normal sodium citrated plasma was prepared as follows. Nine milliliters of blood was drawn by venipuncture into centrifuge tubes containing 1 mL of 3.2% trisodium citrate solution. Platelet-rich plasma (PRP) and platelet-poor plasma (PPP) were prepared by centrifugation at 1,000 rpm and 3,000 rpm for 15 min, respectively. This research was approved by Research Ethics Committee, Huachiew Chalermprakiet University.

Blood coagulation

Modified whole blood clotting time (modified WBCT) assay[31]

Clotting tubes containing 10 µL of dimethyl sulfoxide (DMSO) (Sigma-Aldrich, Germany) (control tube) and 10 µL of 500 µg/mL mangiferin in DMSO (test tube) were incubated at 37 °C. Then, one mL of fresh blood from healthy volunteers was added into each incubated tube. After 5 min, the blood clot formation was determined at 30 sec interval. The time was recorded immediately after complete blood clot.

Platelet aggregation assay[32]

Briefly, 450 µL of platelet-rich plasma (PRP) ($2.5x10^8$ platelets/mL) was mixed with 4.5 µL of 50 mg/mL mangiferin to make the final concentration of 500 µg/mL, incubated at 37 °C for 3 min. After that, twenty microliters of 35 mM adenosine diphosphate (ADP) (Sigma-Aldrich, Germany) were added into 140 µL of the pre-incubated PRP. Platelet aggregation was measured as the increase in light transmission with a CS2500 (Siemens Sysmex®, Germany) analyzer at 660 nm using PPP as the baseline of 100% aggregation.

Activated partial thromboplastin time (aPTT) and prothrombin time (PT) [33] test

In short, 50 µL of normal sodium citrated plasma was incubated with mangiferin (at a final concentration of 500 µg/mL) for 1 min and 100 µL of tissue thromboplastin solution was added. The PT was recorded for the fibrin clot formation. For the aPTT test, 50 µL of normal sodium citrate plasma was incubated with mangiferin at a final concentration of 500 µg/mL for 1 min. Then, 50 µL of aPTT solution was added and incubated at 37 °C for 3 min. After that, 50 µL of 0.25 M calcium chloride ($CaCl_2$) (Sigma-Aldrich, Germany) was added and the time was recorded as a clot was formed. The obtained values were compared with the control unit (vehicle control).

Fibrinolysis activity assay

Clot lysis[34]

In brief, 500 µL of blood from healthy volunteers was drawn into a sterile microcentrifuge tube (the microcentrifuge tube had been weighed and recorded

previously), incubated at 37 °C for 45 min to form a complete clot. The serum was removed, leaving only the clot. The tube was weighed and the value obtained was calculated to find the clot weight (clot weight = weight of the tube in which the clot formed - weight of the tube). After that, mangiferin 100 µL was added to a final concentration of 500 µg/mL and incubated at 37 °C for 90 min and the liquid was aspirated and the weighed of the remaining clot was calculated. The results were displayed in the form of % lysis using phosphate buffer saline (PBS) (Invitrogen, USA) and streptokinase (Sigma-Aldrich, Germany) as negative and positive controls, respectively.

% Lysis = 100 - (clot weight after testing x 100)/initial clot weight)

Fibrinolytic activity

In brief, 100 µL of normal sodium citrated plasma (from 20 volunteers, pooled together) was mixed with 30 µL of 0.25 M $CaCl_2$, incubated at 37 °C for 3 hrs to form a soft fibrin clot. After that, washed the clot with PBS, then added 400 µL of 0.2 M Tris-HCl buffer pH 8.5 (Sigma-Aldrich, Germany) and 100 µL of mangiferin to make the final concentration of 500 µg/mL incubated at 37 °C for 2 hrs. Then, 750 µL of 0.44 M trichloroacetic acid was added at room temperature for 30 min and centrifuged at 3,300 rpm for 15 min. The supernatant was transferred to a new tube, followed by the addition of 1.25 mL of 0.4M sodium carbonate (Na_2CO_3) (Sigma-Aldrich, Germany) and 250 µL of 1:3 diluted Folin Ciocalteu's reagent (Sigma-Aldrich, Germany), leaved for 30 min and the absorbance was recorded at 660 nm. One unit of fibrinolytic activity, which is absorbance increased by 0.01 at 660 nm/hr at 37 °C was calculated.

Anticancer activity

Cell culture

Human lung cancer cell lines (A549 cells) were purchased from the American Type Culture Collection (ATCC). A549 cells were cultured in DMEM, supplemented with 10% FBS and 100 U/mL penicillin and 100 µg/mL of streptomycin. Cells were incubated at 37 °C in a humidified 5% CO_2 atmosphere.

***Cell cytotoxicity assay*[35,36]**

3-(4,5-dimethylthiazol-2-yl)-2,5-diphenyltetrazolium bromide (MTT) assay was performed for cytotoxicity assessment. A549 ($5x10^3$ cells/mL) cells were seeded into 96-well culture plate. Following which, 100 µL fresh medium containing various final concentrations (1-1,000 µg/mL) of mangiferin were added and incubated at 37 °C for 72 hrs. The medium was then replaced with fresh medium containing MTT solution (Bio Basic, Canada) at the final concentration of 0.5 mg/mL. After formazan formation, 50 µL DMSO was added to dissolve the crystals. The samples were measured at 570 nm, along with the reference at 630 nm, using a microplate reader. The data was analyzed using GraphPad Prism v 6.00 software for Windows (GraphPad Software, Inc.). All experiments were performed independently in triplicate.

***Cell migration assay*[37,38,39]**

Effect of mangiferin on cell migration was performed by *in vitro* scratch assay. A549 cells were cultured ($1x10^5$ cell/well) in a 24-well plate. The wound was generated by scratching the cell layer using a 10 µL pipette tip when A549 cells reached approximately 90% confluency. Cells were washed 3 times with PBS and incubated with variour concentrations of mangiferin (0-1,000 µg/mL). The cell images were captured immediately (t=0 hr) under a microscope and then captured again after 24, 48, and 72 hrs of incubation. The area of wound was determined by Image J software. The cell migration was expressed as the percentage change in normalized measurement area to the original open area or wound closure:

$$\%\text{Wound closure} = [(A_{t=0} - A_{t=\Delta t}) / A_{t=0}] \times 100$$

Where $A_{t=0}$ is the area of the wound measured immediately after scratching and $A_{t=\Delta t}$ is the area of the wound measured at t hr after scratching.

Statistical analysis

Statistical analysis of the results was performed using PSPP software version 0.10.4.62724. Data were presented as the mean±SD. The comparison between the groups was carried out by independent samples *t*-test. The results were considered significant at a value of $p<0.05$.

Results

The melting point and molecular weight of isolated mangiferin were 269-271 °C and 422.3 g/mol, respectively. The FT-IR spectral data of isolated mangiferin showed remarkable OH stretch band at 3363 cm^{-1}, conjugated C=O stretch peak at 1648 cm^{-1} and C-O stretch peak at 1250 cm^{-1}. The chemical structure and the interpretation of NMR data of isolated mangiferin were shown in Figure 1 and Table 1, respectively. The ^{1}H-NMR signals at δ 6.35 (1H, H-4), 6.85 (1H, H-5), and 7.38 (1H, H-8) represented Ar-H. The down-field singlet proton at δ 13.80 indicated Ar-OH hydrogen bonding with the carbonyl moiety. The chemical shifts of the sugar moiety were observed at δ 3.15-4.60 ppm. The ^{13}C-NMR indicated 19 carbons atoms in the molecule. The signals of quaternary aromatic carbons were observed at δ 161.8 (C-1), 107.5 (C-2), 163.8 (C-3), 156.2 (C-4a), 101.3 (C-4b), 150.9 (C-6), 143.9 (C-7), 111.4 (C-8a), 154.5 (C-8b), and 179.0 (C=O), and methine carbons at δ 93.3 (C-4), 102.5 (C-5), and 107.8 (C-8). The signals of sugar carbons were observed at δ 61.5-81.6 ppm.

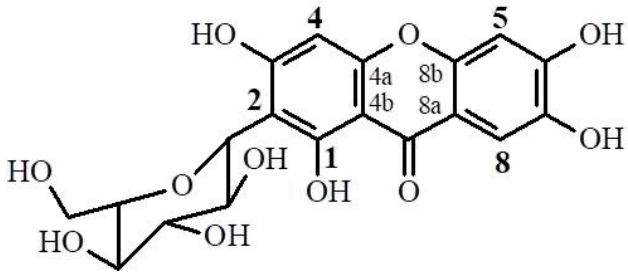

Figure 1 *Chemical structure of mangiferin.*

Table 1 Interpretation of ^{1}H-NMR (500MHz), ^{13}C (125MHz) data of mangiferin.

Position	^{1}H(δ,ppm)	^{13}C(δ,ppm)
1	13.8 (1-OH)	161.8
2		107.5
3		163.8
4	6.35, s	93.3
4a		156.2
4b		101.3
5	6.85, s	102.5
6		150.9
7		143.9
8	7.38, s	107.8
8a		111.4
8b		154.5
CO		179.0
Sugar	3.15-4.60	61.5-81.6

The effect of mangiferin on blood clotting using modified whole blood clotting time method revealed that mangiferin had a significantly slower effect on inducing blood clots than the control group (p<0.05). Mangiferin had a blood coagulation value of 13.09±2.97 minutes compared with the control set with a blood coagulation value of 12.06±2.34 minutes as shown in Table 2.

Table 2 Effect of mangiferin on blood clotting using modified whole blood clotting time method.

Sample (N=60)	Whole blood clot time (WBCT) (min)
Mangiferin (500 µg/mL)	13.09±2.97
Vehicle control	12.06±2.34

It was found that mangiferin decreased platelet aggregation in a statistically significant (p<0.05). Mangiferin had a platelet aggregation value of 65.3±11.1 compared with the control set which had a value of 76.0±6.6 min. The inhibition percentage of platelet aggregation activity of 500 µg/mL mangiferin was 14.1±1.2 as shown in Table 3.

Table 3 Effect of mangiferin on ADP-induced platelet aggregation.

Sample (N=20)	Platelet aggregation (%)	Inhibition (%)
Mangiferin (500 µg/mL)	65.3±11.1	14.1±1.2
Vehicle control	76.0±6.6	

Mangiferin affected the function of coagulation factors in fibrin clot formation in both the extrinsic and intrinsic pathways. Mangiferin at the concentration of 500 µg/mL prolonged the PT with a value of 12.4±1.2 sec slower than the control set with a value of 10.9±0.9 sec, in a statistical significance (p<0.05). Mangiferin showed significant (p<0.05) prolongation of aPTT compared with the control at the value of 29.9±3.1 sec as shown in Table 4.

Table 4 Anticoagulation activity of mangiferin.

Sample (N=60)	Coagulation test (s)	
	Prothrombin time (PT)	Activated partial thromboplastin time (aPTT)
Mangiferin (500 µg/mL)	12.4 ± 1.2	29.9 ± 3.1
Vehicle control	10.9 ± 0.9	27.4 ± 2.6

The study of mangiferin on clot lysis by blood clot lysis time method indicated that mangiferin at a concentration of 500 µg/mL caused blood clot lysis equal to 5.8 ±2.9% whereas the control group had clot lysis at a value of 6.9±1.0%, which was not significantly different at the 95 % confidence level (p>0.05). Studying the effect of mangiferin on the breaking down of fibrin clot by fibrinolytic activity assay revealed that mangiferin was unable to cause fibrin clot dissolution with a value of 0.5±0.4 compared with the control set with statistical significance 5.5±2.1 (p<0.05) as shown in Table 5.

Table 5 Fibrinolysis activity of mangiferin.

Sample (N=20)	Fibrinolysis	
	Blood clot lysis (%)	One unit of fibrinolytic activity
Mangiferin (500 µg/mL)	5.8±2.9	0.5±0.4
Vehicle control	6.9±1.0	5.5±2.1

To determine the effect of mangiferin on cell migration by *in vitro* scratch assay, A549 cells were cultured in the presence of various concentrations of mangiferin. The 90% confluent A549 cells were wounded using a pipette tip. After incubation, the wound closure was observed and imaged under an inverted microscope. Migration of A549 cell line treated with mangiferin (for 72 hrs) was inhibited with the percentage of wound closure reduced to 59.0, 41.1, and 26.8% at the concentration of 250, 500 and 1,000 µg/mL, respectively. Mangiferin at a concentration of 1,000 µg/mL significantly inhibited cell migration with the percentage of wound closure of 17.2, 23.1, and 26.8% after 24, 48 and 72 hrs, respectively (Figure 2) without cytotoxic effects as confirmed by MTT assay (Figure 3).

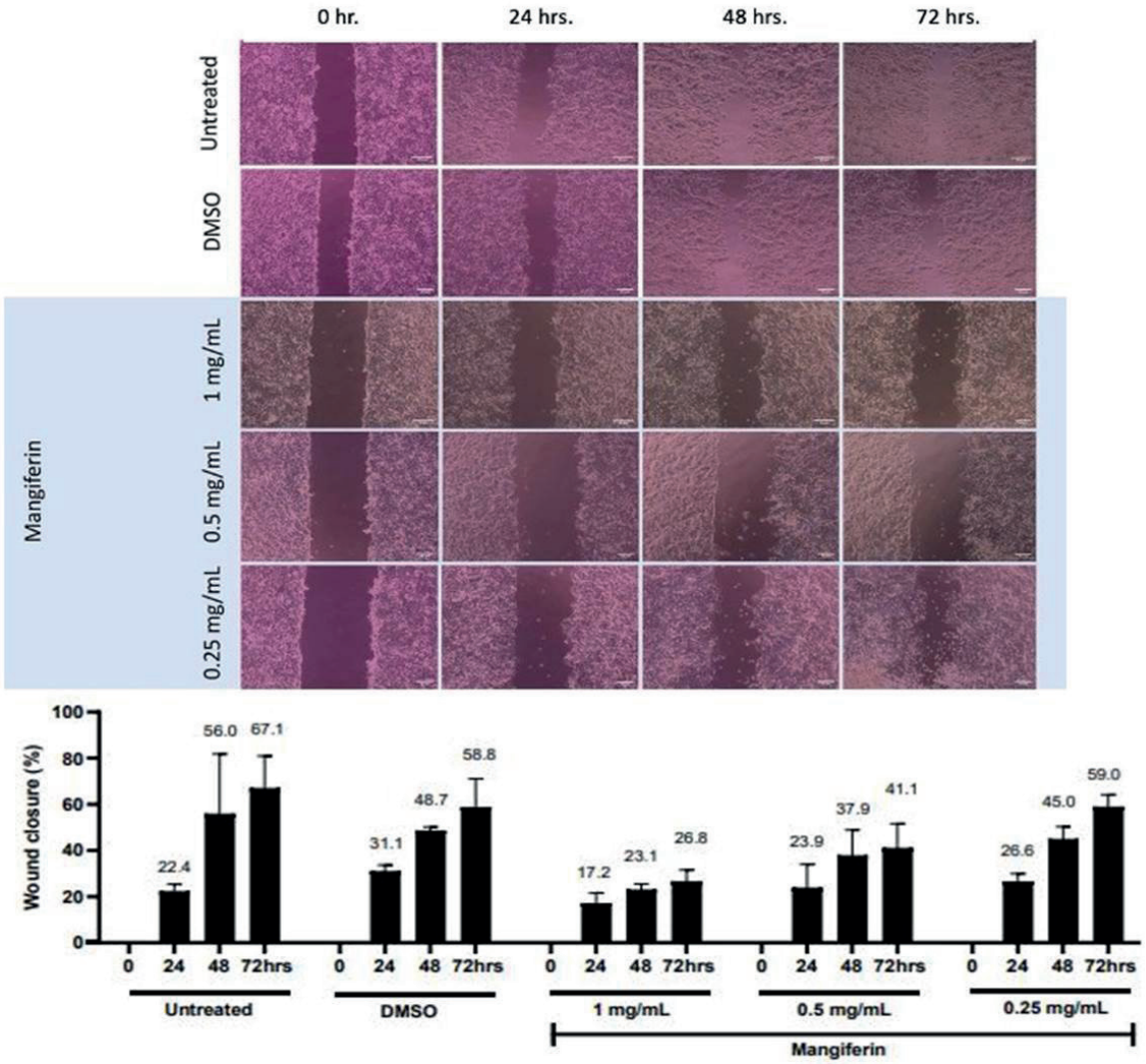

Figure 2 *Image of wound and cell migration to close the wound taken at time 0, 24, 48 and 72 hrs after wounding and the effect of mangiferin on cell migration in A549 cells. (plotted as the percentage of wound closure)*

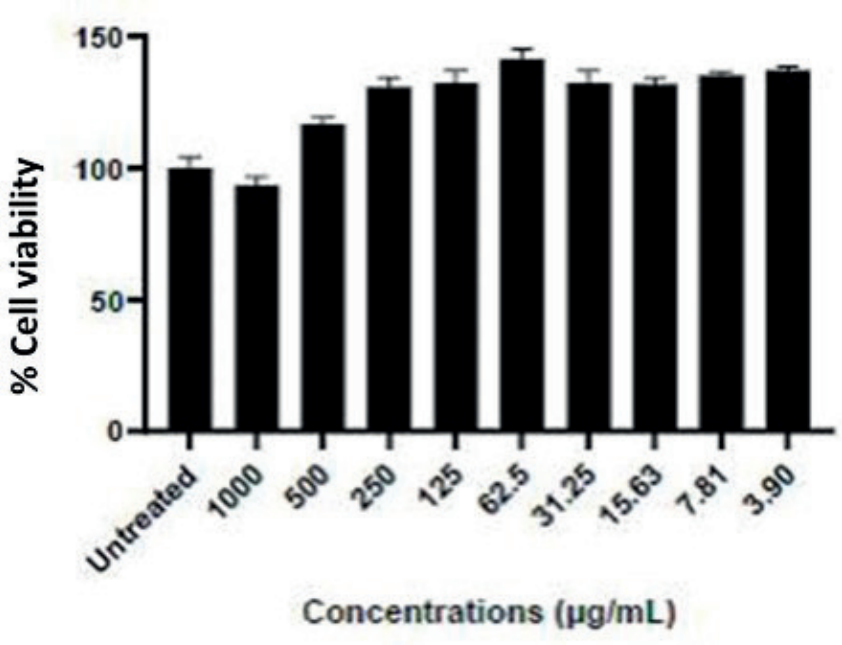

Figure 3 *Effect of mangiferin on the viability of A549 cells.*

Discussion

The extraction of mangiferin from mango leaves used a soxhlet extractor to remove fatty interference substances, then the isolation and purification of mangiferin were performed by column chromatography and crystallization with ethanol to yield 2.7% of mangiferin crystals. The obtained mangiferin characterized by IR, NMR and MS spectroscopic techniques was subjected to evaluate the biological activities. The present study investigated antiplatelet aggregation, anticoagulant, and anticancer activities of mangiferin. Our previous study on cell toxicity of mangiferin indicated that 500 µg/mL of mangiferin had no cytotoxicity on A549 cells (unpublished). Therefore, all the final concentration of mangiferin used in this test experiments were 500 µg/mL. The antiplatelet aggregation activity of mangiferin using conventional light transmission platelet aggregation assay was evaluated on human platelets whose aggregation was induced by using ADP as an agonist. The results showed that mangiferin at a concentration of 500 µg/mL inhibited platelet aggregation in a statistically significant with the inhibition percentage value of 14.1±1.2. This assay was consistent with the research by María Elena Alañón and colleagues who reported that mangiferin extracted from mango seeds had the effect of inhibiting platelet aggregation at a concentration of 1 mg/mL.[32] In addition, using the modified whole blood clotting time method which was one of the simplest methods to evaluate how well the primary blood clotting process was functioning, indicated that mangiferin delayed the time of a blood coagulation at a value of 13.09±2.97 min with statistical significance (p<0.05) when compared with the control set.

The anticoagulant activity of mangiferin was performed *in vitro* in human plasma by prothrombin time (PT) and activated partial thromboplastin time (aPTT) test. PT was mainly applied to measure the activity of coagulation factors of extrinsic and common coagulation pathways while aPTT was used to evaluate the function of coagulation factors of the intrinsic and common coagulation pathways. The prolongation of aPTT, suggested the inhibition of the intrinsic and/or the common pathway. On the other hand, PT prolongation gave information about the inhibition of the extrinsic and/or the common pathway. It was found that mangiferin had the effect of inhibiting the formation of fibrin clot being significantly slower than the control group (p<0.05) for both the PT and aPTT tests. Previous research reported that mangiferin heptasulfate (a polysulfated derivative of mangiferin) interfered blood coagulation by inhibiting the activity of coagulation factor Xa.[40] Consequently, it was considered that mangiferin might exert anticoagulant activity by interfering the function of coagulation factor Xa.

In order to determine the fibrinolysis action of mangiferin, the blood clot lysis and fibrolytic activity assay were also evaluated. The study showed that mangiferin had no fibrinolytic acitivity at the concentration of 500 µg/mL. Qurat U. Ain and colleagues reported that aqueous-methanolic extract of *Mangifera indica* leaves had a significant increment in clot lysis, PT and aPTT due to the presence of polyphenols, flavonoids, alkaloids in its extract.[41] Our studies revealed that isolated mangiferin from *Mangifera indica* leaves had an increment in both PT and aPTT without clot lysis activities. Nevertheless, mangiferin showing no clot lysis activity due to the inappropriate concentration used or entirely lacking fibrinolytic action should be further determined. Several studies reported that mangiferin had many biological activities, especially, anticancer activity against several types of cancers.[5,6]

The anti-lung cancer activity of mangiferin was attractive. was attractive. One *in vitro* experiment showed that mangiferin exerted anti-lung cancer by an influence on cell cycle arrest and induced apoptosis in A549 cells.[26] Another report indicated that mangiferin likely regulated proliferation and apoptosis in lung cancer LUAD cells by reducing the expression levels of miR-92a and miR-27b.[42] Cancer cell migration is one of the important steps in cancer spread and invasion. Inhibitions of A549 cells migration have been widely reported for evaluation of lung carcinogenesis and cancer cells growth.[43-45] In this study the inhibition of cell migration of A549 cells was investigated to determine the anticancer activity of mangiferin by using wound healing (or scratch) assay.

The present data showed that mangiferin significantly decreased the migratory ability of A549 cells in a dose-dependent manner. The cell migration inhibition effect of mangiferin did not result from cytotoxicity as indicated by cytotoxicity assay. It had been previously reported that mangiferin displayed anticancer effects on A549 cells through various mechanisms, such as induction of apoptosis and reduction of miR-92a and miR-27b expression.[26,42]

Our studies demonstrated that mangiferin was able to inhibit cell migration and invasion on A549 cells without cytotoxicity, however, the migration of cancer cells involved multiple mechanistic pathways, the precise molecular mechanism of cell migration inhibition should be further studied.

Conclusion

Mangiferin is a natural bioactive compound possessed a variety of biological activities. In this study, it was clearly showed that mangiferin possessed antiplatelet aggregration and anticoagulation activities without fibrinolysis effect. Nevertheless, the obvious mechanisms of blood coagulation inhibition and optimum concentration used for those activities must be further investigated. In addition, mangiferin showed anticancer activity against A549 cell line by inhibition of cell migration through wound healing assay.

Conflict of interest

No conflict of interest to declare.

Acknowledgements

I would like to thank Huachiew Chalermprakiet Univeristy for financial support of this research project.

References

[1] Dahlbäck B. Blood coagulation. Lancet 2000; 355: 1627-32. doi: 10.1016/S0140-6736(00)02225-X.

[2] Chen A, Stecker E, Warden BA**.** Direct Oral Anticoagulant Use: A Practical Guide to Common Clinical Challenges. J Am Heart Assoc. 2020; 9(13). doi.org/10.1161/JAHA.120.017559.

[3] Schulman S. Advantages and limitations of the new anticoagulants. J Intern Med. 2014; 275:1-11. doi: 10.1111/joim.12138.

[4] Atanasov AG, Zotchev SB, Dirsch VM and Supuran CT. Natural products in drug discovery: advances and opportunities. Nat Rev. 2021; 20: 200-16. doi:10.1038/s41573-020-00114-z.

[5] Du S, Liu H, Lei T, Xie X, Wang H, He X, *et al*. Mangiferin: An effective therapeutic agent against several disorders (Review). Mol Med Rep. 2018; 18(6): 4775-86 doi: 10.3892/mmr.2018.9529.

[6] Imran M, Arshad MS, Butt MS, Kwon JH, Arshad MU and Sultan MT. Mangiferin: a natural miracle bioactive compound against lifestyle related disorders. Lipids Health Dis. 2017; 1-17. doi: 10.1186/s12944-017-0449-y.

[7] Zou B, Wang H, Liu Y, Qi P, Lei T, Sun M, Wang Y. Mangiferin induces apoptosis in human ovarian adenocarcinoma OVCAR3 cells via the regulation of Notch3. Oncol Rep. 2017; 38: 1431–41. doi: 10.3892/or.2017.5814.

[8] Garcia-Rivera D, Hernandez R, Bougarne N, Haegeman G, Berghe W. Gallic acid indanone and mangiferin xanthone are strong determinants of immunosuppressive anti-tumour effects of *Mangifera indica* L. bark in MDA-MB231 breast cancer cell. Cancer Lett. 2011; 305: 21-31. doi: 10.1016/j.canlet.2011.02.011.

[9] Apontes P, Liu Z, Su K, Benard O, Youn DY, Li X, Li W, Mirza RH, Bastie CC, Jelicks LA, Pessin JE, Muzumdar RH, Sauve AA, Chi Y. Mangiferin stimulates carbohydrate oxidation and protects against metabolic disorders induced by high-fat diets. Diabetes. 2014; 63(11): 3626-36. doi: 10.2337/db14-0006.

[10] Sellamuthu PS, Arulselvan P, Muniappan BP, Fakurazi S, Kandasamy M. Mangiferin from *Salacia chinensis* prevents oxidative stress and protects pancreatic β-cells in streptozotocin-induced diabetic rats. J Med Food. 2013; 16(8): 719-27. doi: 10.1089/jmf.2012.2480.

[11] Zhu X, Cheng Y, Du L, Li Y, Zhang F, Guo H, Liu YW, Yin X. Mangiferin attenuates renal fibrosis through down regulation of osteopontin in diabetic rats. Phyther Res. 2015; 29: 295-302. doi: 10.1002/ptr.5254.

[12] Dineshkumar B, Mitra A, Mahadevappa M. Studies on the anti-diabetic and hypolipidemic potentials of mangiferin (Xanthone Glucoside) in streptozotocin-induced Type 1 and Type 2 diabetic model rats. Int J Adv Pharm Sci. 2010; 1: 75-85. doi: 10.5138/ijaps.2010.0976.1055.01009.

[13] Saleh S, El-Maraghy N, Reda E, Barakat W. Modulation of diabetes and dyslipidemia in diabetic insulin-resistant rats by mangiferin: role of adiponectin and TNF-α. An Acad Bras Cienc. 2014; 86(4): 1935-48. doi: 10.1590/0001-3765201420140212.

[14] Stoilova I, Jirovetz L, Stoyanova A, Krastanov A, Gargova S, Ho L. Antioxidant activity of the polyphenol mangiferin. Electron. J Environ Agric Food Chem. 2008; 7: 2706-16.

[15] Garrido G, Gonzalez D, Delporte C, Backhouse N, Quintero G, Nunez Selles A, Morales M. Analgesic and antiinflammatory effects of Mangifera indica L. extract (Vimang). Phytother Res. 2001; 15: 18-21. doi: 10.1002/1099-1573(200102)15:1<18::aid-ptr676>3.0.co;2-r.

[16] Al-rawi A, Dulaimi H, Rawi M. Antiviral activity of mangifera extract on influenza virus cultivated in different cell cultures. J Pure Appl Microbiol. 2019; 13: 455-8. doi: 10.22207/JPAM.13.1.50.

[17] Joshua M and Takudzwa M. Antibacterial properties of *Mangifera indica* on *staphylococcus aureus*. African J Clin Exp. 2013; 14(2): 62-74. doi: 10.4314/ajcem.v14i2.4.

[18] Mazlan NA, Azman S, Ghazali NF, Yusri PZS, Idi HM, Ismail M, Sekar M. Synergistic antibacterial activity of mangiferin with antibiotics against *Staphylococcus aureus*. Drug Invent. Today 2019; 12: 14-7.

[19] Prabhu S, Naraya SH, Shyamala CS. Mechanism of protective action of mangiferin on suppression of inflammatory response and lysosomal instability in rat model of myocardial infarction. Phytother Res. 2009; 23: 756-60. doi: 10.1002/ptr.2549.

[20] Rasool M, Sabina EP, Mahinda PS, Gnanaselvi BC, Mangiferin, a natural polyphenol protects the hepatic damage in mice caused by CCl4 intoxication. Comp Clin Pathol. 2012; 21: 865-72. doi: 10.1007/s00580-011-1190-y.

[21] Mei S, Perumal M, Battino M, Kitts DD, Xiao J, Chen X**.** Mangiferin: a review of dietary sources, absorption, metabolism, bioavailability, and safety. Crit Rev Food Sci Nutr. 2023; 63(18): 3046-64. doi: 10.1080/10408398.2021.1983767.

[22] Singh SK, Kuar Y, Kumar SS, Sharma VK, Dua K, and Samad A. Antimicrobial Evaluation of Mangiferin Analogues. Indian J Pharm Sci. 2009; 71(3): 328-31. doi: 10. 4103/0250-474X.56023.

[23] Li M, Ma H, Yang L, Li P. Mangiferin inhibition of proliferation and induction of apoptosis in human prostate cancer cells is correlated with downregulation of B-cell lymphoma-2 and upregulation of microRNA-182. Oncol Lett. 2016; 11(1): 817-22. doi: 10.3892/ol.2015.3924.

[24] Samadarsi R, Augustin L, Kumar C, and Dutta D. In-silico and in-vitro studies on the efficacy of mangiferin against colorectal cancer. BMC Chem. 2022; 16(1): 42. doi: 10.1186/s13065-022-00835-9.

[25] Peng ZG, Yao YB, Yang J, Tang YL, Huang X. Mangiferin induces cell cycle arrest at G2/M phase through ATR-Chk1 pathway in HL-60 leukemia cells. Genet Mol Res. 2015; 14: 4989-5002. doi: 10.4238/2015.May.12.2.

[26] Shi W, Deng J, Tong R, Yang Y, He X, Wang H, Deng

S, Qi P, Zhang D and Wang Y. Molecular mechanisms underlying mangiferin-induced apoptosis and cell cycle arrest in A549 human lung carcinoma cells. Mol Med Rep. 2016; 13: 3423-32. doi: 10.3892/mmr.2016.4947.

[27] Zou TB, Xia E, He TP, Huang MY, Jia Q and Li HW. Ultrasound-Assisted Extraction of Mangiferin from Mango (*Mangifera indica* L.) Leaves Using Response Surface Methodology. Molecules. 2014; 19: 1411-21. doi: 10.3390/molecules19021411.

[28] Montañez GR, Ragazzo-Sánchez JA, Calderón-Santoyo M, Velázquez-de la Cruz G, Ramírez de León JA, Navarro-Ocaña A. Evaluation of extraction methods for preparative scale obtention of mangiferin and lupeol from mango peels (*Mangifera indica* L.). Food Chem. 2014; 159: 267-72. doi: 10.1016/j.foodchem.2014.03.009.

[29] Jutiviboonsuk A, Sardsaengjun C. Mangiferinin Leaves of Three Thai Mango (*Mangifera indica* L.) Varieties. Isan J Pharm Sci. 2010; 6(3): 122-9. doi: 10.14456/ijps.2010.28.

[30] Shindea SS and Chavanb AR. Isolation of Mangiferin from Different Varieties of *Mangifera Indica* Dried Leaves. Int J Sci Eng Res. 2014; 5(6): 928-34.

[31] Semsri S, Khawon T, Sukasem J, Janwitayanuchit W, Nilsri N and Homvisasevongsa S. Effect of *Eclipta prostrata*, *Chromolaena odorata*, *Centella asiatica* (Linn.) Urban and *Quercus infectoria* Olivier extracts on *in vitro* hemostasis activities. Huachiew Chalermprakiet Sci Technol J. 2017; 3 (2) : 42-53.

[32] Alañón ME, Palomo I, Rodríguez L, Fuentes E, Román DA and Carretero AS. Antiplatelet Activity of Natural Bioactive Extracts from Mango (*Mangifera Indica* L.) and its By-Products. Antioxid. 2019; 8 (517): 1-11. doi: 10.3390/antiox8110517.

[33] Ayodele OO, Anajobi FD, Osoniyi O. *In vitro* anticoagulant effect of *Crassocephalum crepidioides* leaf methanol extract and fractions on human blood. J Exp Pharmacol. 2019; 11: 99-107. doi: 10.2147/JEP.S218261.

[34] Prasad S, Kashyap RS, Deopujari JY, Purohit HJ, Taori GM and Daginawala HF. Development of an *in vitro* model to study clot lysis activity of thrombolytic drugs. Thromb J. 2006; 4(14): 1-4. doi: 10.1186/1477-9560-4-14.

[35] Mosmann T. Rapid colorimetric assay for cellular growth and survival: application to proliferation and cytotoxicity assay. J Immunol Methods. 1983; 65(1-2): 55-63. doi: 10.1016/0022-1759(83)90303-4.

[36] Berridge MV, Herst PM, Tan AS. Tetrazolium dyes as tools in cell biology: new insights into their cellular reduction. Biotechnol AnnU Rev. 2005; 11: 127-52. doi: 10.1016/ S1387-2656(05)11004-7.

[37] Grada A, Otero-Vinas M, Prieto-Castrillo F, Obagi Z, Falanga V. Research Techniques Made Simple: Analysis of Collective Cell Migration Using the Wound Healing Assay. J Invest Dermatol. 2017; 137 (2): e11-e16. doi: 10.1016/j.jid.2016.11.020.

[38] Jonkman JE, Cathcart JA, Xu F, Bartolini ME, Amon JE, Stevens KM, Colarusso P. An introduction to the wound healing assay using live-cell microscopy. Cell Adh Migr. 2014; 8 (5): 440-51. doi: 10.4161/cam.36224.

[39] Cory G. Scratch-wound assay. Methods Mol Biol. 2011; 769: 25-30. doi: 10.1007/978-1-61779-207-6_2.

[40] Correia-da-Silva M, Sousa E, Duarte B, Marques F, Carvalho F, Cunha-Ribeiro LM, Pinto M. Polysulfated Xanthones: Multipathway Development of a New Generation of Dual Anticoagulant/Antiplatelet Agents. J Med Chem. 2011; 54(15): 5373-80. doi: 10.1021/jm2006589.

[41] Ain QU, Abid MUH, Hashim M, Ishaq S, Mansoor A, Perwasha P, Mizgan GE, Munawar SK, Khan IA. Anticoagulant and thrombolytic activities of leaf extract of *Mangifera indica* in smokers. Tob Regul. 2022; 8(1): 1189-201. doi: 10.18001/TRS.8.1.24.

[42] Chi XV, Meng JJ, Lin CY, Su QS, Qin YY, Wei RH, Lan D and Huang C. Mangiferin Inhibits Human Lung Adenocarcinoma by Suppressing MiR-27b and MiR-92a. Evid Based Complement Alternat Med. 2021; 2021: 1-10. doi.org/10.1155/2021/282[29]50.

[43] Cheng XD, Gu JF, Yuan JR, Feng L and Jia XB. Suppression of A549 cell proliferation and metastasis by calycosin via inhibition of the PKCα/ERK1/2 pathway: An *in vitro* investigation. Mol Med Rep 2015; 12: 7992-8002. doi: 10.3892/mmr.2015.4449.

[44] Chen Q, Men Y, Wang H, Chen R, Han X, and Liu J. Curcumin Inhibits Proliferation and Migration of A549 Lung Cancer Cells Through Activation of ERK1/2 Pathwayinduced Autophagy. Nat Prod Commun. 2019: 14(6): 1-7. doi: 10.1177/1934578X19848179.

[45] Kim SY, Shin MS, Kim GJ, Kwon H, Lee MJ, Han AR, Nam JW, Jung CH, Kang KS and Choi H. Inhibition of A549 Lung Cancer Cell Migration and Invasion by Ent-Caprolactin C via the Suppression of Transforming Growth Factor-β-Induced Epithelial-Mesenchymal Transition. Mar Drugs. 2021; 19: 465 doi: 10.3390/md19080465.

Journal of Associated Medical Sciences 2024; 57(2): 76-85

JAMS
Journal of Associated Medical Sciences

Scopus Indexed & Thai-Journal Citation Index Centre (TCI)

Journal of Associated Medical Sciences

Journal homepage: https://www.tci-thaijo.org/index.php/bulletinAMS/index

Sine hunter prey optimization enabled deep residual network for diabetes mellitus detection using tongue image

Jimsha K. Mathew* **and S.Sathyalakshmi**

Computer Science & Engineering, Hindustan Institute of Technology & Science, Chennai, Tamil Nadu.

ARTICLE INFO

Article history:
Received 1 August 2023
Accepted as revised 20 February 2024
Available online 27 February 2024

Keywords:
Sine Cosine Algorithm (SCA), adaptive median filter, Hunter Prey Optimization (HPO), ResUNet++, Deep Residual Network (DRN).

ABSTRACT

Background: Many people suffer from Diabetes Mellitus (DM), a disease caused by high blood glucose levels. In real-time, many methods are implemented to diagnose DM to obtain a good accuracy level, but those methods remain costlier.

Objective: To develop a method for DM detection with good accuracy and minimum cost.

Materials and methods: In this research, DM is detected using tongue image based on DL model, named Deep Residual Network (DRN) that is trained by proposed Sine Hunter Prey Optimization (SHPO). Here, an adaptive median filter is used for the pre-processing phase, and image segmentation is done using ResUNet++, which is trained by Exponential Anti Corona Virus Optimization (ExpACVO). Here, ExpACVO integrates Anti Corona Virus Optimization (ACVO) and Exponential Weighted Moving Average (EWMA). Further, image augmentation and appropriate feature extraction stages are carried out, leading to DM detection by DRN. Moreover, SHPO is formed by combining the Sine Cosine Algorithm (SCA) and Hunter Prey Optimization (HPO). The performance of the proposed method is analyzed using the Tongue image dataset and the Diabetic images dataset.

Results: The performance of SHPO_DRN is found using four evaluation metrics: accuracy, sensitivity, specificity, and f-measure. Here, these metrics exhibit superior performance with high-range values of 0.961, 0.970, 0.948, and 0.961.

Conclusion: The proposed method detects the DM at earlier stages with a good accuracy.

Introduction

Diabetes is attaining potential epidemic status, with more than 62 million diabetic individuals found currently having the disease in India.[1,2] DM and Type 2 diabetes (T2DM), in particular, is increasing importance worldwide by assuming epidemic proportions in many settings and populations.[3,4] The human tongue has many different features with various identifications.[5] Tongue inspection is the most significant diagnostic technique of Traditional Chinese Medicine (TCM) used for observing abnormality or alterations in the tongue and coating of the tongue in diagnosing disease.[6,7] Alterations in the tongue are manifested states of disease in an objective manner that helps in differentiating syndromes, establishing treatment techniques, prescribing herbs, and finding the prognosis of the disease.[8] Deep Learning (DL) methods[9,10] are helpful for diabetic subject's detection by signals of Heart Rate (HR).[11,12] Optimization algorithms are used to improve the performance of the DL methods.[13,14] It can facilitate

* **Corresponding contributor.**
Author's Address: *Computer Science & Engineering, Hindustan Institute of Technology & Science, Chennai, Tamil Nadu.*
E-mail address: rp.20603051@student.hindustanuniv.ac.in
doi: 10.12982/JAMS.2024.029
E-ISSN: 2539-6056

deeper analysis of network data and quicker identification of anomalies. Many techniques were developed for DM detection associated with improvements in self-evaluation of appearance, mental health, and health-related quality of patient's life with DM.[3,15-22]

Main contribution

1. **Developed SHPO_DRN for DM detection:** DM detection is done using DRN, which is trained using SHPO.
2. **SHPO**: It is the integration of SCA and HPO.

Methods

Misbalancing in insulin secretion enhances glucose levels in the blood and, when destroyed completely by the human body's immune system, is an autoimmune system. Initially, input tongue image acquired from databases is forwarded to the pre-processing phase.[23, 24] In the pre-processing phase, an adaptive median filter is utilized to remove the unwanted noises in the image.[25] Further, the pre-processed image is sent to the image segmentation stage. Here ResUNet++is applied for image segmentation, which ExpACVO trains.[26] Then, the segmented image is subjected to the image augmentation phase.[27] Afterwards, the feature extraction takes place. The extracted features are then forwarded to DM detection, which is done by DRN.[28] Here, DRN is trained by SHPO, a combination of SCA and HPO.[29,30] Figure 1 indicates SHPO_DRN for DM detection using tongue image.

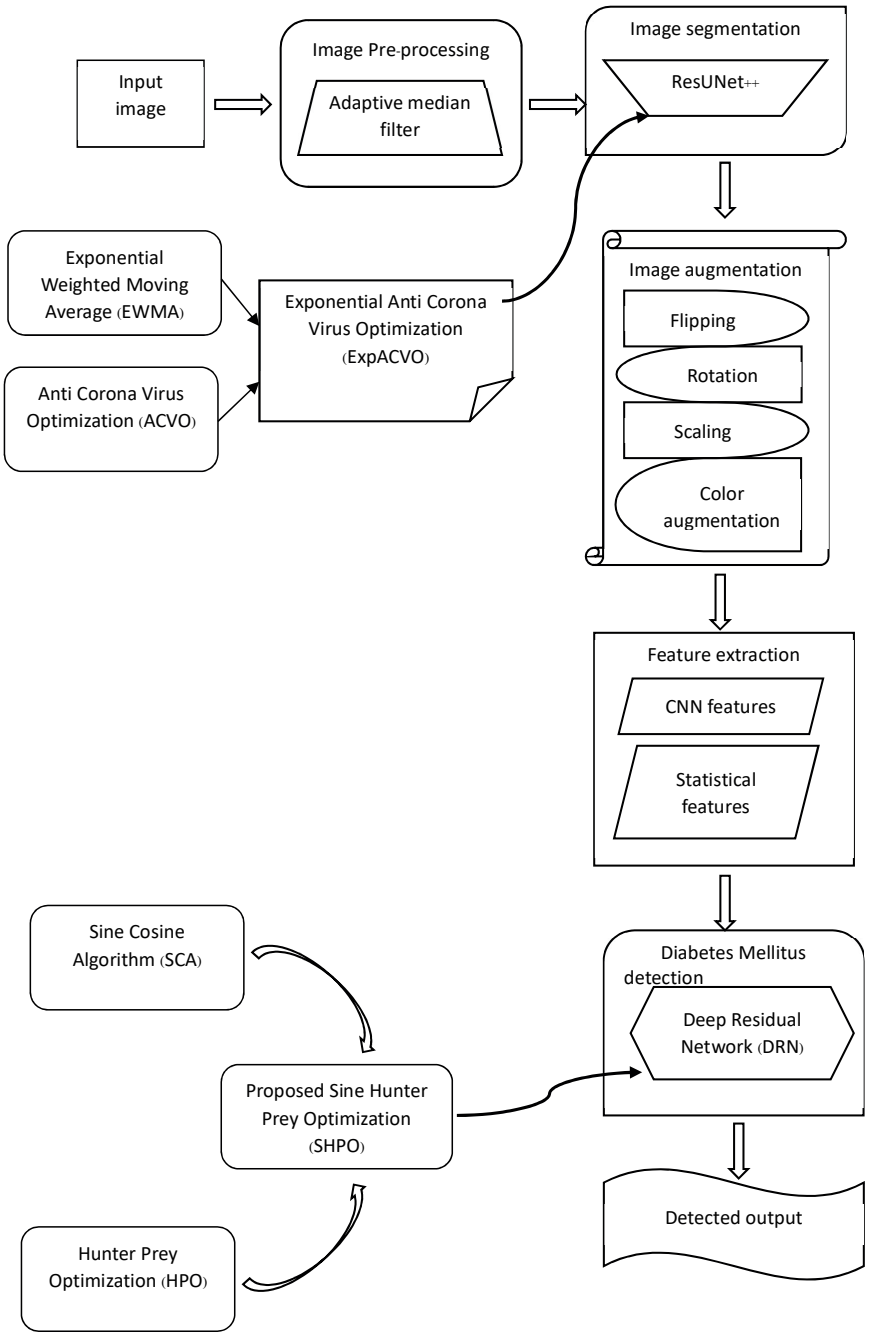

Figure 1. *SHPO_DRN for DM detection using tongue image.*

Acquisition of image

The input image is acquired from datasets that contain various tongue images.[23,24] This dataset is represented as in below format,

$$D_t = \{M_1, M_2, \ldots, M_r, \ldots, M_f\} \quad (1)$$

***Note**: D_t: image dataset, M_r : image in r^{th} position taken as input image, M_f : image in f^{th} position that is full images in the dataset.*

Image pre-processing by adaptive median filter

After the acquisition of the input image field, image pre-processing is done by the adaptive median filter to remove noises in the input image.[25]The pre-processed image is denoted by A_r.

Image segmentation by ResUNet++

Here, the pre-processed image A_r is sent for segmentation. Moreover, image segmentation is done by ResUNet++, which ExpACVO trains.[26] Here, ExpACVO is designed by a combination of ACVO[31] and EWMA.[32] Here, the segmented image is represented by term B_r.

Training of ResUNet++ byExpACVO

ResUNet++ is trained by ExpACVO, which is a combination of both ACVO and EWMA. Updated equation of ExpACVO is formulated below,

$$R_{oj}\left(q+1\right) = \left(\frac{R_{oj}^{E}\left(q\right) - \left(1-\alpha\right) * R_{oj}^{E}\left(q-1\right) + \alpha * \mathrm{B}\left(-1,1\right) * rand}{\alpha} \right) \quad (2)$$

***Note:** B(-1,1) : uniform random number, $R_{oj}(q+1)$: position of o^{th} person in j^{th} dimension at iteration q+1.*

Augmentation of image

This image augmentation includes many manipulation techniques, such as flipping, rotation, scaling, and color augmentation.[22]

Finally, image augmentation is represented in vector form as,

$$X_r = \{V_r(1), V_r(2), V_r(3), V_r(4)\} \quad (3)$$

***Note:** $V_r(1)$: image after the rotation process, $V_r(2)$: image after flipping process, $V_r(3)$: scaled image, $V_r(4)$: image after color augmentation. Thus, the augmented image is given by X_r.*

Extraction of features

Input used for feature extraction is augmented image X_r. Here, features taken are statistical features, such as mean,[33] variance,[33] kurtosis,[34] skewness,[34] standard deviation,[35] entropy,[33] and CNN features.[36]

The statistical features are indicated in vector format,

$$St_r = \{U(1), U(2), U(3), U(4), U(5), U(6)\} \quad (4)$$

***Note:** U(1): mean, U(2): variance, U(3): kurtosis, U(4): skewness, U(5): standard deviation, U(6): entropy. CNN features are indicated by term P_r.*

Thus, overall features are indicated in vector format by,

$$E_r = \{St_r, P_r\} \quad (5)$$

***Note:** E_r: overall feature vector extracted from the augmented image.*

DM detection by DRN

After feature extraction, DM is detected by DRN, trained using SHPO. Here, the overall feature vector E_r is allowed for DM detection.

Architecture of DRN

DRN[37,28] is utilized in works regarding pattern recognition including high training speed with deeper NN and simpler transmission gradient.

Convolution layer

The input at every position given by,

$$Conv2d(Q) = \sum_{y=0}^{x-1}\sum_{z=0}^{x-1} O_{y,z} \cdot Q_{(c+y),(d+z)} \quad (6)$$

$$Conv1d(Q) = \sum_{e=0}^{A_{in}-1} O_e * Q \quad (7)$$

***Note:** Conv2d(Q): process on computation, Conv1d(Q): operator that indicates cross-correlation, Q: prior layers 2D result, c,d: utilized in recording 2D input coordinates, O: x × x kernel matrix, y,z: 2D kernel matrix index position.*

Pooling layer

This layer reduces feature maps spatial size where average pooling is used. Here, the fitting problem is regulated and computes size similar to *Conv1d* and *Conv2d*. Width with a height of 2D matrix output is indicated as,

$$z_{ou} = \frac{z_{in} - O_z}{\mathrm{K}} + 1 \quad (8)$$

$$z_{ou} = \frac{z_{in} - O_z}{\mathrm{K}} + 1 \quad (9)$$

***Note:** z_{in} and y_{in}: height and width of 2D matrix input, o_z and o_y : height and width of kernel dimension.*

Function of activation

This increase features non-linearity stimulates convergence, and alleviates vanishing gradient indicated as ReLu, which is,

$$\mathrm{Re}\,Lu(Q) = \begin{cases} 0, & Q < 0 \\ Q, & Q \geq 0 \end{cases} \quad (10)$$

Batch normalization

This minimizes inputs internal covariate shift via scaling adjustment as well as activations. This enhances the speed of training and reliability while adjusting

gradient explosion and over fitting with a high learning rate.

Residual blocks

This is unity among input as well as output in the residual block. However, if dissimilar, matching factor of size is generated. Thus, input as well as output is represented as,

$$S = N(Q) + Q \quad (11)$$

$$S = N(Q) + M_Q Q \quad (12)$$

Note: *Q, S*: residual blocks input and output, *N*: relationship of mapping from inputs and outputs, M_Q: dimension matching factor.

Linear classifier

Here, the input vector is normalized using softmax to the probability vector of maximal probability, which brings out the last detection.

$$Soft\max(Q_O) = \frac{e^{Q_O}}{\Sigma_{o=1}^{L} e^{Q_O}}, o = 1, 2, .., O \quad (13)$$

Note: *L*: dimension of output, Q_O: layer element of output.

Hence, F_r is obtained result from DRN, trained by SHPO. Figure 2 is the architecture of DRN having many layers.

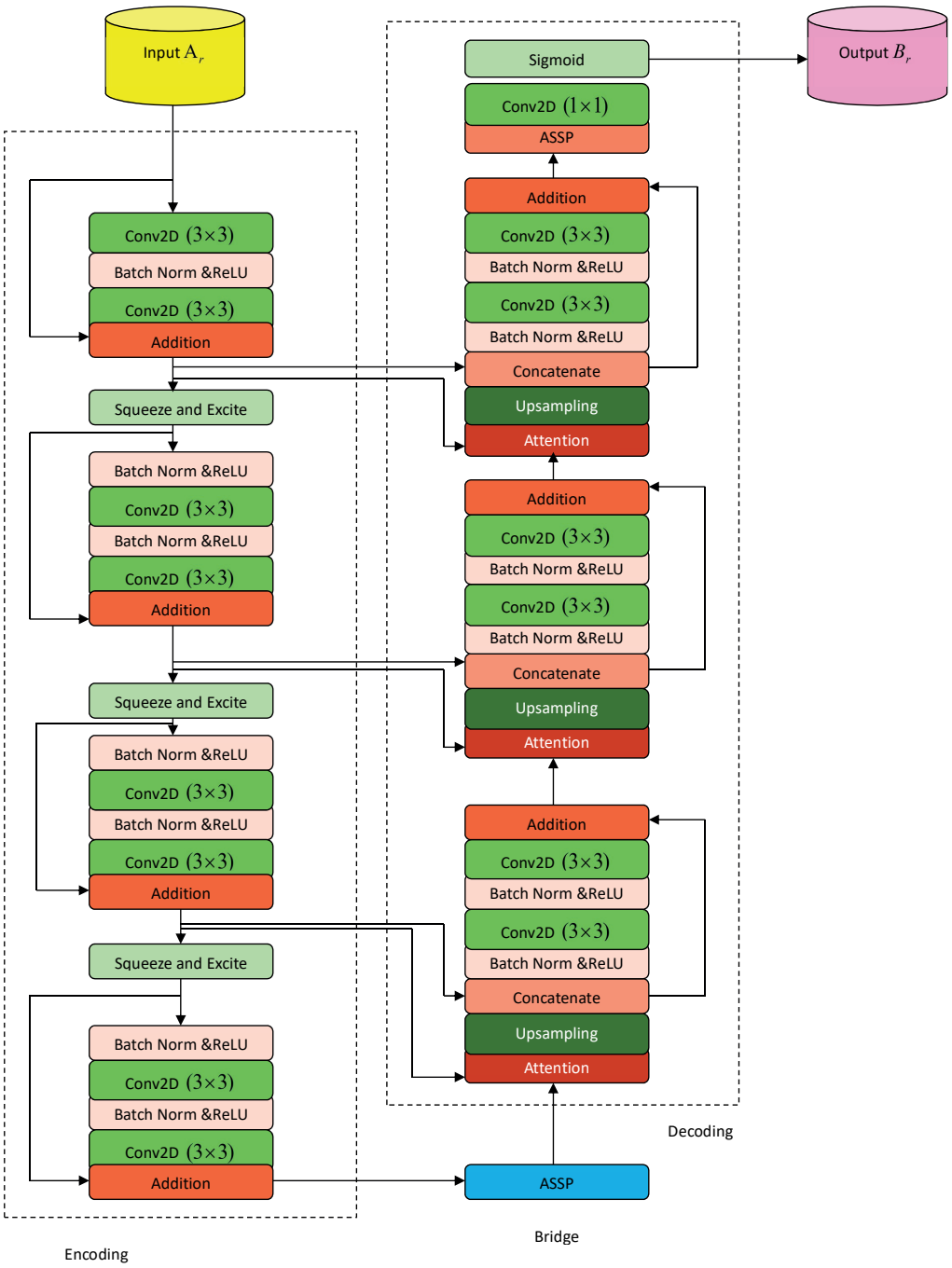

Figure 2. *DRN architecture.*

Training DRN by SHPO

DRN is trained using SHPO, formed by combining SCA and HPO.[29,30]

Hunterposition encoding

In *E* as search space, solution that is best is established, where DRNs learning parameter is indicated by β, which is denoted as *E*= [*1 x* β].

Finding fitness

The fitness function uses results gained from DRNN and targeted results and is denoted as,

$$Fit = \frac{1}{f}\sum_{r=1}^{f}\left[Tar_r^* - F_r\right]^2 \quad (14)$$

Note: *Fit: fitness based on DRN, f: total samples, F_r: DRN result , Tar_r^*: output targeted.*

Step 1: Initialization

Here, population is represented as,

$(s) = \{s_1, s_2, ..., s_t\}$ (15)

Here, the objective function for all members of the population is computed for evaluating the new position of a member and is given as,

$(u) = \{u_1, u_2, ..., u_t\}$ (16)

Every member position of the initial population is created by,

$s_v = rand(1, p)*(U_b - L_b) + L_b$ (17)

Note: *s_v: preys hunter position, L_b: lower boundary, U_b: value upper boundary, p: number of variables*

Step 2: Fitness finding

This is evaluated by attaining the maximum optimal solution that brings a better solution and is represented in Equation (14).

Step 3: Search mechanism

This search mechanism is indicated as,

$$s_{v,o}(n+1) = s_{v,o}(n) + 0.5[(2ACD_{pos(o)} - s_{v,o}(n)) + (2(1-A)C\chi_{(o)} - s_{v,o}(n))] \quad (18)$$

Note: *s(n): current hunter position, s(n+1): hunter next position, D_{pos}: prey position, χ: mean position, C: adaptive parameter.*

Here,

$D = G_1 < A, ind = (D==0)$ (19)

$C = G_2 \otimes ind + G_3 \otimes (\sim ind)$ (20)

Note: *G_2 and G_3: random vectors in range [0,1], D: random vector of 0 and 1 equals variable numbers, ind: index number, A: balance parameter, where value decreases from 1 to 0.02, and is indicated as,*

$$A = 1 - iter\left(\frac{0.98}{Max_{iter}}\right) \quad (21)$$

Note: *iter: current value of iteration, Max_{iter}: maximal iteration. Moreover, search agents distance from mean is,*

$$\chi = \frac{1}{t}\sum_{v=1}^{t}\vec{s}_v \quad (22)$$

Moreover, distance based on Euclidean distance is given as,

$$Dis_{E(v)} = \left(\sum_{o=1}^{p}\left(s_{v,o} - \chi_o\right)^2\right)^{\frac{1}{2}} \quad (23)$$

The search agent with maximal distance from the mean is D_{pos}

$$\vec{D}_{pos} = \vec{s}_v \,|v is index of\, Max(end) sort(Dis_E) \quad (24)$$

If the search agent is considered with maximal distance from Field as an average location in every iteration, then the algorithm has late convergence. Here, the decreasing mechanism is,

$kbest = round(A \times H)$ (25)

Note: *H: search agent numbers. Also, prey position is calculated as,*

$$\vec{D}_{pos} = \vec{s}_v \,|v is sorted\, Dis_E(kbest) \quad (26)$$

Here, value of *kbest* equals *H*. It is assumed that best safe position is optimally global position as it gives prey a survival chance, and hunter chooses another prey, which is represented as,

$$s_{v,o}(n+1) = I_{pos(o)} + AC\cos(2\pi G_4) \times (I_{pos(o)} - s_{v,o}(n)) \quad (27)$$

Note: *s(n): preys current position, s(n+1): further prey position, I_{pos}: optimally global position, G_4: random number ranging [-1,1]. The function of cos and input parameter allows the next position of prey to be positioned at global optimal various radials along angles and increase exploitation performance.*

$$s_{v,o}(n+1) = I_{pos(o)} + AC\cos(2\pi G_4) I_{pos(o)} - AC\cos(2\pi G_4) s_{v,o}(n) \quad (28)$$

$$s_{v,o}(n+1) = I_{pos(o)}[1 + AC\cos(2\pi G_4)] - AC\cos(2\pi G_4) s_{v,o}(n) \quad (29)$$

Basic equation of SCA with condition $m_4 < 0.5$ is,

$$s_{v,o}(n+1) = s_{v,o}(n) + m_1 \times \sin(m_2) \times \left|m_3 J_{v,o}(n) - s_{v,o}(n)\right| \quad (30)$$

Assume, $J_{v,o}(n) > s_{v,o}(n)$,

$$s_{v,o}(n+1) = s_{v,o}(n) + m_1 \times \sin(m_2) \times \left|m_3 J_{v,o}(n) - s_{v,o}(n)\right| \quad (31)$$

$$s_{v,o}(n+1) = s_{v,o}(n) + m_1 \times \sin(m_2) \times \left(m_3 J_{v,o}(n) - s_{v,o}(n)\right) \quad (32)$$

$$s_{v,o}(n+1) = s_{v,o}(n) + m_1 \times \sin(m_2) m_3 J_{v,o}(n) - m_1 \times \sin(m_2) s_{v,o}(n) \quad (33)$$

$$s_{v,o}(n+1) = s_{v,o}(n)[1 - m_1 \times \sin(m_2)] + m_1 \times \sin(m_2) m_3 J_{v,o}(n) \quad (34)$$

$$s_{v,o}(n) = \frac{s_{v,o}(n+1) - m_1 m_3 \sin(m_2) J_{v,o}(n)}{1 - m_1 \times \sin(m_2)} \quad (35)$$

Substitute Equation (48) in Equation (42), which forms a hybridization of SCA with HPO.

$$s_{v,o}(n+1) = I_{pos(o)}[1 + AC\cos(2\pi G_4)] - AC\cos(2\pi G_4)\left(\frac{s_{v,o}(n+1) - m_1 m_3 \sin(m_2) J_{v,o}(n)}{1 - m_1 \times \sin(m_2)}\right) \quad (36)$$

$$s_{v,o}(n+1) + \frac{AC\cos(2\pi G_4) s_{v,o}(n+1)}{1 - m_1 \times \sin(m_2)} = I_{pos(o)}[1 + AC\cos(2\pi G_4)] - AC\cos(2\pi G_4)\left(\frac{-m_1 m_3 \sin(m_2) J_{v,o}(n)}{1 - m_1 \times \sin(m_2)}\right) \quad (37)$$

$$\frac{s_{v,o}(n+1)\left(1 - m_1 \times \sin(m_2)\right) + AC\cos(2\pi G_4) s_{v,o}(n+1)}{1 - m_1 \times \sin(m_2)} = \frac{I_{pos(o)}[1 + AC\cos(2\pi G_4)]\left(1 - m_1 \times \sin(m_2)\right) - AC\cos(2\pi G_4)\left(-m_1 m_3 \sin(m_2) J_{v,o}(n)\right)}{1 - m_1 \times \sin(m_2)} \quad (38)$$

$$s_{v,o}(n+1) = \frac{1}{1 - m_1 \sin(m_2) + AC\cos(2\pi G_4)}\begin{pmatrix} I_{pos(o)}[1 + AC\cos(2\pi G_4)]\left(1 - m_1 \times \sin(m_2)\right) \\ + AC\cos(2\pi G_4)\left(m_1 m_3 \sin(m_2) J_{v,o}(n)\right) \end{pmatrix} \quad (39)$$

This forms basic equation of SHPO for training DRN.

Note: $s_{v,o}$ *(n+1):* v^{th} solution position in o^{th} dimension at iteration *(n+1),* m_1 , m_2 and m_3: random numbers ranging [0,1], *c* : adaptive parameter, G_4: random number ranging [-1,1], a: balance parameter.

Step 4: Choosing hunter and prey

The prey and hunter is chosen based on below formula,

$$s_v(n+1) = \begin{cases} s_v(n) + 0.5\left[\left(2ACD_{pos} - s_v(n)\right) + \left(2(1-a)C\chi - s_v(n)\right)\right] & if\ G_5 < \lambda\ \ (a) \\ I_{pos} + AC\cos(2\pi Q_4) \times (I_{pos} - s_v(n)) & else\ \ \ (b) \end{cases} \quad (40)$$

Note: *Q_5: random number, λ: regulatory parameter set as 0. If Q_5 is less than λ, search agent is hunter. If Q_5 is more than λ then search agent is prey.*

Step 5: End

Thus, fitness is reevaluated as per Equation (14). This brings out an optimal maximal solution to generate best solution for training DRN to detect DM.

Results and discussion

This model is implemented in the python tool with Tongue image dataset[23] and Diabetic images dataset.[24]

Comparative assessment

Analysis of the comparison of SHPO_DRN is carried out in two ways, such as by altering the k-value and by altering the learning set. SHPO_DRN is compared with several methods like CNN,[3] Multi-modal learning,[15] SVM,[16] and ExpACVO-based DQN.

Comparison by varying k-value

Figure 3 represents a comparison of SHPO_DRN byk value change. Figure 3a) indicates accuracy-related comparison by changing k value. When k fold=5, accuracy is 0.796, 0.843, 0.862, 0.917, and 0.940 for CNN, Multi-modal learning, SVM, ExpACVO-based DQN, and SHPO_DRN. Figure 3b) is SHPO_DRN comparison of sensitivity by changing k fold value. While k value=6, sensitivity is 0.952 for SHPO_DRN, other models show lesser sensitivity of 0.828, 0.874, 0.886, and 0.932. Figure 3c) implies specificity-related comparison by altering k-value. For k value of 7, specificity is high at 0.936 for SHPO_DRN, whereas other techniques show lesser specificity of 0.782, 0.837, 0.868, and 0.902. Figure 3d) indicates f-measure based comparison of SHPO_DRN by alteration in k-value. While 8 is k fold value, f-measure is high for SHPO_DRN with 0.961, whereas 0.798, 0.816, 0.848, and 0.887 are f-measure values other models attain.

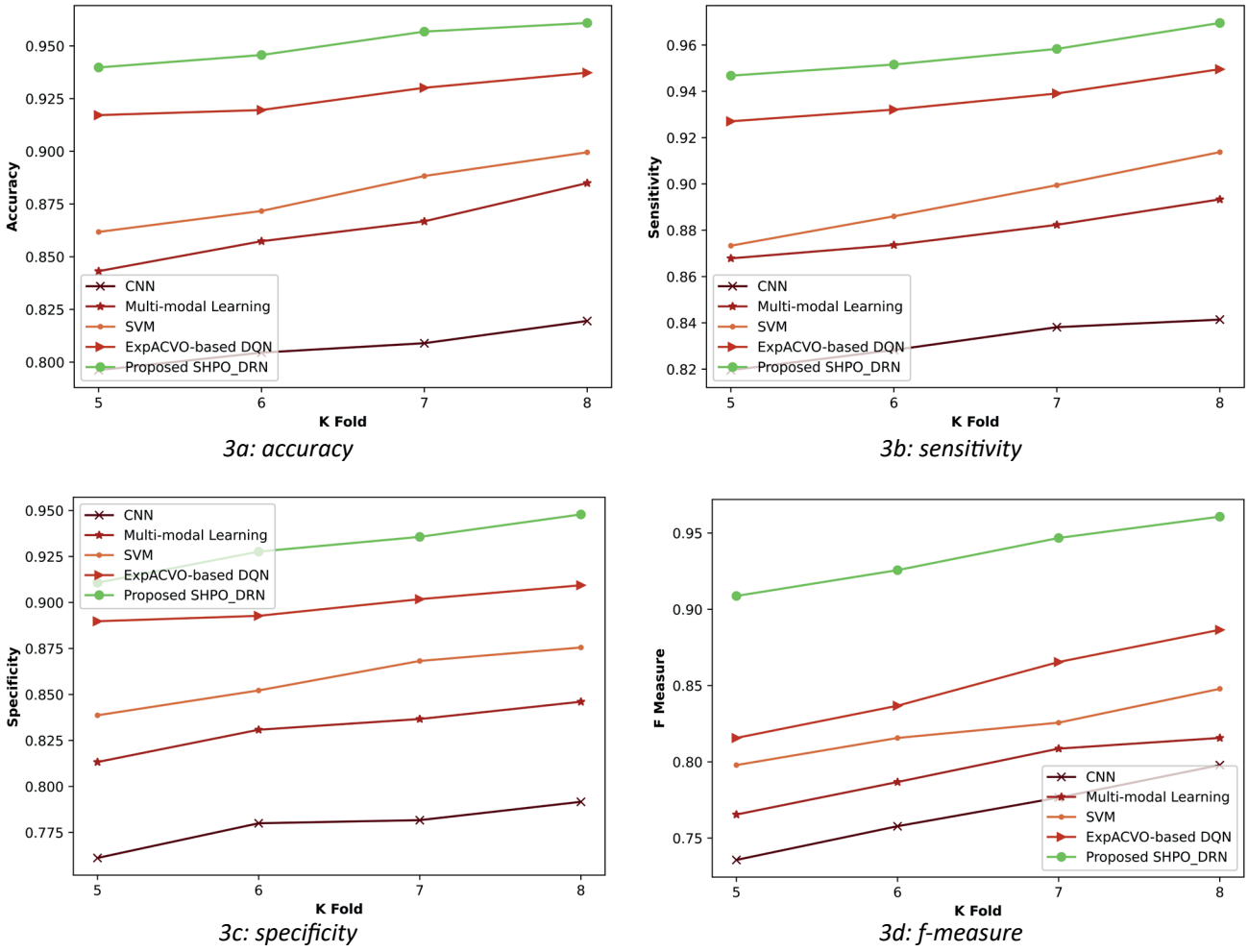

Figure3. *Comparison by varying k-value. a: accuracy, b: sensitivity, c: specificity, d: f-measure*

Comparison by changing learning set

Figure 4 presents a comparative assessment of SHPO_DRN by learning set variation. Figure 4a) is an accuracy comparison by altering learning set. When learning percentage is 90, accuracy is 0.950 for SHPO_DRN, whereas for CNN, Multi-modal learning, SVM, and ExpACVO-based DQN, accuracy values are 0.819, 0.882, 0.907, and 0.931. Figure 4b) is SHPO_DRNs sensitivity comparison by altering learning set. While 80% of learning set, sensitivity is 0.820, 0.868, 0.873, 0.927, and 0.947 for CNN, Multi-modal learning, SVM, ExpACVO-related DQN, and SHPO_DRN. Figure 4c) is specificity-enabled comparison by learning percentage variation. While learning set=70%, specificity is higher of 0.897 for SHPO_DRN, whereas other techniques show less specificity of 0.736, 0.749, 0.786, and 0.821. Figure 4d) implies f-measure based comparison of SHPO_DRN by varying learning set. When training set=60%, f-measure is high for SHPO_DRN with 0.909, whereas0.726, 0.754, 0.787, and 0.809 are f-measure values other techniques attain.

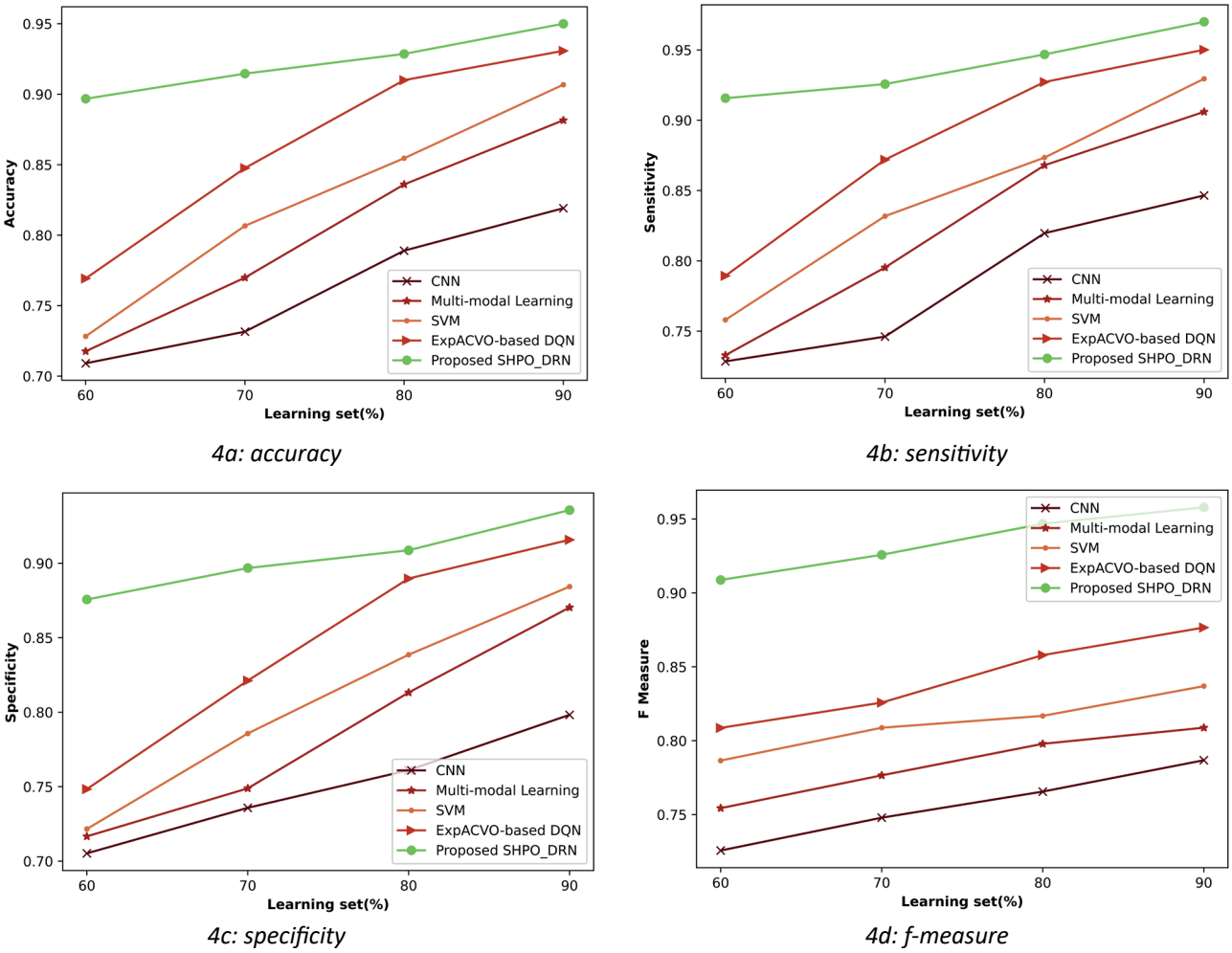

Figure 4. *Comparison by varying learning set. a: accuracy, b: sensitivity, c: specificity, d: f-measure.*

Conclusion

In this study, DM is recognized using a tongue image based on a DL model called DRN, which is trained by SHPO. In this case, an adaptive median filter is used for pre-processing, and picture segmentation is performed by ResUNet++, which has been trained by ExpACVO. Following that, image augmentation and relevant feature extraction phases are performed, culminating in DM detection by DRN. Furthermore, SHPO is created by merging SCA and HPO. Four assessment metrics, such as accuracy, specificity, sensitivity, and f-measure, are utilized to determine performance of proposed SHPO_DRN. These measurements perform well in this context, with high range values of 96%, 97%, 95%, and 96%. In future, this research can be examined for other disease detection with better optimization algorithms.

Conflict of interest

None

Source of funding

Not Applicable

Acknowledgements

I would like to express my very great appreciation to the co-authors of this manuscript for their valuable and constructive suggestions during the planning and development of this research work.

References

[1] Kaveeshwar SA, Cornwall J. The current state of diabetes mellitus in India. Australas Medical J. 2014; 7(1): 45. doi.org/10.4066/AMJ.2013.1979.

[2] American Diabetes Association, Economic consequences of diabetes mellitus in the US in 1997. Diabetes Care. 1998; 21(2): 296-309. doi.org/10.2337/diacare.21.2.296.

[3] Wu L, Luo X, Xu Y. Using convolutional neural network for diabetes mellitus diagnosis based on tongue images. J Eng. 2020; 2020(13): 635-8. doi.org/10.1049/joe.2019.1151.

[4] Lontchi-Yimagou E, Sobngwi E, Matsha TE, Kengne AP. Diabetes mellitus and inflammation. Curr Diabetes Rep. 2013; 13(3): 435-44. doi.org/10.1007/s11892-013-0375-y.

[5] Zhang B, Zhang H. Significant geometry features in tongue image analysis. eCAM. 2015. doi.org/10.1155/2015/897580.

[6] Pang B, Zhang D, Wang K. Tongue image analysis for appendicitis diagnosis. Info Sci. 2005; 175(3): 160-76.

doi.org/10.1016/j.ins.2005.01.010.

[7] Wang X, Zhang D. An optimized tongue image color correction scheme. IEEE T Inf Technol B. 2010; 14(6): 1355-64. doi.org/10.1109/TITB.2010.2076378.

[8] Kanawong R, Obafemi-Ajayi T, Liu D, Zhang M, Xu D, Duan Y. Tongue image analysis and its mobile app development for health diagnosis. Trans Info Smart Healthcare. 2017; 99-121. doi.org/10.1007/978-981-10-5717-5_5.

[9] Yildirim O, Talo M, Ay B, Baloglu UB, Aydin G, Acharya UR. Automated detection of diabetic subject using pre-trained 2D-CNN models with frequency spectrum images extracted from heart rate signals. Comput Biol Med. 2019; 113: 103387. doi.org/10.1016/j.compbiomed.2019.103387.

[10] Bandyopadhyay M, Rout M, Satapathy SC. eds. Machine Learning Approaches for Urban Computing. Springer. 2021. doi.org/10.1007/978-981-16-0935-0.

[11] Ismael HA, Al-A'araji NH, Shukur BK. Enhanced the prediction approach of diabetes using an autoencoder with regularization and deep neural network. Period Eng Nat Sci. 2023; 10(6): 156-67. doi.org/10.21533/pen.v10i6.3394.

[12] Qazi EUH, Zia T, Almorjan A. Deep Learning-Based Digital Image Forgery Detection System. App Sci. 2022; 12(6): 2851. doi.org/10.3390/app12062851.

[13] Mirjalili S, Mirjalili S. Genetic algorithm. Evolu Algo Neu Net: Theo & App. 2019; 43-55. doi.org/10.1007/978-3-319-93025-1.

[14] Wang D, Tan D, Liu L. Particle swarm optimization algorithm: an overview. Soft comp. 2018; 22: 387-408. doi.org/10.1007/s00500-016-2474-6.

[15] Li J, Zhang B, Lu G, You J, Zhang D. Body surface feature-based multi-modal learning for diabetes mellitus detection. Info Sci. 2019; 472: 1-4. doi.org/10.1016/j.ins.2018.09.010.

[16] Sagayaraj AS, Kabilesh SK, Kumar AA, Gokulnath S, Mani T, Dinakaran K. Diabetes Mellitus and Diabetic Retinopathy Detection using Tongue Images. In Journal of Physics: Conference Series. 2021; 1831(1): 012028. doi.org/10.1088/1742-6596/1831/1/012028.

[17] Naveed S. Early diabetes discovery from tongue images. Compu J. 2022; 65(2): 237-50. doi.org/10.1093/comjnl/bxaa022.

[18] Deepa SN, Banerjee A. Intelligent decision support model using tongue image features for healthcare monitoring of diabetes diagnosis and classification. Net Mod Anal Heal Info & Bioinfo. 2021; 10(1): 41. doi.org/10.1007/s13721-021-00319-1.

[19] Logeswaran T, Gowrishankar P, Surendar V, Tamilarasu P, Suresh M. Detection of Diabetes Mellitus using Tongue images. Int J Recent Technol Eng. 2019; 8(4): 2475-82. doi.org/10.35940/ijrte.C6409.118419.

[20] Li J, Yuan P, Hu X, Huang J, Cui L, Cui J, Ma X, Jiang T, Yao X, Li J, Shi Y. A tongue features fusion approach to predicting prediabetes and diabetes with machine learning. J Biomed Inform. 2021; 115: 103693. doi.org/10.1016/j.jbi.2021.103693.

[21] Thirunavukkarasu U, Umapathy S, Krishnan PT, Janardanan K. Human tongue thermography could be a prognostic tool for prescreening the type II diabetes mellitus. Evid-Based Compl Alt. 2020. doi.org/10.1155/2020/3186208.

[22] Shone N, Ngoc TN, Phai VD, Shi Q. A deep learning approach to network intrusion detection. IEEE Trans Emerg Top Comput Intell. 2018; 2(1): 41-50. doi.org/10.1109/TETCI.2017.2772792.

[23] The Tongue image dataset is taken from, https://github.com/BioHit/TongeImageDataset, accessed on May 2023.

[24] The Diabetic images dataset is taken from, https://drive.google.com/drive/u/0/folders/1SsJE1WM-mou5h5yM8TTUy1K44QrtWqE07, accessed on May 2023.

[25] Jubair MI, Rahman MM, Ashfaqueuddin S, Ziko IM. An enhanced decision based adaptive median filtering technique to remove Salt and Pepper noise in digital images. Int Conf Compu & Info Tech (ICCIT 2011), IEEE. 2011; 428-33. doi.org/10.1109/ICCITechn.2011.6164827.

[26] Jha D, Smedsrud PH, Riegler MA, Johansen D, De Lange T, Halvorsen P, Johansen HD. Resunet++: An advanced architecture for medical image segmentation. IEEE Int Sym Multim (ISM), IEEE. 2019; 225-55. doi.org/10.48550/arXiv.1911.07067.

[27] Khalifa NE, Loey M, Mirjalili S. A comprehensive survey of recent trends in deep learning for digital images augmentation. Artif Intell Rev. 2021; 1-27. doi.org/10.1007/s10462-021-10066-4.

[28] He K, Zhang X, Ren S, Sun J. Deep residual learning for image recognition. Proc Cvpr IEEE. 2016; 770-8. doi.org/10.48550/arXiv.1512.03385.

[29] Mirjalili S. SCA: a sine cosine algorithm for solving optimization problems. Knowl-Based Syst. 2016; 96: 120-33. doi.org/10.1016/j.knosys.2015.12.022.

[30] Naruei I, Keynia F, Sabbagh Molahosseini A. Hunter-prey optimization: Algorithm and applications. Soft Comput. 2022; 26(3): 1279-1314. doi.org/10.1007/s00500-021-06401-0.

[31] Emami H. Anti-coronavirus optimization algorithm. Soft Comput. 2022; 26(11): 4991-5023. doi.org/10.1007/s00500-022-06903-5.

[32] Saccucci MS, Amin RW, Lucas JM. Exponentially weighted moving average control schemes with variable sampling intervals. Commun Stat-Simul C. 1992; 21(3): 627-57. doi.org/10.1080/ 036109 19208813040.

[33] Khairandish MO, Sharma M, Jain V, Chatterjee JM, Jhanjhi NZ. A hybrid CNN-SVM threshold segmentation approach for tumor detection and classification of MRI brain images. IRBM. 2021. doi.org/10.1016/j.irbm.2021.06.003.

[34] Hemanth DJ. EEG signal based modified Kohonen neural networks for classification of human mental emotions. J Artif Intell & Sys. 2020; 2: 1-13. doi.org/10.33969/AIS.2020.21001.

[35] Reddy AC. Evaluation of Surface Roughness Using Image Processing Technique. Pentagram Res Cen (P)

Ltd. 2004. doi.org/10.13140/2.1.2687.5207.

[36] Huang K, Liu X, Fu S, Guo D, Xu M, A lightweight privacy-preserving CNN feature extraction framework for mobile sensing. IEEE T Depend Secure. 2019; 18(3): 1441-55. doi.org/10.1109/TDSC.2019.2913362.

[37] Chen Z, Chen Y, Wu L, Cheng S, Lin P. Deep residual network based fault detection and diagnosis of photovoltaic arrays using current-voltage curves and ambient conditions. Energ Convers Manage. 2019; 198: 111793. doi.org/10.1016/j.enconman. 2019.111793.

Journal of Associated Medical Sciences 2024; 57(2): 86-100

JAMS
Journal of Associated Medical Sciences

Scopus Indexed & Thai-Journal Citation Index Centre (TCI)

Journal of Associated Medical Sciences

Journal homepage: https://www.tci-thaijo.org/index.php/bulletinAMS/index

CRISPR 2 spacer architecture analysis and virulotyping for epidemiological study of Salmonella enterica subsp. Enterica circulating in northern Thailand (2015 -2017)

Sudarat Srisong[1] Rungthiwa Srimora[1] Nuttachat Wisittipanit[2] Chaiwat Pulsrikarn[3] Kritchai Pooncharean[4*]

[1]Master of Science Program in Biotechnology, School of Agriculture and Natural Resources, University of Phayao, Phayao Province, Thailand
[2]Department of Material Engineering, School of Science, Mae Fah Luang University, Chiang Rai Province, Thailand
[3]Department of Medical Sciences, WHO National Salmonella and Shigella Center, National Institute of Health, Ministry of Public Health, Nonthaburi province, Thailand
[4]Division of Biochemistry, School of Medical Sciences, University of Phayao, Phayao Province, Thailand

ARTICLE INFO

Article history:
Received 21 December 2023
Accepted as revised 13 February 2024
Available online 27 February 2024

Keywords:
CRISPR 2, spacer analysis, virulotyping, epidemiological study, rapid Salmonella typing, S. 4,[5],12:i:- subtyping.

ABSTRACT

Background: *Salmonella* enterica subsp. enterica, particularly serotype *S.* 4[5],12:i:-, *S.* Typhimurium, and *S.* Enteritidis, represents a significant causative agent of diarrhea, particularly impacting children and immunocompromised individuals on a global scale. Molecular typing of *Salmonella* spp. has a vital role in understand *Salmonella* epidemiology.

Objective: The objective of this study is to utilize CRISPR 2 spacer analysis coupled with multiple-locus variable number tandem-repeat (VNTR) analysis and virulotyping to perform molecular typing and potential subtyping of *Salmonella* spp.

Materials and methods: CRISPR 2 - multiple-locus variable number tandem-repeat (VNTR) analysis, complemented by additional virulotyping, were performed to rapidly characterize those *Salmonella* isolates including eight unidentified strains. Serotype-specific CRISPR 2 amplicons were subjected to sequencing and the obtained sequences were blasted with corresponding whole-genome sequencing (WGS) data in order to extract CRISPR 2 information, especially the number and sequence of spacers which were then utilized to predict *Salmonella* serotypes. Moreover, the similar CRISPR 2 spacer architectures to the corresponding WGS offered the prediction of multilocus sequence types (MLST).

Results: *S.* 4,[5],12:i:-, *S.* Typhimurium, *S.* Enteritidis, *S.* Weltevraden, and *S. Derby* exhibited distinct clustering, while eight unidentified *Salmonella* serotypes displayed unique CRISPR 2-MLVA profiles. Through subsequent sequence analysis and comparison with publicly available whole-genome sequencing data, serotype-specific CRISPR 2 amplicon lengths and spacer architectures were unveiled, enabling precise prediction of MLST types. Intriguingly, a linear correlation emerged between CRISPR 2 amplicon length (500-2000 bps) and the number of spacers (6-32) across diverse *Salmonella* serotypes. Critically, the molecular signatures of CRISPR 2 amplicons accurately predicted the identity of eight unknown *Salmonella* isolates, aligning with conventional serotyping standards. Furthermore, MLST sequences for prevalent *S.* 4,[5],12:i:-, *S.* Typhimurium, and *S.* Enteritidis were unveiled as ST 34, ST 19, and ST 10, respectively. Subtyping of *S.* 4,[5],12:i:- using the *sop*E1 procession (a bacteriophage gene) revealed two major subtypes within ST 34. These subtypes encompassed all six virulent genes, including *Inv*A, *bcf*C, *csg*A, *agf*A, *sod*C1, and *gip*A, either with *sop*E1 (N=8) or without *sop*E1 (N=10). These findings contribute preliminary insights into the genetic diversity and subtyping of *S.* 4,[5],12:i:-.

Conclusion: The combination of CRISPR 2 sequence analysis and virulotyping emerged as a potent epidemiological tool, facilitating the identification of *Salmonella* serotypes and potentially informative subtypes, thereby aiding in the surveillance, and tracking of *Salmonella* transmission in northern Thailand.

∗ **Corresponding contributor.**
Author's Address: *Division of Biochemistry, School of Medical Sciences, University of Phayao, Phayao Province, Thailand*
E-mail address: kof_of@hotmail.com
doi: 10.12982/JAMS.2024.030
E-ISSN: 2539-6056

Introduction

Food poisoning or severe gastroenteritis resulting from the consumption of contaminated Salmonella spp. is a global issue.[1] Predominantly pathogenic to both warm-blooded animals and humans, S. enterica subsp. enterica can be classified into more than 2,463 serovars by assessing their antigenic properties according to the White-Kauffmann-Le Minor Scheme.[2] A limited collection of Salmonella serotypes potentially poses a public concern.[3] Non-Typhoidal Salmonella (NTS) is well-known for causing localized infections, diarrhea, or watery stools, particularly in young individuals.[4] Nevertheless, specific Salmonella serovars, such as S. Enteritidis and S. Typhimurium, are commonly associated with the development of more complicated sepsis.[5]

Nontyphoidal Salmonella (NTS) is commonly found in contaminated commercial meat, eggs, or dairy products. Common sources of the pathogen include well-known animal origins such as cattle, pigs, and chickens.[6] Transmission from animals to humans typically occurs through the consumption of contaminated food, often due to improper cooking or poor sanitation, particularly affecting vulnerable populations such as children, the elderly, or immunocompromised patients.[6,7]

Globally, the incidence of gastroenteritis is approximately 94 million cases per year, with documented rates ranging from 4 to 2741 cases per 100,000 people, varying geographically across the European Union and approximately 14 cases per 100,000 in the United States.[8,9] Furthermore, sporadic cases of multicountry outbreaks have been observed, such as those involving contaminated eggs with *S.* Enteritidis in Poland during 2016-2017 and powdered milk contaminated with *S.* Agona in France during 2017-2018.[10,11] In Thailand, the national documentation for the distribution of *Salmonella* serotypes was conducted during 1993-2002, involving more than 70,000 *Salmonella* isolates. The study identified groups of clinically important *Salmonella* serotypes, with *S.* Weltevreden ranking first, followed by *S.* Enteritidis (2nd), *S.* 4,5,12:i:- (4th), *S.* Typhimurium (5th), and *S.* Stanley (8th).[12] However, food poisoning was publicly documented at up to 163 cases per 100,000 in 2018, without specific causal characterization.[13]

Conventional typing, relying on serological characterization, is considered the standard method for *Salmonella* typing and is endorsed by the ISO system for official reporting.[14] However, the associated laboratory equipment is costly and skilled personnel are scarce. Advancements in *Salmonella* molecular typing have led to the development of rapid characterization methods, utilizing equipment ranging from standard PCR machines to advanced techniques like sequencing, NGS, and high-resolution melting temperature (HRM)-PCR, the latter often combined with multiplex PCR for detailed polymorphism detection.[15,19] For comprehensive epidemiological research, both conventional typing and appropriate molecular approaches are necessary to report *Salmonella* serovars and often their subtypes or even clonal identity in the case of outbreak analysis.[16] Molecular targeting of *Salmonella* typing is rapidly achieved by identifying specified polymorphic alleles of 16S RNA, the *rfb* gene cluster involved in O-antigen biosynthesis, and flagella genes.[17,18] More intricate protocols utilizing advanced technology have been developed to precisely characterize bacterial subtypes or identify clones. Various approaches, including Multilocus Sequence Typing (MLST), Multi Locus Variable number of tandem repeat Analysis (MLVA), Pulsed Field Gel Electrophoresis (PFGE), and Whole Genome Sequencing (WGS), have been established for epidemiologically identifying the transmission routes of *Salmonella* spp. or the causal origins of *Salmonella* outbreaks.[20,21]

Clustered regularly interspaced short palindromic repeats (CRISPR) constitute a novel family of repeated DNA sequences recognized for their adaptive immune protection against foreign mobile genetic elements (MGEs) present in various gram-negative bacteria, including *E.coli*, *Salmonella* spp., and *S.Klebsiella pneumoniae*.[22,23] The distinctive genetic features of the CRISPR locus include an alternating series between direct repeats (DRs), 24-47 bp in length, and DNA variable sequences (spacers) of 21-72 bp.[24] Positioned upstream to the CRISPR locus are a "leader sequence", alternated repeated patterned of directed sequences (DR) and specific spacers and followed by several types of (CRISPR-associated sequence) genes.[25] The CRISPR locus potentially houses unique genetic sequences influenced by evolutionary pressures and is commonly employed for bacterial typing or clonal identification. In *Salmonella* typing, previous studies compared sequence polymorphisms of two CRISPR loci, CRISPR 1 and CRISPR 2, across 783 *Salmonella* strains, observing correlations between *Salmonella* serotypes and multilocus sequence types.[26] Additionally, the characterization of spacer content within CRISPR alleles provided sufficient information for *Salmonella* subtyping.[27] In practical applications, a CRISPR 2 PCR assay was developed for the rapid characterization of three clinically important *Salmonella* spp. using agarose gel electrophoresis.[28] More recently, CRISPR loci polymorphisms have been utilized in a single-step assay to identify multiple contaminated *Salmonella* spp. from poultry samples.[29] As a molecular tool for subtyping bacterial pathogens, multiple-locus variable number tandem-repeat analysis (MLVA) relies on characterizing copy numbers of tandem repetitive DNA elements at different loci. The development of MLVA primarily involves selecting potential loci and designing multiplex primers.[30] This approach has been extensively applied to subtype *S.* Enteritidis and *S.* Typhimurium, demonstrating a high discriminatory index based on amplicon sizing from capillary electrophoresis.[31] Notably, recent MLVA methods have shown promise in characterizing *E. coli* subtypes corresponding to Sequence Types (ST) through visual observation on agarose gel electrophoresis.[32]

Virulotyping or detecting different profiles of virulent gene panels was employed as a potential tool to characterize *Salmonella* heterogenicity among different *Salmonella* serotypes or the same *Salmonella* serovars based on their different phenotypic characteristics. Virulotyping 523 *Salmonella* enterica Serovars Relevant to

Human Health in Europe showed the distribution of most virulence genes corresponding with *Salmonella* serotypes; nevertheless, high variation in the same serotypes was observed with those virulence genes that were prophage encoded, in fimbrial clusters or in the virulence plasmid.[33] The *Salmonella* subtyping of *Salmonella* Typhimurium by differentiating prophage profiles was further performed and found that prophage profiles significantly correspond to MLVA types.[34]

To assess molecular typing methods targeting CRISPR 2 loci, MLVA, and virulent genes as an alternative approach for *Salmonella* typing, preliminary analyses of CRISPR 2-MLVA and CRISPR 2 sequence were rapidly conducted. This evaluation aimed to differentiate 51 standard *Salmonella* strains from various sources (part of a standard collection) and eight *Salmonella* isolates of unknown origin. Moreover, the process involved the sequencing of CRISPR 2 amplicons to determine *Salmonella* serotypes and MLST sequences. These sequences were then compared to the *Salmonella* whole-genome sequencing (WGS) public database available on the public bacterial database (enterobase.com). Furthermore, additional virulent genes were selected and analyzed to provide preliminary information for characterizing *Salmonella* subtypes. This information could potentially offer insights into *Salmonella* transmission patterns in northern Thailand.

Materials and methods

Salmonella isolates in this study

This study analyzed 59 *Salmonella* isolates, comprising 17 identified serotypes via conventional methods and 8 unidentified strains (Table 1). The isolates included 43 samples from hospitalized patients, collected at Phayao Ram Hospital, Phayao Province, between 2015-2017.[35] The remaining 16 isolates were sourced from minced pork and various animal species, acquired across five northern Thailand provinces during 2017-2018.[36]

The collection and use of clinical *Salmonella* isolates were ethically approved by Phayao University's Ethical Committee (Approval No. 57 02 04 0020). Similarly, the procurement of animal-derived isolates adhered to ethical standards, with approval granted by the University's Institutional Animal Care and Use Committee (IACUC), under Project No. 62-02-04-001.

Table 1 Collection of 59 *Salmonella* isolates from various sources in northern Thailand (2015-2017).

Number	Serotypes	Source	Number (N=59)
1	*S.*4,5,12:i:-	Hospitalized patients	16
		Minced pork	4
		Swine	1
2	*S.*Typhimurium	Chicken	2
		Goat	1
3	*S.*Enteritidis	Hospitalized patient	5
		Chicken	1
4	*S.*Weltevreden	Hospitalized patient	4
5	*S.*Stanley	Hospitalized patient	3
6	*S.*Derby	Minced pork	2
7	*S.*Kentucky	Hospitalized patient	1
8	*S.*Agona	Chicken	1
		Hospitalized patient	1
9	*S.*Schwarzen	Minced pork	1
10	*S.*Covallis	Hospitalized patient	1
11	*S.*Krefeld	Swine	1
12	*S.*Braenderup	Chicken	1
13	*S.*Saintpaul	Minced pork	1
14	*S.*Montevideo	Hospitalized patient	1
15	*S.*Barilly	Hospitalized patient	1
16	*S.*Kedougou	Hospitalized patient	1
17	*S.*Give	Hospitalized patient	1
18	Unknown	Hospitalized patient	8

Molecular analyzation of Salmonella isolates from various sources was conducted by performing CRISPR 2 MLVA PCR

Salmonella strains stored in glycerol stocks at -20°C were revived and incubated in NB broth overnight. Confirmation of *Salmonella* identity was conducted by plating on MacConkey agar and SS agar, respectively. A single black colony was selected from SS agar for subsequent DNA isolation. *Salmonella* DNA extraction followed a previously described method.[39] In brief, a one mL aliquot of the culture underwent centrifugation, and the pellet was washed with TE buffer (10 mM Tris HCl, pH 8.0, containing 1 mM EDTA). Subsequently, it was suspended in 400 µL of TE buffer and heated at 80°C for 20 min. Then, 50 µL of lysozyme solution (10 mg/mL) was added, and the mixture was incubated at 37°C for one hr. Following this, 75 µL of a 10% SDS/proteinase K solution was added, and the mixture was incubated at 65°C for 10 min. Next, 100 µL aliquots of 5 M NaCl and prewarmed (65°C) cetyl trimethylammonium bromide (CTAB)/NaCl solution were added. The solution was then incubated at 65°C for 10 min, followed by the addition of 750 µL of chloroform:isoamyl alcohol (24:1) solution. The mixture underwent centrifugation at 11,000×g for 5 min at 4°C, followed by ethanol precipitation. Lastly, the DNA pellet was dissolved in 50 µL of distilled water and stored at -20°C until use.

Multiplex PCR was conducted using specific sets of primers for the amplification of CRISPR 2 alleles and MLVA, as detailed in Table 2. The PCR reactions were performed in a BIO-RAD CFX96TM Real-Time System (Bio-Rad, Hercules, CA, USA). Each PCR mixture (10 µL) contained 1 µL of DNA, 8 pairs of primers at concentrations specified in Table 1, and 2 µL of HOT FIREPol Blend Master Mix Plus 10 mM $MgCl_2$ (Solis Biodye, Tartu, Estonia). The thermocycling conditions for the MLVA set were as follows: initial denaturation at 95°C for 12 minutes, followed by 30 cycles of 94°C for 30 sec, 55°C for 90 sec, and 72°C for 90 sec, with a final extension step at 72°C for 10 minutes. For the CRISPR 2 PCR, the thermocycling conditions included an initial denaturation at 95°C for 12 min, followed by 35 cycles of 94°C for 60 sec, 59°C for 90 sec, and 72°C for 90 sec, with a final extension step at 72°C for 10 min. Subsequently, amplicons from both reactions were combined and subjected to 1% agarose gel electrophoresis in Tris Borate EDTA (TBE, 1X) buffer. Visualization was achieved by staining with RedSafe dye (1:20,000) (INiRON, Washington, United States).

Table 2. Primers used in this study.

Primer	Genes	Sequence (5' → 3')	Size of PCR- product (bps)	Primer Concentration (pmol/ul)	Reference
***Salmonella* typing**					
CHRISPR 2 and MLVA multiplex					
B1	CRSPR 2 loci	GAGCAATACYYTRATCGTTAACGCC	variable	0.2	[24]
B2		GTTGCDATAKGTYGRTRGRATGTRG		0.2	
ECMLV1_f		TCCCTGGACAAACCAGGACTG	162	0.1	[30]
ECMLV1_r1		CGTGCGGACTTATGAGAAAG		0.1	
ECMLV1_r2		CGTGCGGGCTTATGAAAAAG		0.5	
ECMLV2_f		GAAACAGGCCCAGGCTACAC	575	0.05	
ECMLV2_r		CTGGCGCTGGTTATGGGTAT		0.05	
ECMLV3_f		TTCAGGAAATGGATAAAGTAGT	616	0.8	
ECMLV3_r		GGGAGTATGCGGTCAAAAGC		0.8	
ECMLV4_f		ACAACCGGCTGGGGCGAATCC	413	0.05	
ECMLV4_r		GTCAGCAAATCCAGAGAAGGCA		0.05	
ECMLV5_f		GCGGCGCTGAAGAAGAAAGC	413	0.05	
ECMLV5_r		CTCCCGGCAGGCGAAGCATTGT		0.05	
Virulotyping					
Multiplex 1 bcfC; Bovine colonization factor, fimbrial usher, **csgA;** Major fimbrial subunit of thin curled fimbriae and **agfA;** Aggregative fimbria A					
bcfC_f		CAGCTTTTCATGACGCGATA	241	0.4	[35]
bcfC_r		CAATGTCTCTGGTTGCGAGA		0.4	
csgA_f		GGATTCCACGTTGAGCATTT	212	0.4	
csgA_r		CGGAGTTTTTAGCGTTCCAC		0.4	
agfA_f		GGATTCCACGTTGAGCATTT	312	0.4	
agfA_r		GTTGTTGCCAAAACCAACCT		0.4	
Uniplex 1 invA location; Chromosome, Function Enables the bacteria to invade cells					
InvA_f		GTGAAATTATCGCCACGTTCGGGCAA	284	0.125	[36]
InvA_r		GCCCCGGTAAACAGATGAGTATTGA			
Uniplex 2 sopE1 location; Cryptic bacteriophage, Function ; Translocated T3SS effector protein					
sopE1_f		CGGGCAGTGTTGACAAATAAAG	422	0.4	[31]
sopE1_r		TGTTGGAATTGCTGTGGAGCT		0.4	

Table 2. Primers used in this study. *(continued)*

Primer	Genes	Sequence (5' → 3')	Size of PCR- product (bps)	Primer Concentration (pmol/ul)	Reference
Uniplex 3 gipA l location; Gifsy- 1bacteriophage, Function; Peyer's patch-specific virulence factor					
gipA_f		ACGACTGAGCAGGCTGAG	518	0.4	[31]
gipA_r		TTGGAAATGGTGACGGTAGAC		0.4	
Uniplex 4 sodC1 location; Gifsy-2bacteriophage, Function; periplasmic Cu, Zn superoxide dismutase					
sodC1_f		CCAGTGGAGCAGGTTTATCG	424	0.4	[31]
sodC1_r		GGTGCGCTCATCAGTTGTTC		0.4	

[b]Y=T or C; R=A or G; S=G or C; D=A or G or T

Amplicon Profile Analysis and Phylogenetic Tree Construction.

CRISPR 2-MLVA amplicon patterns were analyzed using a curve-based algorithm (Pearson correlation) in the open-source GelJ software.[40] This approach allowed for the creation of a similarity scale, essential for comparing amplicon size variations among different *Salmonella* serotypes. The resultant amplicon profiles were then used to construct phylogenetic trees. An unweighted pair-group method using arithmetic averages (UPGMA) algorithm was employed for this purpose, chosen for its efficacy in illustrating the evolutionary relationships among closely related isolates.

Characterization of CRISPR 2 amplicon sequences

CRISPR 2 amplicons for spacer arrangement analysis were individually examined in separate uniplex experiments for thirty-three isolates (nos. 4, 38, 52, 125, 131, 132, 133, 145, 246, 254, 262, 378, 411, 413, 426, 443, 450, 454, 466, 475, 482, 483, 487, 495, L8, L10, L17, L27, en6, en13, en18, en8, en11). These amplicons were excised and sent for DNA sequencing at First Base (First BASE Laboratories Sdn Bhd, Malaysia).

The obtained CRISPR 2 sequences, in FASTA format, were analyzed using the CRISPRCasFinder tool (https://crisprcas.i2bc.parissaclay.fr/CrisprCasFinder/Index) set to default parameters. This tool was chosen for its accuracy in identifying CRISPR 2 features such as the DR consensus sequence, DR length, and spacer count. Data was presented as sequences or numerical values for further analysis.

Additionally, these CRISPR 2 sequences were compared with Whole Genome Sequences (WGS) of corresponding Salmonella serotypes from the public domain. BLAST analysis, using CRISPR 2 specific primers, was conducted to determine the congruence in amplicon lengths, as visualized in agarose gel electrophoresis.

Molecular analysis of* Salmonella virulent *genes

Amplifications of seven virulent genes were carried out using either multiplex or uniplex PCR with primers obtained from IDT, Singapore (refer to Table 2). Each reaction mixture (10 µL) comprised 1 µL of DNA, the primer set at concentrations specified in Table 2, and 2µL of HOT FIREPol Blend Master Mix Plus 10 mM $MgCl_2$ (Solis Biodye). For all multiplexes and uniplexes, the thermocycling conditions were as follows: an initial denaturation at 95°C for 15 min, followed by 35 cycles of 95°C for 30 sec, 58°C for 30 sec, and 72°C for 1 min, with a final extension step at 72°C for 5 min. The exception was uniplex PCR 1, where the annealing temperature was set at 64 °C for invA. Following amplification, the resulting amplicons were visualized through 1.5% agarose gel electrophoresis, stained with RedSafe dye (1:20000) (INiRON, Washington, United States).

Statistical analysis

Data analysis for descriptive statistics was performed by using of SPSS for Windows, version 10 (SPSS Inc, Chicago, USA) at the University of Phayao.

Results

CRISPR 2-MLVA Profiles in Clinically Important Salmonella Serotypes

The rapid molecular typing of 59 *Salmonella* isolates, including 17 identified and 8 unknown serotypes from northern Thailand (2015-2017), revealed distinct CRISPR 2-MLVA profiles (Figure 1). These profiles allowed us to categorize the isolates into three clusters. Specifically, S. 4,5,12:i:- (N=21), *S.* Enteritidis (N=6), and *S.* Derby (N=2) showed unique profiles with CRISPR 2 fragments at approximately 1600 bps, 800 bps, and 900 or 950 bps, respectively. In contrast, the third cluster exhibited closely related profiles among *S.* Typhimurium, *S.* Stanley, and *S.* Weltevreden, with variations in CRISPR 2 amplicon sizes (1700 bps for *S.* Typhimurium; 1600, 1650, and 1500 bps for *S.* Weltevreden; 1600 and 1500 bps for *S.* Stanley). The other nine serotypes and the eight unidentified isolates presented diverse CRISPR 2-MLVA patterns, with notable faint bands in *S.* Kreldfeld (L8) and *S.* Braenderup (L12), and similar profiles in *S.* Saintpaul (en18) and *S.* Montediveo (38) at approximately 1500 bps.

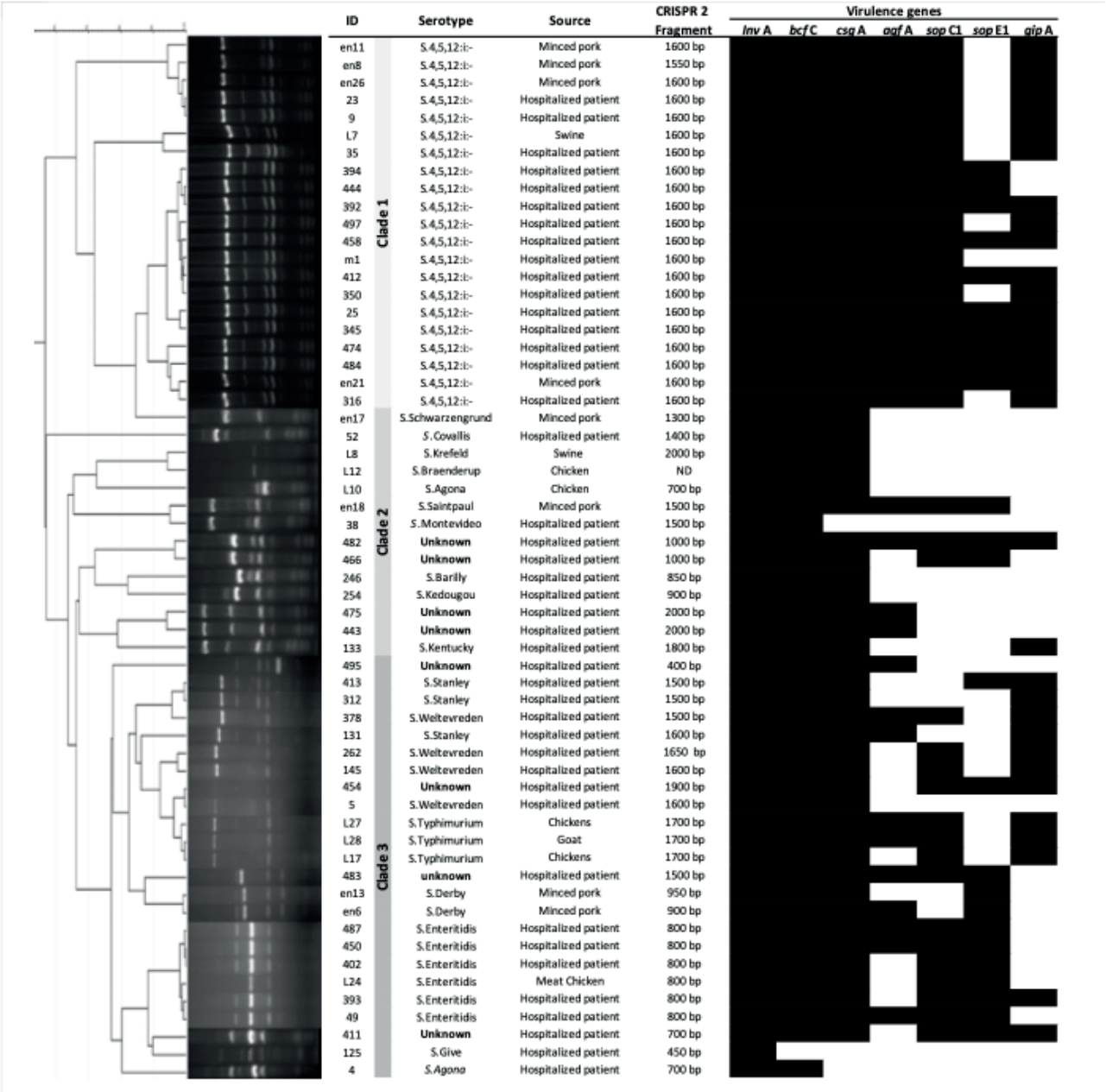

Figure 1 *CRISPR 2 - MLVA Phylogeny tree with associated virulotypes of 59 Salmonella isolates from various sources in northern Thailand (2015-2017). ID: abbreviated name of Salmonella isolates.*

In summary, the CRISPR 2-MLVA profiles of *S.* 4,5,12:i:-, *S.* Enteritidis, and *S.* Derby were consistently distinct and appear suitable for *Salmonella* typing. Further sequence analysis is planned to explore the CRISPR 2 amplicons in more detail, focusing on direct repeats, spacer numbers, and array structures, to confirm serotypes and characterize the unknown isolates.

CRISPR 2 amplicon sequence analysis of 17 *Salmonella* serotypes and 8 unknowns

The analysis of CRISPR 2 loci in 17 identified and 8 unknown *Salmonella* serotypes revealed amplicons ranging from 500 to 2500 bps. Notably, *S.* Braenderup did not produce any CRISPR 2 amplicons (Figure 2). Serotypes like *S.* Give, *S.* Agona, *S.* Enteritidis, *S.* Schwarzen, and *S.* Covallis displayed unique amplicon lengths (480 to 1300 bps). Others, including *S.* 4,5,12:i:- and *S.* Typhimurium, generated amplicons around 1500 bps, indicating serotype-specific profiles.

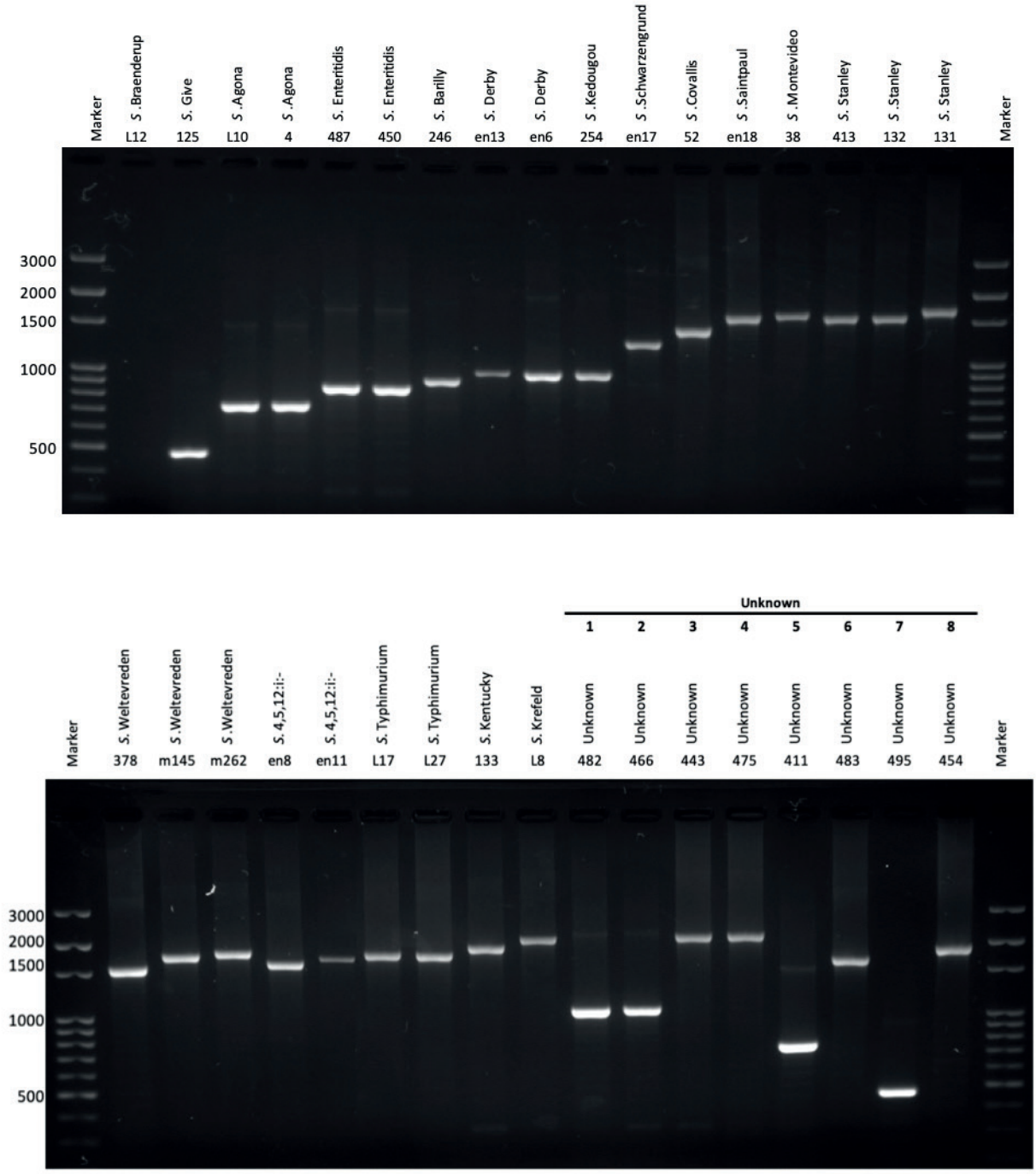

Figure 2 *The CRISPR 2 amplicons of 17 Salmonella serotypes and 8 unknowns of Salmonella isolates from various sources in northern Thailand (2015-2017).*

We sequenced CRISPR 2 amplicons from a representative sample (17 serotypes, 26 isolates; 8 unknowns, 8 isolates) to analyze spacer profiles. Comparing these with public WGS data, we found a close match in molecular weights and spacer counts (Table 3). This alignment suggests a strong correlation between CRISPR 2 amplicons and *Salmonella* serotypes. Particularly, *S.* 4,5,12:i:-, *S.* Typhimurium, and *S.* Enteritidis produced serotype-specific CRISPR 2 amplicons correlating with ST 34, ST 19, and ST 11, respectively. *S.* Stanley and *S.* Weltevreden had similar-sized amplicons corresponding to ST 29 and ST 365. The unknown isolates were identified as various serotypes, including *S.* Typhimurium and *S.* Weltevreden, with novel spacer additions predicted in some cases.

These findings demonstrate the practical utility of CRISPR 2 spacer analysis in predicting *Salmonella* serotypes and STs, offering a viable alternative to conventional typing methods. Furthermore, a linear relationship between the CRISPR 2 amplicon lengths and the number of spacers was observed (Figure 3), underscoring the structured molecular system and potential of using CRISPR 2 loci for indicating other *Salmonella* serotypes from this study.

Table 3 Description of some *Salmonella* serotype specific spacers extracted from raw sequences and further analyzation of the corresponding WGS reference of 17 *Salmonella* serotypes and eight unknowns from various sources in northern Thailand (2015-2017).

NO	Isolated	#C2 Fragment	$S1	S2	S3	S7	S8	S9	S16	S17	Serotypes	Expected C2 Fragments	Expected total number of spacers C2	Expected ST	WGS data Reference
1	L12	0									*S*.Braenderup	0	18	22	SAL_BA8466AA
2	m125	450	ParAB0	CheB1	CheB2						*S*.Give	465	6	516	SAL_XA8594AA
3	L10	700	AgoB1	AgoB2	AgoB3	AgoB7	AgoB8				*S*.Agona	752	8	13	SAL_DB2207AA
4	m4	700	AgoB1	AgoB2	AgoB3	AgoB7	AgoB8				*S*.Agona	752	8	13	SAL_DB2207AA
5	487	850	EntB0	EntB1	EntB2	EntB6	EntB7	EntB8			*S*.Enteritidis	833	10	11	SAL_XA8590AA
6	450	850	EntB0	EntB1	EntB2	EntB6	EntB7	EntB8			*S*.Enteritidis	833	10	11	SAL_XA8590AA
7	m246	900	STMB0	STMB32	STMB2	STMB32	STMB4	STMB5			*S*.Barilly	950	11	909	SAL_XA8606AA
8	en13	1000	DerB1	DerB2	DerB3	DerB13	DerB7	DerB9			*S*.Derby	1014	13	40	SAL_FA4928AA
9	en6	1000	DerB1	DerB2	DerB3	DerB13	DerB7	DerB9			*S*.Derby	1014	13	40	SAL_FA4928AA
10	m254	1000	EnuB1	EnuB2	3	7	Newp13	kra16var			*S*.Kedougou	953	12	1543	SAL_XA8603AA
11	en17	1300	ParBB5	STMB32	BovB1	Swa3	Swa4	Swa5	SwaB12	SwaB13	S. Schwarzengrund	1258	17	96	SAL_DA7383AA
12	m52	1400	MaraB1	NapB4	AltB23	LexB8	LexB8	9	SenB13	JavB1	S.Covallis	1441	20	1541	SAL_XA8588AA
13	en18	1500	ParBB1	StpB3	StpB27	StpB15	StpB7	StpB8	StpB22	StpB23	*S*.Saintpaul	1563	22	50	SAL_FA2386AA
14	m38	1550	JavB1	MonB39	MonB40	MonB44	MonB45	MonB56	MonB46	MonB48	*S*.Montevideo	1625	23	1531	SAL_XA8587AA
15	413	1500	EntB0	IndB1	EntB10	NewpB34var1	BloB1	MbaB38	NiaB2	StaB6	*S*.Stanley	1686	24	29	SAL_XA8593AA
16	132	1500	EntB0	IndB1	EntB10	NewpB34var1	BloB1	MbaB38	NiaB2	StaB6	*S*.Stanley	1686	24	29	SAL_XA8593AA
17	131	1600	EntB0	IndB1	EntB10	NewpB34var1	BloB1	MbaB38	NiaB2	StaB6	*S*.Stanley	1686	24	29	SAL_XA8593AA
18	378	1500	CholB16	WelB2	WelB3	WelB5	WelB6	WelB7	WelB22	WelB23	*S*.Weltevreden	1808	26	365	SAL_XA8578AA
19	m145	1770	CholB16	WelB2	WelB3	WelB5	WelB6	WelB7	WelB22	WelB23	*S*.Weltevreden	1808	26	365	SAL_XA8578AA
20	262	1800	CholB16	WelB2	WelB3	WelB5	WelB6	WelB7	WelB22	WelB23	S.Weltevreden	1808	26	365	SAL_XA8578AA
21	en8	1450	STMB0	STMB32	STMB1	STMB5	STMB6	STMB7	STMB14	STMB15	*S*.4,5,12:i:-	1686	23	34	SAL_XA8579AA
22	en11	1600	STMB0	STMB32	STMB1	STMB5	STMB6	STMB7	STMB15	STMB16	*S*.4,5,12:i:-	1686	24	34	SAL_XA8579AA
23	L17	1700	STMB0	STMB32	STMB1	STMB5	STMB6	STMB7	STMB13	STMB14	*S*.Typhimurium	1809	26	19	SAL_CB8211AA
24	L27	1700	STMB0	STMB32	STMB1	STMB5	STMB6	STMB7	STMB13	STMB14	*S*. Typhimurium	1809	26	19	SAL_CB8211AA
25	m133	1800	EntB39	IndB1	KenB1	KenB5	KenB6	KenB7	KenB59	KenB20	*S*.Kentucky	1809	26	696	SAL_XA8595AA
26	L8	2000	AgoB1	WorB1	WorB2	EntB40	TenB2var1	9	16	17	*S*.Krefeld	2173	32	3157	SAL_YA8552AA
	Unknown										**Conventional Typing**				
27	482	1000	STMB0	STMB32	STMB1	STMB21	STMB22	STMB23			*S*.Typhimurium	1075	14	19	SAL_LA4069AA
28	466	1000	STMB0	2	3	BovB5	BovB6	BovB7			*S*.Bovismorbificans	1076	14	1499	SAL_FA5988AA
29	443	2100	AgoB1	WorB1	WorB2	EntB40	TenB2var1	9			*S*.Krefeld	2173	32	746	SAL_YA8552AA
30	475	2100	AlbB3	AlbB4	Kot26	7					*S*.Albany	2173	32	292	SAL_XA8577AA
31	411	850	PanB1	ParAB0var1	PanB2	PanB3	PanB4	PanB5			*S*.Panama	773	9	48	SAL_ZA4097AA
32	483	1600	ParAB0	InfB1	NewpB1	NewpB11	NewpB43	NewpB13			*S*.Newport	1501	NA	NA	NA
33	495	450	EntB0	IndB1	EntB10	4					*S*.Stanley	NA	NA	NA	NA
34	454	1800	CholB16	WelB2	WelB3	WelB5	WelB6	WelB7			*S*.Weltevreden	1808	26	365	SAL_XA8578AA

Note: *#C2 fragments: PCR amplicons from CRISPR 2 (C2) amplification (base pair: bps), $s(n): the abbreviated name of spacer from 5' of CHRIST 2 locus in sequential order of the number, expected total number of spacers C2, Expected ST: multi locus sequence type (MLST) derived from corresponding WGS data analysis, WGS reference from enterobase.com, NA: not analyzed, Number symbol [1-17] in spacer column defile new spacers (not in database).*

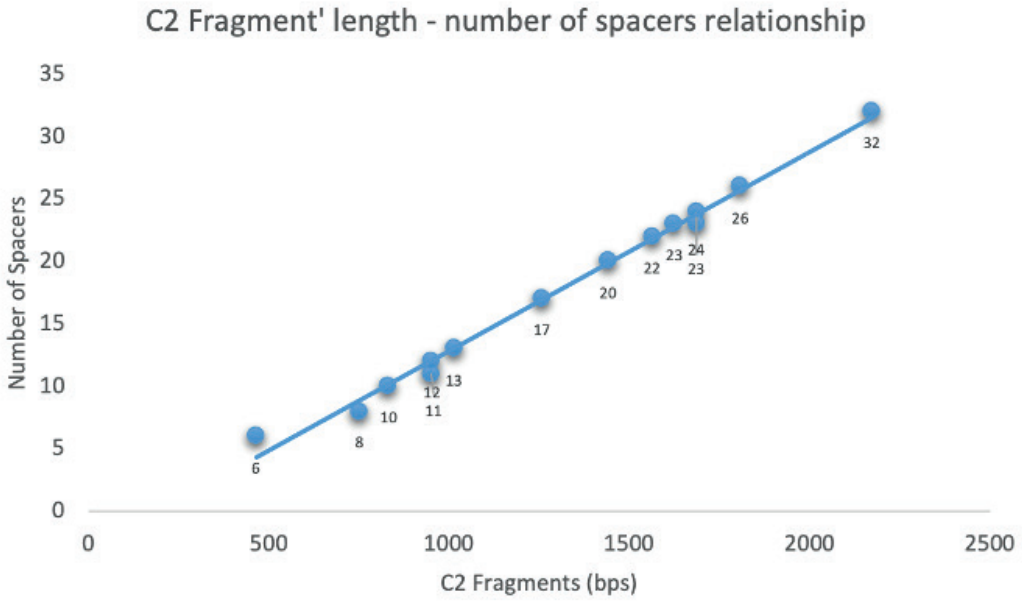

Figure 3 *Graph showed a linear relationship between the length of CRISPR 2 (C2) fragments (bps) and the total number of spacers observed from 14 Salmonella serotypes from various sources in northern Thailand (2015-2017).*

***Salmonella* Virulotypes for Subgrouping**

The study analyzed seven virulent factors in *Salmonella*, including fimbrial genes (*bcf*C, *csg*A, *agf*A), the invasive gene *inv*A, and bacteriophage-related genes (*gip*A, *sop*E1, *sod*C1), employing uniplex or multiplex PCR. Most isolates exhibited *inv*A, *bcf*C, and *csg*A, with exceptions in *S*. Montevideo, *S*. Enteritidis, *S*. Give, and *S.* Derby lacking one or more of these genes (Table 4). Interestingly, serotypes such as *S.* 4,5,12:i-, *S.* Typhimurium, and *S.* Enteritidis demonstrated unique patterns in *agf*A, *gipA*, *sop*E1, and *sod*C1, aiding further subtyping. For instance, the majority of *S.* 4,5,12:i- isolates presented two dominant virulent profiles, mainly distinguished by the presence or absence of *sop*E1. *S.* Typhimurium and *S.* Enteritidis also showed distinct gene patterns, notably in *agf*A and *gip*A.

Table 4 Virulent gene distribution, CRISPR 2 amplicons and Virulotypes of 17 *Salmonella* serotypes and 8 unknowns from various sources in northern Thailand (2015-2017).

Serotypes	Number of strains (N)	Clade	CRISPR 2 (bps)	Virulotypes	Virulent genes						
					*Inv*A	*bcf*C	*csg*A	*agf*A	*sod*C1	*Sop*E1	*gip*A
*S.*4,5,12:i:-	9	1	1600	V_1	■	■	■	■	■		■
	1	1	1550	V_1	■	■	■	■	■		■
	8	1	1600	V_2	■	■	■	■	■	■	■
	2	1	1600	V_3	■	■	■	■	■	■	
	1	1	1600	V_4	■	■	■	■	■		
					100%	100%	100%	100%	100%		
*S.*Typhimurium	2	3	1700 bp	V_1	■	■	■	■	■		■
	1	3	1700 bp	V_5	■	■	■		■		■
					100%	100%	100%		100%		100%
*S.*Enteritidis	3	3	800 bp	V_6	■	■	■	■	■	■	
	2	3	800 bp	V_7	■	■	■		■	■	
	1	3	800 bp	V_8	■	■	■		■	■	■
					100%	100%	100%		100%	100%	
*S.*Weltevraden	2	3	1650	V_5	■	■	■		■		■
	1	3	1500	V_1	■	■	■	■	■		■
	1	3	1600	V_14	■	■	■				■
					100%	100%	100%				100%
*S.*Stenley	1	3	1500	V_9	■	■	■			■	■
	1	3	1500	V_10	■	■	■				■
	1	3	1600	V_11	■	■	■	■			■
					100%	100%	100%				100%
*S.*Derby	1	3	950	V_12	■	■	■			■	
	1	3	900	V_13	■	■	■	■		■	
					100%	100%	100%				
*S.*Agona	1	2	700 bps	V_14	■	■	■				
	1	3	700 bps	V_15	■	■					
					100%	100%					
*S.*Kentucky	1	2	1800	V_16	■	■	■				■
					100%	100%	100%				
*S.*Saintpaul	1	2	1500	V_6	■	■	■	■	■	■	
*S.*Corvallis	1	2	1400	V_14	■	■	■				
*S.*Krefeld	1	2	2000	V_14	■	■	■				
*S.*Braenderup	1	2	ND	V_14	■	■	■				
*S.*Montedeveo	1	2	1550	V_15	■	■					
*S.*Barielle	1	2	850	V_14	■	■	■				
*S.*Kedouko	1	2	900	V_14	■	■	■				
*S.*Give	1	3	450	V_16	■						
*S.*Schwarzengrund	1	2	1300	V_14	■	■	■				
					100%						

Table 4 Virulent gene distribution, CRISPR 2 amplicons and Virulotypes of 19 *Salmonella* serotypes and 8 unknowns from various sources in northern Thailand (2015-2017). *(continued)*

Serotypes	Number of strains (N)	Clade	CRISPR 2 (bps)	Virulotypes	Virulent genes						
					***Inv*A**	***bcf*C**	***csg*A**	***agf*A**	***sod*C1**	***Sop*E1**	***gip*A**
Unknown											
482(*S.*Typhimurium)	1	2	1000	V_2	■	■	■	■	■	■	■
411 (*S.* Panama)	1	2	700	V_8	■	■	■		■	■	■
466 (*S.* Bovismorbificans)	1	2	1000	V_7	■	■	■		■	■	
483 (*S.* Newport)	1	2	1500	V_3	■	■	■	■	■	■	
443 (*S.*Krefeld)	1	3	2000	V_17	■	■	■	■			
475 (*S.* Albany)	1	3	2000	V_17	■	■	■	■			
495 (*S.*Stanley)	1	3	400	V_17	■	■	■	■			
454 (*S.*Weltevraden)	1	3	1900	V_8	■	■	■		■	■	■
					100%	100%	100%				

The analysis revealed that specific virulent gene patterns could significantly differentiate the *S.* 4,5,12:i- isolates into major subtypes, primarily based on *sop*E1 presence. This finding underscores the potential of using virulent gene patterns in *Salmonella* subtyping, especially in understanding the pathogenicity and epidemiology of these serotypes in northern Thailand.

Virulotypes and CRISPR 2 Spacer Profiles in Clinically Important* Salmonella *Serotypes

We analyzed *S.* 4,5,12:i-, *S.* Typhimurium, and *S.* Enteritidis from northern Thailand (2015-2017) for virulent gene profiles and CRISPR 2 spacer patterns. Twenty-one *S.* 4,5,12:i- strains exhibited two dominant virulent gene profiles: one with *sop*E1 (n=10, V_1) and another without *sop*E1 (N=8, V_2). Most of these strains consistently produced a CRISPR 2 fragment of 1600 bps, characterized by a specific spacer architecture (24 spacers; 3' spacer stmB0; 5' spacer stmB33) and MLST type 34 (Table 5). Two *S.* Typhimurium strains shared a virulent gene profile similar to *S.* 4,5,12:i- (V_2), but with a distinct CRISPR 2 fragment length (1700 bps) and spacer architecture (26 spacers; 3' spacer stmB0; 5' spacer stmB36), correlating with MLST type 19. An unknown *S.* Typhimurium strain exhibited a truncated CRISPR 2 fragment (1000 bps) with a different spacer pattern. *S.* Enteritidis strains demonstrated varied virulent gene profiles yet shared a consistent CRISPR 2 fragment length (800 bps) and spacer architecture (10 spacers; 3' spacer entB0; 5' spacer entB9), aligning with MLST type 10.

In summary, combining virulent gene profiling with CRISPR 2 PCR effectively differentiated three clinically significant *Salmonella* serotypes, particularly subtypes of *S.* 4,5,12:i-. This approach shows two subtypes of *S.* 4,5,12:i- circulating in both hospitalized patients and minced pork, facilitating *Salmonella* epidemiological research in northern Thailand.

Table 5. CRISPR 2 – virulent gene-based subtypes of clinically important *Salmonella Typhimurim Enteritidis* and 4,5,12i- isolates from various sources in northern Thailand (2015 -2017).

	Number (N=63)	ID	Source	Virulent genes	Predicted ST type	C2 Fragments (bps)	CRSPR 2 variation	Predicted Number of spacers (C2)	5' Spacer	3' Spacer	WGS data Reference
*S.*4,5,12:i:-	8	25, 345, 392, 412, 458 474, 484	Hospitalized patients	*InvA-bcfC-csgA-agfA-sodC1-sopE1-gipA*	34	1600		24	STMB0	STMB33	SAL_XA8579AA
		en21	Minced pork								
	10	316, 350, 497, 35, 23, 9	Hospitalized patients	*InvA-bcfC-csgA-agfA-sodC1-gipA*		1600		24			
		en11, en26	Minced pork								
		en8	Minced pork			1550	Δ STMB9	23			
		L7	Swine			1600		24			
	2	394, 444	Hospitalized patients	*InvA-bcfC-csgA-agfA-sodC1-sopE1*							
	1	1	Hospitalized patients	*InvA-bcfC-csgA-agfA-sodC1*							
*S.*Typhimurium	4	L27, L28	Chicken, Goat	*InvA-bcfC-csgA-agfA-sodC1-gipA*	19	900		10		STMB31	SAL_CB8211AA
		482 (unknown)	Hospitalized patients	*InvA-bcfC-csgA-agfA-sodC1-sopE1-gipA*							SAL_LA4069AA
		L17	Chicken	*InvA-bcfC-csgA-sodC1-gipA*							SAL_CB8211AA
*S.*Enteritidis	6	49,450,487	Hospitalized patients	*InvA-bcfC-csgA-agfA-sodC1-sopE1*	10	900		10	EntB0	EntB9	SAL_XA8590AA
		402	Hospitalized patients	*InvA-bcfC-agfA-sodC1-sopE1*							
		L24	Minced pork								
		393	Hospitalized patients	*InvA-bcfC-csgA-sodC1-sopE1-gipA*							

Note: *STMB8var1: TGCCAGTGACTACAGAAGCGTCTCTATCGGGG, STMB8var2: TCCCAGTGACTACAGAAGCGTCTCTATCGGGG*

Discussion

Salmonella spp. predominantly affects children and immunocompromised patients, exhibiting varying degrees of virulence, antibiotic resistance, and host specificity associated with different *Salmonella* serovars.[41] *S.* Enteritidis is often linked to bacterial sepsis, while *S.* Typhimurium, including its monophasic forms, frequently leads to prolonged hospitalization due to its high invasiveness and antibiotic resistance.[42] The rapid diagnosis of *Salmonella* serotypes, utilizing advanced molecular tools, is emerging as a highly potential technique for investigating salmonellosis. Various specific endpoint multiplex PCRs have been effectively used to target genes of o-antigens (*wzx*C2, *rfb*J, *prt*, *tyv*, *wzx*E, *wzx*C1, *prt*) and flagella antigens (*fli*C and *flj*B) for typing *Salmonella* serotypes. However, the large number of primers and the complexity of data interpretation often limit their practical application.[43] Alternatively, multiplex PCR combined with High-Resolution Melting (HRM) analysis, targeting sequence polymorphism of three genes, has proven effective in typing several epidemiologically significant *Salmonella* serotypes in Sweden and Thailand.[19,44] Furthermore, machine learning algorithms have been successfully applied to distinguish *Salmonella* serotypes with closely related HRM patterns. CRISPR loci, especially CRISPR 2, have been identified as promising gene targets containing unique DNA signatures capable of specifying S*almonella* subtypes.[45] However, so far, only the CRISPR 2 locus has been developed for characterizing *Salmonella* serotypes through the observation of different DNA amplicons on simple agarose gel electrophoresis.[38] Traditionally, MLVA analysis, typically observed using advanced Capillary Electrophoresis (CE), has been performed to subtype *Salmonella* spp.[46] In this study, however, CRISPR 2 locus analysis, in conjunction with MLVA, was used to generate DNA fingerprint patterns specific to various *Salmonella* serotypes based on agarose gel electrophoresis. To the best of our knowledge, this is the first instance of MLVA analysis being applied in combination with CRISPR 2 PCR to characterize *Salmonella* serotypes using simple agarose gel electrophoresis.

Salmonella enterica serotype 4,5,12:i- is globally prevalent and is often considered to exhibit a high degree of clonal prevalence. Subtyping of *S.* 4,5,12:i- has predominantly been conducted using sophisticated molecular techniques, such as Multilocus Variable-Number Tandem Repeat Analysis (MLVA) with capillary electrophoresis,[46] phage typing, and Pulsed-Field Gel Electrophoresis (PFGE) ,[47] along with CRISPR loci analysis and Whole Genome Sequencing (WGS).[48] Our previous efforts to rapidly subtype *S.* 4,5,12:i- using CRISPR 2 PCR in conjunction with High-Resolution Melting (HRM) analysis achieved limited success.[26] In this study, however, the use of CRISPR 2 and virulent gene amplicons, observed through agarose gel electrophoresis, successfully identified *S.* 4,5,12:i- ST 34 with varying virulotypes in northern Thailand. Genes such as *sop*E1, located on cryptic P2-like prophages, and *gip*A (gipsy-1) have been suggested as markers for subtyping S. 4,5,12:i- ST 34, supporting previous research conducted in China.[49] The heterogeneity of *sop*E1 is likely linked to phage-mediated horizontal gene transfer.[50] Recent research involving a substantial dataset (N=173) focused on the polymorphism of CRISPR 1 and 2, revealing CRISPR type TST4 as the most prevalent subtype of *S.* 4,5,12:i- in pig production in China.[51] Additionally, epidemiological studies have shown that the CRISPR-Cas system, especially the cas genes, used for classifying *S.* Typhi, is associated with varying antimicrobial resistance (AMR) statuses, demographic origins, and endemic isolates in South Asian countries.[51]

In summary, the combination of CRISPR 2 - MLVA analysis and virulotyping provided essential insights into *Salmonella* serotypes. This approach was particularly effective in determining the sequence type (ST) for regional *Salmonella* surveillance. Notably, the majority of *S.* 4,5,12:i- strains were identified as ST 34, with or without the *sop*E1 gene. The prevalence of these subtypes underscores their role in *Salmonella* transmission, contributing to the rate of human infections in northern Thailand between 2015 and 2017. Our future work will focus on using this approach with other serotypes to ascertain its efficiency.

Conclusion

In conclusion, the CRISPR 2 - MLVA analysis, complemented by virulotyping, has been instrumental in identifying and subtyping *S.* 4,5,12:i- in our study region. These methods not only provide preliminary serotype identification but also enable efficient determination of sequence types. This approach has significant implications for understanding *Salmonella* transmission and prevalence in human infections, particularly in northern Thailand between 2015-2017.

Data availability

The raw sequence of CRISPR 2 amplicon of 8 unknowns of *Salmonella* spp. and their CRISPR analyzation using online tool of CRISPRCasMeta [online] https://crisprcas.i2bc.paris-saclay.fr/CrisprCasMeta/Index

Acknowledgements

The authors acknowledge the financial support from a research grant from the Molecular Genetic of Bacterial Pathogen Unit of Excellence (MGBP) numbered FF64-UoE022, University of Phayao. Importantly, the first author wishes to sincerely pay his respects to Prof. Prapon Wilairat, who always supports both knowledge and the passion for mastering knowledge.

Conflicts of Interest

The authors confirm that there are no known conflicts of interest associated with this publication and there has been no significant financial support for this work that could have influenced its outcome.

References

[1] Majowicz SE, Musto J, Scallan E, Angulo FJ, Kirk M, O'Brien SJ, *et al*. The global burden of nontyphoidal Salmonella gastroenteritis. Clin Infect Dis. 2010; 50:

882-9.
[2] Kauffmann F. Serological diagnosis of Salmonella-species Kauffmann-White-Schema (Scandinavian university books) Vind, Denmark: Munksgaard;1972
[3] Hohmann EL.Nontyphoidal Salmonellosis. Clin Infect Dis. 2001; 32: 263-9.
[4] Chung N, Wang SM, Shen CF, Kuo FC, Ho TS, Hsiung CA, *et al*. Clinical and epidemiological characteristics in hospitalized young children with acute gastroenteritis in southern Taiwan. J Microbiol Immunol Infect. 2017; 50(6): 915-22. doi: 10.1016/j.jmii.2017.07.015.
[5] Pegues DA, OhH ME, Miller SI. Nontyphoidal Salmonellosis. Trop Infect Dis. 2006; 1: 241-4.
[6] Eng SK, Pusparajah P, Ab Mutalib NS, Ser HL, Chan KG, Lee LH. a. Salmonella: A review on pathogenesis, epidemiology and antibiotic resistance. Front Life Sci. 2015; 8: 284-293.
[7] Cellucci T, Seabrook JA, Chagla Y, Bannister SL, Salvadori MI. A 10-year retrospective review of Salmonella infections at the Children's Hospital in London, Ontario. Can J Infect Dis Med Microbiol. 2010; 21: 78-82.
[8] De Jong B, Ekdahl K. The comparative burden of salmonellosis in the European Union member states, associated and candidate countries. BMC Public Health. 2006; 6: 1-9.
[9] Centers for Disease Control and Prevention (CDC). 2016. National Enteric Disease Surveillance: Salmonella Annual Report, 2011. Online.
[10] Hörmansdorfer S, Messelhäußer U, Rampp A, Schönberger K, Dallman T, Allerberger F, *et al*. Re-evaluation of a 2014 multi-country european outbreak of Salmonella enteritidis phage type 14b using recent epidemiological and molecular data. Euro Surveill. 2017; 22: 1-7. doi: 10.2807/1560-7917.ES.2017.22.50.17-00196.
[11] Jourdan-da Silva N, Fabre L, Robinson E, Fournet N, Nisavanh A, Bruyand M, et al. Ongoing nationwide outbreak of Salmonella agona associated with internationally distributed infant milk products, France, December 2017. Euro Surveill. 2018; 23: 1-5. doi: 10.2807/1560-7917.ES.2018.23.2.17-00852.
[12] Bangtrakulnonth A, Pornreongwong S, Pulsrikarn C, Sawanpanyalert P, Hendriksen RS, Lo Fo Wong DM a, *et al*. Salmonella Serovars from Humans and Other Sources in Thailand, 1993-2002. Emerg Infect Dis. 2004; 10: 131-6. doi: 10.3201/eid1001.02-0781.
[13] Tungwongjulaniam C. Situation of food poisoning, 2017. Dis Control J. 2018; 44(3): 315-24.
[14] ISO 6579:2000. 2002. Microbiology of food and animal feeding stuffs - Horizontal method for the detection of Salmonella spp. Geneva, Switzerland.
[15] Buchan BW, Ledeboer NA. Emerging technologies for the clinical microbiology laboratory. Clin Microbiol Rev. 2014; 27: 783-822. doi: 10.1128/CMR.00003-14.
[16] Wattiau P, Boland C, Bertrand S. Methodologies for Salmonella enterica subsp. Enterica Subtyping: Gold Standards and Alternatives. Appl Environ Microbiol. 2011; 77: 7877-85. doi: 10.1128/AEM.05527-11.
[17] Masek BJ, Hardick J, Won H, Yang S, Hsieh YH, Rothman RE, *et al*. Sensitive detection and serovar differentiation of typhoidal and nontyphoidal Salmonella enterica species using 16S rRNA gene PCR coupled with high-resolution melt analysis. J Mol Diagn. 2014; 16: 261-6. doi.org/10.1016/j.jmoldx.2013.10.011
[18] Muñoz N, Diaz-Osorio M, Moreno J, Sánchez-Jiménez M, Cardona-Castro N. Development and evaluation of a multiplex real-time polymerase chain reaction procedure to clinically type prevalent Salmonella enterica serovars. J Mol Diagn. 2010; 12: 220-5. doi: 10.2353/jmoldx.2010.090036.
[19] Zeinzinger J, Pietzka AT, Stöger A, Kornschober C, Kunert R, Allerberger F, et al. One-step triplex high-resolution melting analysis for rapid identification and simultaneous subtyping of frequently isolated Salmonella serovars. Appl. Environ. Microbiol. 2012; 78: 3352-60. doi: 10.1128/AEM.07668-11
[20] Leekitcharoenphon P, Nielsen EM, Kaas RS, Lund O, Aarestrup FM. Evaluation of Whole Genome Sequencing for Outbreak Detection of Salmonella enterica. PLoS One. 2014; 4; 9(2): e87991. doi: 10.1371/journal.pone.0087991.
[21] Quick J, Ashton P, Calus S, Chatt C, Gossain S, Hawker J, *et al*. Rapid draft sequencing and real-time nanopore sequencing in a hospital outbreak of Salmonella. Genome Biol. 2015; 16: 1-14. doi: 10.1186/s13059-015-0677-2.
[22] Jansen R, Van Embden JDA, Gaastra W, Schouls LM. Identification of genes that are associated with DNA repeats in prokaryotes. Mol Microbiol. 2002; 43: 1565-75. doi: 10.1046/j.1365-2958.2002.02839.x.
[23] Newsom Sydney, Parameshwaran Hari Priya, Martin Lindsie, Rajan Rakhi. The CRISPR-Cas Mechanism for Adaptive Immunity and Alternate Bacterial Functions Fuels Diverse Biotechnologies. Front Cell Infect Microbiol. 2021; 10: 1-10. doi: 10.3389/fcimb.2020.619763
[24] Shariat N, Dudley EG. CRISPRs: molecular signatures used for pathogen subtyping. Appl Environ Microbiol. 2014; 80(2): 430-9. doi: 10.1128/AEM.02790-13. Epub 2013 Oct 25. PMID: 24162568; PMCID: PMC3911090.
[25] Horvath P, Barrangou R.CRISPR/Cas, the immune system of Bacteria and Archaea. Science. 2010; 327: 167-70. doi: 10.1126/science.1179555.
[26] Fabre L, Zhang J, Guigon G, Le Hello S, Guibert V, Accou-Demartin M, *et al*. Crispr typing and subtyping for improved Laboratory surveillance of Salmonella infections. PLoS ONE. 2012; 7(5): e36995. doi: 10.1371/journal.pone.0036995. Epub 2012 May 18.
[27] Liu F, Kariyawasam S, Jayarao BM, Barrangou R, Gerner-Smidt P, Ribot EM, et al. Subtyping Salmonella enterica serovar enteritidis isolates from different sources by using sequence typing based on virulence genes and clustered regularly interspaced short palindromic repeats (CRISPRs). Appl Environ Microbiol. 2011; 77: 4520-6. doi: 10.1128/AEM.00468-11.
[28] Wisittipanit N, Pulsrikarn C, Srisong S, Srimora R, Kittiwan N, Pooncharoen K. 2020a. CRISPR 2 PCR and

high resolution melting profiling for identification and characterization of clinically-relevant Salmonella enterica subsp. enterica. Peer J. 2020; 8: e9113. doi: 10.7717/peerj.9113.

[29] Thompson CP, Doak AN, Amirani N, Schroeder EA, Wright J, Kariyawasam S, *et al*. High-resolution identification of multiple Salmonella serovars in a single sample by using CRISPRSeroSeq. Appl Environ Microbiol. 2018; 84: 1-13. doi: 10.1128/AEM.01859-18.

[30] Nadon CA, Trees E, KNg L, Nielsen EM, Reimer A, Maxwell N, *et al*. Development and application of MLVA methods as a tool for inter-laboratory surveillance. Euro surveill. 2017; 18: 20565. doi: 10.2807/1560-7917.es2013.18.35.20565.

[31] Wuyts V, Mattheus W, De Laminne De Bex G, Wildemauwe C, Roosens NHC, *et al*. MLVA as a tool for public health surveillance of human Salmonella Typhimurium: Prospective study in Belgium and evaluation of MLVA loci stability. PLoS ONE. 2013; 8(12): e84055. doi.org/10.1371/journal.pone.0084055

[32] Caméléna F, Birgy A, Smail Y, Courroux C, Mariani-Kurkdjian P, Hello S Le, *et al*. Rapid and Simple Universal Escherichia coli Genotyping Method Based on Multiple-Locus Variable-Number Tandem- Repeat Analysis Using Single-Tube Multiplex PCR and Standard Gel Electrophoresis. Appl Environ Microbiol. 2019; 85: 1-15.

[33] Huehn S, La Ragione RM, Anjum M, Saunders M, Woodward MJ, Bunge C, *et al*. Virulotyping and antimicrobial resistance typing of salmonella enterica serovars relevant to human health in Europe. Foodborne Pathog Dis. 2010; 7: 523-35. doi: 10.1089/fpd.2009.0447.

[34] Drahovská H, Mikasová E, Szemes T, Ficek A, Sásik M, Majtán V, *et al*.Variability in occurrence of multiple prophage genes in Salmonella Typhimurium strains isolated in Slovak Republic. FEMS Microbiol Lett. 2007; 270: 237-44. doi: 10.1111/j.1574-6968.2007.00674.x.

[35] Pooncharoen K, Pulsrikarn C, Khamvichai S, Tadee P. Feasibility of high resolution melting curve analysis for rapid serotyping of Salmonella from hospitalised patients. J Assoc Med Sci. 2019; 52(1): 36-40. doi: 10.14456/jams.2018.3.

[36] Pooncharoen K, Pulsrikarn C, Nuanmuang N, Khamai P. Effectiveness of BOX-PCR in Differentiating Genetic Relatedness among Salmonella enterica Serotype 4,[5],12:i:- Isolates from Hospitalized Patients and Minced Pork Samples in Northern Thailand. Int J Microbiol. 2019; 2019: 5086240. doi: 10.1155/2019/5086240.

[37] Borriello G, Lucibelli MG, Pesciaroli M, Carullo MR, Graziani C, Ammendola S, *et al*. Diversity of Salmonella spp. serovars isolated from the intestines of water buffalo calves with gastroenteritis. BMC Vet Res. 2012; 8: 201. doi: 10.1186/1746-6148-8-201.

[38] Rahn K, Grandis A De, Clarke RC, McEwen S. A, Galin JE, Ginocchio C, *et al*. Amplification of invA gene of Salmonella by polymerase chain reaction (PCR) as a specific method for detection of Salmonellae. Mol Cell Probes. 1992; 6: 271-9. doi: 10.1016/0890-8508(92)90002-f

[39] McNerney R, Clark TG, Campino S, Rodrigues C, Dolinger D, Smith L, *et al*.Removing the bottleneck in whole genome sequencing of Mycobacterium tuberculosis for rapid drug resistance analysis: a call to action. Int J Infect Dis. 2017; 56: 130-5. doi: 10.1016/j.ijid.2016.11.422.

[40] Heras, J., Domínguez, C., Mata, E. *et al*. GelJ - a tool for analyzing DNA fingerprint gel images. BMC Bioinformatics 2015; 16: 270. doi.org/10.1186/s12859-015-0703-0

[41] Eng S-KK, Pusparajah P, Ab Mutalib N-SS, Ser H-LL, Chan K-GG, Lee L-HH. Salmonella: A review on pathogenesis, epidemiology and antibiotic resistance. Front Life Sci. 2015; 8: 284-93. doi: 10.1080/21553769.2015.1051243.

[42] Gordon MA, Graham SM, Walsh AL, Wilson L, Phiri A, Molyneux E, *et al*. Epidemics of invasive Salmonella enterica serovar enteritidis and S. enterica serovar typhimurium infection associated with multidrug resistance among adults and children in Malawi. Clin Infect Dis. 2008; 46: 963-9. doi: 10.1086/529146.

[43] Elbagir M, Nori E, Thong KL. Differentiation of Salmonella enterica based on PCR detection of selected somatic and flagellar antigens. Afr J Microbiol Res. 2010; 4: 871-6. doi: 10.5897/AJMR.9000238.

[44] Pooncharoen K, Narong Nuanmuang, Prommuang P, Sriisan S. High-resolution melting-curve analysis for serotyping of Salmonella spp. group B isolated from minced pork in the Northern part of Thailand. J Assoc Med Sci. 2019; 52(1): 62-71. doi: 10.14456/jams.2018.3.

[45] Wisittipanit N, Pulsrikarn C, Wutthiosot S, Pinmongkhonkul S, Pooncharoen K. Application of machine learning algorithm and modified high resolution DNA melting curve analysis for molecular subtyping of Salmonella isolates from various epidemiological backgrounds in northern Thailand. World J Microbiol Biotechnol. 2020; 36: 103. doi: 10.1007/s11274-020-02874-7.

[46] Lindstedt BA, Heir E, Nygård I, Kapperud G. Characterization of class I integrons in clinical strains of Salmonella enterica subsp. enterica serovars Typhimurium and Enteritidis from Norwegian hospitals. J Med Microbiol. 2003; 52: 141-9. doi: 10.1099/jmm.0.04958-0.

[47] Mandilara G, Lambiri M, Polemis M, Passiotou M, Vatopoulos A. Phenotypic and molecular characterisation of multiresistant monophasic Salmonella typhimurium (1,4,[5],12:I:-) in Greece, 2006 to 2011. Euro Surveill. 2013; 18: 1-8.

[48] Xie X, Wang Z, Zhang K, Li Y, Hu Y, Pan Z, *et al*. Pig as a reservoir of CRISPR type TST4 Salmonella enterica serovar Typhimurium monophasic variant during 2009-2017 in China. Emerg Microbes Infect. 2020; 9: 1-4. doi: 10.1080/22221751.2019.1699450.

[49] Yang X, Wu Q, Zhang J, Huang J, Guo W, Cai S.

Prevalence and characterization of monophasic Salmonella serovar 1,4,[5],12:i:-of food origin in China. PLoS ONE. 2015; 10: 1-10. doi: 10.1371/journal.pone.0137967.

[50] Zhang S, Santos RL, Tsolis RM, Mirold S, Hardt WD, Adams LG, *et al*. Phage mediated horizontal transfer of the sopE1 gene increases enteropathogenicity of Salmonella enterica serotype Typhimurium for calves. FEMS Microbiol Lett. 2002; 217: 243-7. doi: 10.1016/S0378-1097(02)01094-7.

[51] Tanmoy AM, Saha C, Sajib MSI, Saha S, Komurian-Pradel F, Belkum A van, *et al*. CRISPR-Cas Diversity in Clinical Salmonella enterica Serovar Typhi Isolates from South Asian Countries. Genes (Basel). 2020; 11(11): 1365. doi: 10.3390/genes11111365. PMID: 33218076; PMCID: PMC7698835.

Journal of Associated Medical Sciences 2024; 57(2): 101-106

JAMS
Journal of Associated Medical Sciences

Scopus Indexed & Thai-Journal Citation Index Centre (TCI)

Journal of Associated Medical Sciences

Journal homepage: https://www.tci-thaijo.org/index.php/bulletinAMS/index

A comparison of the phonation quotient between patients with voice disorders caused by benign vocal fold lesions and normal adults 20-80 years of age

Chalermchai Nilsuwankhosit[1] Jeamjai Jeeraumporn[1*] Sumalee Dechongkit[1] Kunlawat Thadanipon[2]

[1]Department of Communication Sciences and Disorders, Faculty of Medicine Ramathibodi Hospital, Mahidol University, Bangkok, Thailand.
[2]Department of Clinical Epidemiology and Biostatistics, Faculty of Medicine Ramathibodi Hospital, Mahidol University, Bangkok, Thailand.

ARTICLE INFO

Article history:
Received 18 June 2023
Accepted as revised 27 February 2024
Available online 4 March 2024

Keywords:
Voice disorders, benign vocal fold lesions, phonation quotient, vital capacity, maximum phonation time

ABSTRACT

Background: A voice evaluation is an important first step in analyzing voice symptoms and determining appropriate treatment plans. The phonation quotient is a valid aerodynamic parameter in voice evaluations which is an indirect source of information for evaluating the valve function of the vocal folds of patients with voice disorders, especially patients with voice disorders caused by tumors of the vocal folds which is the most common cause in the patients with voice disorders.

Objective: The present study aims to determine and compare the phonation quotient between patients with voice disorders caused by benign vocal fold lesions and normal adults between 20-80 years of age.

Materials and methods: The participants comprised 40 adults with voice disorders caused by benign vocal fold lesions and 40 with normal voices. All participants' voices were evaluated in the Speech Clinic at Ramathibodi Hospital, Bangkok. The phonation quotient (PQ) was calculated by the ratio of vital capacity (VC) to the maximum phonation time (MPT). VC and MPT were measured using a phonatory aerodynamic system (PAS).

Results: The results of the present study indicated that the mean value of the PQ of adults with normal voices was 122.60 cc/sec (SD=16.36). The mean value of the PQ of adults with voice disorders caused by benign vocal fold lesions was 292.08 cc/sec (SD=97.14). The mean value of the PQ in the group with voice disorders caused by benign vocal fold lesions was significantly more significant than the mean value of the PQ in the group with normal voice.

Conclusion: The significant difference between the phonation quotient of adults with voice disorders caused by benign vocal fold lesions and adults with normal voice was that the PQ might be an indicator for indirect evaluation of the airflow leakage related to the efficiency of vocal fold movement during phonation. The PQ can be the optional voice measurement for monitoring and analyzing the outcomes of voice therapy.

Introduction

Voice disorders are impairments that affect a person's communications, social interactions, and occupations. They can also produce emotional and behavioral problems such as anxiety, emotional tension, and aggressive behavior, adversely affecting their quality of life.[1-3] The laryngeal pathology of the patients with voice disorders is diagnosed by an otolaryngologist, and their voice is evaluated by a speech-language pathologist (SLP).[4] Speech-language pathologists evaluate and diagnose voice problems, prepare treatment plans, and provide therapeutic services

∗ **Corresponding contributor.**
Author's Address: *Department of Communication Sciences and Disorders, Faculty of Medicine Ramathibodi Hospital, Mahidol University, Bangkok, Thailand.*
E-mail address: jeamjai.jee@mahidol.ac.th
doi: 10.12982/JAMS.2024.031
E-ISSN: 2539-6056

for patients with voice disorders. The factor that affected the successful results of speech therapy was the ability of SLPs to determine and evaluate the characteristics of their patients' voice problems.[4,5] The voice problems of patients with benign vocal fold lesions arise from incomplete glottic closure, which leads to airflow leakage during phonation, changing the voice by decreasing its loudness and pitch and increasing breathiness.[4,5] From the medical records of the Speech Clinic at Ramathibodi Hospital, Bangkok, the statistics about patients with communication disorders between 2016 and 2017 showed that there were 239 adult patients with voice disorders or 19.1 percent of all adult patients with communication disorders. Benign vocal fold lesions were the most common cause of voice disorders in this group of patients.[6]

Voice evaluations can be generally divided into two types: objective and subjective. A subjective evaluation is an auditory-perceptual evaluation upon which SLPs base their clinical decisions. If a clinician can only conduct a subjective evaluation, more than the voice information from the evaluation will be needed to decide on a proper treatment plan. As a result, an objective evaluation is needed to determine the most effective therapy for patients with voice disorders.[4,7,8] An objective evaluation, such as an acoustic and aerodynamic analysis, is instrumental. Normally, patients with voice disorders will have their maximum phonation time (MPT) evaluated between the steps of their voice therapy programs. These evaluations can be either subjective or objective. However, an additional parameter, called "phonation quotient", is an indirect clinical measurement. In addition to using clinical instruments, the phonation quotient (PQ) is defined as the ratio between two aerodynamic parameters: vital capacity (VC) and maximum phonation time (MPT).[8-12] Vital capacity is the maximum total volume of air that can be expelled after maximum inhalation.[4,9,13,14] Maximum phonation time is the maximum period a vowel sound can sustain after maximum inhalation.[8,9,15]

The VC and MPT of Thai people are different from those of European or American people because of the difference in lung capacity and body size.[15,16] These aerodynamic parameters can be non-invasive and easily measured using the Phonatory Aerodynamic System (PAS).[17] The PAS is an instrument generally used in voice clinics for measuring the airflow, pressure, and parameters associated with speech and voice production. The PAS has two handles attached to the instrument's body, including the required tubing, coupler, microphone, airflow head, face mask, and calibration syringe.

Furthermore, the phonation quotient is a proper aerodynamic parameter in voice evaluations because it indicates the amount of air expelled during phonation.[9,10] PQ is an indirect source of information for evaluating the valve function of the vocal folds of patients with voice disorders, especially patients with voice disorders caused by vocal folds' tumors that may lead to airflow leakage during phonation.[10,12,16] Therefore, one purpose of the present study is to determine the PQ of Thai adults by using the ratio between VC and MPT. Another purpose is to compare the PQ between Thai adults with voice disorders caused by benign vocal fold lesions and adults with normal voices of 20-80 years of age. The results of this study will inform speech-language pathologists about the differences in PQ between Thai adults with voice disorders caused by benign vocal fold lesions and Thai adults with normal voice, and they can use the PQ for an indirect evaluation of the efficiency of vocal fold movement during phonation, or the valve function of the vocal folds. This will enable them to monitor and analyze outcomes in each session after voice therapy and to reconsider the next steps of their voice therapy plans for patients with voice disorders.

Materials and methods

The present study's data was collected from December 2018 to July 2020. The details are as follows:

Participants

The number of participants was determined by sample size determination (two dependent means of phonation quotient for a pair-matched study), which was 80 participants. A total of 80 participants were divided into two groups. There were 40 new cases, 10 males and 30 females, in the group of adults with voice disorders caused by benign vocal folds lesions and 40 adults, 10 males, and 30 females, in the group of adults with a normal voice who were the relatives of patient or personnel at Ramathibodi Hospital. The age and gender of each participant in both groups were matched. The age difference between the participants in both groups was less than 5 years. Furthermore, the members of both groups agreed to participate in this study by signing an informed consent form. In addition to the COVID-19 pandemic, the participants were required to test the COVID-19 Antigen Testing Kit (ATK), and the test result was negative for COVID-19.

In the adults with voice disorders group, the participants were between 26 and 78 years, and the mean age was 49.30 years (SD=14.43). Furthermore, all participants in this group were diagnosed with voice disorders caused by benign vocal fold lesions by Otolaryngologists, and the types of benign vocal fold lesions were divided into 4 types: vocal nodules, vocal polyps, vocal cysts, and vocal masses. There were 22 participants: 8 males and 14 females with vocal nodules, 7 participants: 1 male and 6 females with vocal polyps, 9 females with vocal cysts, and 2 participants: 1 male and 1 female with vocal masses.

In the group of adults with normal voices, there were 37 participants who were the relatives of patients at the speech clinic and 3 participants who were personnel at Ramathibodi Hospital. The participants were between 20 and 80 years old, and the mean age was 48.90 (SD=14.48). All participants in the group of adults with normal voices were healthy adults who did not have diseases of the abdomen, respiratory system, or lung diseases. In addition, the results of their voice analyses were normal.

Participants who did not complete either the test of vital capacity (VC) or the test of maximum phonation time (MPT) by the Phonatory Aerodynamic System (PAS) were excluded.

Procedures

The procedures consisted of two steps: voice analyses to include participants and then aerodynamic analyses. The descriptions of the two steps are as follows:

1. Voice analyses for the inclusion of participants

The participants' voices were analyzed in subjective and objective assessments in a quiet room. Voice analyses were completed in approximately 15 minutes. The subjective assessments were based on the Thai Speech-Language and Hearing Association protocol for auditory perceptual voice analysis, which consisted of participant interviews and history records, respiratory analysis and behavioral voice misuse, auditory perceptual analysis of pitch and loudness, and auditory perceptual analysis of voice quality.[18] In the objective assessment or an instrumental evaluation by Vocal Assessment Program of the Dr. Speech software, version 5, designed by Daniel Z. Huang, Tiger DRS Inc, Shanghai, China, the voice of a participant was evaluated by sustaining the /a/ sound at comfortable pitch and loudness levels. The acoustic parameters of voice were analyzed that consisted including Jitter (%), Shimmer (%), standard deviation of the fundamental frequency or SDF0 (Hz), normalized noise energy or NNE (dB), and the estimated voice quality, which consisted of three parameters: hoarse voice, harsh voice, and breathy voice. Jitter, Shimmer, SDF0, and NNE defaults are 0.5%, 3%, 3 Hz, and -10 dB, respectively.

For voice analysis criteria of the group with normal voice, the results of the subjective and objective assessments: the acoustic parameters and the estimated voice quality of participants were in the normal range.

For the group with voice disorders, the results of participants' subjective and objective assessments were in the abnormal range.

2. Aerodynamic analyses

The vital capacity (VC) and maximum phonation time (MPT) of all participants were measured by using the Phonatory Aerodynamic System (PAS) model 6600 in a quiet room. Both aerodynamic analyses took approximately 15 min. Before aerodynamic analyses in each session, the face mask of the PAS was cleaned with an alcohol solution of 70%, and the airflow head of the PAS was calibrated. The result of the airflow head calibration, which is shown on the computer screen, must be the closest in capacity to 1 liter. After calibration, the VC and MPT of the participants were measured. The participant was informed about the method used to determine VC by breathing in through the nose as deeply as possible (maximum inhalation) and then expelling the air from the mouth as much as possible (maximum exhalation). Furthermore, the participant was informed about the method used to determine MPT by breathing in through the nose as deeply as possible (maximum inhalation) and sustaining the /a/ sound at comfortable pitch and loudness levels for as long as possible. During the tests, the face mask must completely cover the participant's mouth to prevent air leakage. After each session, the PAS face mask was cleaned with soapy water and Hibicet liquid (Savlon). Each of the determinations involved three trials.

Statistical analysis of the data

The statistical analysis of demographic data of all participants was reported by N (%), mean value, and SD.

Using the mean values of VC and MPT, each participant's average values of the VC and MPT were used to determine their phonation quotient (PQ). The PQ is the VC (cc.) ratio to MPT (sec).

After that, the mean value of the phonation quotient in adults with voice disorders and adults with normal voice was transformed by inverse square root (1/sqrt) for normal distribution. The differences in the transformation of the phonation quotient between adults with voice disorders and those with normal voices were analyzed by paired t-test.

Results

The results of the present study were divided into five parts, including the demographic data of the participants, the results of the voice analyses of the participants, the results of the acoustic parameters of the voice of the participants, the results of the aerodynamic analyses of the participants, and the results of the differences in the PQ between adults with voice disorders and adults with normal voice. The details of the results are shown in Table 1 to 5.

Table 1 Demographic data of the participants.

Characteristics	Normal voice (N=40)		Voice disorders caused by benign vocal fold lesions (N=40)			
	Relative of the patients	Personnel	Nodules	Polyps	Cysts	Masses
Gender, N (%)						
Male, 10 (25)	27 (90)	-	8 (80)	1 (10)	-	1 (10)
Female, 30 (75)	10 (100)	3 (10)	14 (35)	6 (15)	9 (22.5)	1 (2.5)
Age, Mean (SD)	48.90 (14.43)		49.30 (14.43)			

Table 2 The results of voice analyses of participants with voice disorders.

Voice analyses	Mild N (%)	Moderate N (%)	Severe N (%)	Total N (%)
Subjective assessment				
Voice disorders	8 (20)	19 (47.50)	13 (32.50)	40 (100)
Objective assessment*				
Hoarse voice	15 (42.86)	14 (40)	6 (17.14)	35 (100)
Harsh voice	5 (25)	6 (30)	9 (45)	20 (100)
Breathy voice	6 (15)	15 (37.5)	19 (47.5)	40 (100)

**Evaluation by Vocal Assessment Program of the Dr. Speech software, version 5, designed by Daniel Z. Huang, Tiger DRS Inc, Shanghai, China.*

Table 3 The results of acoustic parameters of the voice of the participants.

Acoustic parameters of voice*	Normal voice (N=40) Median (QD)	Voice disorders caused by benign vocal fold lesions (N=40) Median (QD)
Jitter	0.19 (0.05)	0.38 (0.48)
Shimmer	1.23 (1.06)	2.35 (2.80)
SDF0	1.36 (0.74)	2.36 (1.65)
NNE	-15.17 (3.50)	-8.17 (4.89)

**Evaluation by Vocal Assessment Program of the Dr. Speech software, version 5, designed by Daniel Z. Huang, Tiger DRS Inc, Shanghai, China.*

Table 4 The results of aerodynamic analyses of the participants.

Groups		Aerodynamic analyses		
		VC (cc)	MPT (sec)	PQ (cc/ sec)
		Mean (SD)	Mean (SD)	Mean (SD)
Normal voice (N=40)	Female (30)	2050.67 (266.38)	17.26 (3.69)	121.66 (17.52)
	Male (10)	2454.00 (374.20)	19.71 (3.39)	125.44 (12.58)
	Total (40)	2151.50 (341.12)	17.87 (3.73)	122.60* (16.36)
	95% confidence interval			117.37-127.83
Voice disorders (N=40)	Female (30)	2240.00 (308.98)	8.31 (2.91)	299.64 (103.68)
	Male (10)	2849.00 (465.58)	11.14 (3.10)	269.40 (74.07)
	Total (40)	2392.25 (438.56)	9.02 (3.17)	292.08* (97.14)
	95% confidence interval			261.01-323.14

**The mean difference of PQ between the two groups was 169.48 cc/sec.*

Table 5 The results of differences in phonation quotient between adults with voice disorders and those with normal voice.

Groups	PQ (1/sqrt)		95 % Confidence interval		*t*	sig
	Mean	SD				
Normal voice (N=40)	0.061	0.010	0.058	0.064	-16.632	<0.001
Voice disorders (N=40)	0.091	0.006	0.089	0.093		

The results of the voice analyses of the participants indicated that the results of subjective and objective assessment in participants with normal voices were in the normal range. On the other hand, subjective and objective assessment results in participants with voice disorders were in the abnormal range. The details of the voice analyses of the participants with voice disorders are shown in Table 2. In addition, the details of the acoustic parameters of the participants' voices are shown in Table 3.

From Tables 4 and 5, the summary of the results indicates that the mean value of the PQ of adults with normal voice was 122.60 cc/sec (SD=16.36), corresponding to a 95% confidence interval of 117.37-127.83 cc/sec and the mean value of the PQ of adults with voice disorder caused by benign vocal fold lesions was 292.08 cc/sec (SD=97.14), corresponding to a 95% confidence interval of 261.01-323.14 cc/sec. In addition, the transformation of the PQ of adults with voice disorders was less than that of adults with normal voice, and the differences were statistically significant (p<0.001). In other words, the PQ of adults with voice disorders (292.08 [97.14] cc/sec) was higher than adults with normal voice (122.60 [16.36] cc/sec),

and the mean difference between the two groups was 169.48 cc/sec. The differences in the PQ between the two groups were statistically significant (p<0.001).

Discussion

From the results of the PQ of adults with normal voices, the mean values of the PQ were 121.66 cc/sec (SD=17.52) for females and 125.44 cc/sec (SD=12.58) for males. The mean values of the PQ for females and males of the present study were in the standard range of adults with normal voice of the study of Hirano, Koike, and Von Leden[10] which agreed with the study of Dobinson and Kendrick,[19] and Morsomme *et al*.[20] The standard range of the PQ for people with normal voice was between 78.00 cc./sec and 241.00 cc/sec (mean=137 cc/sec) for females, and between 69.00 cc/sec and 307.00 cc/sec (mean=145 cc/sec) for males.[10] The PQ of the present study was defined as the ratio between two aerodynamic parameters: the VC and the MPT. In this study, the mean values of the VC were 2050.67 cc. (SD=266.38) for females and 2454.00 cc. (SD=374.20) for males. The mean values of the MPT were 17.26 sec (SD=3.69) for females and 19.71 sec (SD=3.39) for males. The mean values of VC and MPT were in the range of the VC and the MPT in Thai people of Limprasert's study.[15]

Furthermore, the mean value of the PQ of adults with voice disorders caused by benign vocal fold lesions was 292.08 cc/sec, greater than 122.60 cc/sec of adults with normal voice. The lowest value of the PQ in the group of participants with voice disorders was greater than the highest value of the PQ in the group of participants with normal voices. The differences in the mean value of the PQ between both groups of the present study were statistically significant (p<0.01). This finding of the present study agrees with the studies of Hirano, Koike, and Von Leden[10], Iwata and Von Leden,[11] and Aghajanzadeh *et al*.[21] The high PQ values might be interpreted as the tumors of the vocal folds causing incomplete glottic closure[22] and interfering with vocal fold vibrations. Poor vocal fold approximation then causes airflow leakage during phonation, increasing breathiness, and shortening of MPT.[4,5,10,23-25] Breathy voice was one out of three characteristics of objective assessment of the present study, which was found in all of the participants with voice disorders. Moreover, the NNE is the acoustic parameter that is related to a breathy voice. In this study, the NNE value in the group of participants with voice disorders was greater than -10 dB, resulting from an incomplete closure of the glottis. In addition, the short MPT is related to the high PQ value because the MPT has a negative correlation with the PQ. In other words, when MPT decreases, PQ values increase.[10]

Conclusion

The significant difference between the phonation quotient of adults with voice disorders caused by benign vocal fold lesions and adults with normal voice was reflected that the PQ might be an indicator for indirect evaluation of the airflow leakage related to the efficiency of vocal fold movement during phonation. Moreover, the PQ can monitor and analyze therapy outcomes for patients with voice disorders. So, the PQ is one of the airflow measurements in aerodynamic analysis, the optional measurement for voice assessments. Speech and language pathologists (SLPs) can choose the PQ for evaluation in patients with voice disorders caused by laryngeal diseases that affect incomplete glottic closure.

Limitations

The present study was a paired-match study that aimed to determine and compare the phonation quotient between Thai adults with voice disorders caused by benign vocal fold lesions and adults with normal voices. Each participant between both groups was matched by age and gender. Furthermore, the number of participants was not balanced for gender. In addition, there were various types, sites, and sizes of benign vocal fold lesions in the voice disorders group.

Recommendations

For further studies, the participants should be divided equally into genders to better determine and compare the phonation quotient between females and males. The factors that affected the change in the phonation quotient, including the differences in the types, sites, and sizes of benign vocal fold lesions, should be considered. In addition, the instrument Phonatory Aerodynamic System: PAS, can be used for aerodynamic analysis in other types of voice disorders, including organic-physiological voice disorders and functional voice disorders.

Conflict of interest

The authors declare that there is no conflict of interest.

Ethics approval

The present study received approval from the Ethical Committee of the Ramathibodi Hospital, COA. No. MURA2018/863

Reference

[1] Spina A, Maunsell R, Sandalo K, Gusmão R, Crespo A. Correlation between voice and life quality and occupation. Braz J Otorhinolaryngol. 2009; 75(2): 275-9. doi: 10.1016/s1808-8694(15)30790-4.

[2] Wilson JA, Deary IJ, Millar A, Mackenzie K. The quality of life impact of Dysphonia. Clin Otolaryngol. 2002; 27(3): 179-82. doi: 10.1046/j.1365-2273.2002.00559.x.

[3] Krohling L, Pereira de Paula K, Behlau M. Behavior, social competence, and voice disorders in childhood and adolescence. J Voice. 2016; 30(6): 677-83. doi: 10.1016/j.jvoice.2015.08.005.

[4] Boone D, McFarlane S. The voice and voice therapy. 5th ed. New Jersey: Prentice Hall; 1994.

[5] Stemple J, Glaze L, Gerdeman B. Clinical voice pathology: theory and management. 3rd ed. San Diego, CA: Singular Publishing Group; 2000.

[6] Medical Records Section, Faculty of Medicine Ramathibodi Hospital. Statistical report of patients

with communication disorders between 2016 and 2017.
[7] Sataloff R. Vocal health and pedagogy. 5th ed. San Diego, CA: Plural Pub; 2006.
[8] Baken R, Orlikoff R. Clinical measurement of speech and voice. 2nd ed. San Diego, CA: Singular Pub.; 2000.
[9] Dejonckere P.H. Assessment of voice and respiratory function. In: Remacle M, Eckel HE. Surgery of larynx and trachea. Berlin Heidelberg: Springer-Verlag; 2010.
[10] Hirano M, Koike Y, Von Leden H. Maximum phonation time and air usage during phonation. Folia Phoniatr. 1968; 20(4): 185-201. doi: 10.1159/000263198.
[11] Iwata S, Von Leden H. Phonation quotient in patients with laryngeal diseases. Folia Phoniatr. 1970; 22(2): 117-28. doi: 10.1159/000263375.
[12] Joshi A, Watts C. Measurement reliability of phonation quotient derived from three aerodynamic instruments. J Voice. 2016; 30(6): 773.e13-773.e19. doi: 10.1016/j.jvoice.2015.11.015.
[13] Zemlin W. Speech and hearing science: anatomy and physiology. 4th ed. Boston: Allyn and Bacon; 1998.
[14] Pal G, Pal P. Textbook of practical physiology. Calcutta: Orient Longman; 2001.
[15] Limprasert N. Maximum phonation time and vital capacity in normal adult aged 20 to 40 years and the relations between maximum phonation time and vital capacity [Master's thesis]. Bangkok: Mahidol University; 1997.
[16] Aurichayapat P, Khrisanapant W, Aurvichayapat N, Thongaun T,Singhpoo K. Spirometric values in normal Thai. Srinagarind Medical J. 1996; 11(1): 27-34.
[17] KayPENTAX Corp LP, NJ. Instruction Manual, Phonatory Aerodynamic System (PAS), Model 6600.
[18] Thai Speech-Language and Heaing Association. The manual of the professional standards for Thai speech language pathologist. Khon Kaen: Khon Kaen Printing Ltd; 2000.
[19] Dobinson C, Kendrick A. Normal values and predictive equations for aerodynamic function in British caucasian subjects. Folia Phoniatr. 1993; 45(1): 14-24. doi: 10.1159/000266205.
[20] Morsomme D, Jamart J, Boucquey D, Remade M. Presbyphonia: voice differences between the sexes in the elderly. Comparison by maximum phonation time, phonation quotient and spectral analysis. Logoped Phoniatr Vocol. 1997; 22(1): 9-14. doi: 10.3109/14015439709075310.
[21] Aghajanzadeh M, Darouie A, Dabirmoghaddam P, Salehi A, Rahgozar M. The relationship between the aerodynamic parameters of voice and perceptual evaluation in the Iranian population with or without voice disorders. J Voice. 2016; 31(2): 250.e9-250.e15. doi: 10.1016/j.jvoice.2016.07.014.
[22] Joshi A, Watts CR, Hathway J. Phonation quotient using three aerodynamic instruments in the disordered voice. J Voice. 2020; 34(1): 20-4. doi: 10.1016/j.jvoice.2018.08.002.
[23] Ballenger W, Snow J, Wackym P. Otorhinolaryngology. Shelton, Conn.: BC Decker; 2009.
[24] Vasconcelos D, Gomes A, Araújo C. Vocal fold polyps: literature review. Int Arch Otorhinolaryngol. 2019; 23(01): 116-24. doi: 10.1055/s-0038-1675391.
[25] Bjerg-Jensen J, Rasmussen N. Phonosurgery of vocal fold polyps, cysts and nodules is beneficial. Dan Med J. 2013; 60(2): 1-5. PMID: 23461990.

Journal of Associated Medical Sciences 2024; 57(2): 107-114

JAMS
Journal of Associated Medical Sciences

Scopus Indexed & Thai-Journal Citation Index Centre (TCI)

Journal of Associated Medical Sciences

Journal homepage: https://www.tci-thaijo.org/index.php/bulletinAMS/index

Analyzing DNA barcoding and identifying toxins caused by neurotoxic mushroom poisoning using liquid chromatography tandem mass spectrometry

Sriprapa Phatsarapongkul[1] Sittiporn Parnmen[1*] Nattakarn Nooron[1] Rungsaeng Chankunasuka[1] Chidkamon Thunkhamrak[1] Unchalee Nitma[1] Nisakorn Palakul[1] Pornpanna Chonnakijkul[1] Sujitra Sikaphan[1] Chutimon Uttawichai[1] Dutsadee Polputpisatkul[1] Archawin Rojanawiwat[2]

[1]Toxicology Center, National Institute of Health, Department of Medical Sciences, Ministry of Public Health, Nonthaburi Province, Thailand.
[2]National Institute of Health, Department of Medical Sciences, Ministry of Public Health, Nonthaburi Province, Thailand.

ARTICLE INFO

Article history:
Received 3 November 2023
Accepted as revised 27 February 2024
Available online 4 March 2024

Keywords:
Ibotenic acid, LC-MS/MS, neurotoxic mushroom, phylogenetic approach

ABSTRACT

Background: Neurotoxic mushroom poisoning often exhibits rapid symptom onset, typically attributed to compounds such as Ibotenic acid, which affect the central nervous system. This study addresses a new case of mushroom-related food poisoning in southern Thailand.

Objective: The objectives are to determine the presence of ibotenic acid in cases of mushroom-related food poisoning utilizing liquid chromatography-tandem mass spectrometry (LC-MS/MS) and to identify toxic *Amanita* species implicated in these cases.

Materials and methods: Remnant mushroom samples obtained from three clinically reported cases were used. Nucleotide similarity was compared against the rRNA/ITS databases using NCBI BLAST search. Phylogenetic analyses were conducted using maximum likelihood (ML) and FastTree approaches. LC-MS/MS was employed to separate of Ibotenic acid, determine its molecular weight and perform precursor ion fragmentation.

Results: Analysis of the rRNA/ITS databases revealed a high nucleotide similarity between suspected mushroom samples and *Amanita digitosa*. Detailed phylogenetic analysis confirmed that mushroom samples from the three poisoning cases clustered with *A. digitosa*. LC-MS/MS analysis showed the presence of ibotenic acid, with precursor ion (*m/z* 159) and product ion (*m/z* 113.1) as the major toxic substances. Clinically, patients poisoned by ibotenic acid-containing mushrooms exhibited a short latent period with symptoms of nausea, vomiting, vertigo, delirium, confusion, and fatigue.

Conclusion: The genus *Amanita* comprises both edible and inedible species that produce several lethal toxins. The report of ibotenic acid in *A. digitosa* is a novel finding, valuable for food safety monitoring and healthcare decision-maker. This is especially notable due to the accuracy and rapidity of the analytical process.

Introduction

A DNA barcode is a short genetic sequence used to identify and classify species.[1] In investigations of mushroom food poisoning cases, DNA barcoding proves to be valuable tool for identifying samples and determining the species, in conjunction with morphological diagnostics.[2–7] Furthermore, this technique can be applied to case involving remnant or incomplete mushroom samples.[2–7] The most commonly utilized DNA barcode region for fungi is the internal transcribed spacer (ITS) region.[8,9] This region contains two variables ITS1 and ITS2 spacer which are relatively conserved

∗ **Corresponding contributor.**
Author's Address: *Toxicology Center, National Institute of Health, Department of Medical Sciences, Ministry of Public Health, Nonthaburi Province, Thailand.*
E-mail address: sittiporn.p@dmsc.mail.go.th
doi: 10.12982/JAMS.2024.032
E-ISSN: 2539-6056

within a species but exhibit significant variations between species.[8,9]

In Thailand, the ingestion of toxic wild mushrooms remains a significant health concern, resulting in morbidity and mortality.[10] The most frequently encountered lethal wild mushrooms are cytotoxic and myotoxic varieties.[2,4,10] Cytotoxic mushroom poisoning, caused by amatoxins, leads to lethal hepatotoxicity, while myotoxic mushroom poisoning, associated with cycloprop-2-ene carboxylic acid, manifests myotoxic symptoms.[10,11] Well-documented examples include *Amanita brunneitoxicaria*, *A. exitialis*, *A. fuliginea*, *A. gleocystidiosa* and *Russula subnigricans*.[2,4,10,12,13] Mushroom poisoning cases typically fall into two primary categories: gastrointestinal irritation and neurotoxicity.[10] Various mushroom genera, including *Agaricus*, *Chlorophyllum*, *Entoloma*, *Hygrocybe*, *Macrocybe*, and others, are recognized sources of gastrointestinal (GI) irritants.[5,7,10] Nevertheless, the specific GI toxins responsible for these symptoms remain inadequately understood.[14,15] In contrast, neurotoxic mushrooms exhibit less genus diversity compared to GI mushrooms.[10] However, cases of poisoning from toxic mushrooms affecting the nervous system are reported annually among patients, necessitating prompt hospital admission due to the rapid progression of symptoms.[6]

According to the Department of Disease Control, Ministry of Public Health (http://doe.moph.go.th/surdata/disease.php), the incidence of food poisoning from mushroom consumption in the southern region is relatively low compared to other regions. This poisoning typically arises from confusion in distinguishing between poisonous and edible mushrooms. Furthermore, the samples submitted for laboratory analysis often consist of remnants mushroom sample from the patients' meals, rendering some tests incomplete. Therefore, the integration of DNA barcoding techniques alongside morphological analysis of mushrooms can aid in species identification. Moreover, toxin extraction from mushrooms in this study employed microextraction, utilizing minute sample quantities. The primary objective of this study is to identify suspected cases of neurotoxic mushroom poisoning in *Amanita* samples through DNA barcoding and to ascertain their toxins using liquid chromatography-tandem mass spectrometry (LC-MS/MS) employing multiple reaction monitoring (MRM).

Materials and methods

Mushroom specimens

A mushroom sample obtained from 3 poisoning reported cases was used in this study. All poisoning cases occurred in the southern part of Thailand from April to October 2019. In each case, hospitalization was required. Of the 11 patients examined, there were no death cases.

DNA barcode-based fungal identification

The samples containing 20 mg of fruiting bodies were ground in liquid nitrogen and extracted using the Densitʸ Plant Mini Kit (QIAGEN, Germany) according to the manufacturer's instructions. The entire ITS region was amplified with the primers ITS1F and ITS4.[16,17] PCR amplification and sanger sequencing conditions were as described previously.[2,4] The nuclear ITS sequences were compared for nucleotide similarity against the GenBank database using a nucleotide BLAST search of NCBI.[18] The specimens underwent morphological and microscopic examination using a low-magnification stereomicroscope (HumaScope Stereo) and a compound microscope (Olympus CX31) capable of magnifications ranging from 40 to 1,000. For the phylogenetic analysis, the ITS sequences belonging to *Amanita* were downloaded from GenBank. Phylogenetic analyses and genetic distances were performed using Geneious Prime 2022.0.2 (www.geneious.com). Two phylogenetic methods were used including RAxML version 8.2.7 and FastTree version 2.1.11. Branch support was estimated by using 1000 bootstrap replicates. Only clades that received bootstrap support ≥70% under RAxML and SH-like support value ≥90% under FastTree were considered as strongly supported. Phylogenetic trees were depicted using the program FigTree 1.4.4 (http://tree.bio.ed.ac.uk).

Sample preparation and microextraction

Twenty mg of mushroom samples were blended and extracted with 400 uL of 0.1% formic acid in acetonitrile. The extract was incubated at room temperature overnight, followed by centrifugation at 14,000 rpm for 3 min. The clear supernatant was filtered with VertiPure™PVDF(HL) syringe filters (13 mm, 0.2 μm). The filtrate was submitted for subsequent analysis.

Detection of neurotoxins using LC-MS/MS method

The standard reference material of ibotenic acid and alkaloid muscarine were obtained from Sigma-Aldrich (St. Louis, USA). The separation of the peptide toxins and determination of molecular weight as well as the precursor ion fragmentation were using LC-MS/MS method on Agilent 6495 Triple Quadrupole LC/MS and 1290 infinity LC modules with Agilent MassHunter software (California, USA). In the chromatographic system, a Z0RBAX SB-C18 narrow-bore (2.1 mm x 150 mm, 3.5 μm) columns was used for separation of ibotenic acid. The column temperature was 25°C. The mobile phases were deionized water with 0.5% (v/v) formic acid (mobile phase A) and 0.5% (v/v) formic acid in acetonitrile (mobile phase B). A program was started with 30% mobile phase A and 70% mobile phase B at min 1 and 20:80 at min 10. The total run time for each sample was 15 min. The flow rate was 0.2 mL/min. The injection volume was 5 μL, and the Ibotenic acid concentration was 5 μg/L. The MS conditions were as follows: gas temperature, 200°C; gas flow, 14 L/min; nebulizer, 40 psi; and capillary voltage, 4,000 V. The ESI spray was set for positive ion mode detection. Ibotenic acid was detected using multiple reaction monitoring (MRM) for the following unique parent mass-to-charge(m/z)–product m/z combinations: 159 *m/z*-113.1 *m/z*. For detecting alkaloid muscarine, the extraction and MS conditions was followed as described previously.[6]

Results

DNA barcode-based fungal identification

Five remnant mushroom samples obtained from three poisoning cases were analyzed. Results of BLAST search revealed the highest pairwise identity for all samples tested with scores ranging from 95.61 % to 97.01% identity to *Amanita digitosa* (94.98 to 97.01%) and followed by scores ranging from 91.15 to 92.14% identity to a group of *A. ibotengutake* (Table 1). Phylogenetic analyses were used to confirm the relationship of clinical mushroom samples. A matrix of 669 unambiguously aligned nucleotide characters was constructed. All clinical mushroom samples are clustered with *A. digitosa* (100/99) with 95 to 100% identical at the nucleotide level (Figure 1 and 2). Based on the remnant mushroom samples, its general features include pileus brown dark grey at centre towards to haft of greyish at margin, convex to plane; lamellae free, cylindrical stipe, hallow, white to pale grey; bulb subglobose with saccate volva; and subglobose basidiospores, smooth, hyaline, inamyloid (Figure 3).

Table 1 Nucleotide similarity using ITS region.

Sample numbers	Location	GenBank accession numbers	BLAST identification	Nucleotide similarity (%)
D456	Yala province	OR725114	*A. digitosa* KT213722	95.61
			A. ibotengutake AB080987	92.08
D457	Yala province	OR725115	*A. digitosa* KT213722	95.61
			A. ibotengutake AB080987	92.07
D480	Trang province	OR725116	*A. digitosa* KT213722	94.98
			A. ibotengutake AB080990	92.13
D481	Trang province	OR725117	*A. digitosa* KT213722	94.98
			A. ibotengutake AB080990	92.14
D520	Songkhla province	OR725118	*A. digitosa* KT213722	97.01
			A. ibotengutake AB080987	91.15

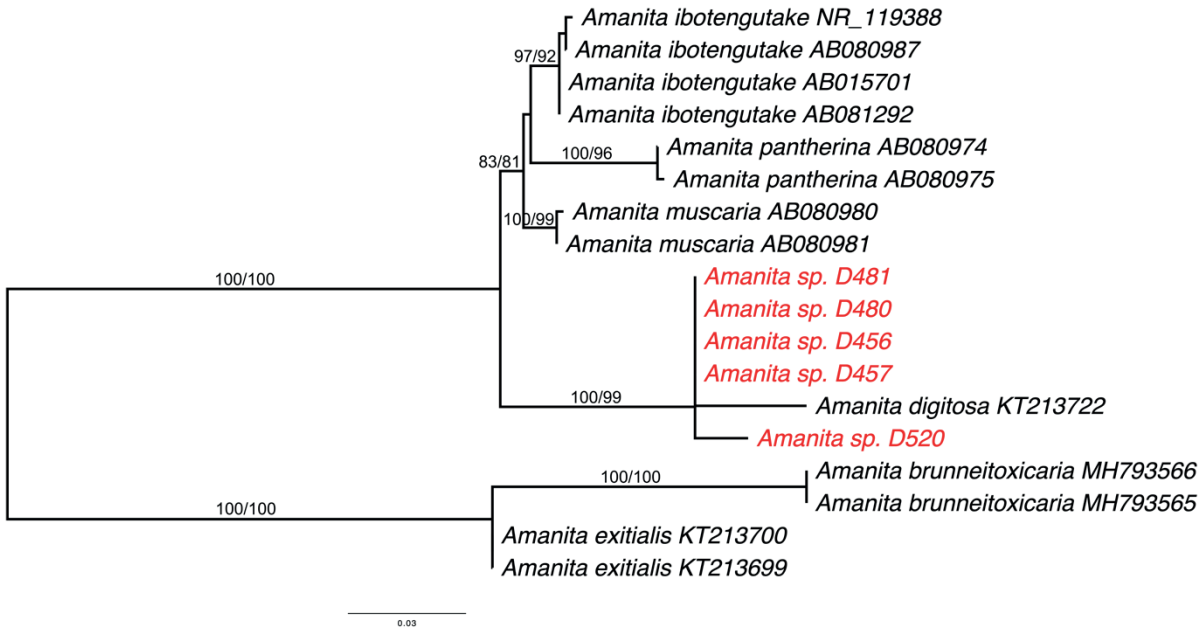

Figure 1 *Phylogenetic tree depicting relationships of the Amanita based on analysis of the ITS region. Mushroom obtained from poisoning cases are written in red. Bootstrap support ≥70% under RAxML and SH-like support value ≥90% under FastTree are indicates above branches.*

Taxon	1	2	3	4	5	6	7	8	9	10	11	12	13	14
1. *A. digitosa* KT213722		95	95	95	95	96	87	87	87	86	85	85	85	85
2. *Amanita* sp. D456	95		100	99	99	99	89	89	90	89	87	88	87	87
3. *Amanita* sp. D457	95	100		99	99	99	89	89	90	89	87	88	87	87
4. *Amanita* sp. D480	95	99	99		100	98	90	90	90	89	87	88	87	87
5. *Amanita* sp. D481	95	99	99	100		98	90	90	90	89	87	88	87	87
6. *Amanita* sp. D520	96	99	99	98	98		89	89	90	89	87	87	86	86
7. *A. ibotengutake* AB080987	87	89	89	90	90	89		100	100	100	94	94	91	91
8. *A. ibotengutake* AB015701	87	89	89	90	90	89	100		100	100	94	94	91	91
9. *A. ibotengutake* AB081292	87	90	90	90	90	90	100	100		99	94	94	92	91
10. *A. ibotengutake* NR_119388	86	89	89	89	89	89	100	100	99		94	94	91	91
11. *A. muscaria* AB080980	85	87	87	87	87	87	94	94	94	94		100	93	93
12. *A. muscaria* AB080981	85	88	88	88	88	87	94	94	94	94	100		93	93
13. *A. pantherina* AB080974	85	87	87	87	87	86	91	91	92	91	93	93		100
14. *A. pantherina* AB080975	85	87	87	87	87	86	91	91	91	91	93	93	100	

Figure 2 *Genetic distance matrix of Amanita. Nucleotide sequence percent (%) identity are shown in the table. Orange color indicates percent identify between A. digitosa and mushroom sample obtained from poisoning cases.*

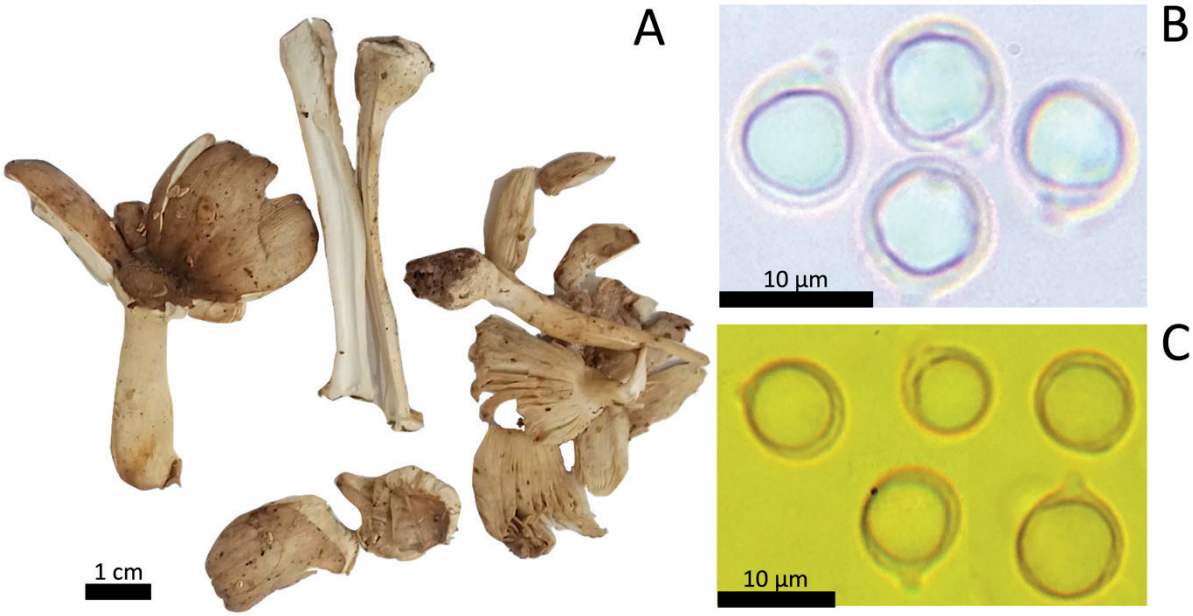

Figure 3 *The remnant mushroom samples. A: Amanita sp. (D480), B: Hyaline subglobose basidiospores, C: Inamyloid subglobose basidiospores.*

Detection of neurotoxin using LC-MS/MS

The purified mushroom extract was analyzed with MS/MS spectra based on the fragmentation of the precursor ion. The LC-MS/MS determination revealed the presence of ibotenic acid with ionic transitions of precursor ion (*m/z* 159) and product ion (*m/z* 113.1) in all *Amanita* samples (Figure 4). All samples did not detect alkaloid muscarine (Figure 5).

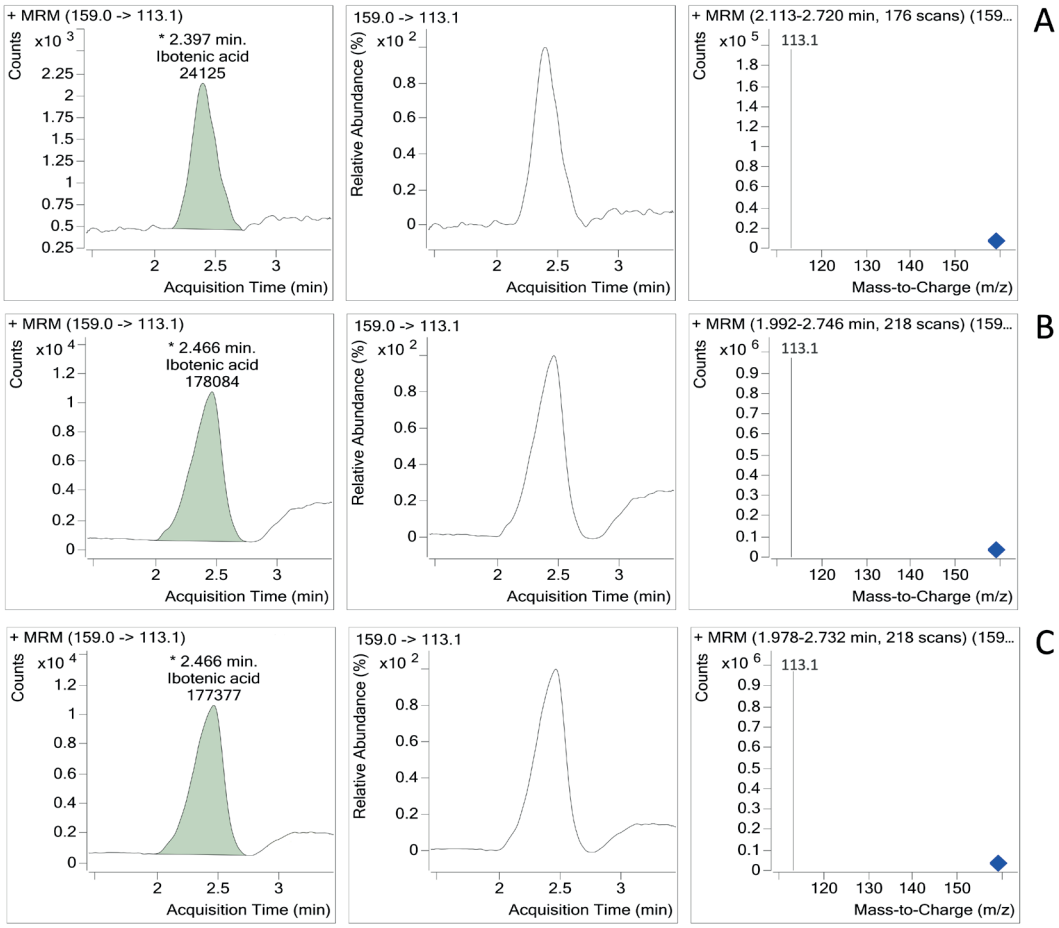

Figure 4. *Liquid chromatography-tandem mass spectrometric MRM chromatograms of Ibotenic acid neurotoxicant obtained from remnant mushroom samples (A) standard Ibotenic acid, (B) Amanita sp. (D480) and (C) Amanita sp. (D481). The diamond-shape represents the molecular ion of ibotenic acid (m/z 159).*

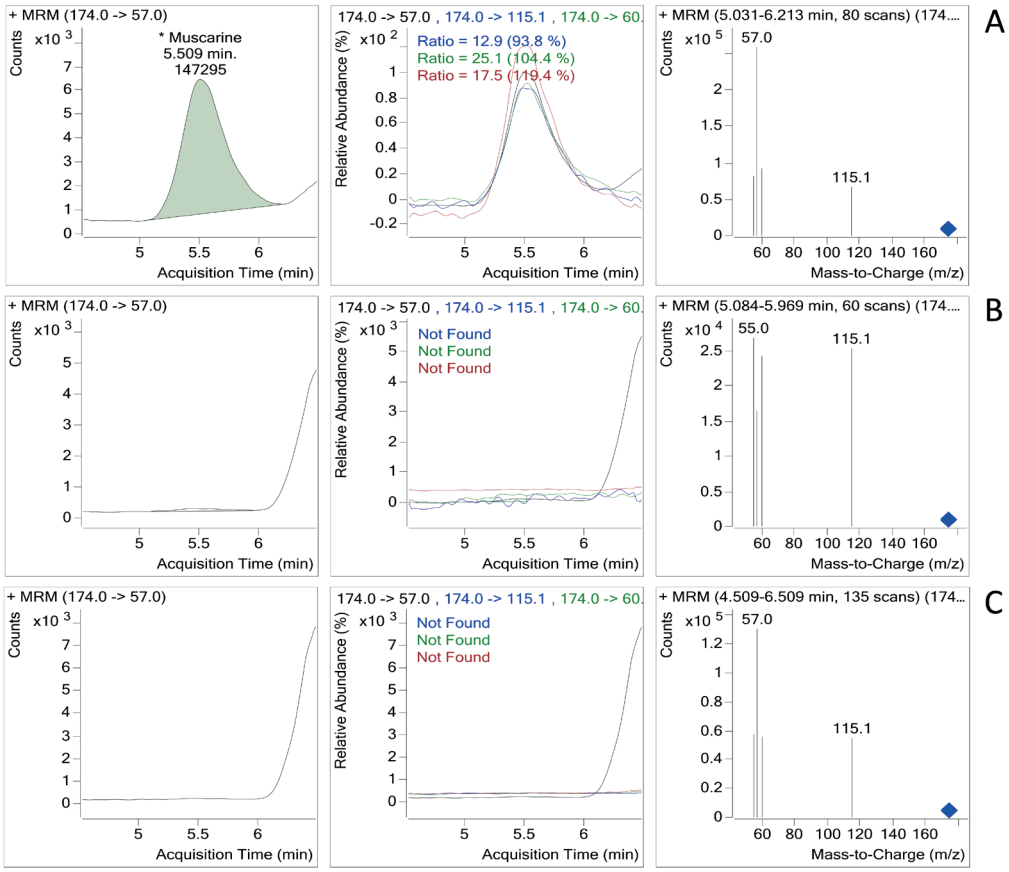

Figure 5. *Liquid chromatography-tandem mass spectrometric MRM chromatograms of alkaloid muscarine obtained from remnant mushroom samples (A) standard alkaloid muscarine, (B) Amanita sp. (D480) and (C) Amanita sp. (D481). The diamond-shape represents the molecular ion of alkaloid muscarine (m/z 174).*

Discussion

Epidemiological data has shown increasing incidence rates of mushroom poisoning cases in Thailand.[19] More than 80% of poisoning cases occur during the rainy season. Mushroom poisoning cases are reported in the north, northeast, east, and west regions from May to October, while in the southern part of the country, they occur from October to April. Food mushroom poisoning, as classified by White *et al*., is divided into six types based on clinical symptoms including group 1 cytotoxic mushroom poisoning, group 2 neurotoxic mushroom poisoning, group 3 myotoxic mushroom poisoning, group 4 metabolic/endocrine toxicity mushroom poisoning, group 5 gastrointestinal irritant mushroom poisoning and group 6 miscellaneous adverse reactions to mushrooms.[11] The most rapid onset of poisoning occurs in group 2, which is associated with neurotoxic mushrooms and manifests within 15-30 minutes. Group 2 includes four subgroups: hallucinogenic mushrooms (2A), autonomic toxicity mushrooms (2B), central nervous system toxicity mushrooms (2C), and morel neurologic syndrome (2D).[11] In Thailand, hallucinogenic mushrooms that produce psilocybin and psilocin are classified as 'category 5' narcotics under the Thai Narcotics Act B.E. 2522 (1979).[20] Mushroom food poisoning caused by neurotoxins has been reported, including cases involving *Inosperma* and *Pseudosperma*.[6] Both genera produce the alkaloid muscarine, which falls under the category of autonomic toxicity mushrooms (group 2B). Patients who ingest these mushrooms typically experience a short latent period of 15 to 30 minutes, with symptoms such as perspiration, hypersalivation, lachrymation, bradycardia, diarrhea, and fatigue.[6]

In this study, we examined mushroom samples obtained from suspected cases of neurotoxic mushroom poisoning. These samples consisted of remnant wild mushrooms harvested by patients and the Surveillance & Rapid Response Team (SRRT) from the Department of Disease Control. The study encompassed three poisoning cases: one in April 2019 from Yala province with one patient, one in August 2019 from Trang province with two patients, and the last cases in October 2019 from Songkhla province with eight patients. All mushroom poisoning cases underwent routine screening for lethal toxic substances, including alpha-amanitin, beta-amanitin, and the neurotoxic substance muscarine. The samples did not detect toxic substances from the above poisoning case. Based on their morphology, the samples were initially identified as belonging to the genus *Amanita*. A BLAST search of the ITS barcode confirmed that all mushroom samples closely matched A. digitosa, followed by *A. ibotengutake*.[12,21] Phylogenetic analyses based on ITS sequences also confirmed that all mushroom samples formed a robust clade with A. digitosa (100/99). While *A.*

digitosa is native to Thailand, *A. ibotengutake* was originally described in Japan. Morphologically, these mushroom samples exhibited greater similarity to *A. digitosa* than *A. ibotengutake*, with similar macroscopic morphology and basidiospore shape.[12,21] *A. ibotengutake* has been reported to contain ibotenic acid and muscimol.[21] These toxins have also been found in species closely related to *A. ibotengutake*, such as *A. muscaria* and *A. pantherina.*[15,22,23] However, the toxic substance of *A. digitosa* remained unknown at the time.[2,12] There have been reports of gastrointestinal irritant symptoms in patients who ingested *A. digitosa*.[2] All the mentioned species belong to the section *Amanita.*[2,12] In Thailand, some species within this section have been identified as causing mushroom food poisoning, with adverse effects ranging from mild gastrointestinal symptoms to severe cytotoxic effects.[2,10,12]

Based on the LC-MS/MS assay, all three poisoning cases involving the ingestion of *A. digitosa* detected the presence of ibotenic acid. Ibotenic acid serves as the main compound, functioning as a prodrug that converts to muscimol through decarboxylation or photochemical reactions.[15,23] Naturally, the ibotenic acid in toxic Amanitas can be converted to muscimol through drying, cooking, or ingestion.[15] Once absorbed into the body, ibotenic acid undergoes decarboxylation, transforming into muscimol. Both ibotenic acid and muscimol readily cross the blood-brain barrier and stimulate glutamate and gamma-aminobutyric acid (GABA) receptors.[15] According to poisoning reports, ingestion of mushrooms containing ibotenic acid and muscimol leads to neuropsychiatric, gastrointestinal irritation, and muscular symptoms.[15,23,24] These toxins are excreted in their original form through the urinary system within six hours.[24] In the reported poisoning cases, patients had ingested what they believed to be an edible species of termite mushroom in the genus *Termitomyces* (Lyophyllaceae). Most patients who ingested *A. digitosa* experienced rapid onset symptoms within five minutes, including nausea, vomiting, vertigo, delirium, confusion, and fatigue. Some patients required intubation in the intensive care unit, but all cases had no reported fatalities.

Conclusions

In summary, this study marks the first documented presence of ibotenic acid in *A. digitosa*. Safeguarding food safety, particularly in cases of mushroom consumption, is of utmost importance. To mitigate the risk of potentially life-threatening incidents, it is crucial to exercise vigilance in mushroom identification, prioritize education, and adhere to safe foraging practices.

Conflict of interest

The authors declare that there is no conflict of interest.

Acknowledgements

This work was financially supported by the Thailand Science Research and Innovation (Grant No. 164021/2022 and 183769/2023).

References

[1] Ratnasingham S, Hebert PDN. bold: The Barcode of Life Data System (http://www.barcodinglife.org). Mol Ecol Notes. 2007; 7(3): 355-64. doi.org/10.1111/j.1471-8286.2007.01678.x.

[2] Parnmen S, Sikaphan S, Leudang S, Boonpratuang T, Rangsiruji A, Naksuwankul K. Molecular identification of poisonous mushrooms using nuclear ITS region and peptide toxins: a retrospective study on fatal cases in Thailand. J Toxicol Sci. 2016; 41(1): 65-76.

[3] Parnmen S, Nooron N, Leudang S, Sikaphan S, Polputpisatkul D, Rangsiruji A. Phylogenetic evidence revealed *Cantharocybe virosa* (Agaricales, Hygrophoraceae) as a new clinical record for gastrointestinal mushroom poisoning in Thailand. Toxicol Res. 2020; 36(3): 239-48. doi.org/10.1007/s43188-019-00024-2.

[4] Ramchiun S, Sikaphan S, Leudang S, Polputpisatkul D, Nantachaiphong N, Khaentaw T, et al. Molecular characterization and liquid chromatography-mass spectrometric multiple reaction monitoring-based detection in case of suspected phalloides syndrome poisoning. J Assoc Med Sci. 2019; 52(1): 48-55. doi: 10.14456/jams.2019.9.

[5] Leudang S, Sikaphan S, Parnmen S, Nantachaiphong N, Polputpisatkul D, Ramchiun S, et al. DNA-based identification of gastrointestinal irritant mushrooms in the genus *Chlorophyllum*: A food poisoning case in Thailand. J Heal Res. 2017; 31(1): 41-9. doi: 10.14456/jhr.2017.6.

[6] Parnmen S, Nooron N, Leudang S, Sikaphan S, Polputpisatkul D, Pringsulaka O, et al. Foodborne illness caused by muscarine-containing mushrooms and identification of mushroom remnants using phylogenetics and LC-MS/MS. Food Control. 2021; 128: 108182. doi.org/10.1016/j.foodcont.2021.108182.

[7] Nooron N, Parnmen S, Chonnakijkul P, Sikaphan S, Chankunasuka R, Phatsarapongkul S, et al. Use of nuclear ITS region as DNA barcode marker for the species identification of mushroom in the genus *Macrocybe* causing foodborne illness. Thai J Toxicol. 2023; 38(1): 55-67. Available from: https://li01.tci-thaijo.org/index.php/ThaiJToxicol/article/view/258482.

[8] Xu J. Fungal DNA barcoding. Genome. 2016; 59(11): 913-32. doi: 10.1139/gen-2016-0046.

[9] Schoch CL, Seifert KA, Huhndorf S, Robert V, Spouge JL, Levesque CA, et al. Nuclear ribosomal internal transcribed spacer (ITS) region as a universal DNA barcode marker for Fungi. Proc Natl Acad Sci USA. 2012; 109(16): 6241-6. doi:10.1073/pnas.1117018109.

[10] Nooron N, Parnmen S, Sikaphana S, Leudang S, Uttawichai C, Polputpisatkul D. The situation of mushrooms food poisoning in Thailand: symptoms and common species list. Thai J Toxicol. 2020; 35(2): 58-69. Available from: https://li01.tci-thaijo.org/index.php/ ThaiJToxicol/article/view/248088.

[11] White J, Weinstein SA, De Haro L, Bédry R, Schaper A, Rumack BH, et al. Mushroom poisoning: A proposed new clinical classification. Toxicon. 2019; 157: 53-65.

doi: 10.1016/j.toxicon.2018.11.007.

[12] Li GJ, Hyde KD, Zhao RL, Hongsanan S, Abdel-Aziz FA, Abdel-Wahab MA, et al. Fungal diversity notes 253--366: taxonomic and phylogenetic contributions to fungal taxa. Fungal Divers. 2016; 1-237. doi.org/10.1007/s13225-016-0366-9.

[13] Trakulsrichai S, Jeeratheepatanont P, Sriapha C, Tongpoo A, Wananukul W. Myotoxic mushroom poisoning in Thailand: clinical characteristics and outcomes. Int J Gen Med. 2020; 13: 1139-46. doi: 10.2147/IJGM.S271914.

[14] He M-Q, Wang M-Q, Chen Z-H, Deng W-Q, Li T-H, Vizzini A, et al. Potential benefits and harms: a review of poisonous mushrooms in the world. Fungal Biol Rev. 2022; 42: 56-68.

[15] Duffy TJ. Toxic Fungi of Western North America. Vol. 2008, Group. MykoWeb; 2008. 166 p. Available from: www.mykoweb.com

[16] Gardes M, Bruns TD. ITS primers with enhanced specificity for basidiomycetes--application to the identification of mycorrhizae and rusts. Mol Ecol. 1993; 2(2): 113-8. doi.org/10.1111/j.1365-294X.1993.tb00005.x.

[17] White TJ, Bruns TD, Lee SB, Taylor JW. Amplification and direct sequencing of fungal ribosomal RNA genes for phylogenetics. In: Innis, M.A., Gelfand, D.H., Sninsky, J.J. & White T., editor. PCR Protocols: a guide to methods and applications. New York: Academic Press; 1990. p. 315-22.

[18] Altschul SF, Gish W, Miller W, Myers EW, Lipman DJ. Basic local alignment search tool. J Mol Biol. 1990; 215(3): 403-10. doi.org/10.1016/S0022-2836(05)80360-2.

[19] Department of Disease Control. Mushroom poisoning. National Disease Surveillance (Report 506). 2023. Available from: http://doe.moph.go.th/surdata/index.php

[20] Saingam D, Assanangkornchai S, Geater AF, Balthip Q. Pattern and consequences of krathom (*Mitragyna speciosa* Korth.) use among male villagers in southern Thailand: a qualitative study. Int J Drug Policy. 2013; 24(4): 351-8. doi: 10.1016/ j.drugpo.2012.09.004.

[21] Oda T, Yamazaki T, Tanaka C, Terashita T, Taniguchi N, Tsuda M. *Amanita ibotengutake* sp. nov., a poisonous fungus from Japan. Mycol Prog. 2002; 1(4): 355-65. doi.org/10.1007/s11557-006-0032-9.

[22] Tsujikawa K, Kuwayama K, Miyaguchi H, Kanamori T, Iwata Y, Inoue H, et al. Determination of muscimol and ibotenic acid in *Amanita* mushrooms by high-performance liquid chromatography and liquid chromatography-tandem mass spectrometry. J Chromatogr B, Anal Technol Biomed life Sci. 2007; 852(1-2): 430-5. doi: 10.1016/j.jchromb.2007.01.046.

[23] Bresinsky A, Besl H. A colour atlas of poisonous fungi: A handbook for pharmacists, doctors, and biologists. London: Wolfe Publishing Ltd; 1990. P.1-295.

[24] Hiroshima Y, Nakae H, Gommori K. *Amanita ibotengutake* intoxication treated with plasma exchange. Ther Apher Dial. 2010; 14(5): 483-4. doi: 10.1111/j.1744-9987.2010.00862.x.

Journal of Associated Medical Sciences 2024; 57(2): 115-124

JAMS
Journal of Associated Medical Sciences

Scopus Indexed & Thai-Journal Citation Index Centre (TCI)

Journal of Associated Medical Sciences

Journal homepage: https://www.tci-thaijo.org/index.php/bulletinAMS/index

Balance abilities in high dynamic-sport athletes with different maximal voluntary contraction

Pornpimol Konkeaw[1] **Sainatee Pratanaphon**[2*]

[1]*Sport Science, Multidisciplinary and Interdisciplinary School, Chiang Mai University, Chiang Mai Province, Thailand.*
[2]*Department of Physical Therapy, Faculty of Associated Medical Sciences, Chiang Mai University, Chiang Mai Province, Thailand.*

ARTICLE INFO

Article history:
Received 23 August 2023
Accepted as revised 28 February 2024
Available online 13 March 2024

Keywords:
Maximal voluntary contraction, balance, core stability, strength, high dynamic-sport athletes

ABSTRACT

Background: Previous studies have shown that muscle force control during submaximal isometric contractions is associated with the ability of dynamic balance to a greater extent than static balance in healthy adults. However, the effect of maximal voluntary contraction (MVC) on balance abilities of athletes with high dynamic-sport, which are most popular in Thailand, needs to be addressed.

Objective: To determine static and balance abilities of high dynamic-sport athletes at different levels of MVC.

Materials and methods: Three groups of high dynamic-sport athletes at different levels of maximal voluntary contraction (MVC), were voluntarily recruited using a sports matrix classification. Outcome measures comprised the Balance Error Scoring System (BESS) and the Star Excursion Balance Test (SEBT). Correlations between BESS and SEBT and confounding variables comprised of performance time of the Mcgill core endurance tests (Core), single-leg sit-to-stand (STS) test, and flexibility were investigated using Pearson's correlation. After controlling for Core and STS, a factorial analysis of covariance (ANCOVA) was used to determine group differences in SEBT and BESS variables.

Results: Athletes with high- and low- MVC had significantly different reaching distances in all SEBT directions (all, $p<0.05$). Significant differences between the high- and the moderate- MVC groups were observed in anterior and lateral directions ($p<0.05$). A significant difference between the moderate- and the low MVC groups was found in the medial direction ($p<0.05$). After controlling for Core and STS, the observed group differences disappeared, except in the posterolateral reaching distance between the high- and the low-MVC groups ($p<0.05$). A significant difference between the high- and the low-MVC groups was only observed in the total foam BESS scores with tandem stance ($p<0.05$) and then disappeared after adjusting for Core and STS (all, $p>0.05$).

Conclusion: The observed differences in all SEBT directions among groups and the difference in the total BESS scores between the high- and the low- MVC, which were observed only in challenged conditions i.e., tandem-foam stance, suggested that dynamic, but not static balance performance of athletes with high dynamic-sport appears to be associated with the magnitude of MVC. Core and STS, but not flexibility, are considered significant contributions to their balance performance.

∗ **Corresponding contributor.**
Author's Address: *Department of Physical Therapy, Faculty of Associated Medical Sciences, Chiang Mai University, Chiang Mai, Thailand*
E-mail address: sainatee.pra@cmu.ac.th
doi: 10.12982/JAMS.2024.033
E-ISSN: 2539-6056

Introduction

Balance control is essential for optimal athletic performance and injury prevention during training and competition. Balance is comprised of static balance, which is the ability to keep the center of mass of a body within the base of support with minimal postural sway, while dynamic balance represents the ability to maintain the body during

movements from one position to another.[1] Evidence in the literature suggested that balance in athletes is likely related to sports type and requires specific motor skills and different sensorimotor systems to control posture and movements.[2-5] For example, Bressel *et al.*[6] demonstrated that although having identical static and dynamic balance, gymnasts and soccer players had different performances in static and dynamic balance compared to basketball players. Most studies showed similarities and differences in balance abilities between each sport. Still, no study offers guidelines to estimate the balanced performance of athletic groups that share some characteristics in common, although their sports are different. Therefore, using a sports matrix as a criterion for grouping a variety of sports that require similar static and dynamic demands and then comparing the differences in balance abilities among sports groups becomes of interest. This may provide a comprehensive guide to estimate athletes' balance ability. Typically, this matrix has been used to guide practitioners and provide recommendations for sports participation.[7] It was developed by the American College of Cardiology Task Force.[8] The program is based on the concept that many similarities can be found among sports, e.g., all sports require a combination of strength and endurance components, although each sport possesses unique characteristics, including rules, culture, environments, the material used, and the numbers of players involved. Nine sports categories are classified by type (strength/static and endurance/dynamic components) according to the estimating of MVC and VO_2max and exercise intensity (low, moderate, and high). Each category is comprised of a variety of sports that require similar static and dynamic demands.

Muscular strength is the ability to exert maximal force in one single contraction, which is essential for controlling motor tasks smoothly and accurately.[9] Previous literature revealed that muscular strength is one of the underlying determinants of strength-power performance,[10,11] and is also associated with enhanced dynamic performance.[12] Recently, a review study of the influence of muscular strength on athletic performance and its beneficial effects revealed that greater muscular strength is associated with athletic performance, thereby affecting the rate of force development, general- and specific- sport skill performance, and decreasing injury risk.[13] However, studies on static balance revealed that the sustainable time for single-leg quiet standing was strongly correlated with force fluctuation in 20% MVC task.[14,15] hip and ankle strategies are more robust predictors for maintaining static balance than maximal strength. Likewise, moderate correlations were observed between knee extensor force control measures during contractions at 40% MVC and dynamic balance.[16] Notably, these studies were conducted in healthy subjects. It is still being determined whether there will be a similar response to athletes with higher performance. We have focused on athletes with high dynamic-sport or sports that required high VO_2max during competition in, which highly popular in Thailand.

It is known that balance control depends on several factors, including sensory input obtained from visual, vestibular, and somatosensory systems, type of sports, competition levels, and fatigue.[2,17-19] However, a systematic review and meta-analysis revealed that gender-related differences in balance performance were inconsistent.[20] Noticeably, potential confounders, including core stability, leg strength, and flexibility, which reported the associations to balance, did not consider the aforementioned studies, which may bias study results. Core stability, defined as the whole trunk, including all the muscles that cross the hip and shoulders, is important for athletic performance while the body is moved outside of the base of support. Studies have shown a significant improvement in balance after receiving a core stabilization training program.[21,22] Also, it has been shown that strength and flexibility are two of the critical indicators of physical performance in sports.[23] Leg strength was significantly correlated to balance performance.[24,25] Asymmetry in the flexibility and strength of the lower extremities can lead to improper control of body movement.[26] Moreover, flexibility, which is the ability of muscles, joints, and soft tissues to move through a range of motion, was positively associated with dynamic balance ability. Previous literature has shown that athletes with high flexibility have better movement proficiency. In contrast, the asymmetry of flexibility between the limbs is a significant risk factor for injury.[27]

This study aimed to investigate the static and dynamic balance abilities of athletes with high dynamic sport at three levels of MVC using a sports matrix classification. Correlations were also investigated between static and dynamic balance abilities and confounders, including core stability, leg strength, and flexibility. We hypothesized that athletes with high-, moderate- and low-MVC balance abilities would significantly differ between groups, and some confounders would dramatically correlate with balance abilities. This may provide more understanding of how MVC can affect static and dynamic balance abilities in athletes with high dynamic sport and clarify which factors are associated with the balance performance of the athletes.

Materials and methods

Study Design

A cross-sectional study was conducted in the three groups of athletes who had high VO_2max during competition at three levels of MVC.

Participants

The sample size was determined by using G*Power 3.1.9.7, F test: ANCOVA Fixed effects, main effects and interactions, with a power of 0.8, effect size of 0.3, numerator df as 1, number of groups as 3, number of covariates as 3, and a significant level of 0.05. Therefore, the total number of subjects is 90, about 30 people for each group. Male college athletes and athletes who participate in sports competitions at the provincial levels, aged 18-25 years, were recruited from Chaing Mai province, Thailand, via advertisements and flyers on university campuses and

in sports communities. All participants had regular physical exercise for at least 3 months. They were excluded if they had a previous history of musculoskeletal injury in the lower limbs in the past six months, received medications that affect balance, had vision problems, such as diplopia, and had diseases affecting postural control, such as vertigo, diabetes mellitus, and Meniere's disease. Based on a sports matrix classification, athletes who had high VO_2max were recruited by levels of MVC into three groups (low-exercise training exposure at <20%MVC e.g. badminton, tennis, moderate- exercise training exposure at 20-50% MVC e.g. basketball, swimming and high-exercise training exposure at >50% MVC e.g. boxing, cycling). Before starting any testing procedures, all participants signed informed consent documents approved by the Institutional Review Board (AMSEC-65EX-001).

Outcome measures

To avoid the effect of fatigue, participants performed a series of measures as follows: 1) body weight (BW), stature, leg length, leg dominance, single-leg sit-to-stand (STS), and the BESS tests were measured in the morning, and 2) core stability tests and the SEBT test were completed in the afternoon. Five-minute rest intervals were provided by sitting quietly between each measure. All outcomes were measured by three well-trained assessors with a physical education background. Before testing, two trials were performed to familiarize with each test.

Anthropometric measures

BW (in kilogram) and stature (in meters) were measured based on the procedure of Tsiros *et al.*[28] Body mass index (BMI) was calculated using weight in kilograms divided by the square of height in meters. Using a tape measure, leg length (in centimeters) was measured in supine from the anterior superior iliac spine to the medial malleolus.[29] Leg dominance was determined by observing which leg the participant preferred to kick the ball at least 2 times.[30]

Balance error scoring system (BESS)

The BESS was used to evaluate the static balance within 5-10 minutes, as described by previous studies.[31,32] The reliability of the BESS ranges from moderate (<0.75) to good (>0.75).[31] Three stances, including double-leg, single-leg, and tandem stances, were conducted on a firm surface (firm BESS) and foam surface (foam BESS) using (AIREX Balance Pad, TN, USA) with and without vision. Starting positions were as follows: hands on the hips and feet together were used to measure balance ability in double-leg stance while standing on the nondominant leg with hands on hips, and then flexed hip for 30 degrees and flexed knee for 45 degrees used for single-leg stance. The nondominant foot behind the dominant foot is used for a tandem stance. Postural error of each 20-second trial was scored as one point if participants did the following criteria, including lifting hands-off hips, opening eyes, stepping, stumbling, falling out of position, abducting the hip by more than 30°, lifting forefoot or heel or failing to return to the test position in more than 5 seconds. Multiple errors occurring simultaneously were counted as one point. All errors observed were summed up and recorded as BESS scores.

Star excursion balance test (SEBT)

Dynamic balance ability was examined using the SEBT based on the guidelines.[1,33] The test-retest reliability was excellent (ICC=0.80-0.94, standard error of measurement =0.00-0.03 cm) for all directions tested.[34] Participants were asked to stand barefoot at the intersection of eight taped lines, with hands placed on the iliac crest. Then, move their legs as far as possible in 8 directions in the same order-anterior, anteromedial, anterolateral, medial, lateral, posterior, posteromedial and posterolateral. Three attempts were made for the right and left leg in each direction. For the left SEBT, the left leg was weight-bearing, and for the right SEBT, the right leg was weight-bearing. The new attempt was performed if the participant failed to maintain a unilateral stance, lifted the stance foot off the ground, stepped hand from the hip, fully stepped on the forefoot, or could not return the reaching foot to the starting position. The average reaching distance (in centimeters) of the 3-trial in each direction was determined and then normalized to leg length (%). The normalized reaching distance was calculated by the maximal reaching distance divided by leg length, then multiplied by 100.

Core stability

As per a previous study, core stability was measured using the McGill core endurance tests.[35,36] McGill tests are popular and practical clinical tests for evaluating the isometric endurance of core muscles, which are shown to have reliability coefficients of between 0.97 and 0.99.[36] The flexor endurance test determined the anterior core endurance (AntCore). In the supine position, participants were asked to bring their hands crossed at the shoulder, bend hip and knee joints at 90° flexion, and the feet were stabilized by the research assistant. Then, flexed the trunk until the lower scapula rose from the bed. The extensor core endurance (ExtCore) test was performed to test the erector spinae and multifidus. This test was initiated with the participant's body hanging down from the table as the spina iliaca anterior superiors aligned with the table edge, the hands folded across at the shoulders, and the feet were stabilized. The lateral bridge test was used to test the lateral core endurance (LatCore). Participants were started in a side-lying position with weight bearing through the arm and extended leg with one foot in front of the other foot while lifting the body in a straight line. The duration (in seconds) of maintaining the three test positions was recorded using a stopwatch.

Leg strength

Leg strength was assessed using the one-leg sit-to-stand (one-leg STS) test, which was developed to measure single-leg muscle strength among young adults.[37] It demonstrated excellent reliability (ICC=0.960) and criterion-concurrent validity against the two-leg STS and

the lower extremity muscle strength. The participant was asked to sit on a chair with bare feet on the ground, slightly behind the knee joint, and arms folded crossed on the chest. After two practice trials, the participant was instructed to rise from a chair using the dominant leg with hip and knee full extension while lifting the other leg above the floor and then returning to the starting position as fast as possible five times. The duration (in seconds) was recorded using a stopwatch. Five trials with a three-minute rest interval were performed. The average of the fastest two trials was used for data analysis.

Flexibility

According to previous research, the sit and reach (SR) test was used to measure lower back and hamstring flexibility.[38] It demonstrated excellent reliability (ICC=0.920), and the criterion-related validity of SR and the passive straight leg raise test is moderate (r=0.63). Participants sat on the floor with the soles of their feet against the end of the SR box and then leaned their trunk and arms to reach forward as far as possible, placing one hand on the other. The average of three trials on each leg (in centimeters) was used for data analysis.

Statistical analysis

The independent variables were groups (low-, moderate- and high- MVC), and the dependent variables were the total BESS score and its subtests and the normalized reaching distances for eight directions. The data were analyzed for normal distribution using the Shapiro-Wilk test, and Levene's test confirmed homogeneity. Analysis of variance (ANOVA) was used, followed by the post-hoc Bonferroni to identify differences in demographic data between groups. Relationships between the balance two tests and core stability, STS, and flexibility were determined using Pearson's correlation and interpreted [0.1=weak; 0.4=moderate; 0.7=strong].[39] To achieve the medium correlation coefficient of at least 0.3 with a power of 80%, a minimum sample size of 84 is needed.[40] Confounders that significantly correlated to each balance test were used as covariates. SEBT variables that were normally distributed were compared between groups after adjustment for covariates using a factorial analysis of covariance (ANCOVA) with Bonferroni-adjusted post hoc tests. The effect size of the ANCOVA was calculated with partial Eta-squared (η^2) [0.01=small; 0.06=medium; 0.14=large].[41] BESS variables that were non-normally distributed were compared between groups after adjustment for covariates using McSweeny and Porter ranked ANCOVA methods with Scheffe post hoc tests. The inter-rater reliability for measuring variables of BESS, SEBT, core stability, leg strength, and flexibility was done in five participants and analyzed using the intraclass correlation coefficient ($ICC_{3,k}$) and was found to be moderate to excellent for all conditions (ICCs for BESS on firm surface =1.000, BESS on foam surface =0.951, SEBT-all directions =>0.90), AntCore=0.998, ExtCore=1.000, LatCore-dominant side=1.000, LatCore-nondominant side=1.000, one-leg STS=0.598, flexibility=1.000, all p<0.05). The test-retest reliability among assessors was moderate to excellent for all conditions ($ICC_{2,1}$ for BESS on firm surface=1.000, BESS on foam surface=0.851-0.872, SEBT-all directions (>0.90), AntCore=0.864-0.868, ExtCore=0.679-0.689, LatCore-dominant side=0.726, LatCore-nondominant side=0.914-0.915, one-leg STS=0.720-0.814, flexibility=0.949-952, all p<0.05. Data analyses were conducted using SPSS, and the significance level was set at p<0.05.

Results

Participant characteristics

Participants in the low MVC group (N=32) were composed of seven badminton players, seven hockey players, eight long-distance runners, and ten football players, and those of the moderate MVC group (N=30) were comprised of ten basketball players, six middle-distance runners, three swimmers, eleven handball players. Participants in the high MVC group (N=23) consisted of eight boxers, two triathlons, one bicycling, and twelve rowers. Participants in the low- and the moderate-MVC groups had marked differences in stature, BW, and limb length (all p<0.05). Participants in the moderate MVC group had age and stature significantly different from the high MVC group (all p<0.05). However, there were no differences in BMI among the three athletic groups (all p>0.05) (Table 1).

Table 1 Characteristics of athletes with low, moderate, and high MVC groups.

Variables	Low MVC (N=32)	Moderate MVC (N=30)	High MVC (N=23)	F test	*p* value
Age (yrs)	20.81 (1.84)	20.17 (1.56)**	21.52 (1.68)	4.151	0.019
Stature (m)	1.72 (0.07)*	1.77 (0.06)**	1.72 (0.06)	6.526	0.002
Body weight (kg)	64.46 (9.68)*	71.60 (12.02)	67.2 6(8.91)	3.691	0.029
Body mass index (kg/m^2)	21.84 (2.69)	22.78 (3.19)	22.69 (2.82)	0.960	0.387
Dominant limb length (cm)	88.00 (4.21)*	92.10 (4.51)	89.87 (4.06)	7.107	0.001
Non-dominant limb length (cm)	87.13 (5.54)*	91.75 (4.76)	89.74 (4.11)	6.905	0.002

Note: *represented as mean (SD), *significant difference from the moderate MVC group (p<0.05), **significant difference from the high MVC group (p<0.05), m: meter, m^2: square meter, cm: centimeter, kg: kilogram, yrs: years, MVC: maximum voluntary contraction*

Bivariate correlations

Errors of the total BESS score and the foam BESS score were significantly correlated with ExtCore and one-leg STS (all $p<0.05$) but not with AntCore, LatCore on both sides and flexibility (all $p>0.05$). The foam BESS error score with tandem stance significantly correlated to AntCore, ExtCore, LatCore-non dominant, and one-leg STS (all $p<0.05$). No correlations were found between errors in the BESS score, subtests performed on the firm surface, and covariates (Table 2). The normalized reaching distance of each SEBT direction of both legs was averaged because there were no differences in reaching distance between the dominant and non-dominant legs (all $p>0.05$). Reaching distances in all directions were significantly associated with AntCore, ExtCore (except anterolateral), LatCore-non-dominant side (except anterolateral), and one-legSTS (all $p<0.05$), but not for flexibility. Reaching distance in anterior and posterior directions was significantly correlated to the LatCore-dominant side (all $p<0.05$) (Table 3).

Table 2 Correlations between BESS variables and Covariates (N=85).

BESS condition	AntCore	ExtCore	LatCore-dominant	LatCore-non-dominant	One-leg sit to stand	Flexibility
Firm *condition*	-0.035 (*p*=0.748)	-0.072 (*p*=0.514)	0.061 (*p*=0.580)	-0.061 (*p*=0.577)	0.052 (*p*=0.638)	-0.186 (*p*=0.087)
Double-leg stance	1.000	1.000	1.000	1.000	1.000	1.000
Single-leg stance	-0.033 (*p*=0.764)	-0.072 (*p*=0.510)	0.037 (*p*=0.733)	-0.056 (*p*=0.610)	0.038 (*p*=0.729)	-0.186 (*p*=0.088)
Tandem stance	-0.020 (*p*=0.853)	-0.019 (*p*=0.866)	0.114 (*p*=0.300)	-0.039 (*p*=0.720)	0.071 (*p*=0.518)	-0.057 (*p*=0.603)
Foam condition	-0.152 (*p*=0.165)	-0.246* (*p*=0.023)	-0.121 (*p*=0.270)	-0.179 (*p*=0.102)	0.346** (*p*=0.001)	0.047 (*p*=0.669)
Double-leg stance	-0.026 (*p*=0.810)	0.092 (*p*=0.404)	0.030 (*p*=0.787)	0.021. (*p*=0.846)	016 (*p*=0.888)	0.071 (*p*=0.516)
Single-leg stance	0.028 (*p*=0.801)	-0.142 (*p*=0.194)	-0.024 (*p*=0.828)	-0.058 (*p*=0.596)	0.256* (*p*=0.018)	0.064 (*p*=0.563)
Tandem stance	-0.307** (*p*=0.004)	-0.273* (*p*=0.011)	-0.192 (*p*=0.079)	-0.252* (p=0.020)	0.298** (*p*=0.006)	-0.004 (*p*=0.973)
Total BESS	-0.133 (*p*=0.225)	-0.221* (*p*=0.042)	-0.069 (*p*=0.528)	-0.165 (*p*=0.132)	0.291** (*p*=0.007)	-0.040 (*p*=0.716)

Note: **correlation is significant at the 0.05 level (two-tailed),**correlation is significant at the 0.01 level (two-tailed), AntCore: anterior core endurance, ExtCore: extensor core endurance, LatCore: lateral core endurance.*

Table 3 Correlations between SEBT variables and Covariates (N=85).

Direction	AntCore	ExtCore	LatCore-dominant	LatCore- non-dominant	One-leg sit to stand	Flexibility
Anterior	0.478** (*p*=0.000)	0.355** (*p*=0.001)	0.277* (*p*=0.010)	0.415** (p=0.000)	-0.378** (*p*=0.000)	0119 (*p*=0.279)
Anteromedial	0.429** (*p*=0.000)	0.369** (*p*=0.001)	0.177 (*p*=0.104)	0.341** (*p*=0.001)	-0.340** (*p*=0.001)	0.019 (*p*=0.864)
Anterolateral	0.223* (*p*=0.040)	0.201 (*p*=0.065)	0.102 (*p*=0.351)	0.108 (*p*=0.325)	-0.280** (*p*=0.009)	0.101 (*p*=0.357)
Medial	0.332** (*p*=0.002)	0.253* (*p*=0.019)	0.065 (*p*=0.552)	0.300** (*p*=0.005)	-0.487** (*p*=0.000)	0.036 (*p*=0.744)
Lateral	0.370** (*p*=0.000)	0.243* (*p*=0.025)	0.135 (*p*=0.217)	0.327** (*p*=0.002)	-0.451** (*p*=0.000)	0.182 (*p*=0.095)
Posterior	0.411** (*p*=0.000)	0.424** (*p*=0.000)	0.232* (*p*=0.032)	0.286** (*p*=0.008)	-0.492** (*p*=0.000)	0.212 (*p*=0.052)
Posteromedial	0.306** (*p*=0.004)	0.259* (*p*=0.017)	0.052 (*p*=0.637)	0.221* (*p*=0.042)	-0.551** (*p*=0.000)	0.103 (*p*=0.347)
Posterolateral	0.348** (*p*=0.001)	0.294** (*p*=0.006)	.0138 (*p*=0.207)	0.259* (*p*=0.017)	-0.479** (*p*=0.000)	0.115 (*p*=0.294)

Note: **correlation is significant at the 0.05 level (two-tailed), **correlation is significant at the 0.01 level (two-tailed), AntCore: anterior core endurance, ExtCore: extensor core endurance, LatCore: lateral core endurance.*

Static balance abilities

After baseline normalization for age, stature, and body weight, the main effects of the group for the total BESS error score, the total foam BESS score, and the foam BESS score for tandem stance were significantly observed (all, $p<0.05$). Post-hoc comparison revealed that the low MVC group had BESS error score for tandem stance on foam surface considerably higher than the high MVC group ($p<0.05$). After controlling for ExtCore and one-leg STS, the main effects of the group for all BESS parameters were not found (all, $p>0.05$) (Table 4).

Table 4 BESS error scores of athletes with different levels of MVC before and after adjustment for potential covariates.

BESS condition	Balance error scoring system (BESS) error scores			F test	*p* value	η^2
	Low MVC	Moderate MVC	High MVC			
After adjustment for age, stature and body weight						
Total BESS-firm surface	46.40 (4.01)	39.49 (4.32)	42.85 (4.80)	0.659	0.520	0.016
Double-leg stance	43.00 (0.00)	43.00 (0.00)	43.00 (0.00)	n/a	n/a	1.000
Single-leg stance	45.03 (3.95)	40.83 (4.25)	43.00 (4.73)	0.249	0.780	0.006
Tandem stance	47.40 (3.12)	39.37 (3.36)	41.62(3.74)	1.605	0.207	0.039
Total BESS-foam surface	51.90 (4.38)	37.41 (4.72)	37.91 (5.25)	3.223	0.045	0.075
Double-leg stance	43.89 (1.43)	42.96 (1.54)	41.81 (1.71)	0.443	0.644	0.011
Single-leg stance	49.78 (4.43)	37.91 (4.77)	40.21 (5.30)	1.850	0.164	0.045
Tandem stance	52.93 (4.16)*	37.91 (4.48)	35.82 (4.98)	4.575	0.013	0.104
Total BESS error score	52.03 (4.38)	36.09 (4.72)	39.45 (5.24)	3.366	0.040	0.079
After adjustment for age, stature, body weight, ExtCore and one-leg STS						
Total BESS-firm surface	46.49 (5.11)	38.46 (5.08)	44.08 (5.00)	0.517	0.599	0.013
Double-leg stance	43.00 (0.00)	43.00 (0.00)	43.00 (0.00)	n/a	n/a	1.000
Single-leg stance	45.65 (5.00)	39.21 (4.98)	44.26 (4.90)	0.375	0.688	0.010
Tandem stance	45.83 (4.00)	40.96 (3.98)	41.72 (3.92)	0.321	0.726	0.008
Total BESS-foam surface	47.69 (5.39)	39.01 (5.36)	41.68 (5.27)	0.502	0.607	0.013
Double-leg stance	44.88 (1.79)	42.60 (1.78)	40.91 (1.76)	1.132	0.328	0.029
Single-leg stance	48.49 (5.65)	38.07 (5.62)	41.80 (5.53)	0.642	0.529	0.016
Tandem stance	47.87 (5.09)	40.37 (5.06)	39.66 (4.98)	0.638	0.531	0.016
Total BESS error score	49.26 (5.42)	36.56 (5.40)	42.69 (5.31)	1.023	0.364	0.026

Note: *Represented as mean (SD),*significant difference from the high MVC group ($p<0.05$), η^2: partial eta squared, MVC: maximum voluntary contraction, one-leg STS: one-leg sit to stand, ExtCore: extensor core endurance.*

Dynamic balance abilities

Normalized reaching distances between the dominant and non-dominant legs were not statistically different for all eight SEBT directions (all $p>0.05$). Therefore, the average reaching distance of both legs was used for further analysis. After baseline normalization for age, stature, and body weight, significant main effects of the group for all eight SEBT directions were found (all, $p<0.005$). Post-hoc comparison indicated that the high MVC had a greater reaching distance in all directions than the low MVC groups, significantly (all $p<0.05$). Normalized reaching distances between the high- and the moderate-MVC groups were only observed considerably in anterior and lateral directions ($p<0.05$). The moderate- and the low- MVC groups significantly differed in medial reaching distance ($p<0.05$). After controlling for AntCore, ExtCore, LatCore-non-dominant side, and one-leg STS, the main effects of the group for all reach directions were not observed ($p<0.05$), except for the posterolateral direction ($p>0.05$). Post-hoc comparison revealed that the low MVC group had posterolateral reaching distance less than the high MVC group significantly ($p<0.05$) (Table 5).

Table 5 Normalized reach distances during SEBT of athletes with different levels of MVC before and after adjustment for potential covariates.

Direction	Normalized reach distances (cm)			F test	*p* value	η^2
	Low MVC	Moderate MVC	High MVC			
After adjustment for age, stature and body weight						
Anterior	0.98 (0.01)**	1.00 (0.02)**	1.07 (0.02)	9.399	0.000	0.192
Anteromedial	1.02 (0.01)**	1.04 (0.02)	1.09 (0.02)	5.819	0.004	0.128
Anterolateral	0.88 (0.02)**	0.94 (0.02)	0.96 (0.02)	5.363	0.007	0.120
Medial	1.03 (0.02)*,**	1.10 (0.02)	1.11 (0.02)	6.441	0.003	0.140
Lateral	0.89 (0.02)**	0.95 (0.03)**	1.05 (0.03)	9.505	0.000	0.194
Posterior	1.06 (0.02)**	1.13 (0.02)	1.19 (0.03)	7.179	0.001	0.154
Posteromedial	1.09 (0.02)**	1.16 (0.02)	1.18 (0.02)	5.315	0.007	0.119
Posterolateral	0.96 (0.02)**	1.05 (0.03)	1.13 (0.03)	10.636	0.000	0.212
After adjustment for age, stature, body weight, AntCore, ExtCore, LatCore - non-dominant side and one-leg STS						
Anterior	0.99 (0.02)	1.00 (0.02)	1.04 (0.02)	1.770	0.177	0.045
Anteromedial	1.03 (0.02)	1.04 (0.02)	1.07 (0.02)	0.881	0.419	0.023
Anterolateral	0.89 (0.02)	0.94 (0.02)	0.96 (0.03)	2.460	0.092	0.062
Medial	1.06 (0.02)	1.10 (0.02)	1.09 (0.02)	1.097	0.339	0.028
Lateral	0.93 (0.03)	0.93 (0.03)	1.02 (0.03)	2.328	0.104	0.058
Posterior	1.09 (0.02)	1.12 (0.03)	1.16 (0.03)	1.181	0.313	0.031
Posteromedial	1.13 (0.02)	1.14 (0.02)	1.16 (0.03)	0.317	0.729	0.008
Posterolateral	0.99 (0.03)**	1.03 (0.03)	1.11 (0.03)	3.361	0.040	0.082

Note: *Represented as mean (SD),*significant difference from the moderate MVC group (p<0.05), **significant difference from the high MVC group (p<0.05), η^2: partial eta squared, cm: centimeter, MVC: maximum voluntary contraction, one-leg STS: one-leg sit to stand, AntCore: anterior core endurance, ExtCore: extensor core endurance, LatCore: lateral core endurance.*

Discussion

Our findings highlight that athletes with high MVC had superior dynamic balance ability to a great extent than those with moderate- and low- MVC. The difference in static balance ability between the high and low-MVC groups was observed only in challenged conditions i.e., tandem stance on foam. AntCore, ExtCore, LatCore-non-dominant side, and one-leg STS, but not flexibility, were associated with dynamic balance ability. ExtCore and one-leg STS, but not AntCore, LatCore, and both sides and flexibility were significantly correlated with static balance, especially during tandem stance on foam condition. These results emphasized the importance of MVC on dynamic balance performance to a greater extent than static balance performance. In addition, core stability and leg strength, but not flexbility are essential contributing factors for controlling the balance of athletes with high dynamic-sport.

These findings support the study of Mear *et al.*[16] in healthy adults, which revealed that knee extensor force control during contraction at 40% MVC, but not at either 10 or 20% MVC, had significantly correlated to dynamic balance in the Y balance test, especially in anterior and posteromedial directions, but not posterolateral direction. In this study, the results of the high-, the moderate- and the low-MVC groups that had the estimated MVC at >50%, 20-50%, and <20%, respectively, revealed that the high MVC group had reaching distance superior to the low MVC group in all 8 directions of SEBT (Table 5). The differences in reaching distance between the high- and moderate-MVC groups, and between the moderate- and low- MVC groups were seen in some directions i.e., anterior, and lateral or medial directions. Consistently, a literature review indicated that maximum strength is moderate to strongly related to endurance capabilities and associated factors, a relationship that is likely stronger for high-intensity exercise endurance activities than for low-intensity exercise endurance. Together, it might be implied that the magnitude of MVC is essential for the dynamic balance performance of athletes.

No differences in BESS performance during the three stances on firm and foam surfaces were observed among the three groups of high dynamic-sport athletes. However, the difference between the high MVC and the low MVC group was observed only under challenging conditions, e.g., a tandem stance on a foam surface. These results were consistent with the results obtained by Knight *et al.* who found no differences in BESS performance among sprinters, distance runners, and throwers, although they had different sports types and energy demands.[42] Studies reported that standing on foam causes body instability in both the sagittal and frontal planes and distorts somatosensory inputs from the lower extremity, and tandem stance perturbs balance in the sagittal and

mediolateral planes.[43,44] Previous observations have shown that standing in tandem stance or on foam requires increments of muscle activity, metabolic cost, and cognitive demands for controlling posture.[44-47] Thus, this would imply that the foam BESS with tandem stance might be a quick screening test for examining the static balance abilities of athletes with high levels of VO_2max. Also, the BESS results of this study were in line with the findings of a previous study that determined the relationship between ankle plantar flexor force steadiness and postural control during single-leg standing on stable and unstable platforms.[15] The authors found that the center of pressure fluctuations, an index for postural control, on a stable platform were not related to maximum strength and force control at high-intensity contractions but were significantly related to force control only at the low-intensity force of 5% of maximum voluntary torque (MVT). Meanwhile, the COP fluctuations on an unstable platform were correlated with force control only at 20% of MVT. Moreover, the extent of muscle activity observed for a single leg standing on both stable and unstable platforms was significantly greater than the muscle activity observed while performing force steadiness tasks at 5% and 20% of MVT. Moreover, a study on static balance has shown that force control in the hip abductors, ankle dorsiflexion, and ankle plantar flexors are stronger predictors of task performance than maximal strength.[14] Together, these findings suggest that high levels of MVC are essential for controlling dynamic, but not static, balance. In addition, the magnitude of MVC becomes crucial to maintaining static balance only in challenged tasks.

Bivariate correlations also showed that Core and one-leg STS, but not flexibility were significantly correlated to SEBT and BESS parameters. After controlling for core stability and one-leg STS, the group differences in SEBT and BESS performance disappeared, except for a group difference in posterolateral reaching distance between the high- and the low-MVC groups. These results emphasized the necessity of core stability and leg strength on both static and dynamic balance abilities of high dynamic-sport athletes and supported the evidence of previous studies.[22,35,48] Therefore, coaches and athletes should incorporate core stability and leg strength into the training program to gain an advantage in maintaining postural balance.

This is the first study that determines the effect of MVC on balance abilities in athletes with high dynamic-sport, and the observed confounders, including core stability and leg strength, were used for statistical analyses. The results provide insights on static and dynamic postural balance control among athletes with high dynamic-sport. However, the findings of this study could not be transferred to practice. Further research using high-precision measurement tools for measuring VO_2max and the level of MVC is needed. Acknowledged limitations in this study may limit the generalizability of the findings. First, the participants of this study were limited to athletes with high VO_2max, but not to athletic groups with low or moderate VO_2max based on Mitchell's classification. Second, the VO2 max and MVC of each participant, which was estimated by Mitchell's classification, can cause distorted results. Third, a small sample of the high MVC group may have affected the power to detect the difference between groups, especially for BESS results. Most data have demonstrated small to medium effect size; therefore, the results should be interpreted cautiously. The unequal number of sports in each athletic group might affect the results of this study. Thus, a larger sample size with equal sports is required for further study.

Conclusion

Dynamic, to a lesser extent, static balance abilities of athletes with high MVC are superior to those with moderate- and low-MVC, emphasizing the extent of the magnitude of MVC on dynamic balance rather than static balance in athletes with high dynamic-sport. Moreover, core stability and leg strength are potential confounders for maintaining postural control.

Conflict of interest

The authors declare no conflict of interest.

Acknowledgements

The authors would like to acknowledge the participants for their contribution as well as extend appreciation to the officers of the Thailand National Sports University, Chiang Mai Campus, for help and support to the study.

References

[1] Gribble PA, Hertel J, Plisky P. Using the star excursion balance test to assess dynamic postural-control deficits and outcomes in lower extremity injury: A literature and systematic review. J Athl Train. 2012; 47(3): 339-57. doi: 10.4085/1062-6050-47.3.08.

[2] Vitale JA, Vitale ND, Cavaleri L, Dazzan E, Laombardi G, Mascagni P, *et al*. Level- and sport-specific star excursion balance test performance in female volleyball players. J Sports Med Phys Fitness. 2019; 59(5): 733-42. doi: 10.23736/S0022-4707.18.08691-7. Epub 2018 Oct 10.

[3] Paillard T. Plasticity of the postural function to sport and/or motor experience. Neurosci Biobehav Rev. 2017; 72: 129-52. doi: 10.1016/j.neubiorev.2016.11.015. Epub 2016 Nov 26.

[4] Itamar N, Schwartz D, Melzer L. Postural control: differences between youth judokas and swimmers. J Sports Med Phys Fitness. 2013; 53(5): 483-89.

[5] Zimmer A, Piecora K, Schuster D, Webbe F. Sport and team differences on baseline measures of sport-related concussion. J Athl Train. 2013 ;48(5): 659-67. doi: 10.4085/1062-6050-48.5.06.

[6] Bressel E, Yonker JC, Kras J, Heath EM. Comparison of static and dynamic balance in female collegiate soccer, basketball, and gymnastics athletes. J Athl Train. 2007; 42(1): 42-6.

[7] Levine BD; Baggish AL, Kovacs RJ, Link MS, Maron MS, Mitchell JH. Eligibility and disqualification recommendations for competitive athletes with

cardiovascular abnormalities: Task Force 1: classification of sports: dynamic, static, and impact: a scientific statement from the American Heart Association and American College of Cardiology. Circulation. 2015; 132: e262-e266. doi: 10.1161/CIR.0000000000000237.

[8] Mitchell JH, Haskell W, Snell P, Camp SPV. Task force 8: classification of sports. J Am Coll Cardiol. 2005; 45(8): 1364-7. doi: 10.1016/j.jacc.2005.02.015.

[9] Pethick J, Winter SL, Burnley M. Physiological complexity: influence of ageing, disease and neuromuscular fatigue on muscle force and torque fluctuations. Exp Physiol. 2021; 106: 2046-59. doi: 10.1113/EP089711.

[10] Stone MH, Moir G, Glaister M, *et al*. How much strength is necessary? Phys Ther Sport. 2002; 3(2): 88-96. doi: 10.1054/ptsp.2001.0102.

[11] Cormie P, McGuigan MR, Newton RU. Developing maximal neuromuscular power: part 2-training considerations for improving maximal power production. Sports Med. 2011; 41(2): 125-46. doi: 10.2165/11538500-000000000-00000.

[12] Stone MH, Stone ME, Sands WA, Pierce KC, Newton RU, Haff GG, *et al*. Maximum strength and strength training-a relationship to endurance? Strength Cond J. 2006; 28(3): 44-53.

[13] Suchomel TJ, Nimphius S, Stone MH. The importance of muscular strength in athletic performance. Sports Med. 2016; 46: 1419-49. doi: 10.1007/s40279-016-0486-0.

[14] Davis LA, Allen SP, Hamilton LD, Grabowski AM, Enoka RM. Differences in postural sway among healthy adults are associated with the ability to perform steady contractions with leg muscles, Exp. Brain Res. 2020; 238: 487-97. doi: 10.1007/s00221-019-05719-4.

[15] Hirono T, Ikezoe T, Yamagata M, Kato T, Kimura M, Ichihashi N. Relationship between ankle plantar flexor force steadiness and postural stability on stable and unstable platforms. Eur J Appl Physiol. 2020; 120: 1075-82. doi: 10.1007/s00421-020-04346-0.

[16] Mear E, Gladwell V. Pethick J. Knee extensor force control as a predictor of dynamic balance in healthy adults. Gait & Posture 2023; 100: 230-5. doi: 10.1016/j.gaitpost.2023.01.004.

[17] Mackinnon CD. Sensorimotor anatomy of gait, balance, and falls. Handb Clin Neurol. 2018; 159: 3-26. doi: 10.1016/B978-0-444-63916-5.00001-X.

[18] Sprenger A, Wojak JF, Jandl NM, and Helmchen C. Postural control in bilateral vestibular failure: its relation to visual, proprioceptive, vestibular, and cognitive input. Front Neurol. 2017; 8, Article 444. doi: 10.3389/fneur.2017.00444.

[19] Seidi F, Hamedani PD, Rajabi R, Sheikhhoseini R, Khoshroo F. A new fatigue protocol to assess postural sway in collegiate female athletes. Fatigue: Biomed Health Behav. 2019; 7(4): 218-28. doi: 10.1080/21641846.2019.1699640.

[20] Schedler S, Kiss R, Muehlbauer T. Age and sex differences in human balance performance from 6-18 years of age: A systematic review and meta-analysis. PLoS ONE. 2019; 14(4): e0214434. doi: 10.1371/journal.pone.0214434.

[21] Sandrey MA, Mitzel JG. Improvement in dynamic balance and core endurance after a 6-week core-stability-training program in high school track and field athletes. J Sport Rehabil. 2013; 22(4): 264-71. doi: 10.1123/jsr.22.4.264. Epub 2013 Jun 24.

[22] Bashir SF, Nuhmani S, Dhall R, Muaidi QI. Effect of core training on dynamic balance and agility among Indian junior tennis players. Back Musculoskelet Rehabil. 2019; 32(2): 245-52. doi: 10.3233/BMR-170853.

[23] Lehance C, Binet J, Bury T, Croisier JL. Muscular strength, functional performances and injury risk in professional and junior elite soccer players. Scand J Med Sci Sports. 2009; 19: 243-51. doi: 10.1111/j.1600-0838.2008.00780.x. Epub 2008 Mar 31.

[24] Castillo-Rodríguez A, Onetti-Onetti W, Mendes RS and Chinchilla-Minguet JL. Relationship between leg strength and balance and lean body mass. Benefits for active aging. Sustainability 2020; 12: 2380. doi: 10.3390/su12062380.

[25] ŚliwowskiJakub R, Marynowicz J, Jadczak L, Grygorowicz M, Kalinowski P, Paillard T. The relationships between knee extensors/ flexors strength and balance control in elite male soccer players. Peer J. 2021; 9: e12461. doi: 10.7717/peerj.12461.

[26] Grygorowicz M, Kubacki J, Pilis W, Gieremek K, Rzepka R. Selected isokinetic test in knee injury prevention. Biol Sport. 2010; 27 (1): 47-51.

[27] Emilio EJM, Hita-Contreras F, Jiménez-Lara PM, LatorreRomán P, Martínez-Amat A. The association of flexibility, balance, and lumbar strength with balance ability: Risk of falls in older adults. J Sports Sci Med. 2014; 13: 349-57.

[28] Tsiros MD, Brinsley J, Mackintosh S, Thewlis D. Relationships between adiposity and postural control in girls during balance tasks of varying difficulty. Obes Res Clin Pract. 2019; 13(4): 358-64. doi: 10.1016/j.orcp.2019.06.003. Epub 2019 Jun 28.

[29] Neelly K, Wallmann HW, Backus CJ. Validity of measuring leg length with a tape measure compared to a computed tomography scan. Physiother Theory Pract. 2013; 29(6): 487-92. doi:10.3109/09593985.2012.755589. Epub 2013 Jan 4.

[30] Schneiders AG, Sullivan SJ, O'Malley KJ, Clarke SV, Knappstein SA, Taylor LJ. A valid and reliable clinical determination of footedness. PM & R. 2010; 2: 835-41. doi: 10.1016/j.pmrj.2010.06.004.

[31] Bell DR, Guskiewicz KM, Clark MA, Padua DA. Systematic review of the balance error scoring system. Sports Health. 2011; 3(3): 287-95. doi: 10.1177/1941738111403122

[32] Iverson GL and Koehle MS. Normative data for the balance error scoring system in adults. Rehabil Res Pract. 2013; 2013: 846418. doi: 10.1155/2013/846418.

[33] Hertel J, Miller SJ, Denegar CR. Intratester and intertester reliability during the star excursion balance test. J Sport Rehabil. 2000; 9(2): 104-16. doi: 10.1123/jsr.9.2.104.

[34] Ortega SL, Ibarra S, Pierce R, Levy S, Gombatto SP. Kinematic and kinetic factors associated with leg reach asymmetry during the Star Excursion Balance Test in division I athletes. Phys Ther Sport. 2020; 45: 63-70. doi: 10.1016/j.ptsp.2020.05.012.

[35] Kocahan T, Ak?noglu B. Determination of the relationship between core endurance and isokinetic muscle strength of elite athletes. J Exerc Rehabil. 2018; 14(3): 413-8. doi: 10.12965/jer.1836148.074. eCollection 2018 Jun.

[36] McGill SM, Childs A, Liebenson C. Endurance times for low back stabilization exercises: clinical targets for testing and training from a normal database. Arch Phys Med Rehabil. 1999; 80(8): 941-4. doi: 10.1016/s0003-9993(99)90087-4.

[37] Thongchoomsin S, Bovonsunthonchai S, Joseph L, Chamnongkich S. Clinimetric properties of the one leg sit to stand test in examining unilateral lower limb muscle strength among young adults. Int J Clin Pract. 2020; 74(9): e13556. doi: 10.1111/ijcp.13556.

[38] Ayala F, Sainz de Baranda P, De Ste Croix M, Santonja F. Reproducibility and criterion-related validity of the sit and reach test and toe touch test for estimating hamstring flexibility in recreationally active young adults. Phys Ther Sport. 2012; 13(4): 219-26. doi: 10.1016/j.ptsp.2011.11.001.

[39] Schober P, Boer C, Schwarte LA. Correlation coefficients: appropriate use and interpretation. Anesth Analg. 2018; 126: 1763-8. doi: 10.1213/ANE.0000000000002864.

[40] Bujang MA and Baharum N. Sample size guideline for correlation analysis. World J Soc Sci Res. 2016; 3(1): 37-46.

[41] Cohen J. A power primer. Psychol Bull. 1992; 112(1): 155-9. doi: 10.1037/0033-2909.112.1.155.

[42] Knight AC, Holmes ME, Chander H, Kimble A, Stewart JT. Assessment of balance among adolescent track and field athletes. Sports Biomech. 2016; 15(2): 169-79. doi: 10.1080/14763141.2016.1159324. Epub 2016 Apr 25.

[43] van MierloJean M, Ormiston JA, Vlutters M, van Asseldonk EHF, van der Kooij H. Pelvis perturbations in various directions while standing in staggered stance elicit concurrent responses in both the sagittal and frontal plane. PloS One. 2023; 18(4): e0272245. doi: 10.1371/journal.pone.0272245.

[44] Mohapatra S, Kukka, KK, Aruin AS. Support surface related changes in feedforward and feedback control of standing posture. J Electromyogr Kinesiol. 2014; 24: 144-52. doi: 10.1016/j.jelekin.2013.10.015.

[45] Mademli L, Mavridi D, Bohm S, Patikas DA, Santuz A, Arampatzis A. Standing on unstable surface challenges postural control of tracking tasks and modulates neuromuscular adjustments specific to task complexity. Sci Rep. 2021; 11: 6122. doi: 10.1038/s41598-021-84899-y.

[46] Sozzi S, Honeine JL, Do MC, Schieppati M. Leg muscle activity during tandem stance and the control of body balance in the frontal plane. Clin Neurophysiol. 2013; 124: 1175-86. doi: 10.1016/j.clinph.2012.12.001.

[47] Dault MC, Geurts AC, Mulder TW, Duysens J. Postural control and cognitive task performance in healthy participants while balancing on different support-surface configurations. Gait Posture. 2001; 14: 248-55. doi: 10.1016/S0966-6362(01)00130-8.

[48] Endo Y, Miura M. Effects of posture and lower limb muscle strength on the results of the Star Excursion Balance Test. J Phys Ther Sci. 2021; 33: 641-5. doi: 10.1589/jpts.33.641. Epub 2021 Sep 1.

Journal of Associated Medical Sciences 2024; 57(2): 125-131

JAMS
Journal of Associated Medical Sciences

Scopus Indexed & Thai-Journal Citation Index Centre (TCI)

Journal of Associated Medical Sciences

Journal homepage: https://www.tci-thaijo.org/index.php/bulletinAMS/index

Preliminary study of distal forearm bone mineral density in residents of Doi Lo District: Observation and comparison with Mae Chaem, and Omkoi Districts, Chiang Mai Province, Thailand

Montree Tungjai[1,2] Monruedee Tapanya[2] Khin Thandar Htun[2] Suratchanee Phadngam[2] Tarika Thumvijit[2] Sompong Sriburee[2] Pisak Chinchai[1,3] Suban Pornwiang[1,4] Suchart Kothan[1,2*]

[1]The Center for Research on Inequality Reduction and Social Opportunity Advancement, Chiang Mai University, Chiang Mai Province, Thailand.
[2]Center of Radiation Research and Medical Imaging, Department of Radiologic Technology, Faculty of Associated Medical Sciences, Chiang Mai University, Chiang Mai Province, Thailand.
[3]Department of Occupational Therapy, Faculty of Associated Medical Sciences, Chiang Mai University, Chiang Mai Province, Thailand.
[4]Department of Educational Foundations and Development, Faculty of Education, Chiang Mai University, Chiang Mai Province, Thailand.

ARTICLE INFO

Article history:
Received 5 February 2024
Accepted as revised 13 March 2024
Available online 19 March 2024

Keywords:
X-ray absorptiometry, osteoporosis, bone mineral density

ABSTRACT

Background: We previously reported distal forearm bone mineral density (BMD) information for individuals residing in Mae Chaem and Omkoi districts, Chiang Mai Province, Thailand.

Objective: This study was aimed to observe distal forearm BMD in residents of Doi Lo District and compare this data with individuals residing in Mae Chaem District and Omkoi District in Chiang Mai Province, Thailand.

Materials and methods: Two hundred fifty-one subjects (215 women, 36 men), aged 24 to 69 years, currently reside in Doi Lo District. BMD was measured on the non-dominant distal forearm using peripheral dual-energy X-ray absorptiometry (pDEXA). Subsequently, data from Doi Lo District were compared with data from Mae Chaem District and Omkoi District obtained from earlier studies.

Results: Distal forearm BMD decreased, and the prevalence of osteoporosis increased in both females and males across age groups. This trend was consistent with data from Mae Chaem District and Omkoi District.

Conclusion: This study demonstrated the prevalence of distal forearm BMD and osteoporosis among females and males in Doi Lo District. The findings from Doi Lo District were consistent with those from Mae Chaem District and Omkoi District in Chiang Mai Province, Thailand. These results provide valuable insights into bone health among residents of Chiang Mai Province, Thailand.

Introduction

Osteoporosis is a common public health issue throughout the world because of its effects on mortality, morbidity, and the costs of medical care related to bone fractures. Osteoporosis is characterized by bone tissue structure deterioration, reduced bone mass, and increased skeletal fragility.[1,2] It has been reported that Europe has approximately 5.5 million males and 22 million females who have been diagnosed with osteoporosis as of 2010.[3]

The prevalence of osteoporosis among women aged greater than 50 years was approximately 5% to 68% in Asia and Africa. In addition, osteoporotic fractures occurred in approximately 17.4% of people residing in Southeast Asia.[4] Moreover, it is estimated that osteoporotic hip fractures occurring in Asia are the cause of 50% of all osteoporotic

∗ **Corresponding contributor.**
Author's Address: *The Center for Research on Inequality Reduction and Social Opportunity Advancement, Chiang Mai University, Chiang Mai Province, Thailand*
E-mail address: suchart.kothan@cmu.ac.th
doi: 10.12982/JAMS.2024.034
E-ISSN: 2539-6056

hip fractures in the world as of 2050.[5]

Osteoporosis is usually an undetected disease until the fracture occurs. The most frequent cause of bone fractures in the elderly occurs mostly in the spine, as well as in the proximal femur (hip) and distal forearm.[6] There are risk factors for osteoporosis such as weight, diet, physical activity, smoking, alcohol abuse, long-term use of certain medications such as glucocorticoids, and lifestyle, which are defined as a modifiable factor. In contrast, gender, age, and race are defined as non-modifiable factors.[7-9] Due to the many risk factors contributing to osteoporosis disease, a serious question is whether different habitation areas can impact BMD within the same province of a country. There have been several studies that have examined BMD among the Thai people who inhabit various provinces of Thailand.[10-14]

We have previously found the prevalence of osteoporosis and distribution of the distal forearm bone mineral density (BMD) in the people living in the Mae Chaem District and the Omkoi District of Chiang Mai Province, Thailand. The Mae Chaem and Omkoi Districts are about 108 and 179 km from Chiang Mai city. This study aimed to observe and compare the distal forearm BMD in the people who live in the Doi Lo District, the Mae Chaem District, and the Omkoi District of Chiang Mai Province, Thailand. Doi Lo District is closer to Chiang Mai city than Mae Chaem and Omkoi Districts.

The most widely used methods to assess BMD are based on X-ray absorptiometry in the bone, and dual energy X-ray absorptiometry (DEXA) is the most commonly used method.[15,16] In this study, the distal forearm BMD of the people who inhabit those three districts was measured by peripheral DEXA (pDEXA). Of note, BMD of the forearm was evaluated using pDEXA and showed strong positive correlation with BMD measured by central DEXA.[17]

Materials and methods

This was a retrospective study. General characteristic information and the distal forearm BMD data was obtained from the Community Services Project of Chiang Mai University in Doi Lo District, Chiang Mai Province, Thailand. BMD data for the distal forearm in Mae Chaem District and Omkoi District, Chiang Mai Province, Thailand, were collected from earlier reports.[18-20]

Subjects and general characteristic information

Two hundred and fifty subjects (214 female, 36 male), ranging from 26 to 69 years old who inhabit the Doi Lo District, Chiang Mai Province, Thailand were recruited through advertisements in the Doi Lo District area. The Doi Lo District is located about 50 km from Chiang Mai city. The general characteristics information (sex, age, height, and weight) was obtained by interviews before measuring the distal forearm BMD. The equation: BMI = kg/m^2 was used for calculating body mass index when BMI is body mass index, kg is kilogram for weight and m is meter for height. The subject's general characteristics information is summarized in Table 1.

Table 1. General characteristic information.

Female	Age groups (yrs)			
	26-39	40-49	50-59	60-69
Age (yrs)	32.28±5.49	45.13±2.87	53.81±2.66	62.33±2.50
Height (cm)	155.15±5.17	155.86±6.31	157.13±7.24	153.56±6.54
Weight (kg)	60.10±13.57	59.73±9.98	60.71±16.12	58.86±9.33
BMI (kg/m^2)	24.88±4.96	24.59±3.89	24.63±6.63	24.98±3.82
Male				
Age (yrs)	-	45.29±4.11	53.78±2.29	64.82±3.09
Height (cm)	-	154.86±3.89	158.11±7.01	159.18±7.64
Weight (kg)	-	60.29±10.32	62.39±13.28	61.82±10.49
BMI (kg/m^2)	-	25.27±5.00	24.86±4.48	24.22±2.12

Distal forearm BMD measurement

The distal forearm BMD was measured according to standard protocol by using peripheral dual energy X-ray absorptiometry (pDEXA) scan (EXA 3000; Osteosys Corp, Seoul, Korea). Briefly, the subjects were asked to remove all items such as wristwatches, bracelets, and rings etc. from the non-dominant distal forearm. The lateral position of the non-dominant distal forearm was positioned between the X-ray source and the detector of the pDEXA machine.

BMD test interpretation

The BMD data was analyzed according to World Health Organization (WHO) guidelines that indicate normal bone mass having a T-score ≥-1, low bone mass or osteopenia (T-score between -1 and -2.5), and osteoporosis (T-score≤ -2.5).[21,22]

Statistical analysis

The data was expressed as mean values±SD. The two sample t-test and linear correlation analysis were used

for comparing the means between the two groups and by performing a Pearson correlation, respectively using a Microsoft excel 2010 program for Windows and origin pro (Originlab Corporation). A $p<0.05$ was considered as statistically significant.

Results

The prevalence of osteoporosis was 6.54% and 13.89% for females (N=214) and for males (N=36), respectively. Table 2 shows the age-group distal forearm BMD and T-scores. For females, the BMD was the highest in the 40-49 year age-group and lowest in the 60-69 year age-group. The T-score at the distal forearm was also highest in the 40-49 year age-group and lowest in the 60-69 year age-group. Similarly, the highest BMD was in the 40-49 year age-group and the lowest was in the 60-69 year age-group for men. Also, the T-score at the distal forearm in men was highest in the 40-49 year age-group and lowest in the 60-69 year age-group.

Figure 1 shows the percentage of prevalence of osteopenia and osteoporosis for females and males, respectively. The percentage of osteopenia and osteoporosis increases as a function of age in while normal bone density decreases occurred in females, not in males.

Table 2. Distal forearm BMD and T-scores for different age-groups.

Age groups (yrs)	Female			Male		
	N	BMD (g/cm²)	T-score	N	BMD (g/cm²)	T-score
26-39	39	0.450±0.054	-0.451±0.901			
40-49	56	0.467±0.075	-0.174±1.242	7	0.532±0.044	-0.824±0.733
50-59	83	0.439±0.078^{I}	-0.639±1.295^{II}	18	0.520±0.070	-1.017±1.165
60-69	36	0.377±0.086^{I,II,III}	-1.664±1.425^{I,II,III}	11	0.486±0.064	-1.595±1.073

Note: *I: value was statistically significant difference from the 26-39 years group (p<0.05), II: value was statistically significant difference from the 40-49 years group (p<0.05), III: value was statistically significant difference from the 50-59 years group (p<0.05). Data are presented as average±sSD.*

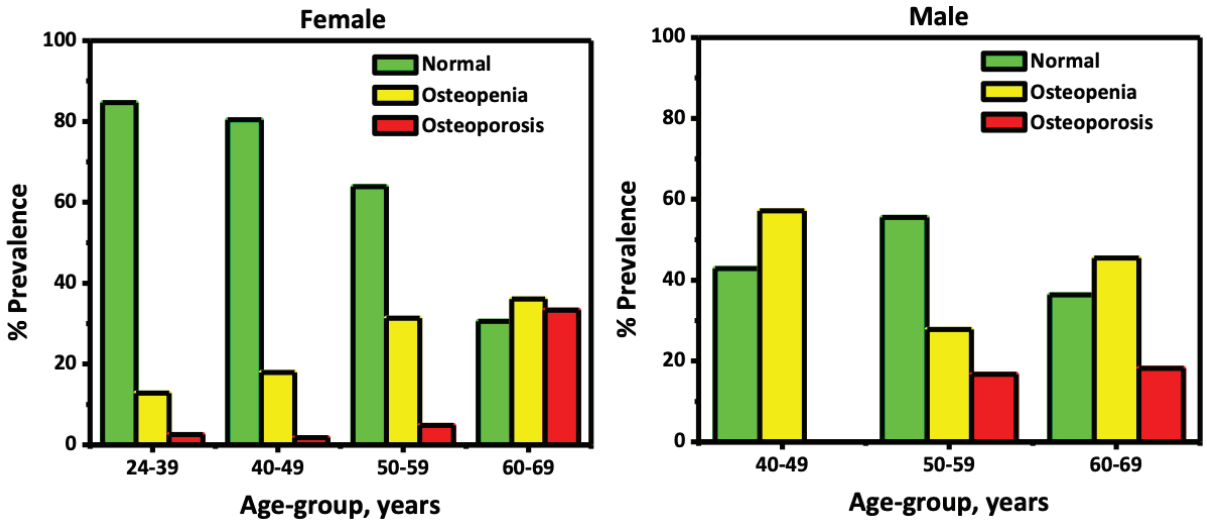

Figure 1. *The percentage of prevalence osteopenia and osteoporosis of females and males.*

Our data was compared to previously reports. Table 3 shows female distal forearm BMD and T-scores obtained from this current study and a study done by Thumvijit *et al*. 2022[19] and Sriburee *et al*. 2019.[18] The current study found incremental decreases in the distal forearm BMD and incrementally decreases took place in the T-scores when age-group increased. The current results were similar to the studies that were conducted by Thumvijit *et al*. 2022[19] and Sriburee *et al*. 2019.[18]

Table 3. Female distal forearm BMD and T-score.

Studies	24-39 (years)		40-49 (years)		50-59 (years)		60-69 (years)	
	BMD (g/cm²)	T-score	BMD (g/cm²)	T-score	BMD (g/cm²)	T-score	BMD (g/cm²)	T-score
Current study	0.450±0.054	-0.451±0.901	0.467±0.075	-0.174±1.242	0.439±0.078	-0.639±1.295	0.377±0.086	-1.664±1.425
Thumvijit *et al.*[19]	0.474±0.058	-0.036±0.959	0.469±0.063	-0.141±1.049	0.413±0.086	-1.099±1.496	0.328±0.091	-2.462±1.460
Sriburee *et al.*[18]			0.392±0.051	-1.414±0.853	0.337±0.063	-2.330±1.049	0.232±0.065	-4.091±1.069

Note: *Data is presented as average±SD.*

Table 4 shows male distal forearm BMD and T-scores from the current study and those of Sriburee *et al.* 2019[18] and Tungjai *et al.* 2017.[20] The current study was compared with a previous study. The current study found incremental decreases in distal forearm BMD and T-scores as age groups increased. The current results was similar to the studies that were conducted by Sriburee *et al*. 2019[18] and Tungjai *et al.* 2017.[20] These finding supported that distal forearm BMD deceased as a function of age in both females and males.

Table 4. Male distal forearm BMD and T-score.

Studies	40-49 (years)		50-59 (years)		60-69 (years)	
	BMD (g/cm²)	T-score	BMD (g/cm²)	T-score	BMD (g/cm²)	T-score
Current study	0.532±0.044	-0.824±0.733	0.520±0.070	-1.017±1.165	0.486±0.064	-1.595±1.073
Sriburee *et al.*[18]	0.530±0.065	-0.857±1.088	0.508±0.087	-1.212±1.448	0.461±0.098	-2.001±1.630
Tungjai *et al.*[20]	0.571±0.071	-0.013±1.163	0.560±0.075	-0.105±1.445	0.500±0.126	-1.411±1.509

Note: *Data is presented as average±SD.*

The female BMD distal forearm plotted against age, BMI, height, and weight are shown in Figure 2. The female BMD at the distal forearm was positively correlated to BMI and weight while being negatively correlated to age and height. However, age had strong impact (Pearson's r=-0.272) and height had weak impact (Pearson's r=-0.002) on female BMD distal forearm when compared with age, BMI, height, and weight factors.

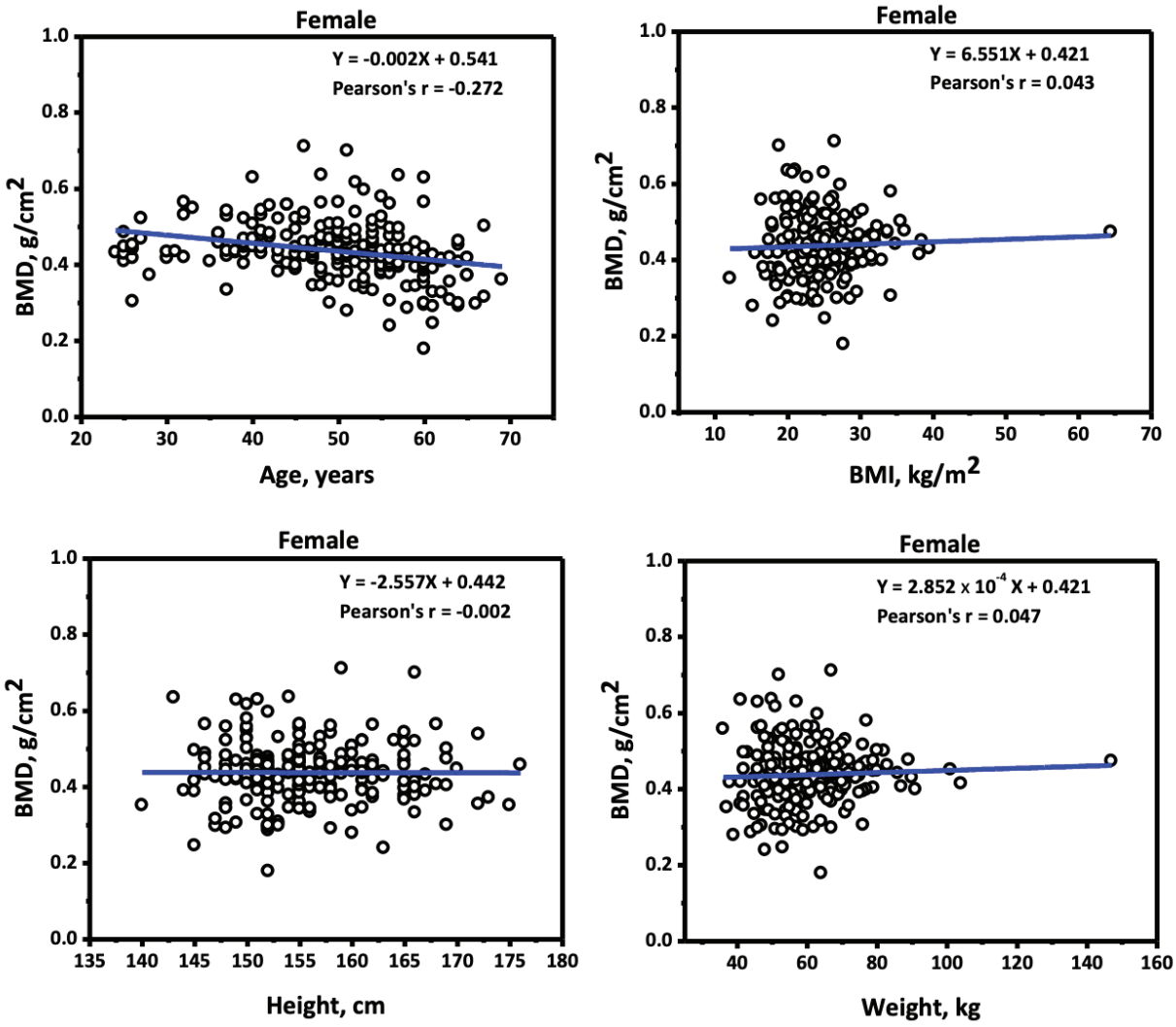

Figure 2. *Female BMD at distal forearm plotted against age, BMI, height, and weight.*

The male BMD distal forearm plotted against age, BMI, height, and weight are shown in Figure 3. The male BMD at distal forearm was positively correlated to BMI (Pearson's r=-0.075), weight (Pearson's r=0.122), and height (Pearson's r=0.120) while it was negatively correlated to age.

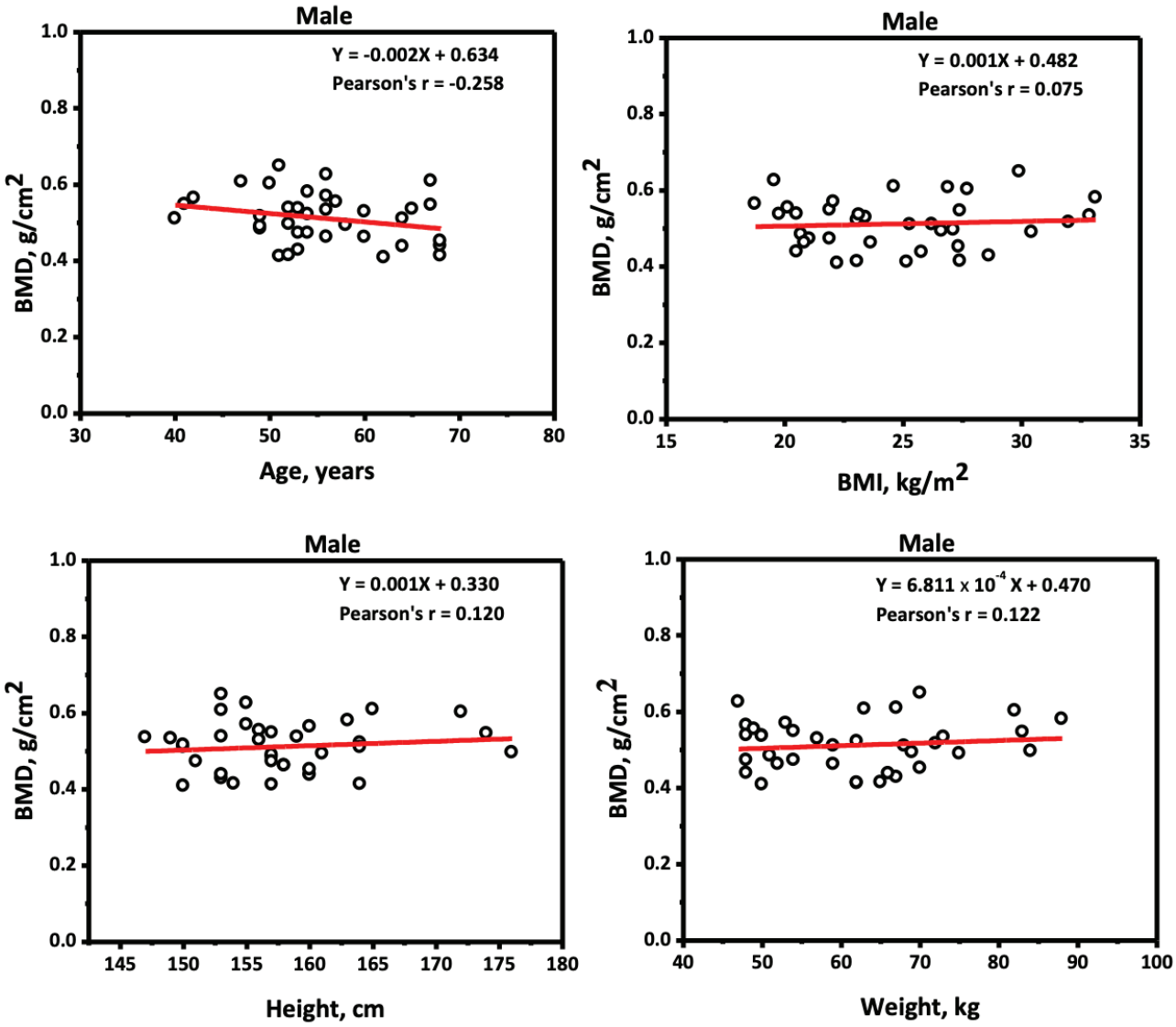

Figure 3. *Male BMD at distal forearm plotted against age, BMI, height, and weight.*

Table 5 shows the linear correlation analysis between distal forearm BMD with age, height, and weight in females and males using a current study and one done by Thumvijit *et al.* 2022,[19] Sriburee *et al.* 2019[18] and Tungjai *et a*l. 2017.[20] The current study was compared to that study. For females, the linear equation of correlation between distal forearm BMD and age were shown as having a negative slope in all studies. Similarly, all studies showed negative slope for linear equation of correlation between the distal forearm BMD and age in men. In contrast, the linear equation of correlation between distal forearm BMD and weight were shown to have a positive slope in all studies. In addition, the linear equation of correlation between the distal forearm BMD and height for males were shown to have a positive slope in the current study and the study done by Tungjai *et al* 2017.[20] These findings suggest that distal forearm BMD was negatively correlated with age and positively correlated with weight, in both females and males. Of note, the linear equation of correlation between the distal forearm BMD and height for females was negatively sloped in the current study whereas Thumvijit *et al*. 2022 showed a positive slope.[19]

Table 5. Linear correlation analysis between distal forearm BMD with age, height, and weight.

	Female			Male		
	Current study	**Thumvijit *et al*.[19]**	**Sriburee *et al*.[18]**	**Current study**	**Sriburee *et al*.[18]**	**Tungjai *et al*.[20]**
Distal forearm BMD (Y-axis) Age (X-axis)	Y=-0.002X +0.541	Y=-0.006X +0.718	Y=-0.006X +0.65	Y=-0.002X +0.634	Y=-0.004X +0.73	Y=-0.006X +0.850
Distal forearm BMD (Y-axis) Height (X-axis)	Y=-2.557X +0.442	Y=0.473X -0.339		Y=0.001X +0.330		Y=0.164X +0.235
Distal forearm BMD (Y-axis) Weight (X-axis)	Y=2.852X 10^{-4} X+0.421	Y=0.004X +0.164		Y=6.811X 10^{-4}X+0.470		Y=0.003X +0.340

Discussion

There are varying prevalences of osteoporosis found in different populations. For example, at the age of 50 years, female and male US Caucasians showed a prevalence of osteoporosis at 18% and 6%, respectively, while Denmark females and males had a prevalence of 41% and 18%, respectively. Moreover, Chinese females and males showed a 50.1% and 22% prevalence, respectively.[17] Of note, this information not only showed variations of prevalence but also showed that the prevalence of osteoporosis was higher in females than males. However, the prevalence of osteoporosis in Sri Lankan females was similar to males (5.8%).[17] In this study, the prevalence of osteoporosis was 6.54% and 13.89% for females and males, respectively. The data from this study seems to contrast with previous studies. This may be due to the fact that the number of samples used in this study for the male group (N=36) were very much less than the female group (N=214).

Moreover, the prevalencey of osteoporosis in populations having the same race and country also varied. Modagan P *et al.* 2018 showed that the prevalence of osteoporosis in a south Indian population at ages of 30-90 years was 24.7%. It was found to be 9.7%, and 15% for males and females, respectively.[23] Similarly, Marwaha, RK *et al*. 2011 showed that the prevalence of osteoporosis in an Indian population aged at 50 years and above who inhabited Delhi was 35.1%. It was 24.6% and 42.5% for males and females, respectively.[17] Moreover, Kaushal N *et al*. 2018 reported that the prevalence of osteoporosis in an Indian population at ages of 20-85 was 6.9%. It was 3.9% for males and 11.1% for females.[24] Of note, the population in those reports had the same race being all an Indian population who hailed from the same country of India.

In this study, we observed the prevalence of osteoporosis and BMD in the Doi Lo District. We also compared the data from Doi Lo District with data obtained from Mae Chaem and Omkoi Districts which are located in the same province of Chiang Mai, Thailand. For the female group, T-scores from Doi Lo district population at 40-49 (years) was similar to Mae Chaem[19] and Omkoi Districts[18] whereas T-scores from Doi Lo District population at 50-59 years and 60-69 years were higher than Mae Chaem[19] and Omkoi Districts.[18] For the male group, T-scores from the Doi Lo District population was less than in Mae Chaem[19] but were higher than the Omkoi District for all age-groups.[18] It should be noted that even though those three districts are located in the same province (Chiang Mai) and country (Thailand), the people who live in each of these districts have different lifestyles and cultures. However, these findings show that distal forearm BMD decreased as a function of age and increased as a function of weight in both females and males who inhabited Doi Lo, Mae Chaem, and Omkoi Districts.

A notable strength in this study is that comparisons were made from three districts (Doi Lo, Mae Chaem, and Omkoi) which are all located in the same province (Chiang Mai), Thailand. This study was supported the notion that lifestyle and culture both contribute to BMD and the prevalence of osteoporosis. However, a limitation of this present study was that the number of our subjects were rather small.

Declaration of conflicting interests

The authors declared no potential conflicts of interest.

Data availability statement

The data are not publicly available due to privacy or ethical restrictions.

Ethics approval

The study was approved by the local institutional review board and was conducted following the Declaration of Helsinki.

Acknowledgements

This research was partially supported by Chiang Mai University. We are thankful to the local government of Doi Lo District, Chiang Mai Province, Thailand for supporting and facilitating this research. We would also like to thank Associate Professor Utumma Maghanemi and Associate Professor Dr. Kwanchai Ratanasthien who kindly supported and participated in this study.

References

[1] Leslie WD, Morin SN. Osteoporosis epidemiology 2013: implications for diagnosis, risk assessment, and treatment. Curr Opin Rheumatol. 2014; 26(4): 440-6. doi: 10.1097/BOR.0000000000000064.

[2] Mauck KF, Clarke BL. Diagnosis, screening, prevention, and treatment of osteoporosis. Mayo Clin Proc.

2006; 81(5): 662-72. doi: 10.4065/81.5.662.

[3] Svedbom A, Hernlund E, Ivergård M, Compston J, Cooper C, Stenmark J, *et al*. Osteoporosis in the European Union: a compendium of country-specific reports. Arch Osteoporos. 2013; 8(1): 137. doi: 10.1007/s11657-013-0137-0.

[4] Bala S, Prabha MLS, Krishna TP. Prevalence and risk factors of low bone mineral density with quantitative ultrasonography among south Indian postmenopausal women. Int J Community Med Public Health. 2016; 3(7): 1735-40. doi: 10.18203/2394-6040.ijcmph20162034.

[5] Johnell O, Kanis JA. An estimate of the worldwide prevalence, mortality and disability associated with hip fracture. Osteoporos Int. 2004; 15(11): 897-902. doi: 10.1007/s00198-004-1627-0.

[6] Sözen T, Özışık L, Başaran N. An overview and management of osteoporosis. Eur J Rheumatol. 2017; 4(1): 46-56. doi: 10.5152/eurjrheum.2016.048.

[7] Askari M, Lotfi Mh, Owlia Mb, Fallahzadeh H, Mohammadi M. Survey of Osteoporosis Risk Factors (Review Article). J Sabzevar Univ Med Sci. 2019; 25(6): 854-63.

[8] Faisal-Cury A, Zacchello KP. Osteoporose: prevalência e fatores de risco em mulheres de clínica privada maiores de 49 anos de idade. Acta Ortop Bra. 2007; 15. doi: 10.1590/S1413-78522007000300005.

[9] Akkawi I, Zmerly H. Osteoporosis: Current Concepts Joints. 2018; 6(2): 122-7. doi: 10.1055/s-0038-1660790.

[10] Iwasaki E, Morakote N, Chaovistsaree S, Matsuo H. Bone mineral density and bone turnover among young women in Chiang Mai, Thailand. Kobe J Med Sci. 2014; 59(5): E149-56. doi

[11] Malairungsakul O, Wiwatanadate P. Factors related to osteoporosis of postmenopausal women in Phayao, Thailand. Arch Osteoporos. 2013; 8: 154. doi: 10.1007/s11657-013-0154-z.

[12] Namwongprom S, Ekmahachai M, Vilasdechanon N, Klaipetch A, Wongboontan C, Boonyaprapa S. Bone mineral density: correlation between the lumbar spine, proximal femur and Radius in northern Thai women. J Med Assoc Thai. 2011; 94(6): 725-31.

[13] Pongchaiyakul C, Nguyen TV, Kosulwat V, Rojroongwasinkul N, Charoenkiatkul S, Rajatanavin R. Effect of urbanization on bone mineral density: a Thai epidemiological study. BMC Musculoskelet Disord. 2005; 6 : 5. doi: 10.1186/1471-2474-6-5.

[14] Sritara C, Thakkinstian A, Ongphiphadhanakul B, Pornsuriyasak P, Warodomwichit D, Akrawichien T, *et al*. Work- and travel-related physical activity and alcohol consumption: relationship with bone mineral density and calcaneal quantitative ultrasonometry. J Clin Densitom. 2015; 18(1): 37-43. doi: 10.1016/j.jocd.2014.04.117.

[15] Kanis JA, Cooper C, Rizzoli R, Reginster JY. European guidance for the diagnosis and management of osteoporosis in postmenopausal women. Osteoporos Int. 2019; 30(1): 3-44. doi: 10.1007/s00198-018-4704-5.

[16] Beck TJ, Ruff CB, Warden KE, Scott WW, Jr., Rao GU. Predicting femoral neck strength from bone mineral data. A structural approach. Invest Radiol. 1990; 25(1): 6-18. doi: 10.1097/00004424-199001000-00004.

[17] Marwaha RK, Tandon N, Garg MK, Kanwar R, Narang A, Sastry A, *et al*. Bone health in healthy Indian population aged 50 years and above. Osteoporos Int. 2011; 22(11): 2829-36. doi: 10.1007/s00198-010-1507-8.

[18] Sriburee S, Tungjai M, Padngam S, Thumvijit T, Hongsriti P, Tapanya M, *et al*. Distal Forearm Bone Mineral Density Among Hill Tribes in the Omkoi District, Chiang Mai Province, Thailand. Open Public Health J 2019; 12: 1-6. doi: 10.2174/1874944501912010001.

[19] Thumvijit T, Sriburee S, Padngam S, Tungjai M, Kothan S. Bone Mineral Density at Distal Forearm in Women in Mae Chaem District, Chiang Mai Province, Thailand: A Cross-Sectional Study. Open Public Health J. 2022; 15: 1-8. doi: 18749445-v15-e2207150.

[20] Tungjai M, Kaewjaeng S, Jumpee C, Sriburee S, Hongsriti P, Tapanya M, *et al*. Bone mineral density at distal forearm in men over 40 years of age in Mae Chaem district, Chiang Mai Province, Thailand: a pilot study. Aging Male. 2017; 20(3): 170-4. doi: 10.1080/13685538.2017.1322058.

[21] Cosman F, de Beur SJ, LeBoff MS, Lewiecki EM, Tanner B, Randall S, *et al*. Clinician's Guide to Prevention and Treatment of Osteoporosis. Osteoporos Int. 2014; 25(10): 2359-81. doi: 10.1007/s00198-014-2794-2.

[22] Humadi A, Alhadithi RH, Alkudiari SI. Validity of the DEXA diagnosis of involutional osteoporosis in patients with femoral neck fractures. Indian J Orthop. 2010; 44(1): 73-8. doi: 10.4103/0019-5413.58609.

[23] Parandaman M, Silambanan S, Menon P, Arunalatha P. Comparison of Bone Mineral Density with Biochemical Parameters and Prevalence of Osteopenia and Osteoporosis in South Indian Population. Biomed Pharmacol J. 2018; 11: 2209-14. doi: 10.13005/bpj/1603.

[24] Kaushal N, Vohora D, Jalali RK, Jha S. Prevalence of osteoporosis and osteopenia in an apparently healthy Indian population - a cross-sectional retrospective study. Osteoporos Sarcopenia. 2018; 4(2): 53-60. doi: 10.1016/j.afos.2018.04.002.

Journal of Associated Medical Sciences 2024; 57(2): 132-140

JAMS
Journal of Associated Medical Sciences

Scopus Indexed & Thai-Journal Citation Index Centre (TCI)

Journal of Associated Medical Sciences

Journal homepage: https://www.tci-thaijo.org/index.php/bulletinAMS/index

A comparative study of pre-processing methods to improve glioma segmentation performance in brain MRI using deep learning

Kasatapad Naknaem[1] Titipong Kaewlek[1,2,3*]

[1]Medical Physics Program, Department of Radiological Technology, Faculty of Allied Health Sciences, Naresuan University, Phitsanulok Province, Thailand.
[2]Department of Radiological Technology, Faculty of Allied Health Sciences, Naresuan University, Phitsanulok Province, Thailand.
[3]Interdisciplinary Health and Data Sciences Research Unit, Faculty of Allied Health Sciences, Naresuan University, Phitsanulok Province, Thailand.

ARTICLE INFO

Article history:
Received 17 February 2024
Accepted as revised 17 March 2024
Available online 19 March 2024

Keywords:
Glioma, image segmentation, image enhancement, deep learning, U-net architecture.

ABSTRACT

Background: Glioma is the most common brain tumor in adult patients and requires accurate treatment. The delineation of tumor boundaries must be accurate and precise, which is crucial for treatment planning. Currently, delineating boundaries for tumors is a tedious, time-consuming task and may be prone to human error among oncologists. Therefore, artificial intelligence plays a vital role in reducing these problems.

Objective: This study aims to find a relationship between improving image enhancement and evaluating the performance of deep learning models for segmenting glioma image data on brain MRI images.

Materials and methods: The BraTs2023 dataset was used in this study. The image dataset was converted from three dimensions to two dimensions and then subjected to pre-processing via four image enhancement techniques, including contrast-limited adaptive histogram equalization (CLAHE), gamma correction (GC), non-local mean filter (NLMF), and median and Wiener filter (MWF). Subsequently, it was evaluated for structural similarity index (SSIM) and mean squared error. The deep learning segmentation model was created using the U-Net architecture and assessed for dice similarity coefficient (DSC), accuracy, precision, recall, F1-score, and Jaccard index for tumor segmentation.

Results: The performance of enhanced image results for CLAHE, GC, NLMF, and MWF techniques shows SSIM values of 0.912, 0.905, 0.999, and 0.911, respectively. The dice similarity coefficient (DSC) for segmentation without image enhancement was 0.817. The DSC of segmentation for CLAHE, GC, NLMF, and MWF techniques were 0.818, 0.812, 0.820, and 0.797, respectively.

Conclusion: The enhanced image technique could affect the performance of tumor segmentation. by the enhanced image for use in a trained model may increase or decrease performance depending on the chosen image enhancement technique and the parameters determined by each method.

Introduction

Glioma is the most frequent primary central nervous system cancer in adults, exhibiting extreme intrinsic heterogeneity in appearance, shape, and histology. Gliomas can be classified into high-grade glioma (HGG) and low-grade glioma (LGG). The prognosis of gliomas depends on the grade and genomic profile. HGG is a tumor that shows a severe clinical prognosis and rapid invasion, with a median survival rate of two years or less. It differs from low-grade glioma in that it has a worse prognosis and is more invasive

∗ **Corresponding contributor.**
Author's Address: *Medical Physics Program, Department of Radiological Technology, Faculty of Allied Health Sciences, Naresuan University, Phitsanulok Province, Thailand.*
E-mail address: titipongk@nu.ac.th
doi: 10.12982/JAMS.2024.035
E-ISSN: 2539-6056

or noninvasive.[1,2] Whether HGG or LGG, there is a similarity in the tumor volume, including the whole tumor, tumor core, and active tumor region. As a result, many different types of MR imaging exist because the T1-weighted MRI image can't clearly define the tumor boundary. Therefore, other types of MR imaging, such as T1-contrast, T2-weighted, and T2-FLAIR, are used to indicate the three tumor regions mentioned clearly. Accurate identification of brain tumor sub-regions boundaries in MRI is of profound importance in many clinical applications, such as tumor detection, treatment planning, image-guided procedures, and monitoring tumor growth. However, manual tumor detection and delineation are tedious, time-consuming, and depend on the experience of the oncologist. This may cause human error while delineating the boundaries of the tumor, including disruption of work when dealing with many patients.[3] For the above reasons, automatic tumor boundaries delineation is necessary to reduce the problems mentioned.

The science of deep learning has been used to develop knowledge. Deep learning is a part of the science of artificial intelligence. Since deep learning is more flexible than machine learning, it can automatically find features within image data. For this reason, deep learning is popular in medical image segmentation. Nevertheless, Lin M *et al*. 4's research found a Dice Similarity Coefficient (DSC) of 0.887. The study of Franziska Knuth *et al*.[5] found a DSC of 0.770, and the research of Zhao C *et al*.[6] found a DSC of 0.774. The results depend on various factors, including the architecture used, specific details related to deep learning modeling, and the image quality used to train the deep learning model. The research of Güneş AM *et al*.[7] shows that image quality affects the quality of the segmentation model. When the dataset has increased noise and artifacts during the training of a large dataset, the model's performance increases, which shouldn't be the case. Therefore, the researcher is interested in studying the comparison of pre-processing methods to improve the performance of image segmentation of glioma on brain MRI images using deep learning. The objective is to find a relationship between improving image enhancement and the performance of deep learning models and to develop a deep learning model for segmenting glioma image data on brain MRI images.

Materials and methods

This study conducted a comparative analysis of pre-processing methods aimed at enhancing glioma segmentation performance in brain MRI using deep learning. It consists of two main parts: the first part compares the effectiveness of various pre-processing methods, while the second part assesses the performance of the deep learning model, as shown in Figure 1. Initially, the input image dataset is fed into the program, followed by image pre-processing, which involves converting 3D images to 2D grayscale images and resizing them to 128x128 pixels. Subsequently, the image dataset undergoes enhancement techniques and is evaluated using metrics such as the Structural Similarity Index and the Mean Squared Error. The enhanced dataset is then utilized to train and test the deep learning model. Finally, the model's performance is evaluated using metrics including the Dice similarity coefficient, F1 score, Jaccard similarity coefficient, recall, precision, and accuracy. The result is a predicted mask. The study's detailed aspects include patient data preparation, pre-processing techniques, tumor segmentation architecture, model training, and statistical analysis.

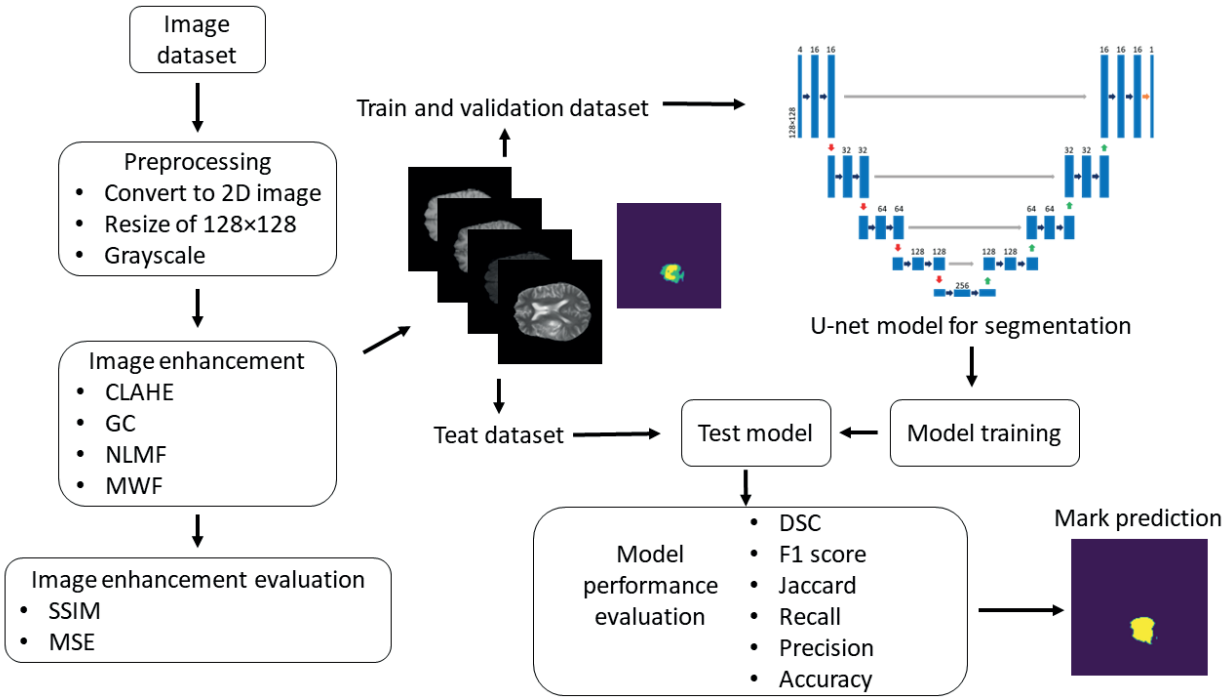

Figure 1 *Workflows of image enhancement and model.*

Patient data preparing

The MR images used in this study were collected from a public dataset, the Brain Tumor Segmentation (BraTS) Challenge 2023 dataset.[1,3,8] The dataset comprises T1, post-contrast T1-weighted (T1Gd), T2-weighted, and T2 Fluid Attenuated Inversion Recovery (T2-FLAIR) MR images of 1,470 brain glioma patients. The volume of 3D MR images is 240×240×155 pixels, and the image voxel size is 1.0 mm^3. The ground truth includes the GD-enhancing tumor region, the peritumoral edematous or invaded tissue region, and the necrotic tumor core region. Experienced neuroradiologists approved these annotations.

Pre-processing technique

The 3D image files in nii.gz format are converted to 2D image files with the png extension. This process involves selecting only the axial MRI images from all four types of MRI images, with the condition that a mask must be present and the extent of the tumor is more than 1% compared to all the data within the mask. The result yields 54,031 axial images for each type. Subsequently, 5,000 images are randomly selected, and the image and mask data are transformed into numpy arrays (npy file extension). Additionally, the images are resized and converted to grayscale, resulting in image and mask data with dimensions of 128×128×1.

This study applies four image enhancement techniques, including contrast-limited adaptive histogram equalization, gamma correction, non-local mean filter, and median and Wiener filter, to enhance the details of all images. Each technique is explained in detail as follows:

Contrast-Limited Adaptive Histogram Equalization (CLAHE)

CLAHE is a technique for reducing noise and over-enhancement by dividing the image into sub-images or tiles. Each tile expands the image intensity range by adjusting the difference in intensity of objects within the image to be similar and limits the height of the histogram by setting a level to eliminate the histogram (clip limit). This distributes the signal exceeding the limit to other parts of the histogram without exceeding the limit.[9,10] This study set the parameters as follows: the clip limit (cl) values and tile sizes (ts) are (0.1, 8×8), (0.2, 2×2), (0.2, 6×6), (0.2, 8×8), and (0.3, 6×6), respectively.

Gamma Correction (GC)

GC is a technique for image processing that adjusts the gamma value according to the characteristics of the image to suit its brightness and contrast.[11,12] Gamma correction is given by the following equation (1). When, the enhanced image will be brighter than the original image, and when, the enhanced image will be darker than the original image. The disadvantage of gamma correction is that it involves an unvaried modification due to a predefined value.[13] This study set the parameters as follows: the gamma values (g) are 0.7, 1.3, 1.5, 1.7, and 1.9, respectively.

$$T(I) = I_{max}\left(\frac{I}{I_{max}}\right)^{\gamma} \quad (1)$$

Where I_{max} is maximum pixel intensity, is pixel intensity, and is gamma correction.

Non-local mean filter

NLMF is an algorithm that filters out noise from images while maintaining the sharpness of the edges of objects within the image. It also adjusts areas within the image to be smoother. NLMF calculates the average of all pixels within the image by considering the similarity between pixels. The resulting averaging eliminates noise and gives the pixels of the image similar values.[14,15] This study set the parameters as follows: set the smoothing kernel value (s), patch size (p), and window size (w) to (1, 6, 20), (1, 7, 15), (1, 7, 20), (2, 2, 20), and (2, 8, 15), respectively.

Median and Wiener filter (MWF)

The Median filter is a filter used to remove noise from images, especially salt and pepper noise. The Median Filter works by taking the pixel values around the position of the pixel of interest, arranging them from least to greatest, and selecting the median value to use. Next, the data is processed through WF to reduce noise and improve signal quality by trying to make the mean square error between the original image and the enhanced image as low as possible.[16] This study set the parameters as follows: set the kernel sizes (k) to 3×3, 5×5, 7×7, 9×9, and 11×11, respectively.

In the final step, all four types (CLAHE, GC, NLMF, and MWF) of MRI images are combined to create a new dataset with a size of 128×128×4. Subsequently, the combined dataset is divided into 4,000 training sets and 1,000 validation sets out of the 5,000 sets of image and mask data. Additionally, 1,000 data sets are randomly selected to create a test set. In each set, the data will include a mask or the boundary of the tumor based on the number of data sets. Therefore, a total of five data sets will be obtained for training the model, comprising a dataset with no image enhancement, a dataset enhanced with the CLAHE technique, a dataset enhanced with the GC technique, a dataset enhanced with the NLMF technique, and a dataset enhanced with the MWF technique.

Tumor segmentation architecture

The U-Net architecture was employed to segment the tumor from the brain tissue area in the brain MRI images. The details of the U-Net for this proposed adaptation were derived from Ronneberger *et al*.,[17] and the structure consists of an encoder path, decoder path, and connecting path. These three paths follow the typical architecture of a conventional network. The encoder path comprises two 3×3 convolutions, with each layer followed by a rectified linear unit (ReLU) and a 2×2 max-pooling operation with two strides for downsampling. With each downsampling step, the number of feature channels increases twofold. On the other hand, the decoder path consists of two 3×3

convolutions, with each layer followed by ReLU and 2×2 up-convolutions for upsampling. With each upsampling step, the number of feature channels decreases twofold. The decoder path is concatenated with the encoder path through the connecting path, linking to the corresponding feature map from the encoder path. Finally, the last layer consists of a 1×1 convolution, utilizing a sigmoid activation function for the final output, as shown in Figure 2.

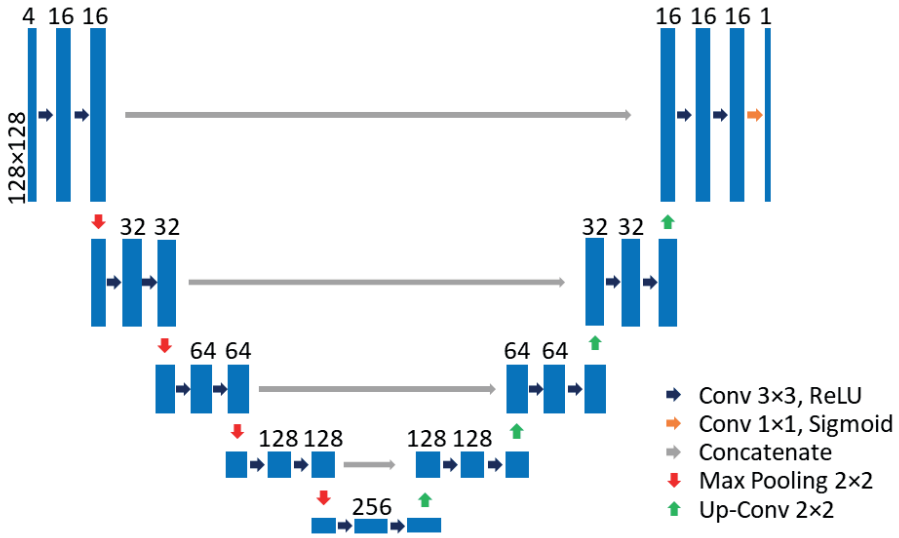

Figure 2 *U-Net architecture of this study.*

Model training

The training used Tensorflow version 2.13 as the backend in Python version 3.10.9, utilizing an NVIDIA GeForce RTX 3050 Laptop GPU. The image segmentation model was trained to employ the Adam optimizer, a learning rate set at 0.001 with a lower bound on the learning rate of 0.0000001, a Dice Similarity Coefficient (DSC) loss function, and a batch size of 32 for 100 epochs. Initially, the model underwent training with a combination image dataset without image enhancement. Throughout the training process, the model was validated using a validation dataset to estimate errors in the training. The early stopping technique was employed to mitigate the overfitting problem. Upon completing the training of the model with the combination image dataset without image enhancement, the dataset was modified to a combination image dataset with image enhancement using four techniques (CLAHE, GC, NLMF, and MWF).

Statistical analysis

The statistical analysis is divided into image enhancement and segmentation model performance.

For image enhancement, evaluation involves using the structural similarity index (SSIM) and mean squared error (MSE). SSIM serves as a metric (luminance, contrast, and structure) to measure the similarity between two given images. At the same time, MSE is employed to compare the true pixel values of the original image to the degraded image. The equations for SSIM and MSE are provided in (2)-(3).

$$SSIM = i(x,y) \times c(x,y) \times s(x,y) \quad (2)$$

Where i is the luminance similarity index, c is the contrast similarity index, s is the structure similarity index, x is the original image, and y is the enhanced image.

$$SSIM = \frac{1}{mn} \sum_0^{m-1} \sum_0^{n-1} | |f(i,j)-g(i,j)| |^2 \quad (3)$$

Where f is the original pixel image, g is the enhanced pixel image, m is the row number of image, n is the column number of image, i is the row index, and j is the column index.

The model performance is assessed through the confusion matrix, which consists of values such as the dice similarity coefficient (DSC), Jaccard similarity coefficient, accuracy, precision, sensitivity (recall), and F1-score. The evaluation values for model performance are presented in equations (4)-(9).

$$DSC = \frac{2|A \cap B|}{|A| + |B|} \quad (4)$$

$$Jaccard = \frac{|A \cap B|}{|A| + |B| - |A \cap B|} \quad (5)$$

Where A and B are datasets A and B, and $A \cap B$ is the intersection part of the two datasets.

$$Accuracy = \frac{TP + TN}{TP+TN+FP+FN} \quad (6)$$

$$Precision = \frac{TP}{TP + FP} \quad (7)$$

$$Recall = \frac{TP}{TP + FN} \quad (8)$$

$$F1\ score = \frac{2 \times precision \times recall}{precision \times recall} \quad (9)$$

Where True Positives (TP) is the model predicting a tumor boundary when it is a tumor boundary, True Negatives (TN) is the model correctly predicting it not to be a tumor boundary, False Positive (FP) is the model predicting a tumor boundary when it is not a tumor boundary, and False Negative (FN) is the model predicting something different than the tumor boundary.

Results

Evaluation of image enhancement

Table 1 shows the results of the evaluation parameters for each image enhancement. NLMF exhibits the highest SSIM compared to other techniques, followed by GC, MWF, and CLAHE, respectively. Regarding the MSE value, NLMF has the lowest MSE compared to other techniques, followed by CLAHE, GC, and MWF, respectively.

Table 1 Results of the image enhancement techniques.

Technique	Parameter	T1		T1c		T2		T2f	
		SSIM	MSE	SSIM	MSE	SSIM	MSE	SSIM	MSE
CLAHE No.1	cl= 0.1, ts=8	0.721	395.03	0.695	288.53	0.701	314.16	0.703	460.31
CLAHE No.2	cl=0.2, t=2	0.914	6.013	0.91	11.64	0.912	7.358	0.912	8.381
CLAHE No.3	cl=0.2, ts=6	0.743	108.31	0.721	156.38	0.732	92.08	0.735	113.68
CLAHE No.4	cl=0.2, ts=8	0.721	395.03	0.695	288.53	0.701	314.16	0.703	460.31
CLAHE No.5	cl=0.3, ts=6	0.743	108.31	0.721	156.38	0.732	92.08	0.735	113.68
GC No.1	g=0.7	0.923	1231.2	0.895	2388.57	0.896	2260.82	0.905	1834.04
GC No.2	g=1.3	0.956	684.21	0.938	1311.27	0.94	1241.86	0.945	1012.54
GC No.3	g=1.5	0.959	624.8	0.938	1167.96	0.94	1107.54	0.947	912.38
GC No.4	g=1.8	0.957	601.61	0.929	1045.05	0.933	995.04	0.943	845.03
GC No.5	g=1.9	0.956	607.09	0.924	1020.6	0.929	973.67	0.94	838.26
NLMF No.1	s=1, p=6, w=20	0.999	0.007	0.999	0.015	0.999	0.006	0.999	0.001
NLMF No.2	s=1, p=7, w=15	0.999	0.006	0.999	0.014	0.999	0.001	0.999	0.006
NLMF No.3	s=1, p=7, w=20	0.999	0.007	0.999	0.015	0.999	0.006	0.999	0.001
NLMF No.4	s=2, p=2, w=20	0.999	0.015	0.998	0.212	0.999	0.169	0.999	0.116
NLMF No.5	s=2, p=8, w=15	0.999	0.061	0.999	0.114	0.999	0.023	0.999	0.059
MWF No.1	k = 3	0.957	1080.54	0.836	4242.03	0.912	1376.93	0.939	1021.88
MWF No.2	k = 5	0.95	1105.33	0.834	4340.87	0.906	1474.32	0.929	1057.57
MWF No.3	k = 7	0.942	1132.57	0.832	4425.22	0.897	1572.39	0.919	1092.08
MWF No.4	k = 9	0.932	1160.39	0.829	4497.25	0.888	1668.26	0.908	1125.35
MWF No.5	k = 11	0.922	1188.02	0.825	4560.84	0.878	1760.5	0.898	1157.18

Evaluation of model performance for segmentation

Figure 3 shows the learning curves of the model during training with a dataset, with and without the image enhancement process. We can observe that all models don't exhibit a gap between training and validation loss; as a result, none of the models suffer from overfitting or underfitting problems.

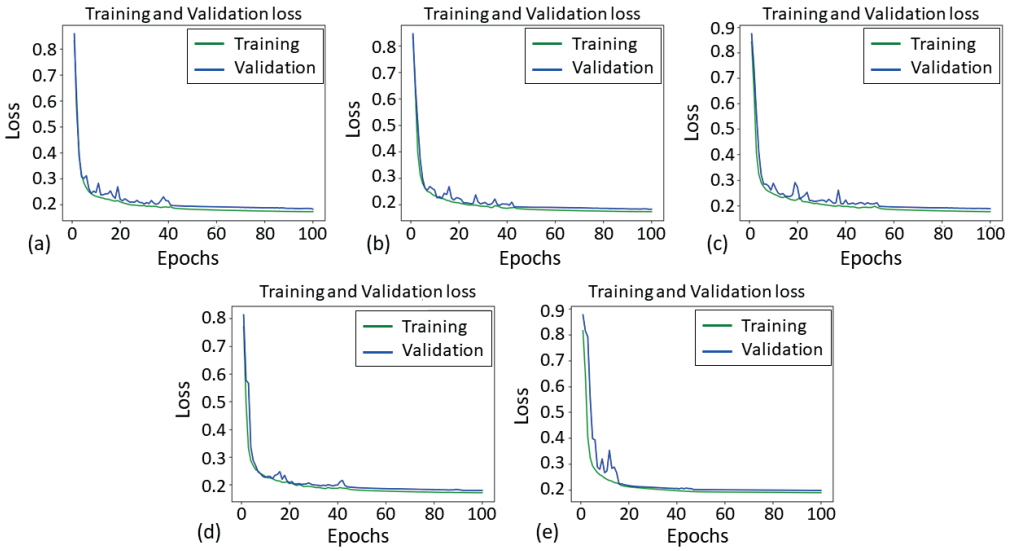

Figure 3 *Loss curve of training and validation set. a: standard MRI image dataset without image enhancement, b-e: MRI image dataset with image enhancement (CLAHE, GC, NLMF, and MWF, respectively).*

Table 2 presents the results of the evaluation parameters for various models. A trained model with original MRI images has a DSC of 0.8171 compared to a trained model with MRI images via image enhancement techniques. We can observe that CLAHE and NLMF techniques can increase the DSC value, while GC and MWF techniques decrease the DSC value. Specifically, CLAHE, NLMF, GC, and MWF have a maximum DSC of 0.818, 0.820, 0.812, and 0.797, respectively, in this study.

Table 2 The performance of tumor segmentation in various models.

Technique	Parameter	DSC	F1	Jaccard	Recall	Precision	Accuracy
Normal	-	0.817	0.892	0.815	0.943	0.860	0.994
CLAHE No.1	cl=0.1, ts=8	0.817	0.896	0.820	0.943	0.865	0.994
CLAHE No.2	cl=0.2, ts=2	0.818	0.895	0.818	0.940	0.866	0.994
CLAHE No.3	cl=0.2, ts=6	0.811	0.884	0.801	0.926	0.858	0.994
CLAHE No.4	cl=0.2, ts=8	0.814	0.888	0.806	0.938	0.854	0.994
CLAHE No.5	cl=0.3, ts=6	0.812	0.886	0.805	0.931	0.858	0.994
GC No.1	g=0.7	0.812	0.885	0.801	0.922	0.861	0.994
GC No.2	g=1.3	0.811	0.890	0.809	0.930	0.863	0.994
GC No.3	g=1.5	0.808	0.878	0.792	0.923	0.851	0.993
GC No.4	g=1.8	0.803	0.872	0.782	0.917	0.844	0.993
GC No.5	g=1.9	0.802	0.870	0.780	0.917	0.843	0.993
NLMF No.1	s= 1, p=6, w=20	0.819	0.899	0.824	0.942	0.870	0.994
NLMF No.2	s=1, p=7, w=15	0.819	0.895	0.818	0.950	0.856	0.994
NLMF No.3	s=1, p=7, w=20	0.820	0.900	0.826	0.946	0.869	0.994
NLMF No.4	s=2, p=2, w=20	0.819	0.898	0.823	0.940	0.870	0.994
NLMF No.5	s=2, =8, w=15	0.820	0.900	0.827	0.948	0.867	0.994
MWF No.1	k=3	0.797	0.866	0.774	0.900	0.851	0.993
MWF No.2	k=5	0.792	0.859	0.763	0.893	0.842	0.992
MWF No.3	k=7	0.781	0.846	0.744	0.880	0.831	0.992
MWF No.4	k=9	0.789	0.855	0.755	0.892	0.833	0.992
MWF No.5	k=11	0.761	0.816	0.702	0.854	0.800	0.990

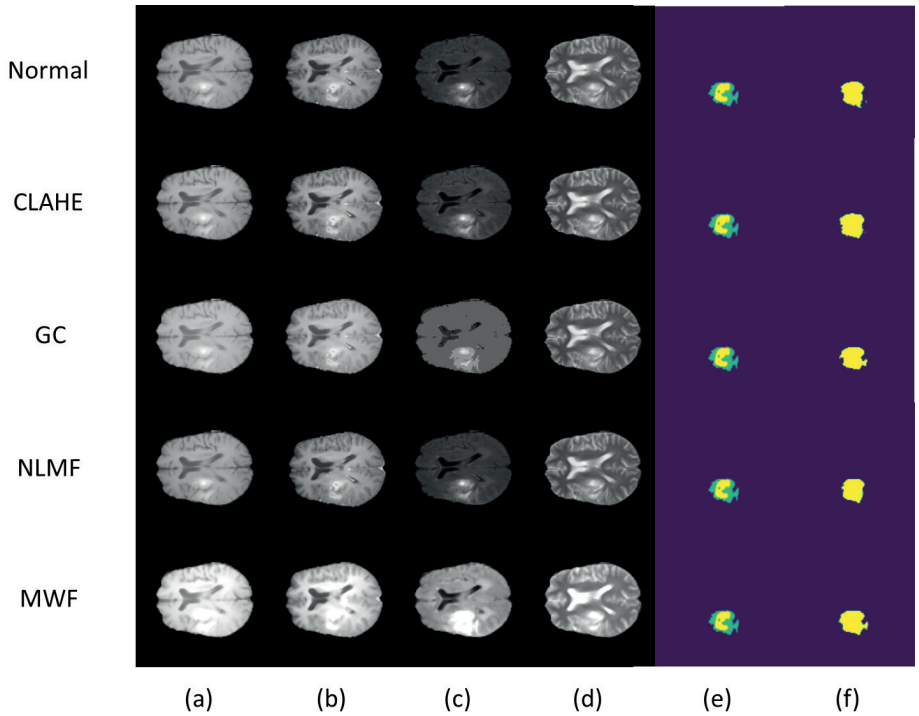

Figure 4 *Image of image enhancement and mark prediction from the model. A: T1-weighted, b: post-contrast T1, c: T2-weighted, d: T2-FLAIR, e: gound truth or mask, e: mask prediction.*

Table 3 compares each image enhancement technique's DSC and average SSIM values.

Table 3 Comparative of DSC and average SSIM values.

Technique	Parameter	DSC	Average SSIM
CLAHE No.1	cl=0.1, ts=8	0.817	0.705
CLAHE No.2	cl=0.2, ts=2	0.818	0.912
CLAHE No.3	cl=0.2, ts=6	0.811	0.733
GC No.1	g=0.7	0.812	0.905
GC No.2	g=1.3	0.811	0.945
GC No.3	g=1.5	0.808	0.946
NLMF No.1	s=1, p=6, w=20	0.819	0.999
NLMF No.2	s=1, p=7, w=15	0.819	0.999
NLMF No.5	s=2, p=8, w=15	0.820	0.999
MWF No.1	k=3	0.797	0.911
MWF No.4	k=9	0.789	0.889
MWF No.5	k=11	0.761	0.881

Discussion

This study examines the relationship between image enhancement and the performance of deep learning models, comparing the results of enhancement techniques to increase the efficiency of glioma tumor segmentation on brain MRI images. Four image quality enhancement techniques, CLAHE, GC, NLMF, and MWF, are used to assess image quality based on SSIM and MSE values. Additionally, this report investigates a deep learning model for glioma tumor image segmentation on brain MRI images, developing the model using the U-net architecture. The study compares models trained with image datasets that have undergone all four image enhancement techniques.

Regarding the relationship between image enhancement and deep learning model performance, it was observed that image quality significantly impacts the performance of deep learning models, as indicated in Table 3 when comparing the same techniques. For instance, the trained model with the CLAHE technique (CLAHE No. 1), featuring a cliplimit parameter of 0.1 and a tile size of 8, displayed a DSC value of 0.817 and an SSIM value of 0.705. In comparison, adjusting the parameters to cliplimit equal to 0.2 and tile size equal to 6 (CLAHE No. 3) resulted in a DSC value of 0.811 and an SSIM value of 0.733. It is evident that, despite the improved image quality of the CLAHE No. 3 model, it reduces the efficiency of the model. Furthermore, models trained with datasets of similar image quality exhibited varying performance, as seen in the CLAHE No.2 and MWF No.1 models, in the MWF No.4 and MWF No.5 models, and the GC No.2 and GC No.3 models. These results indicate that poorer image quality may contribute to better model performance, aligning with the research by Güneş AM *et al.*, which stated that reducing the image quality of training data by reducing contrast or adding artifacts makes the resulting model more effective.[7]

The developed deep learning model for glioma tumor segmentation on brain MRI images revealed that trained models with datasets that did not undergo image enhancement techniques had a DSC value of 0.817, while the image segmentation trained model with the CLAHE enhancement technique had a DSC value of 0.818, GC had a DSC value of 0.812, NLMF had a DSC value of 0.820, and MWF had a DSC value of 0.797. Table 3 indicates that the model with image enhancement using the NLMF technique has the highest DSC value, while the model with image enhancement using the MWF technique has the least, being 2.4% lower than the trained model without image enhancement techniques. Table 2 shows that the F1-score, Jaccard, recall, precision, and accuracy values of the trained model without image enhancement techniques were 89.2%, 81.5%, 94.3%, 86.0%, and 99.4%, respectively. For the trained models with the CLAHE technique, the values were 89.5%, 81.8%, 94.0%, 86.6%, and 99.4%, respectively. The GC values were 88.5%, 80.1%, 92.2%, 86.1%, and 99.4%, respectively. NLMF values were 90.0%, 82.7%, 94.8%, 86.7%, and 99.4%, respectively, and MWF values were 86.6%, 77.4%, 90.0%, 85.1%, and 99.3%, respectively.

Comparing the trained model with the enhanced dataset with previous works on glioma segmentation on brain MRI images, Table 4 shows that the DSC values of the U-Net+CLAHE, U-Net+GC, U-Net+NLMF, and U-Net+CLAHE models are lower than all previous works, both in the trained model with similar and completely different datasets. Adding image enhancmore than ement techniques alone is sufficient to increase model performance. However, the proposed model accuracy and recall demonstrate high performance for all models, at least 0.993 for U-Net+MWF, close to Ghosh S. 2019[18] and Al Nasim MA 2022.[19]

Table 4 Compares of previous works.

Author	Image	Network	Recall	Precision	Accuracy	DSC
Ghosh S. 2019[18]	TCGA-LGG	U-Net+ResNeXt50	-	-	0.996	0.932
		U-Net+FPN	-	-	0.993	0.899
Al Nasim MA 2022[19]	BraTS2019	U-Net+empirical analysis	0.997	-	0.998	0.920
Manasa K. 2022[20]	Brast2018	U-Net+Zernile Moments	0.877	0.810	-	0.852
Yan C. 2022[21]	BraTS2018	SEResU-Net	0.923	-	-	0.911
Our proposed	BraTS2023	U-Net+CLAHE	0.940	0.866	0.994	0.818
		U-Net+GC	0.922	0.861	0.994	0.812
		U-Net+NLMF	0.948	0.867	0.994	0.820
		U-Net+MWF	0.900	0.851	0.993	0.797

Limitation

Limitations related to this study: First, using image datasets in two dimensions may reduce the quality of model training because the original image dataset used for training is designed in 3D. Second, different types of MRI images should be separated for enhancement because each type has distinct characteristics. However, this study used the same parameters for enhanced images in each technique since the mask design is used to label the tumor's boundaries, designed for all four MRI types together. Finally, this study did not introduce imperfections within the dataset to compare image enhancements, which would help better understand the relationship between increased image enhancement and model performance.

Conclusion

In conclusion, the study explores the relationship between image enhancement and the performance of deep learning models, aiming to develop a deep learning model for segmenting glioma tumors on MRI images using the U-net architecture with image enhancement techniques. The results demonstrate that pre-processing significantly improves image quality and can enhance brain segmentation on brain MRI images. Specifically, the non-local mean filter technique performed best, followed by gamma correction, median and wiener filter technique, and contrast-limited adaptive histogram equalization was the lowest. However, when using enhanced images for trained models, it was found that image enhancement techniques can increase performance, precisely the non-local mean filter technique, the contrast-limited adaptive histogram equalization technique, while the gamma correction technique and the median and wiener filter decrease model performance. Enhanced images for trained models may increase or decrease performance depending on the chosen image enhancement technique and the parameters determined by each method.

Conflict of interest

None

Funding

None

Ethical approval

The study was approved by the ethics committee of Naresuan University, Thailand (IRB No. P1-0155/2566).

References

[1] Baid U, Ghodasara S, Mohan S, Bilello M, Calabrese E, Colak E, *et al*. The rsna-asnr-miccai brats 2021 benchmark on brain tumor segmentation and radiogenomic classification. arXiv. 2021; 2107.02314. doi.org/10.48550/arXiv.2107.02314

[2] Lin M, Momin S, Lei Y, Wang H, Curran WJ, Liu T, *et al*. Fully automated brain tumor segmentation from multiparametric MRI using 3D context deep supervised U-Net. Med Phys. 2021; 48(8): 4365-74. doi.org/10.1002/mp.15032.

[3] Menze BH, Jakab A, Bauer S, Kalpathy-Cramer J, Farahani K, Kirby J, *et al*. The multimodal brain tumor image segmentation benchmark (BRATS). IEEE Trans Med Imaging. 2014; 34(10): 1993-2024. doi: 10.1109/TMI.2014.2377694.

[4] Lin M, Momin S, Lei Y, Wang H, Curran WJ, Liu T, *et al*. Fully automated brain tumor segmentation from multiparametric MRI using 3D context deep supervised U-Net. Med Phys. 2021; 48(8): 4365-74. doi.org/10.1002/mp.15032.

[5] Knuth F, Adde IA, Huynh BN, Groendahl AR, Winter RM, Negård A, *et al*. MRI-based automatic segmentation of rectal cancer using 2D U-Net on two independent cohorts. Acta Oncol. 2022; 61(2): 255-63. doi.org/10.1080/0284186X.2021.2013530.

[6] Zhao C, Zhao Z, Zeng Q, Feng Y. MVP U-Net: Multi-view pointwise U-Net for brain tumor segmentation. InBrainlesion: Glioma, Multiple Sclerosis, Stroke and Traumatic Brain Injuries: BrainLes 2020, Lecture Notes in Computer Science, October 4, 2020: Lima, Peru, 12659: 93-103. Springer, Cham. doi.org/10.1007/978-3-030-72087-2_9

[7] Güneş AM, van Rooij W, Gulshad S, Slotman B, Dahele M, Verbakel W. Impact of imperfection in medical imaging data on deep learning-based segmentation performance: An experimental study using synthesized data. Med Phys. 2023; 50(10): 6421-32. doi: 10.1002/mp.16437

[8] Bakas S, Akbari H, Sotiras A, Bilello M, Rozycki M, Kirby JS, *et al*. Advancing the cancer genome atlas glioma MRI collections with expert segmentation labels and radiomic features. Sci Data. 2017; 4(1): 1-3. doi.org/10.1038/sdata.2017.117.

[9] Wen H, Qi W, Shuang L. Medical X-ray image enhancement based on wavelet domain homomorphic filtering and CLAHE. Proceedings of In 2016 International Conference on Robots & Intelligent System (ICRIS), IEEE. 2016 Aug 27: 249-54. doi: 10.1109/ICRIS.2016.50.

[10] Zuiderveld K. Contrast limited adaptive histogram equalization. Graphics gems. 1994; 474-85. doi.org/10.1016/B978-0-12-336156-1.50061-6.

[11] Cao G, Huang L, Tian H, Huang X, Wang Y, Zhi R. Contrast enhancement of brightness-distorted images by improved adaptive gamma correction. Comput Electr Eng. 2018; 66: 569-82. doi.org/10.1016/j.compeleceng.2017.09.012.

[12] Huang Z, Zhang T, Li Q, Fang H. Adaptive gamma correction based on cumulative histogram for enhancing near-infrared images. Infrared Phys Technol. 2016; 79: 205-15. doi.org/10.1016/j.infrared.2016.11.001.

[13] Sahnoun M, Kallel F, Dammak M, Mhiri C, Mahfoudh KB, Hamida AB. A comparative study of MRI contrast enhancement techniques based on Traditional Gamma Correction and Adaptive Gamma Correction: Case of multiple sclerosis pathology. Proceedings of In 2018 4th international conference on advanced technologies for signal and image processing (ATSIP), IEEE. 2018 Mar 21, 1-7. doi: 10.1109/ATSIP.2018.8364467.

[14] Shreyamsha Kumar BK. Image denoising based on non-local means filter and its method noise thresholding. SIViP. 2013; 7: 1211-27. doi.org/10.1007/s11760-012-0389-y

[15] Chandrashekar L, Sreedevi A. Assessment of non-linear filters for MRI images. Proceedings of In 2017 2nd International Conference on Electrical, Computer and Communication Technologies (ICECCT), IEEE. 2017 Feb 22, 1-5. doi: 10.1109/ICECCT.2017.8117852.

[16] Min A, Kyu ZM. MRI images enhancement and tumor segmentation for brain. In2017 18th International Conference on Parallel and Distributed Computing, Applications and Technologies (PDCAT) 2017 Dec 18 (pp. 270-275). IEEE. doi: 10.1109/PDCAT.2017.00051.

[17] Ronneberger O, Fischer P, Brox T. U-net: Convolutional networks for biomedical image segmentation. Proceedings of InMedical Image Computing and Computer-Assisted Intervention-MICCAI 2015: 18th International Conference, Munich, Germany, October 5-9, 2015, 234-241). Springer, Cham. doi.org/10.1007/978-3-319-24574-4_28.

[18] Ghosh S, Santosh KC. Tumor segmentation in brain MRI: U-Nets versus feature pyramid network. Proceedings of In2021 IEEE 34th International Symposium on Computer-Based Medical Systems (CBMS), IEEE. 2021 Jun 7, 31-6. doi: 10.1109/CBMS52027.2021.00013.

[19] Al Nasim MA, Al Munem A, Islam M, Palash MA, Haque MM, Shah FM. Brain tumor segmentation using enhanced u-net model with empirical analysis. In2022 25th International Conference on Computer and Information Technology (ICCIT) 2022 Dec 17 (pp. 1027-32). IEEE. doi: 10.1109/ICCIT57492.2022.10054934.

[20] Manasa K, Krishnaveni V. Brain Tumor Segmentation Using Zernike Moments in U-Net. In 2022 International Conference on Intelligent Innovations in Engineering and Technology (ICIIET) 2022 Sep 22 (pp. 342-6). IEEE. doi: 10.1109/ICIIET55458.2022.9967618.

[21] Yan C, Ding J, Zhang H, Tong K, Hua B, Shi S. SEResU-Net for Multimodal Brain Tumor Segmentation. IEEE Access. 2022; 10: 117033-44. doi: 10.1109/ACCESS.2022.3214309.

Journal of Associated Medical Sciences 2024; 57(2): 141-148

JAMS
Journal of Associated Medical Sciences

Scopus Indexed & Thai-Journal Citation Index Centre (TCI)

Journal of Associated Medical Sciences

Journal homepage: https://www.tci-thaijo.org/index.php/bulletinAMS/index

Evaluation of the offset couch parameter between kilovoltage on-board imaging and cone-beam computed tomography in patients with prostate cancer

Tanaporn Guawgumnerdtong[1,2] Nuanpen Damrongkijudom[3] Achawee Suwanarat[3] Piyawan Chailapakul[2] Tawatchai Ekjeen[3*]

[1]Master of Science in Radiological Technology Programme, Faculty of Medical Technology, Mahidol University, Nakhon Pathom Province, Thailand.
[2]Department of Radiation Oncology, Chulabhorn Hospital, Chulabhorn Royal Academy, Bangkok, Thailand.
[3]Department of Radiological Technology, Faculty of Medical Technology, Mahidol University, Nakhon Pathom Province, Thailand.

ARTICLE INFO

Article history:
Received 25 October 2023
Accepted as revised 18 March 2024
Available online 21 March 2024

Keywords:
Prostate cancer, IGRT protocol, PTV margin.

ABSTRACT

Background: External Beam Radiation Therapy (EBRT) is a curative therapy technique for prostate cancer. Since the prostate is unstable and surrounded by the bladder and rectum, precision of the target location is critical. Image Guided Radiation Therapy (IGRT) can improve treatment precision. The bladder and rectum may alter volume during IGRT, shifting the prostate's position and resulting in missed target volume doses and extra organs at risk (OARs) doses.

Objective: To assess setup error and residual error during patient positioning, as well as the current IGRT protocol efficiency, in prostate cancer patients while recommending a planning target volume (PTV) margin.

Materials and methods: The offset couch parameter of on-board imaging (OBI) and cone-beam computed tomography (CBCT) was computed to determine the error distribution, magnitude, and error difference between treatment phases. The systematic and random errors were calculated using the van Herk equation to determine the planning target volume (PTV) margin.

Results: The setup error was -0.86 to 0.25 mm, and the residual error was -0.15 to 0.32 mm. The couch displacement percentage for OBI was 29.44% to 58.89%, and for CBCT was 8.10% to 34.12%. The systematic error was 1.65 to 3.21. The random error was 1.78 to 3.29. The setup error was greatest in the longitudinal (Lng) direction, residual error was greatest in the vertical (Vrt) direction, and systematic and random error were greatest in the Vrt and lateral (Lat) direction, respectively. The PTV margin was greatest in the Vrt direction, while the Lng direction was the narrowest margin for every treatment phase.

Conclusion: The highest setup error occurs in the Lng direction for all treatment phases. For the 46 Gy and 60 Gy phases, the highest residual error is in the Vrt direction. However, in the 78 Gy phase, the error is relatively close to 0.01mm in every direction. The current IGRT protocol is effective in detecting setup and residual errors. The 78 Gy phase has the greatest PTV margin, whereas the 46 Gy phase shows the narrowest margins in all directions.

Introduction

In 2021, prostate cancer will be the fourth most frequent cancer among Thai men.[1] EBRT is one of the curative approaches for prostate cancer. The bladder and rectum are OARs for prostate cancer treatment. Position accuracy is limited by various factors, including clinical site, tumor volume, treatment technique, and immobilization device. IGRT reduces positional error by imaging the target region before administering radiation.[2] OBI and CBCT are IGRT methods for precise target volume localization that

* **Corresponding contributor.**
Author's Address: *Department of Radiological Technology, Faculty of Medical Technology, Mahidol University, Nakhon Pathom, Thailand.*
E-mail address: tawatchai.ekj@mahidol.ac.th
doi: 10.12982/JAMS.2024.036
E-ISSN: 2539-6056

may decrease the PTV margin.[3] Although CBCT takes longer than OBI, leading to increased intrafraction motion and necessitating a larger PTV margin, daily CBCT decreases errors more than non-daily CBCT.[4] According to ESTRO ACROP, the bone anatomy for prostate IGRT is insufficient since the prostate position does not correspond to the pelvic bone.[5] Fiducial markers or CT-based IGRT with soft tissue matching are recommended for detecting prostatic movements.[5] The van Herk equation is commonly used for PTV margin calculations.

At Chulabhorn Hospital, the most frequently used dose protocol for prostate cancer is 78 Gy in 39 fractions (Fx) using Volumetric Modulated Arc Therapy (VMAT). The treatment can be divided into three phases: 46Gy, 60Gy, and 78Gy. The treatment regions in each phase are as follows: 1) Prostate, seminal vesicle, and pelvic node; 2) Prostate and seminal vesicle; and 3) Prostate. For the 46 Gy and 60 Gy phases, the IGRT protocol is daily OBI and weekly CBCT, but daily OBI and daily CBCT for the 78 Gy phase. Before CT simulation and daily treatment, patients are required to maintain a full bladder to ensure accurate prostate positioning. Patients are positioned supine with hands on the chest, utilizing a cushion and foot support as immobilization devices secured to the treatment couch. On the treatment day, skin markers and in-room lasers are utilized for positioning. In this study, setup error refers to the error from the positioning, measurable using OBI, whereas residual error refers to the error that remains after OBI correction and can be measured using CBCT. After patient setup, OBI-based bone matching was performed to rectify the setup error and adjust the couch position, then CBCT-based soft tissue matching to correct the residual error and adjust the couch position before delivering radiation.

The objective of this study was to evaluate the setup error, residual error, and efficiency of the current IGRT protocol in prostate cancer. Another objective was to propose the PTV margin for the current IGRT protocol.

Materials and methods

Patients

This study was approved by Mahidol University Central Institutional Review Board (Protocol number 2022/199.2507**)** and Ethic Committee Chulabhorn Royal Academy. A total of 60 prostate cancer patients were selected from Chulabhorn Hospital's electronic medical record using a blinding procedure conducted by the participant who was not part of the study. Before the patient selection, the patient's name and hospital number were anonymized. The study included patients who underwent VMAT treatment with a dose of 78 Gy in 39 Fx following the IGRT protocol of Chulabhorn Hospital from October 2018 to January 2022. Patients for this study are treated with Varian TrueBeam LINAC (Varian Medical System, Palo Alto, CA).

Data acquisition

The offset couch parameters, representing couch values in three translation directions, were gathered from the offline review feature of the ARIA Oncology Information System (ARIA OIS) and recorded. The three translation directions were lateral (Lat: Left to Right), vertical (Vrt: Anterior to Posterior), and longitudinal (Lng: Superior to Inferior). All offset couch parameters for OBI and CBCT across fractions were collected. The offset couch parameters were vector parameters. For each patient, OBI data consisted of 39 sets, whereas CBCT data were at least 16 sets**.**

Data analysis

The 3 subprocesses were applied to each data set.

1. The offset couch parameter division

Offset couch parameters were categorized into two groups: OBI and CBCT. Each category included parameters for the three treatment phases. The total OBI data comprised 7,020 values, while the total CBCT data consisted of 3,708 values, for all treatment phases and directions.

2. Examining the setup and the residual error distribution and magnitude

The mean, standard deviation (SD), minimum, and maximum values were calculated. Box plots with a 95% confidence interval (CI) were constructed for each data set using IBM SPSS. The setup error magnitude was determined using the following equation:

$$\text{Setup error magnitude} = \sqrt{\text{SE}_{\text{Lat}}^2 + \text{SE}_{\text{Lng}}^2 + \text{SE}_{\text{Vrt}}^2}$$

where the SE_{Lat}, SE_{Lng}, and SE_{Vrt} were the lateral, longitudinal, and vertical setup errors, respectively.

3. Investigating the significant error difference between treatment phases in each direction of OBI and CBCT and observing the error direction

The Brown-Forsythe test was applied at a 95% CI to determine the error difference between treatment phases in each direction. This statistic was utilized for both OBI and CBCT. The couch displacement percentage for each direction of OBI and CBCT was calculated using Microsoft Excel to determine the error direction.

PTV margin

The PTV margin was calculated using the van Herk equation to account for setup errors observed by the current IGRT protocol. The formula was defined as 2.5 times the total SD of systematic errors plus 0.7 times the total SD of random errors.[6]

$$PTV\ margin = 2.5\Sigma + 0.7\sigma$$

The systematic error impacts all treatment fractions due to preparation error, including discrepancies in the isocenters of the LINAC, imager, and laser, as well as changes in organ shape. The population systematic error was defined as the standard deviation of all individual mean following this equation.[7]

$$\Sigma = \sqrt{\frac{1}{N-1}\sum_{i}^{N}(m_i - \bar{m})^2}$$

The random error occurs in different directions and fractions during treatment execution such as prostate motion. The population random error was defined as the root mean square of the individual SD of all patients following this equation.[8]

$$\sigma = \sqrt{\frac{1}{N}\sum_{i}^{N} s_i^2}$$

where Σ was a systemic error of all patients
σ was a random error of all patients
N was the number of patients
m_i was a systematic error of the *i*th individual patient
s_i was a random error of the *i*th individual patient
$\overline{m}$ was a mean systematic error of all patients

Results

Distribution of setup errors and magnitudes

Table 1 presented the distribution setup error in each treatment direction for every treatment phase, whereas Figure 1 showed a setup error boxplot of all phases. The median and interquartile range (IQR) of all directions and magnitudes in the three phases were similar. Although the setup error distribution of magnitude and every direction for each phase was similar, the variance of each phase differed due to large variations in sample sizes. Notably, the largest average setup error was found in the Lng direction, while the lowest was in the Lat direction for every phase.

Table 1 Distribution of setup errors in each treatment direction for each treatment phase.

Direction	Phase	Mean±SD (mm)	Maximum (mm)	Minimum (mm)
Lat	46	0.25±3.63	22.90	-13.50
	60	-0.07±3.38	11.30	-13.80
	78	0.04±3.73	14.40	-13.00
Lng	46	-0.63±2.46	14.10	-16.60
	60	-0.76±2.72	19.90	-8.40
	78	-0.86±2.73	9.20	-13.50
Vrt	46	-0.48±3.16	14.10	-11.80
	60	-0.54±3.57	10.00	-10.30
	78	-0.52±3.67	7.80	-10.40
Magnitude	46	4.69±2.81	23.89	0
	60	5.07±2.59	22.10	0
	78	5.32±2.73	16.17	0

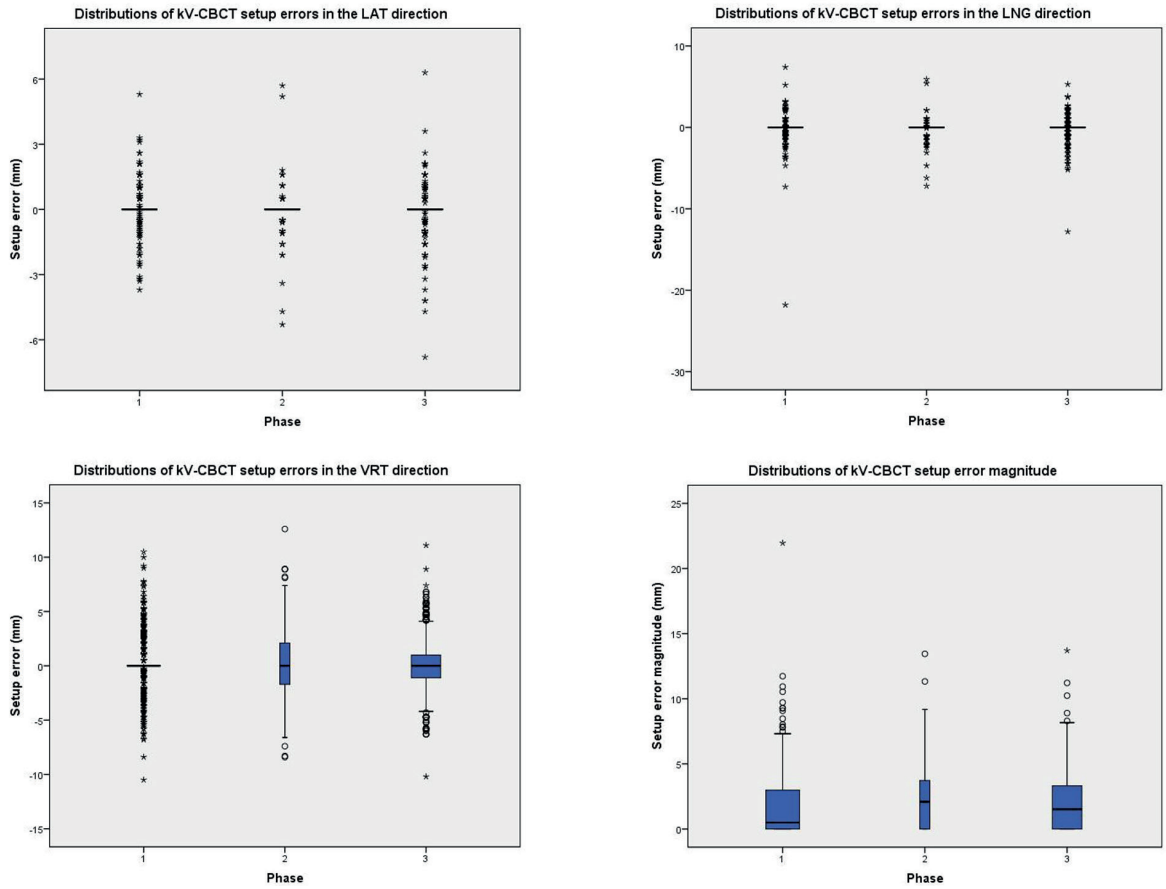

Figure 1 *Boxplot of setup error distribution of three treatment phases (Lat, Lng, Vrt, and magnitude).*

Distribution of residual errors and magnitudes

Table 2 illustrates the distribution of residual errors in each treatment direction for every treatment phase, while Figure 2 provides corresponding boxplots. The IQR for both Lat and Lng were narrow across all three phases, indicating minimal dispersion in residual error distributions. Notably, the IQR of Vrt differed among phases, with the 60 Gy phase having the widest range and the greatest dispersion in its distribution. Although the IQR of magnitudes was similar in all phases, the median for the 46 Gy phase was approximately around Q1. The distribution is right skewed for all phases. The largest average residual error was in the Vrt for the 46 Gy and 60 Gy phases but for the 78 Gy phase, the largest was in the Lat. The lowest average residual error was in the Lat for all phases.

Table 2 Distribution of residual errors in each treatment direction for each treatment phase.

Direction	Phase	Mean±SD (mm)	Maximum (mm)	Minimum (mm)
Lat	46	0.01±0.69	5.30	-3.70
	60	-0.05±1.00	5.70	-5.30
	78	-0.08±0.86	6.30	-6.80
Lng	46	-0.09±1.24	7.40	-21.80
	60	-0.15±1.19	5.90	-7.20
	78	-0.07±1.09	5.30	-12.80
Vrt	46	0.18±2.47	10.50	-10.50
	60	0.32±3.35	12.60	-8.40
	78	0.02±2.60	11.10	-10.20
Magnitude	46	1.66±2.32	21.95	0
	60	2.52±2.71	13.45	0
	78	1.98±2.19	13.71	0

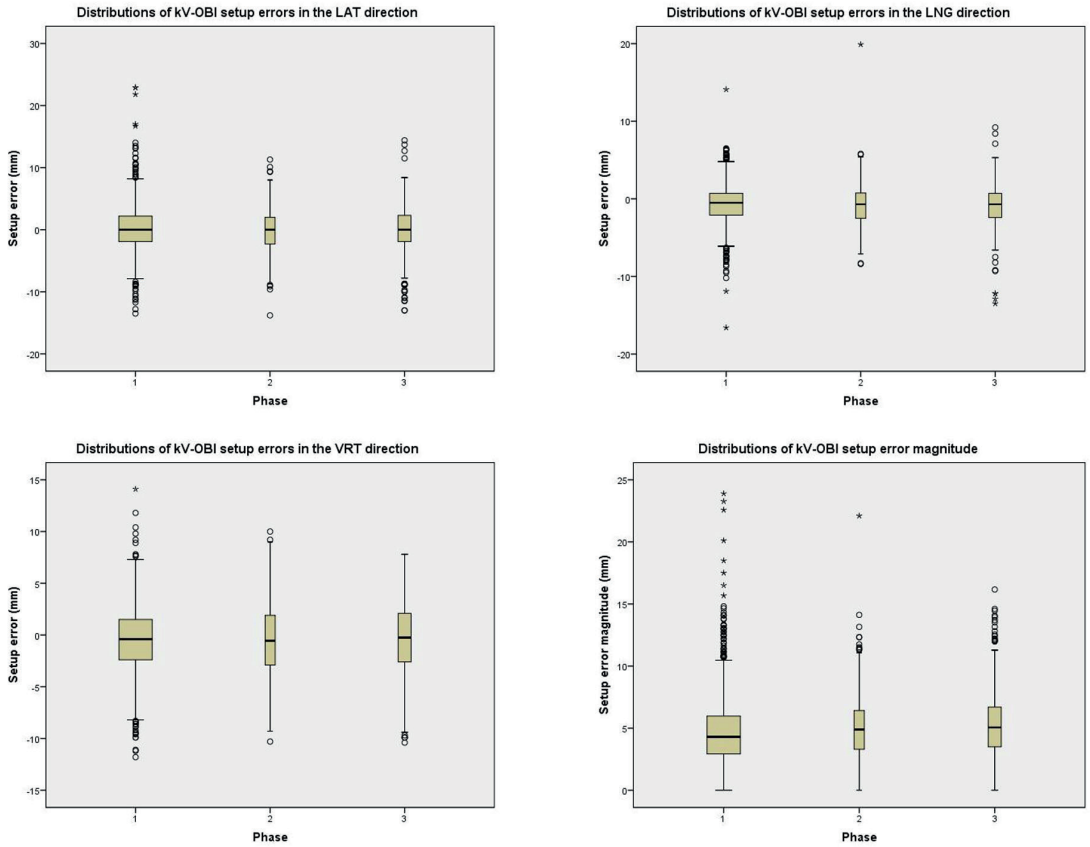

Figure 2 *Boxplot of residual error distribution of three treatment phase (Lat, Lng, Vrt, and magnitude).*

Mean difference between the three treatment phases for setup error and residual error in each direction.

The *p* values for all directions, both OBI and CBCT, were greater than 0.05. Table 3 showed that the OBI *p* values were 0.215, 0.188, and 0.926 for the Lat, Lng, and Vrt, respectively. Meanwhile, the CBCT *p* values were 0.254, 0.770, and 0.411 for the Lat, Lng, and Vrt, respectively. Notably, there were no significant differences between within-group variance and between-group variance in each phase for all directions. Table 4 showed that in the 46 Gy phase, both OBI and CBCT exhibited the highest displacement in the Vrt, and the lowest in Lng. Like the 60 Gy phase, the highest displacement was found in Vrt for both OBI and CBCT, whereas the lowest displacement of OBI was in Lat, with the CBCT in Lng. For the 78 Gy phase, the highest and lowest displacements of OBI were in Lat and Vrt, respectively, while the highest and lowest displacements of CBCT were in Vrt and Lng.

Table 3 Distribution of error difference between treatment phases in each direction of OBI and CBCT.

IGTR Protocol		*p* value
OBI	LAT-OBI	0.215
	LNG-OBI	0.188
	VRT-OBI	0.926
CBCT	LAT-CBCT	0.254
	LNG-CBCT	0.770
	VRT-CBCT	0.411

Table 4 Percentage of couch displacement of OBI and CBCT in each direction for each treatment phase.

Direction	OBI (%)			CBCT (%)		
	Phase 46 Gy	Phase 60 Gy	Phase 78 Gy	Phase 46 Gy	Phase 60 Gy	Phase 78 Gy
Left	45.32	44.76	46.85	12.15	14.12	14.46
Right	43.00	44.29	44.81	12.15	15.88	20.08
No shift	11.68	10.95	8.33	75.70	70.00	65.46
Superior	32.12	32.86	29.44	8.10	8.24	11.45
Inferior	54.82	57.38	58.89	10.39	12.94	12.25
No shift	13.05	9.76	11.67	81.51	78.82	76.31
Anterior	51.41	53.10	50.56	24.47	31.18	30.32
Posterior	38.36	37.38	37.04	24.65	34.12	28.11
No shift	10.22	9.52	12.41	50.88	34.71	41.57

Evaluation of systematic and random errors and suggested PTV margin

Table 5 displayed the computer systematic and random setup errors, along with the PTV margin for all directions and phases. The Vrt presented the greatest systematic error for all phases, while Lng presented the smallest. The random error was largest in the Lat for all phases and lowest in the Lng for the 46 Gy and 60 Gy phases, but the lowest in the 78 Gy phase was in the Lng and Vrt. For all phases, the PTV margin was greatest in the Vrt and lowest in the Lng. The PTV margin of the 78 Gy phase was the largest in all directions except the PTV margin in the Lng of the 60 Gy, which was greater than 78 Gy and 46 Gy, respectively.

Table 5 Systematic and random error and suggested PTV margins in each direction for each treatment phase.

Phase	Direction	Systematic error: Σ (mm)	Random error: σ (mm)	PTV (mm)
46 Gy	Lat	1.68	3.29	6.50
	Lng	1.65	1.88	5.43
	Vrt	2.30	2.23	7.31
60 Gy	Lat	2.21	2.77	7.46
	Lng	2.18	1.78	6.70
	Vrt	3.06	2.03	9.07
78 Gy	Lat	2.38	3.00	8.04
	Lng	2.06	1.92	6.48
	Vrt	3.21	1.91	9.36

Note: Σ: systematic error, σ: random error.

Discussion

In this study, the greatest setup error was in the Lng, followed by the Vrt and Lat in every phase. This finding contrasts with previous studies[7-10] that reported the highest setup error in Vrt. Hurkmans' study found that employing a skin marker could increase the setup error due to deviations from the respiratory, weight loss, and relaxation.[8] In our study, the incorporation of a skin marker may have contributed to the highest setup error in the Lng direction. Mayyas's study highlighted the skin marker had a large effect on the setup error in Vrt but lesser in Lat. By controlling this factor, the setup error could be reduced.[9]

Another factor influencing setup error is online image registration, but this variable is very responsive to prostate motion.[11] While 2d-kV imaging can correct the setup error, it doesn't account for prostate motion in the correction,[12] implying that the residual error was prostate motion.[13] Our study found that Vrt exhibited the highest residual error, except in the 78 Gy phase. This aligns with van Herk's findings that prostate motion was typically small, except in the Vrt direction,[14] particularly in the posterior direction.[15] Previous research found that movement of internal organs and/or targets caused variations in prostate location.[16,17] Contrary to Millender's study indicated that most of the position error was caused by setup error rather than prostate motion,[18] our findings reveal that setup errors were significantly greater than residual errors in our study.

This study observed that the setup and residual errors in the 46 Gy phase tended to have the same variation while the 60 Gy and 78 Gy phases did not, indicating that an increase in CBCT was required to correct the residual error. The current IGRT protocol for the 46 Gy and 78 Gy phases appears to be adequate; however, the protocol for the 60 Gy phase should be modified. However, when considering the PTV margin employed in treatment, the residual error in the 60 Gy phase was effectively covered by this PTV, no

adjustments were required for this protocol. Moseley's study supports the feasibility of using CBCT as the daily online IGRT for the prostate since it provided target and organ at-risk localization and enables the evaluation treatment response.[19]

In each treatment phase, the greatest PTV margin was observed in Vrt direction. Consistent with previous studies, Vrt demonstrated the greatest PTV margin.[7,9,11,20] The suggested Vrt margin ranged from 7-9 mm while the Lng margin was suggested to be 5-6 mm, corresponding to previous studies. However, this study had a larger Lat margin than previous studies due to the larger random error. Mayyas's study suggests a 10-11 mm PTV margin for skin markers and OBI before CBCT to decrease PTV by 3-5 mm.[9]

The systematic error impacts the PTV margin and is more significant than a random error since it influences the course error.[21] Daily IGRT can reduce both systematic and random error.[22,23] Daily CBCT before treatment has been shown to decrease prostate deformation with rectum and bladder control.[3] Huang's study found that daily CBCT can reduce PTV margin by 1-2 mm.[3] At Chulabhorn Hospital, the employed PTV margin for prostate cancer was 8 mm in all directions except the posterior, where it is set as 5 mm. The suggested PTV margin generally aligns within the 8 mm range, except the Vrt margin for the 60 Gy and 78 Gy phases, which exceeded the current PTV recommendation. This study was limited by the omission of the intrafraction motion error and an absence to account for the volume of the rectum and bladder.

Conclusion

The highest setup error occurs in the Lng direction for all treatment phases, with the 46 Gy phase exhibiting the least error. For the 46 Gy and 60 Gy phases, the highest residual error is in the Vrt direction. However, in the 78 Gy phase, the error is close together in every direction, with a size of no more than 0.01mm. The current IGRT protocol used for prostate cancer patients is effective in detecting setup and residual errors. The suggested PTV margin are proposed at 6.50 mm to 8.00 mm for Lat, 5.5 mm to 6.70 mm for the Lng, and 6.50 mm to 9.40 mm for Vrt direction. Notably, the 78 Gy phase has the greatest PTV margin, whereas the 46 Gy phase shows the narrowest margins in all directions.

These findings underscore the effectiveness of the current IGRT protocol and provide valuable insights for optimizing PTV margins based on specific treatment phases and directions.

Conflict of Interest

The authors declare no conflict of interest.

Funding

None

References

[1] Naravejsakul k, Pothisa T, Saenrak N. Incidence of Prostate Cancer in Physical Checkup Population with Rising of Serum Prostatic Specific Antigen. Vajira Med J. 2022; 66(5): 361-8. doi: 10.14456/vmj.2022.37.

[2] Somboon S, Malila W, Tamon S, Nueangwong W, Yeenang N, Rueansri J. Evaluation of optimal kilovoltage-cone beam technique on image quality, registration accuracy, time of imaging and relative dose for head radiotherapy: A phantom study. J Assoc Med Sci. 2022; 55(2): 10-5. doi: 10.12982/JAMS.2022.011.

[3] Huang K, Palma D, Scott D, McGregor D, Yartsev S, Louie A, *et al*. Inter- and Intrafraction Uncertainty in Prostate Bed Image-Guided Radiotherapy. Int. J. Radiat. Oncol Biol Phys. 2012; 84: 402-7. doi: 10.1016/j.ijrobp.2011.12.035.

[4] Ariyaratne H, Chesham H, Pettingell J, Alonzi R. Image-guided radiotherapy for prostate cancer with cone beam CT: dosimetric effects of imaging frequency and PTV margin. Radiother Oncol. 2016; 121(1): 103-8. doi: 10.1016/j.radonc.2016.07.018.

[5] Ghadjar P, Fiorino C, Munck Af Rosenschöld P, Pinkawa M, Zilli T, van der Heide UA. ESTRO ACROP consensus guideline on the use of image guided radiation therapy for localized prostate cancer. Radiother Oncol. 2019; 141: 5-13. doi: 10.1016/j.radonc.2019.08.027.

[6] van Herk M. Errors and margins in radiotherapy. Semin Radiat Oncol. 2004; 14(1): 52-64. doi: 10.1053/j.semradonc.2003.10.003.

[7] Hashido T, Nakasone S, Fukao M, Ota S, Inoue S. Comparison between manual and automatic image registration in image-guided radiation therapy using megavoltage cone-beam computed tomography with an imaging beam line for prostate cancer. Radiol Phys Technol. 2018; 11(4): 392-405. doi: 10.1007/s12194-018-0476-z.

[8] Hurkmans CW, Remeijer P, Lebesque JV, Mijnheer BJ. Set-up verification using portal imaging; review of current clinical practice. Radiother Oncol. 2001; 58(2): 105-20. doi: 10.1016/s0167-8140(00)00260-7.

[9] Mayyas E, Chetty IJ, Lu M, Stricker H, Pradhan D, Movsas B, *et al*. Evaluation of multiple image-based modalities for image-guided radiation therapy (IGRT) of prostate carcinoma: a prospective study. Med Phys. 2013; 40(4): 041707. doi: 10.1118/1.4794502.

[10] Ghilezan MJ, Jaffray DA, Siewerdsen JH, Van Herk M, Shetty A, Sharpe MB, *et al*. Prostate gland motion assessed with cine-magnetic resonance imaging (cine-MRI). Int J Radiat Oncol Biol Phys. 2005; 62(2): 406-17. doi: 10.1016/j.ijrobp.2003.10.017.

[11] McNair HA, Hansen VN, Parker CC, Evans PM, Norman A, Miles E, *et al*. A comparison of the use of bony anatomy and internal markers for offline verification and an evaluation of the potential benefit of online and offline verification protocols for prostate radiotherapy. Int J Radiat Oncol Biol Phys. 2008; 71(1): 41-50. doi: 10.1016/j.ijrobp.2007.09.002.

[12] Zucca S, Carau B, Solla I, Garibaldi E, Farace P, Lay G, *et al*. Prostate image-guided radiotherapy by megavolt cone-beam CT. Strahlenther Onkol. 2011; 187(8): 473-8. doi: 10.1007/s00066-011-2241-7.

[13] Poulsen PR, Muren LP, Høyer M. Residual set-up errors and margins in on-line image-guided prostate localization in radiotherapy. Radiother Oncol. 2007; 85(2): 201-6. doi: 10.1016/j.radonc.2007.08.006.

[14] van Herk M, Bruce A, Kroes AP, Shouman T, Touw A, Lebesque JV. Quantification of organ motion during conformal radiotherapy of the prostate by three dimensional image registration. Int J Radiat Oncol Biol Phys. 1995; 33(5): 1311-20. doi: 10.1016/0360-3016(95)00116-6.

[15] Ost P, De Meerleer G, De Gersem W, Impens A, De Neve W. Analysis of prostate bed motion using daily cone-beam computed tomography during postprostatectomy radiotherapy. Int J Radiat Oncol Biol Phys. 2011; 79(1): 188-94. doi: 10.1016/j.ijrobp.2009.10.029.

[16] Nakamura N, Shikama N, Takahashi O, Ito M, Hashimoto M, Uematsu M, *et al*. Variability in bladder volumes of full bladders in definitive radiotherapy for cases of localized prostate cancer. Strahlenther Onkol. 2010; 186(11): 637-42. doi: 10.1007/s00066-010-2105-6.

[17] Schallenkamp JM, Herman MG, Kruse JJ, Pisansky TM. Prostate position relative to pelvic bony anatomy based on intraprostatic gold markers and electronic portal imaging. Int J Radiat Oncol Biol Phys. 2005; 63(3): 800-11. doi: 10.1016/j.ijrobp.2005.02.022.

[18] Millender LE, Aubin M, Pouliot J, Shinohara K, Roach M, 3rd. Daily electronic portal imaging for morbidly obese men undergoing radiotherapy for localized prostate cancer. Int J Radiat Oncol Biol Phys. 2004; 59(1): 6-10. doi: 10.1016/j.ijrobp.2003.12.027.

[19] Moseley DJ, White EA, Wiltshire KL, Rosewall T, Sharpe MB, Siewerdsen JH, *et al*. Comparison of localization performance with implanted fiducial markers and cone-beam computed tomography for on-line image-guided radiotherapy of the prostate. Int J Radiat Oncol Biol Phys. 2007; 67(3): 942-53. doi: 10.1016/j.ijrobp.2006.10.039.

[20] Bylund KC, Bayouth JE, Smith MC, Hass AC, Bhatia SK, Buatti JM. Analysis of interfraction prostate motion using megavoltage cone beam computed tomography. Int J Radiat Oncol Biol Phys. 2008; 72(3): 949-56. doi: 10.1016/j.ijrobp.2008.07.002.

[21] van Herk M, Remeijer P, Rasch C, Lebesque JV. The probability of correct target dosage: dose-population histograms for deriving treatment margins in radiotherapy. Int J Radiat Oncol Biol Phys. 2000; 47(4): 1121-35. doi: 10.1016/s0360-3016(00)00518-6.

[22] Ding GX, Coffey CW. Radiation dose from kilovoltage cone beam computed tomography in an image-guided radiotherapy procedure. Int J Radiat Oncol Biol Phys. 2009; 73(2): 610-7. doi: 10.1016/j.ijrobp.2008.10.006.

[23] Wang G, Wang WL, Liu YQ, Dong HM, Hu YX. Positioning error and expanding margins of planning target volume with kilovoltage cone beam computed tomography for prostate cancer radiotherapy. Onco Targets Ther. 2018; 11: 1981-8. doi: 10.2147/ott.S152915.

Journal of Associated Medical Sciences 2024; 57(2): 149-156

JAMS
Journal of Associated Medical Sciences

Scopus Indexed & Thai-Journal Citation Index Centre (TCI)

Journal of Associated Medical Sciences

Journal homepage: https://www.tci-thaijo.org/index.php/bulletinAMS/index

AI-based diagnosis of chronic obstructive pulmonary disease from low-dose CT images

Chayanon Pamarapa[1] Salisa Kemlek[1] Wichasa Sukumwattana[1] Pharinda Sitthikul[1] Sichon Khuanrubsuan[1] Akkarawat Chaikhampa[1] Paritt Wongtrakool[2] Ammarut Chuajak[3] Monchai Phonlakrai[1] Ruedeerat Keerativittayayut[1*]

[1]School of Radiological Technology, Faculty of Health Science Technology, Chulabhorn Royal Academy, Bangkok, Thailand.
[2]Department of Diagnostic and Therapeutic Radiology, Faculty of Medicine, Ramathibodi Hospital, Mahidol University, Bangkok, Thailand.
[3]Queen Savang Vadhana Memorial Hospital, Chonburi Province, Thailand.

ARTICLE INFO

Article history:
Received 21 November 2023
Accepted as revised 9 April 2024
Available online 10 April 2024

Keywords:
Chronic obstructive pulmonary disease, Low dose computed tomography, ResNet, convolutional neural network.

ABSTRACT

Background: Chronic obstructive pulmonary disease (COPD) is a group of diseases characterized by airflow blockage. It is one of the leading causes of global mortality and is primarily attributed to smoking. COPD patients are usually diagnosed by spirometry test. Although regarded as the gold standard for COPD diagnosis, the spirometry test carries contraindications, thus prompting the development of low-dose computed tomography (low-dose CT) scan as an alternative for COPD screening. However, a practical limitation of diagnosing COPD from CT images is its reliance on the expertise of a skilled radiologist.

Objective: To address this limitation, we aimed to develop a deep-learning model for the automated classification of COPD and non-COPD from low-dose CT images.

Materials and methods: We examined the potential of a convolutional neural network for identifying COPD. Our dataset consisted of 10,000 low-dose CT images obtained from a lung cancer screening program, involving both ex-smokers and current smokers deemed at high risk of lung cancer. Spirometry data served as the ground truth for defining COPD. We used 90% of the datasets for training and 10% for testing.

Results: Our developed model achieved notable performance metrics: an area under the receiver operating characteristic curve (AUC) of 0.97, an accuracy of 0.89, a precision of 0.85, a recall of 0.96, and an F1-score of 0.90.

Conclusion: Our study demonstrates the potential of deep learning models to augment clinical assessments and improve the diagnosis of COPD, thereby enhancing diagnostic accuracy and efficiency. The findings suggest the feasibility of integrating this technology into routine lung cancer screening programs for COPD detection.

Introduction

Chronic obstructive pulmonary disease (COPD) is a term used to denote a group of diseases that result in the obstruction of airflow and consequent respiratory difficulties.[1,2] In 2024, the Global Initiative for Chronic Obstructive Lung Disease (GOLD) highlighted COPD as a leading cause of mortality globally, ranking among the top three.[3] In the large majority of COPD patients, this pathology is associated with smoking.[4] The absence of symptoms does not represent a dependable marker of disease and may instead delay diagnosis until more pronounced airflow obstruction becomes manifest.[4] Accurate detection of COPD is vital for promptly introducing therapies that reduce the risk of future exacerbation, delay disease

* **Corresponding contributor.**
Author's Address: *School of Radiological Technology, Faculty of Health Science Technology, Chulabhorn Royal Academy, Bangkok, Thailand.*
E-mail address: ruedeerat.kee@cra.ac.th
doi: 10.12982/JAMS.2024.037
E-ISSN: 2539-6056

progression, and enhance patient prognosis. However, a large amount of literature indicates that a significant proportion of patients are incidentally diagnosed with COPD during lung cancer screening, resulting in delayed treatment.[4]

Spirometry represents a widely accepted pulmonary function test and the gold standard for evaluating bronchial obstruction and lung elasticity.[5] However, spirometry presents certain limitations in patients with specific conditions such as aneurysms, respiratory tract infections, untreated pneumothorax, unstable vascular or cardiovascular systems, and those who have undergone thoracic or abdominal surgery. Additionally, spirometry may not be appropriate for patients with untreated or poorly controlled high blood pressure, low blood pressure, recent myocardial infarction, pulmonary embolism, or hemoptysis.[6,7] Therefore, physicians frequently rely on low-dose computed tomography (low-dose CT) as an alternative diagnostic technique, particularly in cases where spirometry may not be advisable.[8,9] Low-dose CT scanning is attractive because it reduces radiation exposure by nearly fourfold compared with conventional chest computed tomography,[10] however, COPD diagnosis through this technology demands the expertise of a skilled radiologist, thus putting pressure on clinical resources.

The objective of this study was to develop and evaluate a residual network-based artificial intelligence model that could effectively screen individuals for COPD from low-dose CT images. We hypothesized that only images from a specific portion of the upper lobe may carry reliable information for detecting COPD. Without human guidance, deep neural networks can identify patterns at various spatial scales that could distinguish between COPD and non-COPD.

Materials and methods

Participants

We retrospectively obtained low-dose CT images and spirometry data from individuals enrolled in a lung cancer screening program at Chulabhorn Hospital, Thailand. The study encompassed 295 participants who underwent follow-up assessments over 8 years from 2012 to 2020. Our analysis focused on a subset of this cohort, yielding 1,000 datasets comprising 500 chronic obstructive pulmonary disease (COPD) and 500 instances of non-COPD. Participants in the lung cancer screening initiative had to meet specific criteria: age exceeding 40 years, current smokers or individuals who had refrained from smoking for less than 15 years, and maintaining a minimum consumption of ten packs of cigarettes per year. The quantification of pack-years was based on the average daily packs smoked multiplied by the number of years smoked, with one pack equivalent to 20 cigarettes.

Additionally, prospective participants were required to have no prior history of lung disease or cancer. They were excluded if they self-reported history of lung cancer or congenital lung diseases, had lung surgery, used oral steroids, had blood transfer or dyspnea that required hospitalization for 4 weeks before the study, were unable to walk, or carried metallic implants in their thoracic region. Before engagement in the lung cancer screening program, all participants provided informed consent. Approval for the lung cancer screening program and this retrospective study was obtained from the institutional review board of Chulabhorn Royal Academy, Thailand, and complied with the Declaration of Helsinki.

Spirometry test

Spirometry is the gold standard for testing pulmonary or breathing functions during the identification and classification of COPD severity.[11] Participants were asked to perform the spirometry test before low-dose CT examination. COPD evaluation can be conducted using forced expiratory volume within one second (FEV1), which measures the air expelled in the first moments of a rapid exhalation, and forced vital capacity (FVC), which represents the total amount of air exhaled during the FEV test. Spirometry information served as the ground truth for this study. COPD can be defined using post-bronchodilator spirometry (FEV1/FVC ratio of less than 70%). COPD severity can be graded into four stages based on GOLD criteria: stage I (mild) for FEV1 values ≥80%, stage II (moderate) for FEV1 values between 50% and 79%, stage III (severe) for FEV1 values between 30% and 49%, and stage IV (very severe) for FEV1 values <30%.[4] Based on these criteria, 500 datasets from 164 participants were labeled as COPD, while 500 datasets from 131 regular participants were labeled as non-COPD. In the COPD cohort, 59%, 35%, 5%, and 1% of participants were categorized into GOLD stages 1, 2, 3, and 4, respectively.

Low-dose CT scans

Low-dose CT data were acquired using 192-detector row CT (SOMATOM Force, Erlangen, Germany) following the chest low-dose CT Protocol at Chulabhorn Hospital, Thailand, as outlined in Table 1. Scanning was performed in a head-first supine position. Participants were asked to raise their arms above their heads, fully inspire, and suspend breathing during scanning.

Table 1 Low-dose CT scanning parameters.

Scanning Parameters	Details
Surview image coverage	Cover Mid Neck to Anterior Superior Iliac Spine (ASIS)
Chest low-dose image coverage	Cover Supraclavicular to Adrenal glands
Reconstruction	Lung Window
Matrix size	512×512 pixels
Detector width	192 mm × 0.625 mm
Slice thickness	0.6-1.0 mm.
kV Mode	120 kV
mA Mode	25-50 mA
Pitch	1
Radiation dose ($CTDI_{vol}$)	≤1.9 mGy

Note: mA: milliampere; kV: kilovoltage, $CTDI_{vol}$: Computed Tomography dose index volume

Image pre-processing

Lung segmentation

All low-dose CT image volumes with lung window underwent the same processing pipeline, which consisted of approximate lung mask generation and extraction of regions of interest. Lung volumes were segmented from other organs and tissue in the thoracic region using the U-net model developed by Ronneberger and collaborators.[12] The U-net model is a convolutional U-shaped symmetrical neural network that won first place in the 2015 ISBI cell monitoring competition and is currently the most popular model for segmenting chest CT images.[13] Lung segmentation involved the following steps: 1) fully automated contouring of lung volume using the U-net model, 2) creation of a binary mask of lung volume, and 3) application of the acquired binary mask to the original CT images to isolate pixels associated with lung volume from those associated with other organs.

The examples of a low-dose chest CT input image are shown in Figure 1: the raw image before segmentation (a), the associated binary mask image (b), and the resulting segmented lungs (c). Initially, the U-net model classifies each pixel of the input image, resulting in a mask of lung regions to be extracted. As shown in Figure 1b, this mask assigns a value of 1 to pixels associated with the lung volume (white), and 0 to the remaining areas. Information within the segmented lung volume is utilized for model training in the next step.

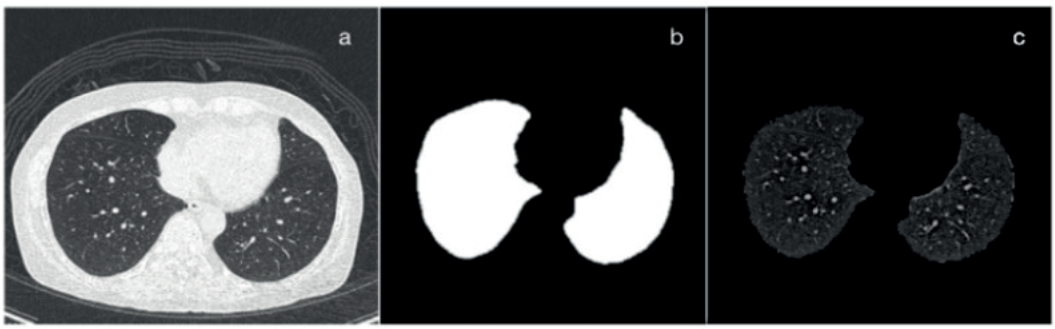

Figure 1 *Example of lung volume segmentation: (a) original image, (b) lung mask derived from the input image, (c) lung volume after segmentation.*

Slice selection

Previous studies identified the upper lobe of the lungs as the region with the highest likelihood of COPD presence.[14,15] Based on this evidence, we focused only on this region to optimize our computational resources. Slice selection was performed using in-house Python software. The first slice of segmented lung volume is determined by the presence of less than 0.5% black pixels of the selected slice. With a slice thickness of 1.0 mm and a slice interval of 0.7 mm, we uniformly sectioned slice numbers 52 to 61 in the axial direction (at a distance of 37.0-43.4 mm from the apex of the lung) based on the average lung dimensions of Thai individuals (240 mm).[16] These slices served as the center of the upper lobe. After slice selection, we obtained ten CT images for each dataset.

Following the above procedures, we obtained 10,000 input images (5,000 COPD and 5,000 non-COPD) for model training and testing. We used 90% of this dataset (9,000 images: 4,500 COPD and 4,500 non-COPD) for training and 10% (1,000 images: 500 COPD and 500 non-COPD) for testing.

The images, which initially measured 512×512 pixels, were resized to 224×224 pixels to comply with the input requirements of the model.

Model development

ResNet-50 architecture

This study adopted a pretrained ResNet-50 model, a convolutional neural network trained on the ImageNet dataset. ResNet-50 is employed as the default model to minimize the necessary input datasets and accelerate the construction of a new model for efficient classification.[17] We utilized the learned weighting factors from pre-training on ImageNet, where these factors dynamically adjust during model training, capturing the relationship between input and output data. The proposed architecture is illustrated in Figure 2.

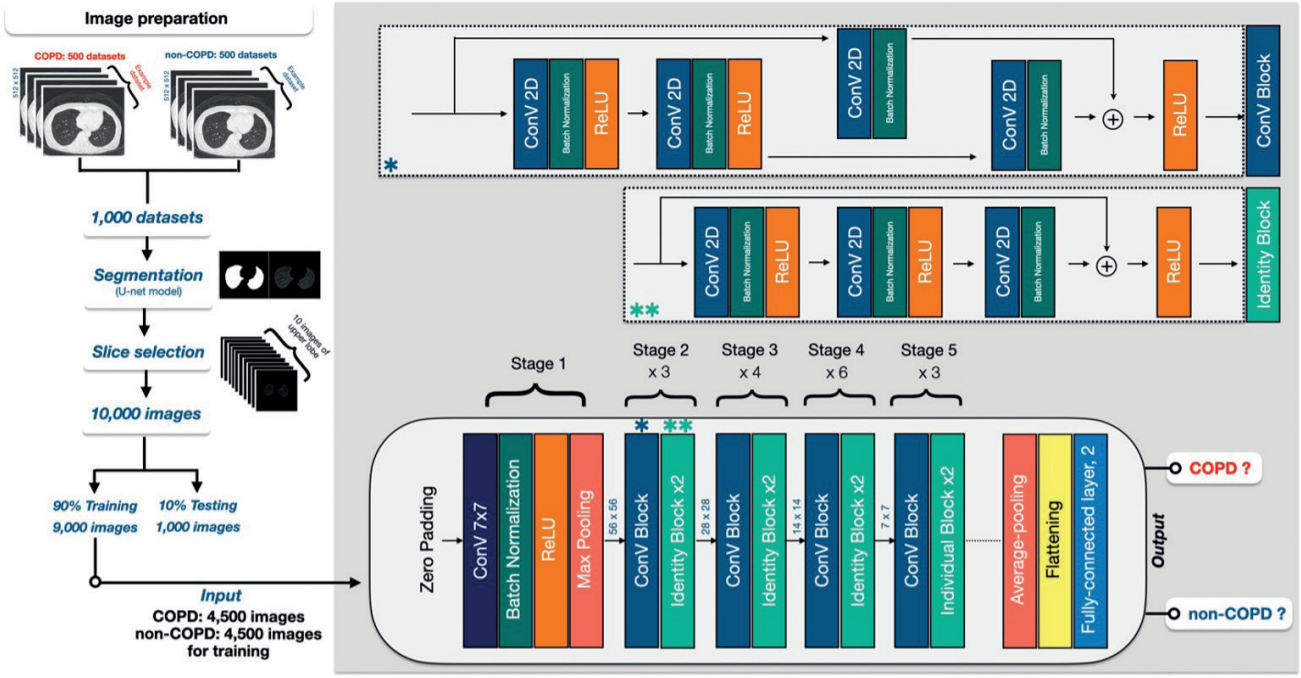

Figure 2 *Overall framework of the proposed architecture.*

Evaluation of model performance

We assessed the performance of the artificial intelligence model by analyzing the following metrics:

- A confusion matrix is a method for describing the performance of classification outcomes obtained when applying the model to the testing dataset. It consists of four fundamental characteristic values: True Positive (TP) represents the number of participants who are correctly classified as having COPD lesions under the spirometry-based diagnosis of COPD; True Negative (TN) represents the number of participants who are correctly classified as not having COPD lesions, by the spirometry-based diagnosis of non-COPD (healthy); False Positive (FP) represents the number of participants that are misclassified as suffering from COPD, in disagreement with the spirometry-based diagnosis of non-COPD (healthy); False Negative (FN) represents the number of participants misclassified as healthy, in dispute with the spirometry-based diagnosis of COPD.
- The accuracy of our model can be assessed by analyzing the values derived from the confusion matrix as follows:

a) Accuracy reflects the agreement between model predictions and spirometry-based diagnoses as detailed by equation 1:

$$\text{Accuracy} = \frac{TP + TN}{TP + TN + FP + FN} \quad (1)$$

b) Precision reflects model accuracy by comparing TP with FP, as detailed in equation 2:

$$\text{Precision} = \frac{TP}{TP + FP} \quad (2)$$

c) Recall reflects model accuracy by comparing TP with FN, as detailed in equation 3:

$$\text{Recall} = \frac{TP}{TP + FN} \quad (3)$$

d) F1-score is the average between precision and recall as indicated in equation 4:

$$\text{F1 score} = 2 \times \frac{(\text{Precision} \times \text{Recall})}{(\text{Precision} + \text{Recall})} \quad (4)$$

- Area under the receiver operating characteristic curve (AUC)

The relationship between the True Positive Rate (TPR) and False Positive Rate (FPR) is indicated by the area under the Receiver Operating Characteristic (ROC) curve. An area under the ROC curve (AUC) close to 1 indicates excellent model performance.

Results

Model implementation

We performed hyperparameter optimization to identify the highest network classification performance. This tuning procedure optimized the use of weights returned by pre-training. The best-performing pre-trained ResNet-50 network was trained with the following hyperparameters: the optimization algorithm (sgdm) for optimization algorithm, batch size (32), maximum of epochs (100), learning rate (0.0001), momentum (0.9), L2 regularization (0.0001), and L2 normalization with a gradient threshold method. The model training accuracy and loss function of ResNet-50 are presented in Figure 3.

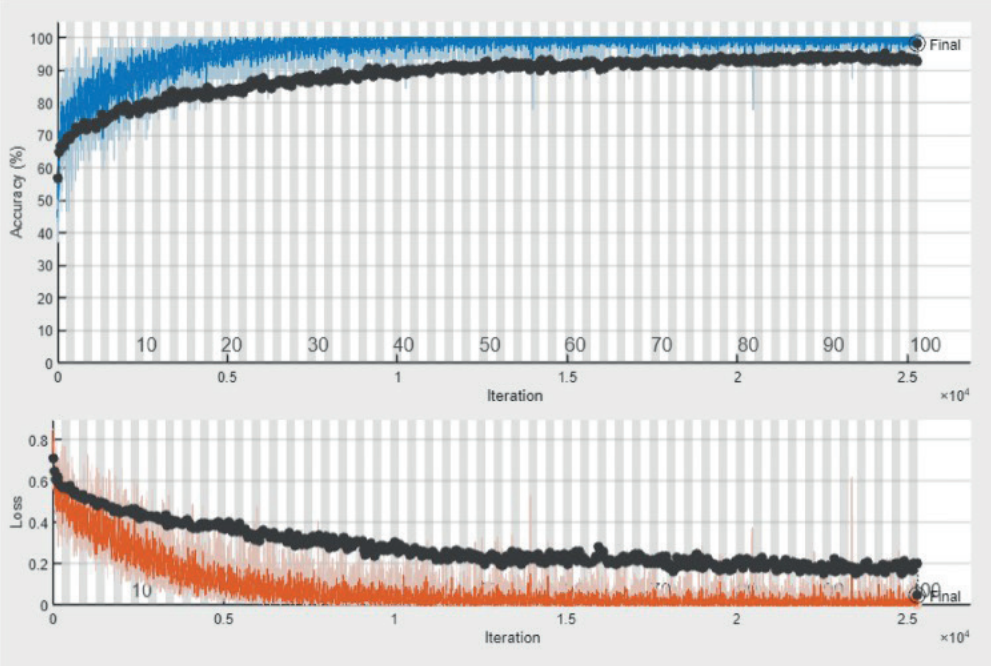

Figure 3 *Model accuracy and loss function. Upper: model training accuracy (blue) with validation accuracy (black) in the upper graph, lower: loss function (orange) with validation loss (black) after 100 epochs of training*

Model testing performance

Table 2 presents the classification results of testing images into COPD or non-COPD. The consistency between model prediction and ground truth (spirometry test) is notable, encompassing 894 images, with 481 identified as TP and 413 as TN. However, inconsistencies were observed in 106 images, with 19 identified as FN and 87 FP.

The performance evaluation of ResNet-50 achieved an accuracy of 0.89, precision of 0.85, recall of 0.96, and F1-score of 0.90. Figure 4 demonstrates the ROC curve from ResNet-50 model with AUC of 0.97. Notably, ResNet-50 demonstrated superior model performance compared with VGG16 and Inception V3 (see Table 3 and Figure 4).

Table 2 Confusion matrix of model prediction versus spirometry test.

		Spirometry test	
		COPD	non-COPD
Model prediction	COPD	481 images (TP)	87 images (FP)
	non-COPD	19 images (FN)	413 images (TN)

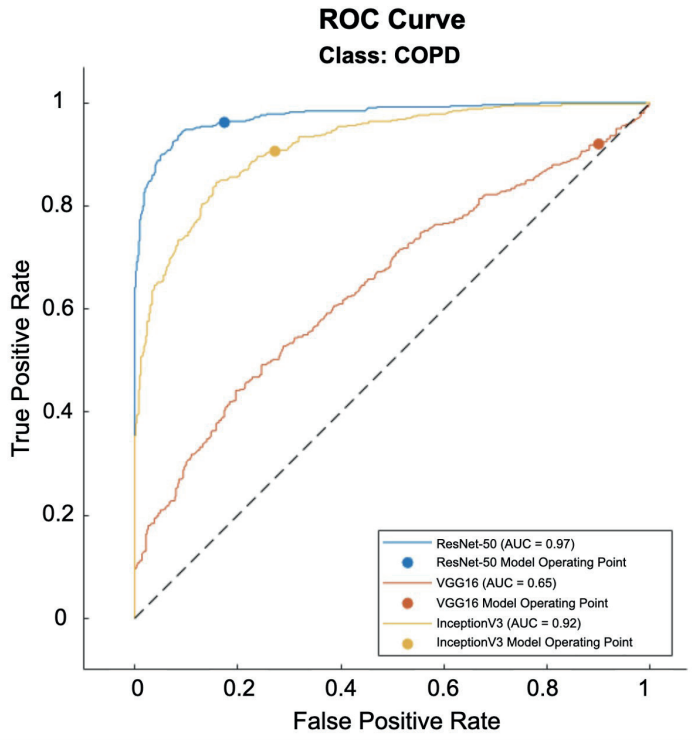

Figure 4 *Receiver operating characteristic (ROC) curve of ResNet-50, Inception V3, and VGG16.*

The performance evaluation of other pre-trained models, including Inception V3 and VGG16, was elaborated. Inception V3 achieved an accuracy, precision, recall, and F1-score of 0.82, 0.77, 0.91, and 0.83, respectively. Meanwhile, VGG16 attained an accuracy, precision, recall, and F1-score of 0.51, 0.51, 0.92, and 0.65, respectively. Each model exhibited an AUC of 0.92 and 0.65 (Figure 4), respectively, lower than that of ResNet-50. The detailed performance characteristics of Inception V3 and VGG16 are provided in supplementary figures 1-2. Furthermore, a comprehensive summary of model performance and comparative analysis with previous studies is presented in Table 3.

Table 3 The comparison of predictive model performance across previous studies

Authors	Models	Number of CT datasets	Model performance				
			AUC	Accuracy (%)	Precision (%)	Recall	F1-score
Present study	ResNet-50	1,000	0.97	89.40	84.68	0.96	0.90
	Inception V3	1,000	0.92	81.70	76.91	0.91	0.83
	VGG16	1,000	0.65	51.00	50.55	0.92	0.65
Ho TT *et al.* [18]	3D-CNN (Naive model)	596	0.93	89.30	82.60	0.88	0.85
Tang *et al.*[15]	Deep residual networks with 152 layers	2,589	0.889	n/a	74.00	0.79	n/a
González *et al.*[1]	CNN analysis	7,963	0.856	74.95	n/a	n/a	n/a

Note: AUC: area under the ROC Curve, CNN: convolutional Neural Network, 2D: two-dimensional image, 3D: three-dimensional image or volumetric data.

Discussion

The present study used a pretrained ResNet-50 to identify COPD from low-dose CT images. Specifically, we capitalized on clinical evidence indicating a prominent presence of COPD lesions in the upper lobe of the lung. This observation prompted us to focus only on upper lung slices, rather than the whole lung, as input to the model, to reduce computational time and workload. Remarkably, the proposed model achieved an AUC value of 0.97, accuracy of 0.89, precision of 0.85, recall of 0.96, and F1-score of 0.90. The performance of our model is comparative with previous studies [1,15,18] (see Table 3). Notably, we achieved comparable predictive efficacy using a significantly smaller number of participants than the previous studies.[1,15]

While our model demonstrated acceptable performance for classifying COPD, the confusion matrix revealed 87 instances of non-COPD images being misclassified as COPD, and 19 misclassified as non-COPD. These instances of misclassification may be attributed to inaccuracies in labeling the COPD input during the training phase. While it is the case that COPD participants were labeled using the gold standard method of spirometry testing, we cannot be sure that all images from these participants necessarily contain COPD lesions. Some slices without lesions were labeled and integrated into the COPD training set. Consequently, the model may have misinterpreted and erroneously classified some non-COPD images as COPD during the testing phase. Future studies should establish robust techniques to improve the accuracy of input labeling.

To develop a more precise and reliable COPD classification, we must acknowledge and address certain limitations of our study. First, given that over half of the COPD patients were categorized into GOLD stage 1 (mild COPD), there is a potential concern that the model could misclassify them as usual. This observation underscores the importance of future studies with larger populations representing each COPD stage. Such studies could facilitate the development of more robust classification models capable of distinguishing between COPD and non-COPD individuals, as well as accurately identifying different COPD stages.

Second, the reliance on spirometry to label individuals as COPD or non-COPD introduces potential uncertainties when using 2D CT images as input to the model. While we deliberately tried to incorporate ten slices from the upper lobe of labeled COPD individuals, this approach does not guarantee the presence of COPD lesions in all slices. It is, therefore, advisable to submit all input images to thorough verification by experienced radiologists, thereby ensuring precise and reliable labeling. This verification process may entail the exclusion of numerous images, which may potentially result in an inadequate number of images for training. Training with 3D input data may address this issue. A 3D image of the entire lung or some relevant part from an individual labeled as COPD may guarantee the inclusion of COPD lesion characteristics for each training input. Although the adoption of 3D input data is promising,[1,15,18] it is essential to balance performance optimization and computational feasibility.

Additionally, no practical protocol for selecting specific lung regions has been established yet. Thus, further research and refinement are warranted to determine the most pragmatic and effective means of harnessing 3D input data for improved classification performance. Striking a balance between computational feasibility and the comprehensive representation of essential features remains a central challenge.

In addition to substantial computational demands, implementing 3D input data requires a significantly larger dataset to ensure the availability of a sufficiently large training dataset. A viable solution to this problem may involve collaborations among multiple centers, to collect more diverse and extensive datasets.[19] Such collaborative efforts have the potential to enrich the variety and representation of COPD cases, allowing models to generalize across different patient populations. However, to effectively utilize CT datasets from diverse sources, careful standardization and normalization procedures must be implemented.[20] These essential procedures could address differences in imaging protocols, acquisition parameters, and equipment variations.[19]

Third, we specified the upper lobe of all lungs at slice numbers 52 to 61, guided by the average lung dimensions observed in Thai individuals.[16] Nevertheless, individual lung sizes may vary due to age, ethnicity, and physiological profiles. Future studies should consider implementing advanced segmentation techniques[21,22] for the precise delineation of individual lungs before their division into distinct components. This refined approach would enable the accurate selection of the upper portion of each lung as input for the model, thereby enhancing the precision and customization of assessments.

Lastly, k-fold validation is a fundamental feature that addresses the common challenge of overfitting in deep learning. By adopting batch image processing and implementing k-fold validation, the generalization capacity and accuracy of the model are significantly enhanced. These critical steps contribute to a more robust and reliable classification system, minimizing overfitting concerns and bolstering the ability of the model to handle diverse datasets effectively.[23,24]

Conclusion

In conclusion, our study provides empirical evidence supporting the efficacy of deep learning for classifying COPD from non-COPD cases using low-dose CT images. Notably, our model achieved 89.40% accuracy using less input data than previous studies. This result highlights the potential utility of our model as a pre-screening aid for radiologists, particularly in lung cancer programs for smokers. It may also serve as a valuable screening tool for COPD in participants who may be limited in their ability to undergo spirometry. In the future, this model may be able to classify COPD severity if provided with sufficient data.

Additionally, the incorporation of activation maps shows promise for highlighting precise lesion locations and expediting diagnosis. Ultimately, diagnostic aids in deep learning models may offer invaluable insights for

radiologists and clinicians, enhancing clinical observations and patient follow-up care. These advancements elevate the diagnostic process, rendering it more accurate and efficient.

Acknowledgements

We would like to express our sincere gratitude to Chulabhorn Royal Academy for the generous support through grant number RAA2564/036 and RCP2555/002. In addition, we would like to extend our appreciation to all the participants in Chulabhorn Royal Academy Integrated Lung Cancer Screening Program.

References

[1] González G, Ash SY, Vegas-Sánchez-Ferrero G, Onieva JO, Rahaghi FN, Ross JC, *et al*. Disease staging and prognosis in smokers using deep learning in chest computed tomography. Am J Respir Crit Care Med. 2018; 197(2): 193-203. doi: 10.1164/rccm.201702-0388OC.

[2] MacNee W. Pathology, pathogenesis, and pathophysiology. BMJ. 2006; 332(7551): 1202-4. doi: 10.1136/bmj.332.7551.1202.

[3] Global strategy for the diagnosis, management, and prevention of chronic obstructive pulmonary disease [Internet]. 2024. Available from: https://goldcopd.org/2024-gold-report/. Accessed February 18, 2024.

[4] Lamprecht B, Soriano JB, Studnicka M, Kaiser B, Vanfleteren LE, Gnatiuc L, *et al*. Determinants of underdiagnosis of COPD in national and international surveys. Chest. 2015; 148(4): 971-85. doi: 10.1378/chest.14-2535.

[5] Johns DP, Walters JA, Walters EH, *et al*. Diagnosis and early detection of COPD using spirometry. J Thorac Dis. 2014; 6(11): 1557-69. doi: 10.3978/j.issn.2072-1439.2014.10.11.

[6] Coates AL, Graham BL, McFadden RG. Spirometry in primary care. Can Respir J. 2013; 20(1): 13-22. doi: 10.1155/2013/485906.

[7] Cooper BG. An update on contraindications for lung function testing. Thorax. 2011; 66(8): 714-23 doi: 10.1136/thx.2010.140236.

[8] Gierada DS, Black WC, Chiles C, Pinsky PF, Yankelevitz DF, *et al*. Low-dose CT screening for lung cancer: Evidence from 2 decades of study. Radiol Imaging Cancer. 2020; 2(2): e190058. doi: 10.1148/rycan.2020190058.

[9] Nawa T. Low-dose CT screening for lung cancer reduced lung cancer mortality in Hitachi City. Int J Radiat Biol. 2019; 95(10): 1441-6. doi: 10.1080/09553002.2019.1614235.

[10] Larke FJ, Kruger RL, Cagnon CH, Flynn M, McNitt-Gray MM, Wu X, *et al*. Estimated radiation dose associated with low-dose chest CT of average-size participants in the National Lung Screening Trial. AJR Am J Roentgenol. 2011; 197(5): 1165-9. doi: 10.2214/AJR.11.6707.

[11] Bailey KL. The importance of the assessment of pulmonary function in COPD. Med Clin North Am. 2012; 96(4): 745-52. doi: 10.1016/j.mcna.2012.03.009.

[12] Ronneberger O, Fischer P, Brox T. U-Net: Convolutional Networks for Biomedical Image Segmentation. Springer International Publishing; 2015. p. 234-41.

[13] Tan W, Huang P, Li X, Ren G, Chen Y, Yang. J. Analysis of segmentation of lung parenchyma based on deep learning methods. J Xray Sci Technol. 2021; 29(6): 945-59. doi: 10.3233/XST-218010.

[14] Nemec SF, Bankier AA, Eisenberg RL. Upper lobe-predominant diseases of the lung. AJR Am J Roentgenol. 2013; 200(3): W222-W237. doi: 10.2214/AJR.12.9544.

[15] Tang LYW, Coxson HO, Lam S, Leipsic j, Sin D. Towards large-scale case-finding: Training and validation of residual networks for detection of chronic obstructive pulmonary disease using low-dose CT. Lancet Digit Health. 2020; 2(5): e259–e267. doi: 10.1016/S2589-7500(20)30100-1.

[16] Bradley P, Fuhrman M, Zimmerman M. Pediatric critical care (Fourth Edition). St. Louis; 2011.

[17] He K, Zhang X, Ren S, Sun J, editors. Deep Residual Learning for Image Recognition. 2016 IEEE Conference on Computer Vision and Pattern Recognition (CVPR); 2016 27-30 June 2016.

[18] Ho TT, Kim T, Kim WJ, Lee CH, chae KJ, Bak SH, *et al*. A 3D-CNN model with CT-based parametric response mapping for classifying COPD subjects. Sci Rep. 2021; 11: 34. doi: 10.1038/s41598-020-79336-5.

[19] Gierada DS, Bierhals AJ, Choong CK, Bartel ST, Ritter JH, Das NA. et al. Effects of CT section thickness and reconstruction kernel on emphysema quantification relationship to the magnitude of the CT emphysema index. Acad Radiol. 2010; 17(2): 146-56. doi: 10.1016/j.acra.2009.07.025.

[20] Selim M, Zhang J, Fei B, Zhang GQ, Chen J. STAN-CT: Standardizing CT Image using Generative Adversarial Networks. AMIA Annu Symp Proc. 2020; 2020: 1100-9.

[21] Ait Skourt B, El Hassani A, Majda A. Lung CT Image Segmentation Using Deep Neural Networks. Procedia Computer Science. 2018; 127: 109-13.

[22] Murugappan M, Bourisly AK, Prakash NB, Sumithra MG, Acharya UR. et al. Automated semantic lung segmentation in chest CT images using deep neural network. Neural Comput Appl. 2023; 35(21): 15343-64. doi: 10.1007/s00521-022-07399-7.

[23] Rodriguez JD, Perez A, Lozano JA. Sensitivity analysis of k-fold cross validation in prediction error estimation. IEEE Trans Pattern Anal Mach Intell. 2010; 32(3): 569-75. doi: 10.1109/TPAMI.2009.187.

[24] Anguita D, Ghelardoni L, Ghio A, Oneto L, Ridella S. The 'K' in K-fold cross validation. In: ESANN 2012 proceedings, European Symposium on Artificial Neural Networks, Computational Intelligence and Machine Learning. Bruges (Belgium), 25-27 April 2012. i6doc.com publ. ISBN 978-2-87419-049-0. Available from: https://www.esann.org/sites/default/files/proceedings/legacy/es2012-62.pdf.

Journal of Associated Medical Sciences 2024; 57(2): 157-165

JAMS
Journal of Associated Medical Sciences

Scopus Indexed & Thai-Journal Citation Index Centre (TCI)

Journal of Associated Medical Sciences

Journal homepage: https://www.tci-thaijo.org/index.php/bulletinAMS/index

Community rehabilitation by the trained village health volunteers on activities of daily living and quality of life in stroke survivors

Pisak Chinchai[1*] Siriphan Kongsawasdi[2] Pornpen Sirisatayawong[1] Sopida Apichai[1] Busaba Chuatrakoon[2] Nipaporn Thonglorm[2]

[1]Department of Occupational Therapy, Faculty of Associated Medical Sciences, Chiang Mai University, Chiang Mai Province, Thailand.
[2]Department of Physical Therapy, Faculty of Associated Medical Sciences, Chiang Mai University, Chiang Mai Province, Thailand.

ARTICLE INFO

Article history:
Received 3 February 2024
Accepted as revised 17 April 2024
Available online 24 April 2024

Keywords:
Functional ability, cerebrovascular disease, basic activities of daily living, instrumental activities of daily living, hemiplegia.

ABSTRACT

Background: The number of people with disabilities resulting from strokes is increasing in Thailand. The major sequela of the disease was weakness in one side of the body that causes difficulty in activities of daily living (ADL) and poor quality of life (QOL) for stroke survivors. Community-based rehabilitation could be one of the strategies that enhances functional performance and improves QOL in these individuals. There were many disabled people in Mae Ka subdistrict, San Pa Tong District, Chiang Mai Province, where health care providers and local people were enthusiastic to take care of each other's health in the community.

Objective: The present study aimed to investigate rehabilitation outcomes in ADL and QOL of stroke participants who received rehabilitation services from trained village health volunteers (VHVs).

Materials and methods: This study was a quasi-experimental research design. Subjects were recruited using purposive sampling, including 10 stroke survivors. Instruments used were 1) ADL Assessment for Occupational Therapy Clients; and 2) World Health Organization Quality of Life Assessment, Short Form-Thai version. The statistics used were descriptive, as well as the Wilcoxon Signed Ranks Test.

Results: Results demonstrated that scores of basic activities of daily living (BADL) in the participants increased significantly (p<0.05) except for sexual expression. The score in the instrumental activities of daily living (IADL) was also significantly higher at post-rehabilitation than pre-intervention (p<0.05), as was the total ADL score. Stroke patients had significantly higher QOL scores after intervention than the pretest (p<0.05).

Conclusion: These indicated that the community rehabilitation center at Mae Ka Subdistrict Administrative Organization, San Pa Tong District, Chiang Mai Province, run by the trained VHVs could promote ability in daily activities and improve QOL in stroke participants who come for their services.

Introduction

Stroke is the leading cause of death and long-term disability in those who survive.[1,2] In 2012, stroke mortality was 30.7 per 100,000 people in Thailand,[3] and this increased to 44.8 in 2014, 47.8 in 2017, and 52.8 in 2020.[3-5] In 2016, the total recorded incident rate of stroke was 451.4 per 100,000 people, which increased to 467.5 in 2017, 506.2 in 2018, and 542.54 in 2019.[4] Approximately 90% of stroke victims suffer from the sequelae of stroke, mainly weakness of the muscles and sensory deficits on the affected side, problems with uncontrolled muscle spasms, perception and cognition disorders, blurry or double vision, problems with chewing and swallowing

∗ **Corresponding contributor.**
Author's Address: *Department of Occupational Therapy, Faculty of Associated Medical Sciences, Chiang Mai University, Chiang Mai Province, Thailand.*
E-mail address: pisak.c@cmu.ac.th
doi: 10.12982/JAMS.2024.038
E-ISSN: 2539-6056

(dysphagia), etc. which resulted in these disabled people lacking the ability to do various activities in daily life, and many have to depend on others and have a poor quality of life.[6-8]

After the stroke, it has a significant impact on daily life activities for those who survive. Activities of daily living (ADL) are generally divided into two aspects.[9] One is the basic activities of daily living (BADL), which refer to daily routine activities that people perform regularly in their everyday lives.[9,10] The other is instrumental activities of daily living (IADL), which refer to activities that are more complex than the BADL and mostly require the use of equipment or tools to accomplish the tasks.[11] Walker, Leonardi-Bee, Bath, Langhorne, Dewey, Corr, *et al*.[12] found in their study of the data meta-analysis of community occupational therapy (OT) for stroke individuals that community OT significantly improved personal ADL (e.g., dressing, washing, feeding) and extended ADL (walking, domestic skills, leisure). Park, and Lee found in their study of the effects of community-based rehabilitation on ADL in chronic stroke survivors that the program improved ADL performance significantly.[13] Lee, Lee, Choi, and Pyun found in their study of community integration and QOL in aphasia after a stroke that score of QOL significantly correlated with ADL performance, which indicated that enhancement of ADL abilities could promote QOL of these individuals.[14]

For those unable to do daily activities by themselves, it may cause a poor quality of life. Hopman, and Verner noted in their study of QOL in 85 stroke patients at 6 months post-discharge from hospital without community rehabilitation that 5 of the 8 domains in QOL in these survivors, as measured by the SF-36, declined significantly.[15] The term quality of life has many definitions. This can be summarized as the level of satisfaction that has been met in terms of physical, mental, social, and various goal achievements in life.[16]

In Thailand, rehabilitation services are mostly still in hospital institutes, while those with permanent paralysis or various chronic diseases still require continuous care even when returning to the home.[17] Today, many communities are health conscious. There has been an effort by people in the community to help each other take care of each other's health in their localities. Personnel who play an essential role in this group are village health volunteers (VHVs). Some communities, led by local organizations such as subdistrict municipalities and subdistrict administrative organizations (SAOs), have set up rehabilitation centers in their localities to provide health care and essential rehabilitation for people with disabilities in the community. The VHVs, trained by medical personnel such as occupational therapists (OTs) and physical therapists (PTs), are providers of care for service recipients in the community. According to the Act Promotion and Development of Quality of Life for Persons with Disabilities, B.E. 2007, Section 20/3, local government units are allowed to establish service centers for persons with disabilities with their own budget.[18] A previous similar study to this research project was conducted by Chinchai, Sirisatayawong, and Jindakum, who investigated community integration and QOL of stroke survivors who received rehabilitation from the trained VHVs twice a week for 12 weeks (a total of 24 times) in four community rehabilitation centers, revealed that stroke participants had better community integration skills and QOL at the posttest than the pretest.[19] However, it is not easy for stroke individuals and family caregivers who live in the community to prepare themselves to come for services as many as twice a week. A lower frequency of services, for example, once a week, could be an alternative that may encourage more participation from these groups of people.

Mae Ka SAO, San Pa Tong District, Chiang Mai Province, is classified as one of the SAOs, with administrators and personnel who are responsible for caring for the health and welfare of the people being very alert. There is an idea to open a rehabilitation center to care for disabled people in their area, with VHVs who have received training in basic rehabilitation from PTs and OTs as service providers. Mae Ka subdistrict has a total population of 7,258 people, divided into 3,473 men, 3,785 women (from a survey as of February 2014).[20] Of these, there are a total of 343 registered disabled people, most of whom are persons with physical and movement disabilities, which includes people who are disabled due to stroke.[20]

The researcher is therefore interested in such a rehabilitation center, with service providers being the trained VHVs who live in that community, and how this affects the ability to do daily activities and the QOL of stroke patients before and after receiving once a week of the service.

Materials and methods

Study Design

This study was a quasi-experimental research design that compared the ability to do daily activities and QOL of stroke participants before and three months after receiving services at the community rehabilitation center, Mae Ka SAO, San Pa Tong District, Chiang Mai Province.

Participants

Stroke patients who were residents of Mae Ka SAO, San Pa Tong District, Chiang Mai Province, came to receive treatment at the rehabilitation center at Mae Ka SAO from July 2022 to September 2022. There was a total of 16 stroke clients during this period.

The sample was selected using a purposive sampling method according to the inclusion criteria as follows:

1. Be a person who has been discharged from the hospital and at home for over 3 months. This is because we can only accept stroke recipients with stable medical symptoms to come to services at the community rehabilitation center. The medical doctor prescribed medicine to the patients around 2 to 3 months after discharge from the hospital until the subsequent follow-up to check if their physical condition was stable at home.
2. There are no complications that are obstacles or risk factors for rehabilitation activities, such as

uncontrolled high blood pressure, heart disease, pressure sores, etc.
3. Do not regularly receive rehabilitation services at other rehabilitation centers.
4. Be a person who can come to receive services at the rehabilitation center once a week, for 1.5 hours each time, for 12 weeks (a total of 12 times).
5. Willing to participate in the research.

From a total population of 16 stroke recipients, 12 were selected as a sample according to the inclusion criteria.

Withdrawal criteria

People who receive services at a community rehabilitation center less than 80 percent of the designated time (less than 10 times out of 12 times).

Instrument

Data was collected using a general socio-demographic questionnaire for people with disabilities. In addition, there are tools to collect data on study variables, including.

1. Activities of Daily Living (ADL) Assessment for Occupational Therapy Clients: It is a tool used to measure the ability to perform daily activities in people with disabilities, especially those suffering from stroke. This instrument was developed by Apichai, Chinchai, Dhippayom, and Munkhetvit.[21] This tool has Likert scales for scoring ability in each activity in five levels, ranked from 1 to 5, where 1 means unable to do activities independently or can do it yourself less than 25% (dependence), and 5 means able to do that activity normally, you can do it yourself with the help of equipment, or you can do it yourself but have someone to guide you. There are two main aspects of daily activities: 1) Basic activities of daily living (BADLs), divided into self-care, functional mobility, and sexual expression. There are 23 questions in this aspect of the test: 2) Instrumental activities of daily living (IADLs), daily routines that require the use of tools or equipment, which has 12 test questions in this aspect of daily routines. The total possible score on the test from both aspects ranges from 35 to 175 points. This instrument has been explored for its psychometric properties with 45 stroke survivors and 45 normal adults. The results found that this test had an inter-rater reliability value of 0.98 and an internal consistency value with the Cronbach's alpha coefficient of 0.88. The results of the known-groups validity test found that stroke participants demonstrated significantly lower scores than normal adults (p<0.001), indicating good construct validity of the instrument.[21]
2 World Health Organization Quality of Life Assessment, Short Form-Thai version (WHOQOL-BREF-THAI), which has been updated and translated into Thai by Mahatnirunkul, Tuntipivatanaskul, Pumpisanchai, Wongsuwan, and Ponmanajirungkul.[22] This tool has 26 items that cover four components of quality of life: the physical, the psychological, the social relationship, and the environmental aspects. There are 5 levels of scoring criteria based on Likert scales, arranged from 1 to 5. Questions with opposing meanings are scored in reverse. Possible scores are 26-130 points with the following criteria: 1) scores of 26-60 mean having a poor quality of life; 2) a score of 61–95 means having a moderate quality of life; and 3) a score of 96-130 means having a good quality of life.[22] The reliability of this tool, calculated by the Cronbach's alpha coefficient, was 0.8406, and its concurrent validity was 0.6515. The reliability of WHOQOL-BREF-THAI in patients with chronic diseases such as HIV/AIDS revealed that the Cronbach's alpha ranged from 0.61 to 0.81 across domains.[23] This tool can be used to measure an indicator of treatment or a health intervention program.[22] It can also be used to assess the changes in quality of life resulting from treatment.[22] In cases where the respondent is old and cannot read, data collection may be used in the interview format. In a pilot study for the reliability of this tool among 15 stroke survivors who lived in Chaing Mai province, the result, as determined by Cronbach's alpha coefficient, was 0.84.[24]

Procedure

1. Following the ethics approval from the Human Research Ethics Committee, Faculty of Associated Medical Sciences, Chiang Mai University, the main researcher contacted the mayor of Mae Ka SAO, San Pa Tong District, Chiang Mai Province, to request permission to use the SAO's rehabilitation center as a place to implement the rehabilitation program for people with disabilities and conduct research.
2. The researcher prepared rehabilitation training equipment for stroke participants: a walking rail and steps, a training bed, arm and hand training equipment, tables, and chairs for practicing activities, etc.
3. The researchers coordinated with the SAO and Subdistrict Health Promotion Hospital officials to make an appointment to organize a basic rehabilitation training program for the VHVs. In selecting the VHVs for the study, officials from Mae Ka's SAOs asked for the village headman's cooperation in posting invitation announcements at the village headman's house and making announcements using voice calls in the village to invite. We recruited two VHVs per village. As there are 14 villages in this subdistrict, 28 VHVs were accepted by those who applied first. After the program, there was a posttest of the knowledge and training skills of VHVs. The questions in the test were drawn from the 2-day training program

by the PTs and OTs who conducted the practice session. Those who pass the test could be able to become service providers at the rehabilitation center. Those who received better scores have a higher chance of being selected. The training took two days, as we believed it was sufficient for this group's basic rehabilitation knowledge and skills. In addition, the VHVs of this community have received one to two weeks of training in caring for bedridden patients and caring for people with disabilities, in general, every year. In the two days of the program, the first day was a presentation of theoretical knowledge, and the second was a practical training session, starting from 8:30 am. to 4:30 pm. each day. In the theory section, OT taught basic knowledge of stroke in terms of risk factors, causes, symptoms, consequences, stroke rehabilitation, and psychological support. In the practice session, OTs trained the VHVs on proper positioning (lying, sitting, and standing), hand function, and ADL techniques for stroke. PTs trained the VHVs in general exercise (passive and active), bed mobility, weight training, balance (sitting and standing), and walking with and without aids.

4. The researchers visited the homes of the stroke disabled together with VHVs to screen the samples according to the inclusion criteria and invited them to participate in this research project. Home visits were conducted in all 14 villages of the Mae Ka SAO.
5. The researchers and the officials at Mae Ka SAO selected 12 VHVs who passed the training exam, arranged in order of their test scores, to be service providers at the rehabilitation center. Services are provided weekly, Tuesday, and Friday, 9:00 am. To 12:00 pm., and there are two VHVs working each day. The researchers and team, who are OTs and PTs, were the people who assessed people with disabilities together with the VHVs and recommended individual treatment methods for the VHVs. The recommended treatment is essential rehabilitation with training methods according to a structured program where there is no or minimal risk of injury to the stroke participants. The VHVs can provide rehabilitation such as passive and active range of motion (ROM) to the joints, strengthening exercise to the muscles, functional movement of the affected extremity, walking locomotion, and ADL training, all upon the recommendation of the OTs and PTs. One VHV could take care of two to three disabled people each day. Each disabled person received rehabilitation for 12 weeks, once per week, for one hour and 30 minutes each time, for 12 times. Before every training session, VHVs measured blood pressure, checked the vital signs of all stroke participants, and asked about general physical symptoms. Medicines and first-aid equipment are prepared at the center. Mae Ka SAO's emergency vehicles are always available when rehabilitation services are being provided to service recipients.
6. A research assistant (RA), who is an occupational therapist (OT) with more than five years of experience working with stroke patients and does not know the research objectives, and who has been trained in using research tools, collected data on the study variables within seven days before the disabled person received rehabilitation. Data collection was conducted at the homes of disabled people. When the disabled person was uncomfortable participating in the data collection process at home, the RA made an appointment with stroke subjects to meet at the community rehabilitation center, where Mae Ka SAO vehicles pick up disabled people at convenient times during official hours. Data were collected again within seven days after the disabled person received 12 weeks of rehabilitation. To prevent differences in environmental conditions that may affect the study variables, for those with disabilities who first collected information at home, data collection will be conducted at home the second time. In the same way, disabled people initially received data collection at a community rehabilitation center. The second time, the data was collected at the rehabilitation center.
7. When the VHVs provided services to people with disabilities at the rehabilitation center, the researchers, both OTs and PTs, visited the work of the VHVs once every two weeks to see what they needed to help with. The VHVs could also immediately contact OTs and PTs via phone if they have a problem or want to ask about rehabilitation issues.

Data Analysis

Descriptive statistics for the demonstration of socio-demographic data in the sample. As the data in the study variables were not normally distributed, a Wilcoxon Signed Rank test was used to see differences in these variables before and after receiving the rehabilitation program. Statistical significance was set at $p<0.05$. The effect size (Cohen's d) was also calculated to demonstrate the practical significance of the study's findings. The intermediate or medium (d ranges from 0.45 to 0.75) and large effect sizes (d>0.75) were preferable as these indicate significant practical results from the experiment.[25]

Results

Of the 12 stroke participants selected according to the study criteria, two subjects were withdrawn due to participating in rehabilitation for less than 80 percent of the designated time. There was a total of 10 participants remaining in the research project. The results of the study can be shown as follows:

Data from Table 1 show that the majority (80%) of the sample were married, the level of education is mainly at the primary level, and almost all of them (80%) suffered

from stroke for more than two years. Data from Table 2 show that the sample's BADL ability in nearly all aspects and the total BADL, except sexual expression, improved significantly (p<0.05). Participants also significantly improved the IADL, as was the total ADL (p<0.05). Data from Table 3 show that every aspect of the sample's QOL, including the overall QOL, improved significantly (p<0.05).

Table 1. Socio-demographic information in stroke participants (N=10).

Variables		Number
Sex	Male	6
	Female	4
Age (year)	51-60	4
	61-70	3
	71-80	3
	Mean±SD = 64.60±10.68	
	Minimum = 51, Maximum = 80	
Marital status	Married	8
	Divorced	1
	Widowed	1
Education level	Elementary	8
	Secondary	1
	College/University	1
Body affected side	Left	6
	Right	4
Diagnosis	Hemorrhagic stroke	4
	Thrombotic stroke	3
	Embolic stroke	3
Time since onset (month)	<12	1
	13-24	1
	>24	8
Time since discharged from hospital (month)	<12	1
	13-24	1
	>24	8
Motor recovery (Brunnstrom stages)	3	4
	4	1
	5	5
Caregiver	Spouse	6
	Son/daughter	2
	Relatives	2

Table 2. Comparisons of the activities of daily living in stroke participants before and after receiving the rehabilitation program (N=10).

ADL			Median (Q3-Q1)	*p* value	Effect size
BADL**	Self-care	Pretest	92.9 (98.1-76.3)	0.012*	0.56
		Posttest	100 (100-86.3)		
	Bed mobility	Pretest	95.0 (100-88.8)	0.039*	0.46
		Posttest	100 (100-95.0)		
	Transferring	Pretest	45.7 (80.0-26.4)	0.018*	0.53
		Posttest	80.0 (88.9-45.7)		
	Locomotion	Pretest	80.0 (100-75.0)	0.020*	0.52
		Posttest	100 (100-87.5)		
	Sexual expression	Pretest	4.5 (5.0-2.5)	0.317	0.22
		Posttest	5.0 (5.0-2.5)		
	Total BADL	Pretest	77.9 (89.1-70.7)	0.008*	0.60
		Posttest	92.4 (95.8-75.4)		
IADL***	Total IADL	Pretest	48.2 (79.6-29.4)	0.012*	0.56
		Posttest	62.7 (87.4-30.0)		
Total ADL	BADL + IADL	Pretest	69.7 (86.2-62.2)	0.008*	0.60
		Posttest	85.6 (93.1-64.9)		

*Note: *statistically significant, **BADL stand for Basic activities of daily living, ***IADL stand for Instrumental activities of daily living*

Table 3. Comparisons of QOL in stroke participants before and after receiving the rehabilitation program (N=10).

QOL		Median (Q3-Q1)	*p* value	Effect size
Physical	Pretest	18.0 (24.0-15.0)	0.009*	0.58
	Posttest	22.0 (26.0-20.0)		
Mental	Pretest	19.0 (25.0-18.0)	0.024*	0.50
	Posttest	23.0 (24.0-20.0)		
Social relationship	Pretest	9.0 (10.0-7.0)	0.027*	0.50
	Posttest	10.0 (11.0-9.0)		
Environmental	Pretest	23.0 (25.0-22.0)	0.007*	0.60
	Posttest	28.0 (30.0-25.0)		
Total QOL	Pretest	74.0 (93.0-67.0)	0.008*	0.60
	Posttest	90.0 (96.0-82.0)		

*Note: *Statistically significant.*

Discussion

The results of the study can be discussed as follows:

Activities of daily living ability

The results of the present study found that almost every aspect of the sample's ability to do BADL and the total BADL, except sexual expression, improved significantly (p<0.05), with medium effect sizes (Table 2). The BADL includes self-care activities, bed mobility, transferring, wheelchair propelling, and walking locomotion. This is likely because rehabilitation service providers at Mae Ka community rehabilitation center are the VHVs who have been trained to have the ability to care for people with disabilities in these BADL. BADL is a preliminary activity that requires training for people with disabilities to engage to their potential. This is consistent with the study of Chinchai and Kongsawasdi[26,] who studied the ability to perform daily activities of 11 stroke survivors who received a rehabilitation program at the community rehabilitation center of Doi Lor SAO, Doi Lor District, Chiang Mai Province. The stroke participants in that study received twice a week of rehabilitation for 8 weeks, provided by the VHVs who have been trained in the basic rehabilitation program, and the results revealed that the stroke subjects had better ability in BADL. However, the essential daily routine of sexual expression in the present study has not changed significantly from before and after the program. This may be because, in the general social context of many places, sexual communication is still a subject that people still find shameful and sensitive,[27] especially in Asian countries, including Thailand. Therefore, disabled people themselves will avoid talking about sexual problems. Health professionals, themselves, are underprepared to address sexuality with stroke survivors and rarely provide information or ask about sexuality.[28,29] Moreover, service providers (VHVs) in the present study do not have adequate training or knowledge in this area to provide counseling to disabled people.

For the results of the ability to do IADL in the sample group, it was found to be significantly improved (p<0.05) with a medium effect size comparing before and after receiving the rehabilitation program (Table 2). This is likely because daily routines that use assistive devices in the IADL, such as caring for others, traveling within the community, shopping, cooking, washing utensils, taking care of one's own health, etc., are connected to the BADL. For example, when people with disabilities can perform walking locomotion better in the BADL, it will increase their abilities to travel around the community and do better shopping, etc. in the IADL. In addition, the trained VHVs who worked at the rehabilitation center provided rehabilitation and encouraged the clients to participate in household activities such as meal preparation and clean-up and community events such as religious and spiritual activities in their own community, which increased IADL performance. Congruence with a study by Chinchai, Sirisatayawong, and Jindakum, who investigated community integration, including household activities that are like those in the IDL, in stroke survivors that received rehabilitation from the trained VHVs in four community rehabilitation centers in Chiang Mai province, Thailand.[19] The study revealed that stroke participants had significantly better scores in household and community engagement at the posttest than the pretest.

The results of the present study also demonstrated that the ability to perform the overall ADL improved after receiving the rehabilitation program, the same as BADL and IADL. This is consistent with a study by Chinchai and Kongsawasdi, which explored the ability to perform daily activities of 11 stroke subjects who received a rehabilitation program at the community rehabilitation center of Doi Lor SAO, Doi Lor district, Chiang Mai province, twice a week for eight weeks, provided by the trained VHVs.[26] The results revealed that the stroke participants had better ability to perform the BADL, IADL, and overall ADL.

Quality of Life

The results of the study demonstrated that after receiving rehabilitation programs from the trained VHVs, the stroke patients' overall QOL and all its components (physical, psychological, social interactions, and the environment) significantly improved (p<0.05) with medium effect sizes (Table 3). Beside the rehabilitation programs that the VHVs provided to disabled people, which consist of general exercise, walking locomotion, wheelchair propelling, upper extremity function training, ADL practice, etc., the VHVs also provided advice on how to behave to take care of themselves at home, such as

taking medicine as prescribed by a doctor, taking care of cleanliness of the body, making simple home modification suggestions, e.g., making handrails in the bathroom, substituting a squat toilet with the flush toilet, etc. The VHVs also encouraged stroke recipients to participate in community and social activities. In addition, when disabled people come to receive services at the rehabilitation center in the community, they could meet with peers and talk or express their feelings, discuss, and exchange knowledge about treatment with each other, etc. All these processes are essential factors that result in the improvement of QOL. Consistent with the study of Chinchai, Kongsawasdi, Kapwang, and Chanchai on the QOL and community integration of 11 stroke subjects who receive rehabilitation services from the trained VHVs at the community rehabilitation centers for eight weeks, two times a week, one hour thirty minutes each time, which demonstrated that the overall QOL of the sample improved significantly (p<0.05).[30] In addition, when the ability to ADL increases in these people, it may be a factor that leads to good QOL. According to a study by Jönsson, Lindgren, Hallström, Norrving, and Lindgren[31] that examined QOL in 304 stroke survivors at four and 16 months after the onset, functional ability was a good predictor for improving QOL. Enhancement of functional performance in daily activities in stroke individuals could induce good QOL in these people.[32-35]

Limitations

Due to the small number of samples as we conducted a study in only one community rehabilitation center, it may not be appropriate to calculate the IADL on a per-area basis because in the IADL there are 12 assessment topics, and it is not necessary for patients to complete all activities in the IADL. Patients may do one or not complete another according to their ability and necessity. This is not like BADL, where every patient must complete all aspects of their daily lives. Another limitation of the study is that the time since onset for most subjects in the present study was above 12 months (Table 1). This meant that stroke survivors who attended rehabilitation in our research were chronic, as we recruited only participants with stable medical symptoms. A study in more acute cases may need health professionals such as PTs, OTs, etc., as these require complicated therapy and many physical precautions. Another concern is that the VHVs in the present study recognized that stroke participants under their care would be evaluated for functional ability and QOL after the rehabilitation, which might affect the study results. However, these VHVs did not know the objectives of the research project, and the researchers were not involved in promoting their work positions.

Conclusion

The ability to do BADL in almost all aspects, the total IADL, and the overall daily routine of ten stroke participants were significantly improved (p<0.05) after receiving rehabilitation practices from the trained VHVs for 12 weeks, once a week, for one hour and 30 minutes each time. Except for sexual expression in the BADL, that score has not changed from pretest to posttest. The QOL scores, which consist of physical, mental, social relationship, and environmental aspects, and the overall QOL in these stroke recipients were also significantly increased (p<0.05) comparing before and after receiving rehabilitation programs. All these indicate the advantages of services provided by the trained VHVs at the Mae Ka SAO rehabilitation center, San Pa Tong District, Chiang Mai Province, to the ADL and QOL of stroke survivors in the present study.

Conflicts of Interest

The authors declared no potential conflicts of interest concerning this article's research, authorship, and/or publication.

Ethical Approval

Ethical approval was obtained from the Human Research Ethics Committee, Faculty of Associated Medical Sciences, Chiang Mai University, Thailand; project number AMSEC-64EX-002; and the ethics clearance number 069/2564.

Acknowledgements

The authors would like to thank the stroke participants who lived in Mae Ka Subdistrict, San Pa Tong District, Chiang Mai Province, who volunteered their time to participate in the study.

References

[1] Suwanwela NC. Stroke epidemiology in Thailand. J Stroke. 2014; 16(1): 1-7. doi: 10.5853/jos.2014.16.1.1.

[2] World Health Organization. Cardiovascular Diseases (CVDs) [Internet]. World Health Organization; 2021 [cited 2022 January 7]. Available from: https://www.who.int/news-room/fact-sheets/detail/cardiovascular-diseases-(cvds).

[3] Division of Non Communicable Diseases, Ministry of Public Health. Numbers and motality rate in 5 NCD Year 2016 – 2019 [Internet]. Division of Non-Communicable Diseases, Ministry of Public Health; 2020 [cited 2023 July 15]. Available from: http://thaincd.com/2016/mission/documents-detail.php?id=13893&tid=32&gid=1-020. (in Thai).

[4] Division of Non-Communicable Diseases, Ministry of Public Health. Number and mortality rate of non-communicable diseases Year 2016-2018 (Hypertension, diabetes, ischemic heart disease, cerebrovascular disease, bronchitis and chronic obstructive pulmonary disease) [Internet]. Division of Non-Communicable Diseases, Ministry of Public Health; 2022 [cited 2023 July 15]. Available from: http://thaincd.com/2016/mission/documents-detail. php?id=14220&tid=32&gid=1-020. (in Thai).

[5] Srivanichakorn S. Morbidity and mortality situation of non-communicable diseases (diabetes type 2 and cardiovascular diseases) in Thailand during 2010-

2014. Dis Control J 2017; 43(4): 379-90. doi: 10.14456/dcj.2017.4. (in Thai).
[6] Bunyamark T. Occupational therapy in stroke. In: Chinchai P, Bunyamark T, editors. Occupational therapy for persons with neurological conditions. 4th ed. Chiang Mai, Thailand: Siam Pimnana Company Limited; 2017. p. 177-202. (in Thai).
[7] Gillen G. Cerebrovascular accident/stroke. In: Pendleton HM, Schultz-Krohn W, editors. Pedretti's occupational therapy: Practice skills for physical dysfunction. 7th ed. St. Louis, MO: Elsevier Mosby; 2013. p. 844-80.
[8] Gillen G. Upper extremity function and management. In: Gillen G, editor. Stroke rehabilitation: A function-based approach. 4th ed. St. Louis, MO: Mosby; 2016. p. 424-85.
[9] Foti D. Activities of daily living. In: Pedretti LW, Early MB, editors. Occupational therapy practice skills for physical dysfunction 5th ed. St. Louis, Missouri: Mosby, Inc.; 2001. p. 124-71.
[10] Fasoli SE. Assessing roles and competence. In: Radomski MV, Latham CAT, editors. Occupational therapy for physical dysfunction. 7th ed. Baltimore, MD: Lippincott Williams &Wilkins; 2014. p. 76-102.
[11] Woodson AM. Stroke. In: Radomski MV, Latham CAT, editors. Occupational therapy for physical dysfunction. 7th ed. Baltimore, MD: Lippincott Williams &Wilkins; 2014. p. 999-1041.
[12] Walker MF, Leonardi-Bee J, Bath P, Langhorne P, Dewey M, Corr S, *et al*. Individual patient data meta-analysis of randomized controlled trials of community occupational therapy for stroke patients. Stroke. 2004; 35: 2226-32. doi: 10.1161/01.STR.0000137766.17092.fb.
[13] Park Y-J, Lee C-Y. Effects of community-based rehabilitation program on activities of daily living and cognition in elderly chronic stroke survivors. J Phys Ther Sci. 2016; 28(11): 3264-6. doi: 10.1589/jpts.28.3264.
[14] Lee H, Lee Y, Choi H, Pyun S-B. Community integration and quality of life in aphasia after stroke. Yonsei Med J. 2015; 56(6): 1694-702. doi: 10.3349/ymj. 2015.56.6.1694.
[15] Hopman W, Verner J. Quality of life during and after inpatient stroke rehabilitation. Stroke. 2003; 34(3): 801-5. doi: 10.1161/01.STR.0000057978.15397.6F.
[16] Dedhiya S, Kong SX. Quality of life: An overview of the concept and measures. Pharm World Sci 1995; 17: 141-8. doi: 10.1007/BF01879707.
[17] Chinchai P, Marquis R, Passmore A. Functional performance, depression, anxiety, and stress in people with spinal cord injuries in Thailand: A transition from hospital to home. Asia Pac Disabil Rehabil J. 2003; 7(2): 32-9.
[18] Empowerment of Persons with Disabilities Act, B.E. 2550 (2007).[cited 2024 January 19]. Available from: http://web1.dep.go.th/?q=th/node/446.
[19] Chinchai P, Sirisatayawong P, Jindakum N. Community integration and quality of life: Stroke survivors as recipients of rehabilitation by village health volunteers (VHVs) in Thailand. Occup Ther Health Care. 2020; 34(3):277-90.doi:10.1080/07380577.2020.1773010.
[20] Mae Ka Subdistrict Administrative Organization. Fundamental Data: History and general information; 2023 [cited 2024 January 19]. Available from: https://maeka.go.th/public/list/data/index/menu/1142. (in Thai).
[21] Apichai S, Chinchai P, Dhippayom JP, Munkhetvit P. A new assessment of activities of daily living for Thai stroke patients. CMU J Nat Sci 2020; 19(2): 176-90. doi: 10.12982/CMUJNS.2020.0012.
[22] Mahadnirunkul S, Tantipiwattanasakul W, Pumpaisanchai W, Wongsuwan K, Ponmanajirungkul R. Comparison of the WHOQOL-100 and the WHOQOL-BREF (26 items). J Ment Health. 1998; 5(3): 4-15. (in Thai).
[23] Sakthong P, Schommer J, Gross C, Sakulbumrungsil R, Prasithsirikul W. Psychometric properties of WHO-QOL-BREF-Thai in patients with HIV/AIDS. J Med Assoc Thai 2007; 90(11): 2449-60. (in Thai).
[24] Chinchai P, Bunyamark T, Sirisatayawong P. Effects of caregiver education in stroke rehabilitation on the quality of life of stroke survivors. World Fed Occup Ther 2010; 61(1): 56-63. doi: 10.1179/otb.2010.61.1.015.
[25] Lenhard W, Lenhard A. Computation of effect sizes 2016 [Available from: https://www.psychometrica.de/effect_size.html.
[26] Chinchai P, Kongsawasdi S. Activities of daily living performance in stroke survivors receiving services from the trained village health volunteers at Doi Lor Community Rehabilitation Center, Doi Lor District, Chiang Mai Province, Thailand. J Assoc Med Sci 2021; 54(3): 11-7.
[27] Tipton-Burton M, Delmonico R. Sexuality and physical dysfunction. In: Pendleton HM, Schultz-Krohn W, editors. Occupational therapy: Practice skills for physical dysfunction. 8th Ed. St. Louis, MO: ELSEVIER; 2018. p. 289-304.
[28] McLaughlin J, Cregan A. Sexuality in stroke care: A neglected quality of life issue in stroke rehabilitation? A pilot study. Sex Disabil. 2005; 23: 213-26. doi: 10.1007/s11195-005-8929-9.
[29] Richards A, Dean R, Burgess GH, al. e. Sexuality after stroke: An exploration of current professional approaches, barriers to providing support and future directions. Disabil Rehabil. 2016; 38: 1471-82. doi: 10.3109/09638288.2015.1106595.
[30] Chinchai P, Kongsawasdi S, Kapwang S, Chanchai N. Quality of life and community integration of stroke survivors receiving services from trained village health volunteers at the community rehabilitation center, Doi Lor Sub-district Administrative Organizations, Doi Lor District, Chiang Mai Province. J Health Sci 2022; 31: S304-S17. (in Thai).
[31] Jönsson AC, Lindgren I, Hallström B, Norrving B, Lindgren A. Determinants of quality of life in stroke survivors and their informal caregivers. Stroke. 2005; 36(4): 803-8. doi: 10.1161/01.STR.0000160873.32791.20.
[32] Abubakar SA, Isezuo SA. Health related quality of life of stroke survivors: Experience of a stroke unit. Int J Biomed Sci 2012; 8(3): 183-7.

[33] Jaracz K, Kozubski W. Quality of life in stroke patients. Acta Neurol Scand. 2003; 107: 324-9. doi: 10.1034/j.1600-0404.2003.02078.x.

[34] King RB. Quality of life after stroke. Stroke. 1996; 27(9): 1467-72. doi: 10.1161/01.STR.27.9.1467.

[35] Thanakiatpinyo T, Dajpratham P, Kovindha A, Kuptniratsaikul V. Quality of life of stroke patients at one year after discharge from inpatient rehabilitation: A multicenter study. Siriraj Med J 2021; 73(4): 216-23. doi: 10.33192/Smj.2021.29.

Journal of Associated Medical Sciences 2024; 57(2): 166-172

JAMS
Journal of Associated Medical Sciences

Scopus Indexed & Thai-Journal Citation Index Centre (TCI)

Journal of Associated Medical Sciences

Journal homepage: https://www.tci-thaijo.org/index.php/bulletinAMS/index

Development and implementation of the external quality assessment program for erythrocyte sedimentation rate in hematology laboratories in Thailand

Suwit Duangmano[1,2*] Panida Kulawong[2] Puwadon Lawapakull[2] Panida Pongpunyayuen[2] Saowanit Chairatanapiwong[2]

[1]Division of Clinical Microscopy, Department of Medical Technology, Faculty of Associated Medical Sciences, Chiang Mai University, Chiang Mai Province, Thailand.
[2]AMS CMU EQA Unit, Department of Medical Technology, Faculty of Associated Medical Sciences, Chiang Mai University, Chiang Mai Province, Thailand.

ARTICLE INFO

Article history:
Received 25 December 2023
Accepted as revised 24 April 2024
Available online 26 April 2024

Keywords:
Control materials, erythrocyte sedimentation rate, proficiency testing, quality control

ABSTRACT

Background: The erythrocyte sedimentation rate (ESR) remains the most widely used screening test for monitoring the course of infections, inflammatory diseases, and some types of cancer. Proficiency Testing (PT) programs are unavailable in Thailand for ESR.

Objective: This study aimed to develop and initiate the PT program to improve testing quality through evaluation and analysis of the laboratory test results for ESR.

Materials and methods: The PT program for ESR was established at the AMS CMU EQA Unit by the ISO/IEC17043:2010 requirements. The unit produced and sent the ESR control materials to participants for laboratory analysis; the test results were returned to the unit. The PT program was carried out in two cycles per year, with two samples in each cycle. The performance of each laboratory was assessed using robust Z score and performance score.

Results: ESR control materials presented with satisfactory homogeneity and stability according to ISO 13528: 2015. One hundred and four laboratories were enrolled in the PT program. Of these laboratories, 96 (92.3%) returned their data: 40 (42.7%) used the modified Westergren method, 29 (29.2%), 14 (15.7%), and 13 (12.4%) used Microsed, Mixrate, and other methods, respectively. Satisfactory and questionable performance was obtained in 82/96 (85.4.%) and 8/96 (8.3%), respectively. Unsatisfactory performance was noted at 6/96 (6.3%). The level of excellent performance was achieved by 82 (approx. 85%) of these laboratories. Two main types of errors found from analyzing the received data were (i) specimen processing and (ii) incorrect identification of the analytical method.

Conclusion: Our results indicate that the advantage of participation in the PT program for ESR is that the laboratories can monitor and investigate the source of laboratory errors. Therefore, the PT program for ESR testing should become an integral part of the quality assurance system in the laboratory.

Introduction

The erythrocyte sedimentation rate (ESR) test is commonly used in clinical laboratories that help indicate and monitor an increase in inflammatory activity such as infections, inflammations, or cancers.[1] It is based on the principle that the sedimentation of red cells in plasma provides a measure of the level of acute-phase proteins and, therefore, of inflammation. In general, the ESR is increased in all acute and inflammatory conditions. Variations in the ESR depend on a variety of factors,

* **Corresponding contributor.**
Author's Address: *Division of Clinical Microscopy, Department of Medical Technology, Faculty of Associated Medical Sciences, Chiang Mai University, Chiang Mai Province, Thailand.*
E-mail address: suwit.du@cmu.ac.th
doi: 10.12982/JAMS.2024.039
E-ISSN: 2539-6056

including age, sex, hematocrit, fibrinogen concentration, and fibrinogen availability (amount of fibrinogen per red blood cell).[2] Lifestyle factors (physical activity, smoking, and alcohol consumption) and common metabolic abnormalities (obesity and related metabolic syndrome) may also influence ESR values.[3] ESR is increased in anemia, more in megaloblastic than iron-deficiency anemia, and pronounced polycythemia inhibits sedimentation.[4] The ESR is not specific for any diseases but can be used with C-reactive protein (CRP) to evaluate distinct acute inflammatory conditions, especially in orthopedic conditions.[5] In recent decades, several methods and instruments have been used to perform the test, such as modified versions of the Westergren method (e.g., measurements after only 15–30 min), as well as instruments based on entirely different principles than the Westergren method (e.g., centrifugation or photometric rheology).[6-8] However, the Westergren method was still confirmed as the reference method 2011 by the International Committee for Standardization in Hematology (ICSH) and the Clinical and Laboratory Standards Institute (CLSI).[9,10] The reference method for measurement of the ESR should use either whole blood anticoagulated with EDTA and later diluted with sodium citrate or saline (4:1) or whole blood anticoagulated with sodium citrate (4:1) in Westergren pipettes.[9]

Proficiency testing (PT) is an external quality assessment (EQA) tool for providing information that satisfies regulatory requirements and improves laboratory quality, patient care, and safety. In addition to the value to individual laboratories, data from PT programs benefits the laboratory community in multiple ways by providing a snapshot of laboratory practice and summarizing the performance of various methods in identifying normal and abnormal specimens and the effects of therapies or interfering substances. Participation in proficiency testing is associated with improved laboratory quality, particularly in the laboratory-developed test setting. Laboratories are familiar with EQA/PT schemes since participating in the scheme is a prerequisite for accreditation according to the International Organization for Standardization (ISO) 15189 standard requirement. However, some laboratories still need to participate in external quality assessment programs due to the lack of a national or international proficiency testing program, including ESR. Because the erythrocyte sedimentation reaction occurs in fresh blood and is transient, usual reference or control materials are unavailable. This study aimed to develop and initiate the PT program for ESR in Thailand to improve the quality of testing through the evaluation and analysis of the laboratory tests for ESR.

Materials and methods

Preparation of EQA materials for ESR

The ESR control materials were produced at the Faculty of Associated Medical Sciences Chiang Mai University External Quality Assessment Unit (AMS CMU EQA), Chiang Mai University, Chiang Mai, Thailand. The control material comprises a synthetic plasma base with an aggregating agent component and a chemically fixed red blood cell component. The synthetic plasma base comprises a carrying buffer that, in conjunction with the aggregating agent, high molecular weight polymer, or combination of high molecular weight polymers, produces predictable and reproducible red blood cell sedimentation rate values for a given ESR testing apparatus and method. Chemical fixing of the red blood cells modified by Herz and his colleague provides the ESR control capable of providing valuable results in citrate and/or saline[11].

Assessment of homogeneity and stability of ESR control materials

The homogeneity and stability of ESR control materials were assessed according to the ISO/IEC17043:2010 requirements.[12] Ten samples were randomly chosen at each level, and each bottle was duplicated and analyzed for the homogeneity of control materials. The degree of homogeneity of the samples was determined by using the statistical criteria based on ISO13528:2015[13], according to Equation B.1, comparing the between-sample standard deviation S_s with the standard deviation for proficiency assessment σ_{pt}. The proficiency test items may be considered to be adequately homogeneous when $S_s \leq 0.3\ \sigma_{pt}$.

In addition, four samples were randomly selected for the stability assessment in transport conditions to assess the conditions of shipping and handling and stability conditions at the expiration date. These four samples were sent to 2 participants and were then returned to the provider. The provider tested the returned samples in duplicate within 5 days after receiving the samples to assess the stability of the samples in transport conditions. Two samples were kept at 2-8 °C and tested for ESR to determine their stability within 3 days after the expiration date (14 days). The ESR test is performed by using Westergren method. The assessment criterion for the stability of the ESR samples was taken from the ISO standard 13528:2015[13] as follows: $|\bar{y}_1 - \bar{y}_2| \leq 0.3\ \sigma_{pt}$ where $\bar{y}_1$ is the average value of the parameter obtained from the homogeneity content, $\bar{y}_2$ is the average value of the parameter investigated during the stability test, and σ_{pt} is the standard deviation used in the PT.

Determination of the assigned values

The assigned value of each control lot is determined by using consensus value from participants (referring to algorithm A referring to the ISO 13528: 2015[13] that the assigned value of the quantitative test is the robust mean of the results reported by all participants in a subgroup). The z-scores, standardized performance measure, were calculated using the following equation: $z\ score = (x_i - x_{pt})/\ \sigma_{pt}$ where x_i = participant's value for each run, X_{pt} = assigned value and σ_{pt} = standard deviation for proficiency assessment. When the uncertainty of an assigned value $U(x_{pt}) > 0.3\ \sigma_{pt}$, the z'-scores were used to evaluate the performance. The z'-scores can be interpreted similarly as z-scores depending on the design for the proficiency testing scheme.

Operation of PT program

The PT program was established in compliance with ISO/IEC17043:2010 in 2020 at the AMS CMU EQA Unit. EQA samples were packed in a box with ice packs by the instruction of the Proficiency Testing Centre (4.6.3 "Packaging, labelling and distribution of proficiency test items"). EQA samples were immediately distributed by registered post twice a year, with two samples each cycle, with instructions and the return forms.

Participants must fill in the return form to show details of the person responsible, dates of sample reception and sample analysis, type of analytical instrument, and reports of unexpected events during the testing of each sample. Results could be returned by post or submitted online. After the closing date, 14 days after distribution, the results were analyzed and reported back to the participants by post with suggestions for improvement for those with extreme outliers. The turnaround time of the scheme was about 1 month.

Statistical analysis

Data was analyzed using SPSS 13.0. Robust mean, robust standard deviation, and standard uncertainty of assigned value were calculated and used to evaluate the performance of the participant. To compare the performance between measurement system and overall correct recognition rate among PT program, performance scores of the participants were shown as z-score of each sample. For monitoring the performance, absolute z-score at most 2.0 is considered to be acceptable.

Results

EQA sample

Homogeneity and stability tests were performed in accordance with the ISO/IEC 17043:2010 requirement. Stability in transport conditions was performed within 5 days after the return date, and stability at the expired date was undertaken at 4 °C storage for 14 days, which results showed no deterioration in sample quality (Supplementary data S1). Moreover, homogeneity testing results indicated that all 10 samples were adequately homogenous (Supplementary data S2).

Participant laboratories

Of 104 laboratories enrolled in the program, 96 laboratories (92.3%) submitted their results within the specified deadline. The majority of the results were from modified Westergren methods (42.7%), followed by Microsed (29.2%), Mixrate (15.7%), Vesmatic Easy (5.3%), conventional Westergren (3.1%), Vision-B YHLO Biotech (1%), XC-A10 (1%), Mini CUBE (1%), and Vesmatic Cube 30 (1%). The summary of participants and analytical methods is shown in Table 1.

Table 1. Number of participating laboratories in 2020.

Method	Cycle 1/2020		Cycle 2/2020	
	N	%	N	%
Modified Westergren	40	41.7	41	42.7
Microsed	29	30.2	28	29.2
Mixrate	14	14.6	15	15.7
Vesmatic Easy	6	6.3	5	5.3
Westergren	4	4.2	3	3.1
Vision-B YHLO Biotech	1	1.0	1	1.0
XC-A10	1	1.0	1	1.0
Mini CUBE	1	1.0	1	1.0
Vesmatic Cube 30	0	0.0	1	1.0
Total	**96**	**100.0**	**96**	**100.0**

Precision of participants

As previously reported, two replicate samples were sent to participating laboratories. Z score was calculated to determine participants' precision; *z*-scores and *z'*-scores were considered *Satisfactory* when |z or z'| ≤2.0, *Questionable* when 2.0 < |z or z'| <3.0, and *Unsatisfactory when* |*z*|≥3. Precision levels of participants of the PT program are shown in Table 2. In 82/96 (85.4.%) and 8/96 (8.3%), respectively, were satisfactory and questionable performance. Unsatisfactory performance was noted at 6/96 (6.3%).

Table 2. Precision results obtained from the participants.

Method	Precision					
	|z or z'| ≤ 2.0		2.0 < |z or z'| <3.0		|z or z'| ≥ 3.0	
	N	%	N	%	N	%
Modified Westergren	33	40.2	6	75.0	2	33.3
Microsed	24	29.3	2	25.0	2	33.3
Mixrate	15	18.3	0	0.0	0	0.0
Vesmatic Easy	4	5.0	0	0.0	1	16.7
Westergren	2	2.4	0	0.0	1	16.7
Vision-B YHLO Biotech	1	1.2	0	0	0	0.0
XC-A10	1	1.2	0	0.0	0	0.0
Mini CUBE	1	1.2	0	0.0	0	0.0
Vesmatic Cube 30	1	1.2	0	0.0	0	0.0
Total	**82**	**100.0**	**8**	**100.0**	**6**	**100.0**

Note: |z or z'| ≤ 2.0: Satisfactory, 2.0 < |z or z'| <3.0: Questionable, |z| ≥ 3: Unsatisfactory

Proficiency levels of participants

Assigned value, robust standard deviation, and standard uncertainty of assigned value were calculated using the algorithm A, and the results are shown in Table 3. To facilitate the performance evaluation by the participating laboratories, the methodology described in ISO13528:2015[13] was applied. The scores from both cycles were calculated and used to determine the proficiency levels of participants. Scoring criteria for participant performance levels are as follows: |z or z'| ≤ 2.0 scored 3, 2.0 < |z or z'| <3.0 scored 2, |z or z'| ≥3.0 scored 1. The criteria for proficiency levels of participants from both cycles are as follows: Excellent (score 9-12), Fair (score 5-8), and Poor (score <5). Proficiency levels of participants of the PT program are shown in Figure 1. Laboratories performed well in the analysis of the EQA samples: 85.42% (82/96) were excellent, 13.54% (13/96) were fair, and only 1.04% (1/96) were poor.

Table 3. Assigned values (x_{pt}), standard deviation (σ_{pt}) and standard uncertainties (u_{xpt}) of each control material given by the compared methods.

Method	Cycle 1/2020						Cycle 2/2020					
	ESR63-A1			ESR63-A2			ESR63-B1			ESR63-B2		
	x_{pt}	σ_{pt}	u_{xpt}	x_{pt}	σ_{pt}	u_{xpt}	x_{pt}	σ_{pt}	u_{xpt}	x_{pt}	σ_{pt}	u_{xpt}
All method	2.7	1.5	0.2	51.8	16.1	2.2	32.2	8.8	1.1	29.7	8.2	1.1
Modified Westergren	2.8	1.7	0.3	46.2	17.8	3.6	33.6	8.4	1.6	29.7	10.2	2.0
Microsed	2.0	0.0	0.0	53.7	7.0	1.6	28.3	8.3	1.9	26.7	6.7	1.6
Mixrate	3.0	1.3	0.4	60.7	15.6	6.1	30.3	11.9	3.8	30.0	5.2	1.7

Note: ESR63-A1: normal level, ESR63-A2, B1, and B2: abnormal level

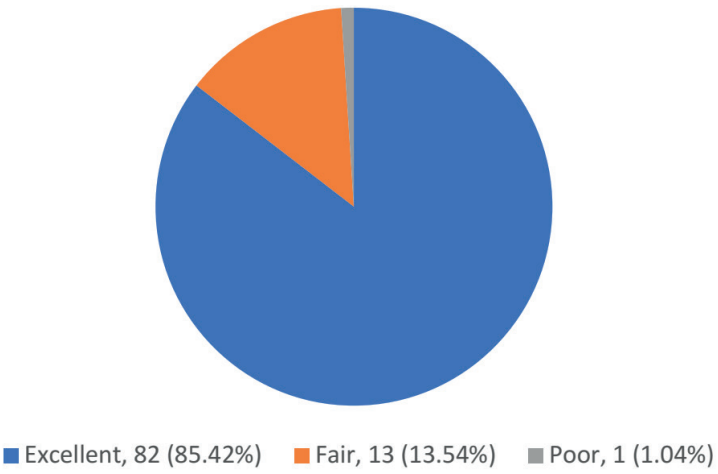

Figure 1. *Distribution of 96 laboratory participants performance result in PT program.*

Discussion

The erythrocyte sedimentation rate determination is a simple and inexpensive laboratory test frequently ordered in clinical medicine. Recent studies have evaluated the ESR as a screening test for infection in specific clinical instances, such as infection associated with orthopedic prostheses, pediatric bacterial infection, and gynecologic inflammatory disease.[14-16] Because the ESR determination is frequently performed in hematology laboratories, careful attention to all factors that may produce erroneous values is essential. The proficiency testing scheme has provided an assessment of the participant's measured values and their evaluated uncertainties. In addition to identifying the individual laboratory performance, it also determines the characteristics of the different reagents and methods used in other laboratories.

In this study, we reported the ESR analysis results from the participants on our control materials prepared from chemically fixed red blood cells and synthetic plasma for the EQA/PT scheme. Here, the addition of an aggregating agent to the synthetic plasma base behaves similarly to an abnormal increase of large plasma proteins such as Fibrinogen and Alpha 2 macro-globulins in whole blood. Using chemically fixed red blood cells provides the ESR control with the ability to operate in the presence of citrate or saline solution.

We found that the in-house developed ESR control materials can be applicable as surveillance material for the PT program of ESR testing. Since the Westergren method is the reference method, we used the Westergren method to assess homogeneity and stability. Our control materials presented with satisfactory homogeneity $S_s \leq 0.3\ \sigma_{pt}$ and stability $|\bar{y}_1 - \bar{y}_2| \leq 0.3\ \sigma_{pt}$ according to ISO 13528: 2015.

Participating laboratories performed well in the analysis of EQA control materials. Excellent and fair performance was obtained in 82/96 (85.42%) and 13/96 (13.54%). Poor performance was respectively noted at 1/96 (1.04%). The participating laboratory with poor performance was contacted for remediation and corrective actions. Analysis of receiving data found that two main types of errors were (i) specimen processing and (ii) incorrect identification of the analytical method.

The preanalytical and specimen processing are crucial parts of the analysis and equally important as the analytical process. ICSH recommended that before testing, the EDTA samples should be diluted with sodium citrate/NaCl in the proportion of 4 volumes of blood to 1 volume of citrate/NaCl. Blood samples may be drawn into sodium citrate directly, diluted in proportion to the rate of 4 volumes of blood and 1 volume of citrate. Moreover, mixing blood samples should be a minimum of eight complete inversions with the air bubble traveling from end to end of the tube. Mixing should be continued until immediately before the ESR pipette is filled at the start of the test.[9] When reporting laboratory testing, the analytical methods should be fully described. Reference ranges often depend on the analytical method used.[17,18] According to the ISO 15189 standard, reporting information about the laboratory, patient, sample identifiers, results, methodology, and interpretation is essential. We showed herein our PT program for ESR testing was successfully conducted by AMS CMU EQA Unit. Our results indicated that the advantage of participation is that the laboratories can monitor and investigate the source of laboratory errors. Since the implementation of this program has led to improved precision and interlaboratory agreement on ESR testing, PT program for ESR testing should become an integral part of quality assurance in the hematology laboratory.

Conclusion

The stabilized ESR EQA samples prepared using a synthetic plasma base with an aggregating agent and chemically fixed red blood cells in this study meet the ISO 13528:2015 requirements of homogeneity and stability for the ESR PT scheme. The PT program is designed as an enthusiastic effort to help participating laboratories determine their performance, resolve any problem areas, assess instruments and reagents, and influence national policy. Therefore, the PT program for ESR testing should be integrated into the laboratory's entire quality assurance system.

Conflict of interest

None declared.

Acknowledgements

The authors thank Kallayanee Treesuwan and Tanyarat Jomkaew for their expert technical assistance.

Author contributions

All the authors have accepted responsibility for the entire content of this submitted manuscript and approved the submission.

References

[1] Tishkowski K, Gupta V. Erythrocyte Sedimentation Rate. [Updated 2023 Apr 23]. In: StatPearls [Internet]. Treasure Island (FL): StatPearls Publishing; 2024 Jan-. Available from: https://www.ncbi.nlm.nih.gov/books/NBK557485/

[2] Bain BJ. Some influences on the ESR and the fibrinogen level in healthy subjects. Clin Lab Haematol. 1983; 5(1): 45-54. doi: 10.1111/j.1365-2257.1983.tb00495.x.

[3] Alende-Castro V, Alonso-Sampedro M, Vazquez-Temprano N, Tuñez C, Rey D, García-Iglesias C, Sopeña B, Gude F, Gonzalez-Quintela A. Factors influencing erythrocyte sedimentation rate in adults: New evidence for an old test. Medicine (Baltimore). 2019 Aug; 98(34): e16816. doi: 10.1097/MD.0000000000016816. PMID: 31441853; PMCID: PMC6716712.

[4] Guidelines on selection of laboratory tests for monitoring the acute phase response. International Committee for Standardization in Haematology (expert panel on blood rheology). J clin Pathol. 1988; 41(11):1203-12. doi: 10.1136/jcp.41.11.1203.

[5] Lapić I, Padoan A, Bozzato D, Plebani M. Erythrocyte Sedimentation Rate and C-Reactive Protein in Acute

Inflammation: Meta-Analysis of Diagnostic Accuracy Studies. Ame J Clin Pathol. 2020; 153(1): 14-29. doi: 10.1093/ajcp/aqz142.

[6] Baskurt OK, Uyuklu M, Hardeman MR, Meiselman HJ. Photometric measurements of red blood cell aggregation: light transmission versus light reflectance. J Biomed Opt. 2009; 14(5): 54044. doi: 10.1117/1.3251050.

[7] Shelat SG, Chacosky D, Shibutani S. Differences in Erythrocyte Sedimentation Rates Using the Westergren Method and a Centrifugation Method. Am J Clin Pathol. 2008; 130(1): 127-30. doi: 10.1309/E5R9P5YPHXFE3198.

[8] Vennapusa B, de La Cruz L, Shah H, Michalski V, Zhang Q-Y. Erythrocyte Sedimentation Rate (ESR) Measured by the Streck ESR-Auto Plus Is Higher Than With the Sediplast Westergren Method: A Validation Study. Am J Clin Pathol. 2011; 135(3): 386-90. doi: 10.1309/AJCP48YXBDGTGXEV.

[9] Jou JM, Lewis SM, Briggs C, Lee SH, de La Salle B, Mcfadden S. ICSH review of the measurement of the erythocyte sedimentation rate. Int J Lab Hematol. 2011; 33(2): 125-32. doi: 10.1111/j.1751-553X.2011.01302.x.Epub 2011 Feb 25.

[10] Clinical and Laboratory Standards Institute., Jou JM. Procedures for the erythrocyte sedimentation rate test: approved standard. Clinical & Laboratory Standards Institute; 2011. 25.

[11] Herz F, Kaplan E. Effect of Glutaraldehyde Fixation on Erythrocyte Agglutinability. Proc Soc Exp Biol Med. 1973; 144(3): 1017-9. doi: 10.3181/00379727-144-37732.

[12] ISO/IEC 17043 (2010) Conformity assessment-general requirements for proficiency testing. ISO, Geneva.

[13] ISO/IEC 13528 (2015) Statistical methods for use in proficiency testing by interlaboratory comparisons. ISO, Geneva; 2015.

[14] Nilsdotter-Augustinsson A, Briheim G, Herder A, Ljunghusen O, Wahlström O, Ohman L. Inflammatory response in 85 patients with loosened hip prostheses: a prospective study comparing inflammatory markers in patients with aseptic and septic prosthetic loosening. Acta Orthop. 2007; 78(5): 629-39. doi: 10.1080/17453670710014329.

[15] Shaikh KJ, Osio VA, Leeflang MM, Shaikh N. Procalcitonin, C-reactive protein, and erythrocyte sedimentation rate for the diagnosis of acute pyelonephritis in children. Cochrane Database Syst Rev. 2020; 9: CD009185. doi: 10.1002/14651858.CD009185.pub3.

[16] Łój B, Brodowska A, Ciecwiez S, Szydłowska I, Brodowski J, Łokaj M, Starczewski A. The role of serological testing for Chlamydia trachomatis in differential diagnosis of pelvic pain. Ann Agric Environ Med. 2016; 23(3): 506-10. doi: 10.5604/12321966.1219196.

[17] Jones G, Barker A. Reference intervals. Clin Biochem Rev. 2008 Aug;29 Suppl 1(Suppl 1):S93-7. PMCID: PMC2556592.

[18] Lenicek Krleza J, Honovic L, Vlasic Tanaskovic J, Podolar S, Rimac V, Jokic A. Post-analytical laboratory work: national recommendations from the Working Group for Post-analytics on behalf of the Croatian Society of Medical Biochemistry and Laboratory Medicine. Biochem Med. 2019; 29(2): 20502. doi: 10.11613/BM.2019.020502.

Supplementary data S1. Stability results.

Number of PT item	Stability in transport conditions		Stability at the expired date	
	1	**2**	**1**	**2**
ESR63-A1	3	3	3	3
	3	4	3	3
Mean	3.3 mm/hr		3.0 mm/hr	
Result	sufficiently stable		sufficiently stable	
ESR63-A2	40	41	45	42
	43	43	43	41
Mean	41.8 mm/hr		42.8 mm/hr	
Result	adequately stable		adequately stable	
ESR63-B1	28	28	26	22
	25	26	23	27
Mean	26.8 mm/hr		24.5 mm/hr	
Result	adequately stable		sufficiently stable	
ESR63-B2	25	24	18	24
	28	28	19	25
Mean	26.3 mm/hr		21.5 mm/hr	
Result	adequately stable		sufficiently stable	

Adequately stable: The acceptance criterion for the PT Items to be adequately stable for the proficiency test when $|\bar{y}_1 - \bar{y}_2| \leq 0.3\sigma_{pt}$

Sufficiently stable: If adequately stable is not met, the expanded criterion for the PT Items to be sufficiently stable for the proficiency test were apply when $|\bar{y}_1 - \bar{y}_2| \leq 0{,}3\sigma_{pt} + 2\sqrt{u^2(\bar{y}_1) + u^2(\bar{y}_2)}$

Supplementary data S2. Homogeneity results.

No	Number of PT item							
	ESR63-A1		ESR63-A2		ESR63-B1		ESR63-B2	
	1	**2**	**1**	**2**	**1**	**2**	**1**	**2**
1	2	2	40	39	28	27	27	26
2	3	2	41	40	31	28	25	25
3	3	3	41	42	27	26	26	26
4	3	2	43	42	26	28	28	29
5	3	2	42	43	27	27	25	25
6	3	3	42	38	29	30	27	27
7	3	2	42	41	28	27	27	27
8	2	2	43	40	27	27	27	25
9	2	2	44	40	29	30	26	26
10	2	3	40	41	26	27	25	25
Mean	2.4 mm/hr		41.2 mm/hr		27.8 mm/hr		26.2 mm/hr	
Result	Sufficiently homogeneous		Sufficiently homogeneous		Sufficiently homogeneous		Sufficiently homogeneous	

Sufficiently homogeneous: The expanded criterion for the PT Items to be sufficiently homogeneous for the proficiency test when $Ss \leq \sqrt{c}$; $c = F_1\sigma^2_{allow} + F_2S^2_w$

Journal of Associated Medical Sciences 2024; 57(2): 173-182

JAMS
Journal of Associated Medical Sciences

Scopus Indexed & Thai-Journal Citation Index Centre (TCI)

Journal of Associated Medical Sciences

Journal homepage: https://www.tci-thaijo.org/index.php/bulletinAMS/index

Updated research trend and clustering algorithm on virtual reality and pulmonary rehabilitation: Scopus-based bibliometric and visual analysis

Jirakrit Leelarungrayub[1,2*] Pongkorn Chantaraj[1] Supattanawaree Thipcharoen[1] Jutamat Jintana[1]

[1]Department of Data Science and Digital Innovation, Faculty of Innovation Technology and Creativity, The Far Eastern University, Chiang Mai Province, Thailand.
[2]Department of Physical Therapy, Faculty of Associated Medical Sciences, Chiang Mai University, Chiang Mai Province, Thailand.

ARTICLE INFO

Article history:
Received 30 December 2023
Accepted as revised 24 April 2024
Available online 28 April 2024

Keywords:
Bibliometric, clustering, pulmonary rehabilitation, virtual reality

ABSTRACT

Background: Virtual reality (VR) is a new innovative technology that can enhance intervention and should promote the effectiveness of rehabilitation, but there is a lack of scientific evidence on the clustering and topic research trend, especially on VR and pulmonary rehabilitation (PR). More evidence about network clusters and trends will encourage the research in the future.

Objective: This study aimed to explore, identify, cluster, and forecast analysis for the research trend of VR and PR from the research articles on the SCOPUS database.

Materials and methods: In this study, the search terms "virtual reality" AND "pulmonary rehabilitation" were extracted from specific English research articles published on the SCOPUS database between 2013-2023. RStudio software was used to perform bibliometric and visual analysis. During the analysis in the bibliometric tool, the normalization process with Salton's Cosine and network clustering via trend topic with the Walktrap algorithm was analyzed before specific visualization with the network clustering mapping, Treemap, and trend topic line by Kamada-Kawai layout algorithm.

Results: From the 1,396 articles on "VR" published between 2010 and 2023, there were 13 research articles on "VR AND PR" published between 2013 and 2023. The bibliometric result from 13 articles showed total of 36 subdisciplines correlated networks among virtual reality (20, 7%), male (16, 6%), female (15, 5%), aged (12, 4%), chronic obstructive lung disease (12, 4%), exercise (11, 4%), human (10, 4%), humans (10, 4%), middle-aged (10, 4%), quality of life (10, 4%), article (9, 3%), pulmonary rehabilitation (9, 3%), controlled study (8, 3%), adult (6, 2%), chronic obstructive (6, 2%), clinical article (6, 2%), forced expiratory volume (6, 2%), pulmonary disease (6, 2%), randomized controlled trial (6, 2%), and forced vital capacity (5, 2%), etc., respectively. Three network clusters were reported after the normalization process and clustering evaluation by factorial analysis. The first cluster was composed of virtual reality, male, female, aged, chronic obstructive lung disease, exercise, human, humans, middle-aged, quality of life, article, pulmonary rehabilitation, controlled study, adult, chronic obstructive, clinical article, forced expiratory volume, randomized controlled trial, forced vital capacity, six-minute walk test, depression, technology, telerehabilitation, breathing exercise, Covid-19, dyspnea, functional status, hospital patient, and physical activity, respectively. The second cluster consisted of procedure and exercise therapy, and the last cluster consisted of exercise tolerance, lung, treatment outcome, health program, and convalescence. Finally, trend research topics were presented in virtual reality, male, female, aged, chronic obstructive lung disease, human, exercise, quality of life, and middle-aged, respectively, in 2023.

Conclusion: Therefore, the contribution from data analysis in this article can identify the clustering and trend topics of VR, chronic obstructive lung disease, aging participants, exercise, and quality of life in future research.

∗ **Corresponding contributor.**
Author's Address: *Department of Data Science and Digital Innovation, Faculty of Innovation Technology and Creativity, The Far Eastern University, Chiang Mai Province, Thailand.*
E-mail address: jirakrit@feu.edu
doi: 10.12982/JAMS.2024.040
E-ISSN: 2539-6056

Introduction

New innovative technology, Virtual Reality (VR), is one of many devices that can answer future challenges.[1] Various types of VR such as non-immersive, immersive, and 3D-displays, is a novel technology defined as "the use of interactive simulations created with computer hardware and software to present users with synchronized virtual environments that feel similar to real-world situations.[2] In a VR system, the complexities of the real world can be simulated in a controlled program.[3] The rehabilitation field can be facilitated using different devices or equipment.[4] Some evidence reported that the manual rehabilitation process following many injuries and disabilities is long, arduous, and tedious; therefore, patients mostly lack the motivation to follow the program, which can lead to ineffective rehabilitation outcomes and less quality of improvement.[5,6] The advantages of VR for rehabilitation have been applied and performed because of real-time feedback, individual setup, ease of adjustment, and simple measurement possibility,[7,8] especially in physical therapy that has been documented in the fact sheet in the International Association for the Study of Pain (IASP) 2022 as the same as other digital modalities with medical applications (mHealth apps), and telemedicine.[9]

Presently, VR shows initial promising results in clinical studies. VR integrates mechanisms of distraction, behavioral modification, relaxation, and education in many conditions such as neuropathic pain and low back pain.[10] Several VR systems have been developed for rehabilitation. Moreover, clinical engagement through VR can reduce pain perception and improve physical movement.[11] Different studies have investigated the effectiveness of VR in rehabilitation or the design and development of VR systems to facilitate rehabilitation exercises. For example, using Kinect for motor disabilities and exercises for shoulder abduction, path following, play along, and balloon pop, Roy and coworkers found that both patients and clinicians considered it an engaging and motivational intervention in rehabilitation.[12] In addition, Su and coworkers designed a VR to help patients do lower back exercises and the result showed a high degree of acceptance in motivating the patients to perform the exercises.[13] Moreover, Kim and co-workers evaluated the effects of an unsupervised VR-based exercise program on hip muscle strength and balance control in older adults. The results reported that the VR group had shown a great improvement in hip strength of extensors, flexors, and adductors (changes = 55.5%, 29.9%, and 48.6%, respectively). In contrast, the control group did not show significant improvements (changes = 1.5%, 4.6%, and 2.1%, respectively).[14] As well, the study of Bryanton *et al*. reported that greater mean ankle active ranges of motion to hold time after practicing with VR-based ET when compared to conventional therapies.[15] Moreover, many reviews have further investigated specific patients or goals to use VR with exercise to achieve rehabilitation, e.g., in multiple sclerosis,[16] chronic stroke,[17] balance and gait,[18] and Down syndrome, and cerebral palsy.[19]

Therefore, the previous evidence shows that VR programs are considered more effective tools for rehabilitation than traditional approaches in the new digital technology.[20] Because VR is an enjoyable activity with valuable feedback and improves motor learning and adherence to exercise with non-immersive,[21] semi-immersive, and fully immersive systems.[22] Unfortunately, there were rare previously published articles that showed the applications of VR in pulmonary rehabilitation and suggested a trend study in the future. Therefore, this study aimed to explore and identify the network cluster and forecast the research topic trend of VR and PR from the prior data based on the SCOPUS that can be useful to encourage future research.

Methodology

This study employs a research design combining quantitative and qualitative methods to analyze and visualize data. It is a component of a large-scale research project that was approved by the Human Ethics Committee at the Faculty of Associated Medical Science, Chiang Mai, Thailand (STUDY CODE: AMSEC-67Ex-004). Bibliometric analysis under RStudio Software (version 4.3.2) is one of many software related to various databases, i.e., Web of Science, PubMed, Cochrane, or SCOPUS.[23] However, this study aimed to explore the network clustering and trend topics in the research between 2010 and 2023. The search terms or inclusion criteria were focused on specific keywords, such as "Virtual Reality (VR)" and "Pulmonary Rehabilitation" in the research articles based on the particular SCOPUS database with literature type of research article and English language. As a property of Scopus, it is relatively more comprehensive than PubMed or Web of Science (WoS). For example, Garrido-Cardenas et al. argue that Scopus covers 84% of the WoS titles, whereas only 54% of the publications in Scopus are indexed in WoS.[24] Scopus is also more precise than Google Scholar because of its superior control over the referred publications and the controlled indexing.[25] As a result, the Scopus database was the only reasonable option for conducting the study because of its accessibility and extensive coverage of peer-reviewed academic literature.[26] Exclusion criteria were types of literature categorized as letters, reports, conferences, proceedings, or review data (Cochrane). Generally, Cobo *et al*. proposed the method of bibliometric analysis for application to the analysis of scientific domains.[27] There are eight steps: data collection, selection of analyzed units, data processing, normalization process, creation of science mapping, analysis methods, visualization techniques, and interpretation.

This research ran on the methodology of bibliometric analysis from Steps 1 to 5 [28] as in Figure 1, which was modified from Aria and Cuccrullo.[29] The data from research articles on "virtual reality" and "pulmonary rehabilitation" was collected on the SCOPUS database in steps I and II. All data was transformed into a " BibTex " file type before processing in the Bibliometric method within RStudio Software in Step III. Then, the data processing on bibliometric analysis, the primary most relevant sources or journals, number of documents, keyword occurrences,

most relevant words, or most frequency words was computerized evaluated. During processing in bibliometric analysis, the normalization process with Salton's Cosine [27] (Step IV) and network clustering and trend topic analysis were identified by the Walktrap distance algorithm.[30] The creation of science mapping visualization in the bibliometric tool as network clustering mapping, Treemap, or trend topic was presented by the Kamada-Kawai layout algorithm which is used to present a specific visualized layout with weight edged based on the distance among all data.[28,32] In this study, Salton Cosine normalization was selected because previous evidence reported that Salton's cos is similar to the Person's cosine that was used to investigate the potential co-cited in the library environment.[33] The Walktrap distance algorithm was used to analyze the network clustering and trend research topic in a small database,[34] and following as in the previous suggestion.[35,36] Therefore, all algorithms in this study were used to analyze either a big or small database.

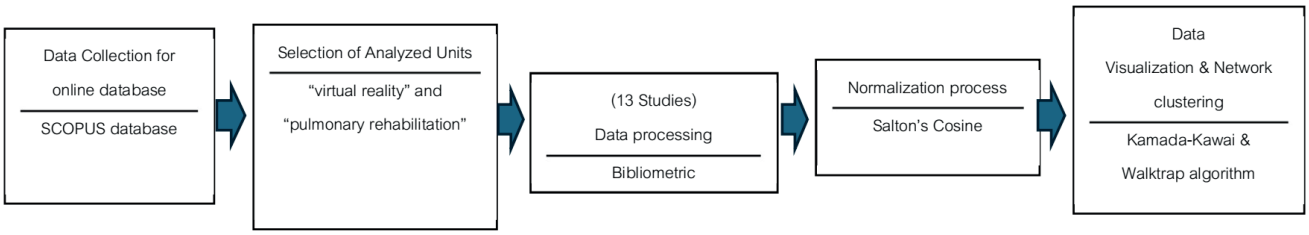

Figure 1. *Five steps of data collection, analysis, data processing, normalization, and clustering processes.*[28]

Results

Distribution by Time and Journal publication

A total of 1,396 original publication articles on "Virtual reality" or VR were found between 2010 and 2023. Still, there were only 13 research articles published in 11 journals with 63 authors under the specific words of "Virtual Reality AND Pulmonary Rehabilitation" published between 2013 and 2023. All articles with the author's name, journal, research title, and published page were presented in Table 1. The most relevant sources or journals and the number of documents were the International Journal of COPD (N=2), International Journal of Environmental Research and Public Health (N=2), BMJ Open (N=1), Canadian Respiratory Journal (n=1), Contrast Media and Molecular Imaging (n=1), Frontiers in Public Health (N=1), Journal of Medical Internet Research (N=1), Journal of Clinical Medicine (N=1), Journal of Healthcare Engineering (N=1), Journal of Human Kinetics (N=1), and Journal of Medical Internet Research (N=1).

Table 1. Cited Article Results in SCOPUS database between 2013-2023.

Authors	Title
Li Y, *et al*.[37]	Virtual reality as an adjunct to pulmonary rehabilitation of patients with chronic obstructive pulmonary disease: a protocol for systematic review and meta-analysis.
Rutkowski S, *et al*. [38]	Inpatient post-COVID-19 rehabilitation program featuring virtual reality-preliminary results of randomized controlled trial.
Rutkowski S, *et al*.[39]	Effectiveness of an inpatient virtual reality-based pulmonary rehabilitation program among COVID-19 patients on symptoms of anxiety, depression, and quality of Life: preliminary results from a randomized controlled trial.
Cerdan-De-las-heras J, *et al*. [40]	Tele-rehabilitation program in idiopathic pulmonary fibrosis-A single-center randomized trial
Rutkowski S, *et al*. [41]	Evaluation of the efficacy of immersive virtual reality therapy as a method-supporting pulmonary rehabilitation: A randomized controlled trial.
Liu H, *et al*.[42]	Study on adjuvant medication for patients with mild cognitive impairment based on VR technology and health education.
Xie X, *et al*.[43]	Virtual reality technology combined with comprehensive pulmonary rehabilitation on patients with stable chronic obstructive pulmonary disease.
Jung T, *et al*.[44]	A virtual reality-supported intervention for pulmonary rehabilitation of patients with chronic obstructive pulmonary disease: Mixed methods study.
Rutkowshi S, *et al*. [45]	Virtual reality rehabilitation in patients with chronic obstructive pulmonary disease: A randomized controlled trial.
Alves da Cruz MM, *et al*.[46]	Acute hemodynamic effects of virtual reality-based therapy in patients of cardiovascular rehabilitation; a cluster randomized crossover trial.
Knox L, *et al*.[47]	Safety, feasibility, and effectiveness of virtual pulmonary rehabilitation in the real world.
Rutkowski S, *et al*.[48]	Effect of virtual reality-based rehabilitation on physical fitness in patients with chronic obstructive pulmonary disease.
Wardini R, *et al*.[49]	Using a virtual game system to innovate pulmonary rehabilitation: Safety, adherence, and enjoyment in severe chronic obstructive pulmonary disease.

Co-occurring keywords and Network Clustering analysis

The result of the bibliometric analysis of 13 articles with specific keywords of "VR and PR" from the research articles in SCOPUS showed a total of 36 subdisciplines. The most frequency words, word clustering, and Treemap used subdisciplines in 13 articles including virtual reality (N=20, 7%), male (N=16, 6%), female (N=15, 5%), aged (N=12, 4%), chronic obstructive lung disease (N=12, 4%), exercise (N=11, 4%), human (N=10, 4%), humans (N=10, 4%), middle-aged (N=10, 4%), quality of life (N=10, 4%), article (N=9, 3%), pulmonary rehabilitation (N=9, 3%), controlled study (N=8, 3%), adult (N=6, 2%), chronic obstructive (N=6, 2%), clinical article (N=6, 2%), forced expiratory volume (N=6, 2%), pulmonary disease (N=6, 2%), randomized controlled trial (N=6, 2%), and forced vital capacity (N=5, 2%), etc., respectively. After the normalization with Salton's Cosine, the science mapping from 36 subdisciplines was presented from the bibliometric analysis with the Kamada-Kawai algorithm, shown in Figures 2-4.

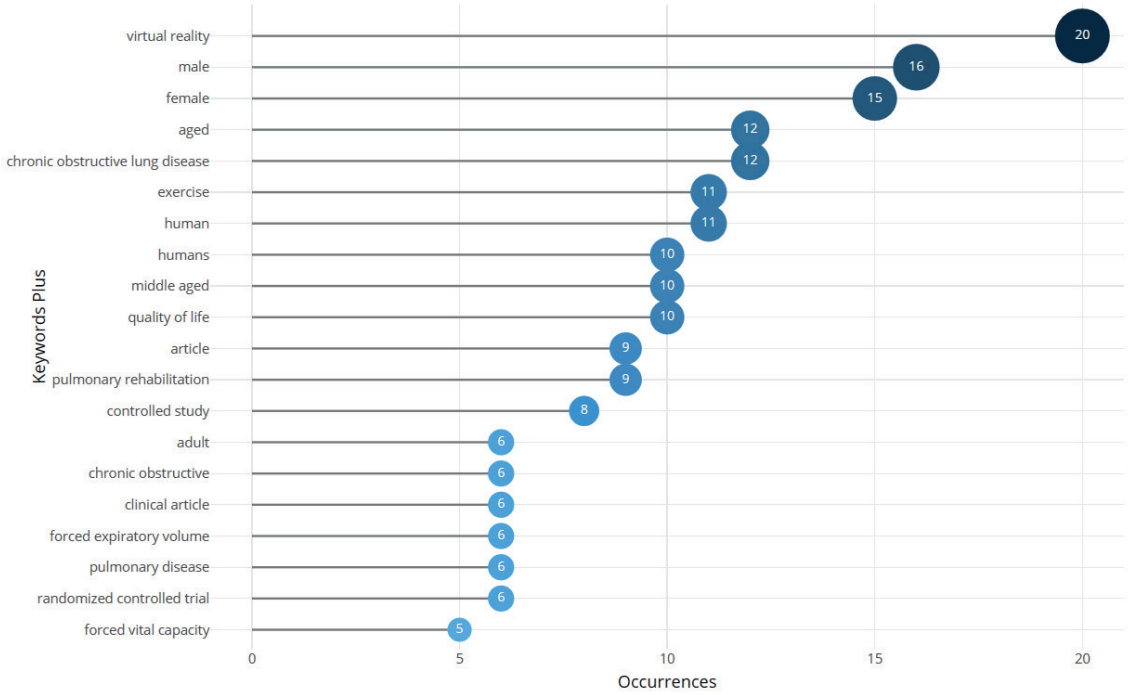

Figure 2. *Most frequency words in 13 published articles between 2013 and 2023.*

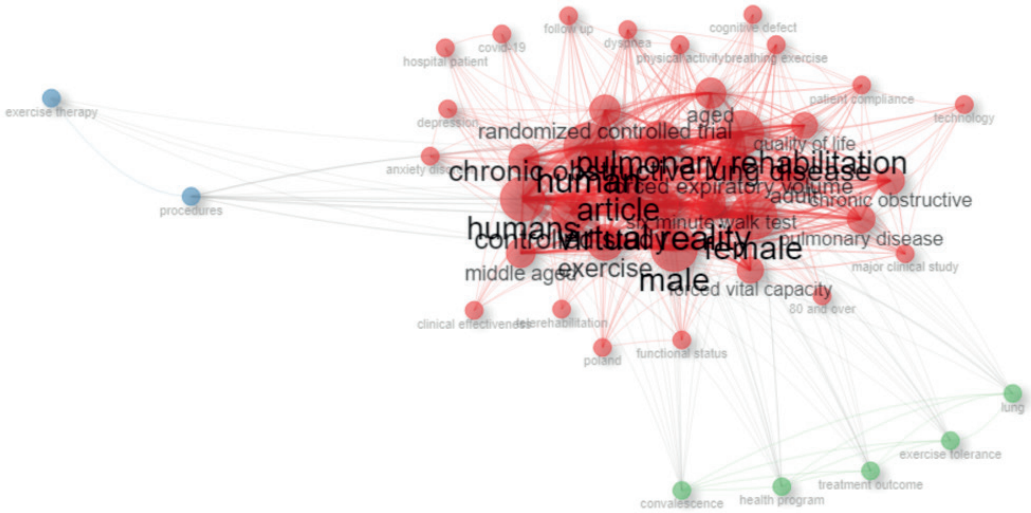

Figure 3. *Network clustering visualization with Walktrap distance algorithm of 36 subdisciplines from 13 cited articles.*

Figure 4. *Treemap analysis of a total of 36 subdisciplines from "virtual reality" and "pulmonary rehabilitation" after citation between 2013 and 2023 in the SCOPUS database.*

The results represented three clusters and map network clustering as presented in Table 2 and Figure 5. The first cluster was composed of 29 subdisciplines: Virtual reality, male, female, aged, chronic obstructive lung disease, exercise, human, humans, middle-aged, quality of life, article, pulmonary rehabilitation, controlled study, adult, chronic obstructive, clinical article, forced expiratory volume, randomized controlled trial, forced vital capacity, six-minute walk test, depression, technology, telerehabilitation, breathing exercise, Covid-19, dyspnea, functional status, hospital patient, physical activity, respectively. The second cluster of 2 subdisciplines consisted of procedure and exercise therapy, and the last cluster of 5 subdisciplines consisted of exercise tolerance, lung, treatment outcome, health program, and convalescence.

Table 2. Network Clustering and 36 subdisciplines from "virtual reality" and "pulmonary rehabilitation"

Network Clustering	Subdisciplines
1	Virtual reality, male, female, aged, chronic obstructive lung disease, exercise, human, humans, middle-aged, quality of life, article, pulmonary rehabilitation, controlled study, adult, chronic obstructive, clinical article, forced expiratory volume, randomized controlled trial, forced vital capacity, six-minute walk test, depression, technology, telerehabilitation, breathing exercise, Covid-19, dyspnea, functional status, hospital patient, physical activity
2	Procedures, exercise therapy
3	Exercise tolerance, lung, treatment outcome, health program, convalescence

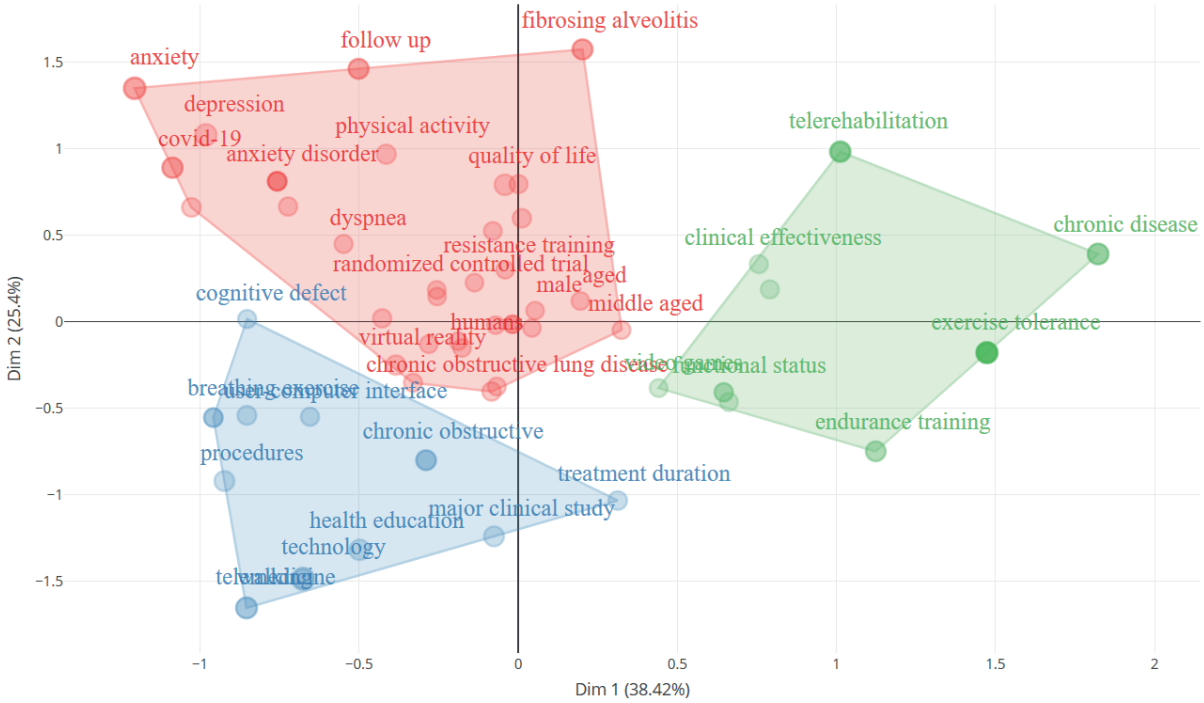

Figure 5. *Three-map network clustering analysis from all 36 subdisciplines or words in 13 published articles between 2013 and 2023.*

Trend research Topic related to the keywords of Virtual reality and Pulmonary rehabilitation.

From the words' frequency over time since 2013, the results showed an increased trend of the top ten words. Trend research topics were virtual reality (1 to 20), male (2 to 16), female (2 to 15), aged (3 to 12), chronic obstructive lung disease (1 to 12), human (2 to 11), exercise (2 to 11), humans (2-10), quality of life (0 to 10) and middle-aged (1 to 10), respectively in 2023 when compared to 2013 (Figure 6).

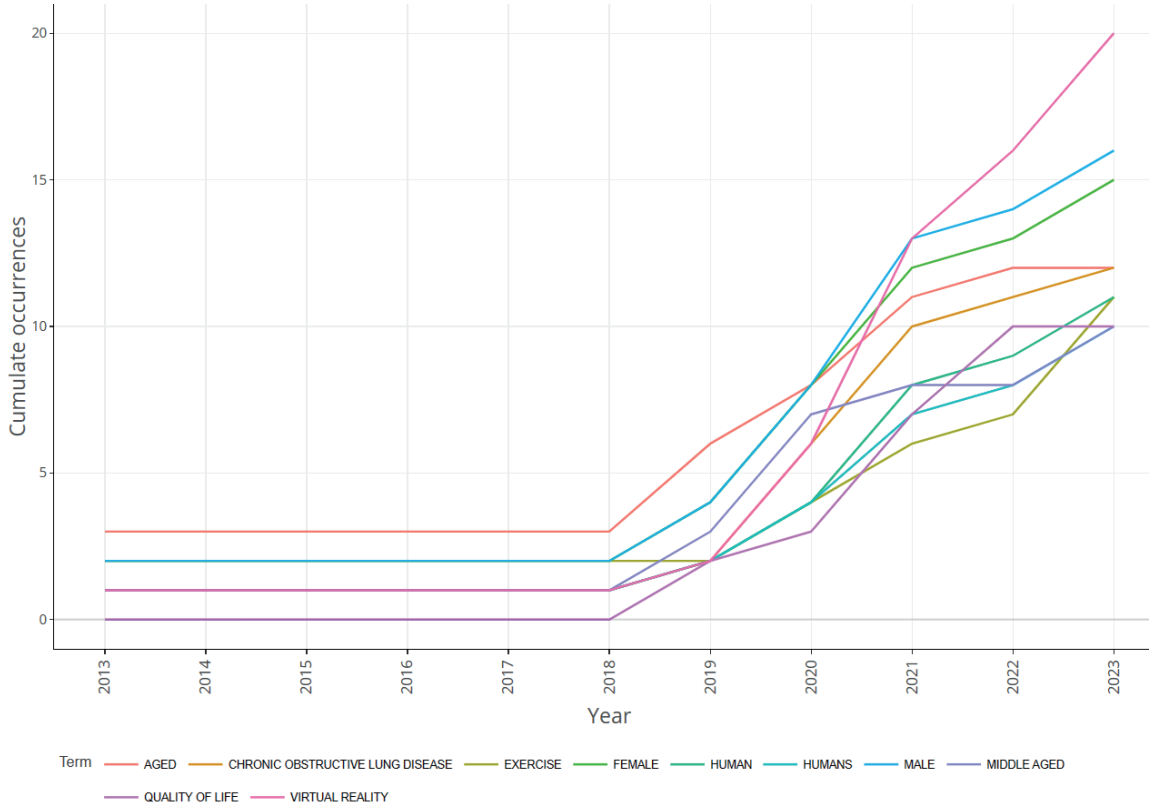

Figure 6. *Trend topics from the words' frequency over time from 2013 to 2023 analysis.*

Discussion

The bibliometric analysis used mainly in this study is one of many software product line engineering at lower costs, in a shorter time, and with higher quality.[50] Bibliometric analysis has been popular in business research in recent years which can be attributed to the advancement, availability, and accessibility of software such as Gephi, VOSviewer, and scientific databases such as SCOPUS in this study.[35] In addition, this method can be applied for discovering knowledge and identifying novel ideas for investigation or research and the position of the intended contributions to all fields.[51] The advantages of this method are that it can be used and tested repeatability in a broad scope from either small or big datasets from the globally published articles in SCOPUS or PubMed with both quantitative as most frequency words or Treemap percentages and qualitative as network clustering, trend topic, and network clustering visualization analysis when compared to other qualitative analysis in Meta-analysis, and Systematic literature review.

This study applied the bibliometric tool to explore and identify the network clustering analysis because it was popularly used in business research; for example, to analyze risk management from the SCOPUS database.[52] That report could identify the six clusters of all risk parameters in the same way as the three network clustering identifications that can be evaluated in this study. Thus, bibliometric analysis in this study is reflected as a great tool to get reliable, clear, and unbiased quantitative estimate results as a prior report.[53]

Network clustering and most frequency words.

The results of 13 research articles showed the top ten frequency words of virtual reality, male, female, aged, chronic obstructive lung disease, exercise, human, humans, middle-aged, quality of life, article, pulmonary rehabilitation, controlled study, and adults, etc. No previous studies have been reported on data citations, which is likely this result. However, a previous report documented seven electronic libraries and 32 review studies from 2010 to 2023 from Digital Library, Google Scholar, IEEE Explore, MEDICINE, PubMed, Sage, and ScienceDirect.[54] Therefore, the meaning of this study can be suggested that VR and PR have been studied concerning VR's impact on the quality of life from exercise and pulmonary rehabilitation in humans with chronic lung disease under a controlled study design. Moreover, the validity of the results of the three clusters in this study with the Cosine normalization algorithm can be supported by previous evidence, [33]data visualization from the occurrence matrix,[55] network mapping visualization with Kamada-Kawai layout algorithm,[56,] and related to the Walktrap algorithm.[35] The network clustering visualization from this study can be represented as same as in the network in various research areas[57] with other algorithms such as Edge, Fast Greedy, Eigenvector, Infomap, Label Propagation, Louvain,[58] and Walktrap algorithm in this study.[59] Moreover, the small data from 13 research articles and three networks in this results, the Walktrap algorithm can be selected automatically in the RStudio and bibliometric analysis. In addition, some previous research reports on data mining or data analysis on the different algorithms, various modularity, processing time, and cluster members, suggested that frequency analysis and co-occurring networks should be identified and applied.[59,60] This study showed partial results on network clustering from database citations. However, this study aims mainly to present the clustering of words related to the research topic in the future. From the network clustering analysis from the most frequent words in this study, "Virtual Reality" and "Pulmonary Rehabilitation" were dominant outcomes in research articles automatically presented in the SCOPUS database between 2013 and 2023. This confirms the future view on VR, which is a promising technology for implementing personalized, motivating, and controlled rehabilitation scenarios as previous evidence.[61]

Trend research topics of virtual reality and pulmonary rehabilitation

Identifying the research trend in the future of this study is consistent with a previous review document.[62] The reviewed report of Patsaki and co-workers claimed that VR application has been recommended for COPD patients and variables examined with aerobic capacity for exercise, lung function, anxiety, depression, six-minute walk test, and FEV1. In this study, the Bibliometric tool successfully analyzed the summarizing articles, which is the same as the previous suggestion.[63] Although the 13 research articles were cited between 2013 and 2023, the frequency of the words over time could also be analyzed. Trend topics were virtual reality (1 to 20), male (2 to 16), female (2 to 15), aged (3 to 12), chronic obstructive lung disease (1 to 12), human (2 to 11), exercise (2 to 11), quality of life (0 to 10) and middle-aged (1 to 10), respectively in 2023 when compared to 2013. Unfortunately, the sub-classified analysis found nine articles published between 2019 and 2023 and one research article in 2023 that studied "VR and pulmonary rehabilitation and chronic obstructive lung disease." In addition, breathing exercise, breathing exercise gaming, pulmonary rehabilitation, respiratory biofeedback, and virtual reality were the keywords that have been continued respectively citation that help to improve the quality of life in patients with chronic lung disease.[38] Therefore, future research on VR-innovative technology in pulmonary rehabilitation in case of chronic pulmonary disease should be encouraged.

Limitation of study

This data was mainly cited from the SCOPUS database, English literature, and specific research articles on the keywords "Virtual reality and Pulmonary rehabilitation". Moreover, some new research articles in the in-press situation may not appear in the SCOPUS database. Therefore, continuous study should be followed or performed for the strong evidence. In addition, the keywords such as specific programs such as "chest mobilization exercise" or/and "purse-lip breathing exercises" or/and "incentive spirometer" or/and "education", etc.,

were not recorded. Thus, the limitation of the network clustering and trend topic analysis cannot be evaluated for future research studies.

Conclusion and Clinical Application

The bibliometric analysis of specific research articles in the SCOPUS database in the 10-year update on the keywords "VR and Pulmonary rehabilitation" can be helpful and suggest more future studies and encouraged in the cardiopulmonary research area, relating to the other keywords such as chronic obstructive lung disease, exercise, breathing exercise, pulmonary rehabilitation, quality of life, forced expiratory volume, forced vital capacity, six-minute walk test, dyspnea, functional status, and physical activity". Moreover, this study encourages future research in clinical cardiopulmonary rehabilitation through the discovery of knowledge from the data-mining analysis tool.

Acknowledgments

This study is a part of all segments of the Master's thesis conducted at the Department of Data Science and Digital Innovation, Faculty of Innovation Technology and Creativity, The Far Eastern University, Chiang Mai, Thailand. I am standing as a corresponding author thanks to all the chief and co-advisors for their excellent suggestions, recommendations, and full support. In addition, we would like to express our gratitude to the Faculty of Associated Medical Sciences at Chiang Mai University in Thailand for their kind funding support of this research study.

Conflict of Interest

The authors declare no conflict of interest.

References

[1] Dockx K, Bekkers EM, Van den Bergh V, Ginis P, Rochester L, Hausdorff JM, et al. Virtual reality for rehabilitation in Parkinson's disease. Cochrane Database Syst Rev. 2016; 12(12): CD010760. doi: 10.1002/14651858. CD010760.pub2.

[2] Weiss PL, Kizony R, Feintuch U, Katz N. Virtual reality in neurorehabilitation. In: Gage F, Cohen L, Selzer M, Duncan P, Clarke S, editors. Textbook of neural repair and rehabilitation: Volume 2: Medical Neuro-rehabilitation. 2nd Ed. Cambridge: Cambridge University Press; 2006: 182-97.

[3] Keshner EA. Virtual reality and physical rehabilitation; a new toy or a new research and rehabilitation tool? J Neuroeng Rehabil. 2004: 1(1): 8. doi: 10.1186/1743-0003-1-8.

[4] Lee LG, Krovi VN. Musculoskeletal simulation-based optimization of rehabilitation program. International Workshop on Virtual Rehabilitation, New York, NY, USA, 2006, pp. 36-41, doi: 10.1109/IWVR.2006.1707524.

[5] Kizony R, Katz N, Weiss PL. Adapting an immersive virtual reality system for rehabilitation. Comput Animat Virtual Worlds. 2003; 14(5): 261-8. doi: 10.1002/vis.323.

[6] Weiss PL, Rand D, Katz N, Kizony R. Video captures virtual reality as a flexible and effective rehabilitation tool. J Neuroeng Rehabil. 2004; 1(1): 12. doi: 10.1186/1743-0003-1-12.

[7] Burdea GC. Virtual rehabilitation benefits and challenges. Methods Inf Med. 2003; 42: 519-23. doi: 10.1267/METH03050519.

[8] Yang X. Virtual reality in rehabilitation. Rehabilitation Engineering. [Internet]. Tan Yen Kheng (Ed), ISBN: 978-953-307-023-0, InTech, Available from: http://www.intechopen.com/books/rehabilitation-engineering/virtual-reality-in-rehabilitation.

[9] Schäfer AGM, Zalpour C, von Piekartz H, Hall TM, Paelke V. The efficacy of electronic health supported home exercise interventions for patients with osteoarthritis of the knee: systematic review. J Med Internet Res. 2018; 20(4): e152. doi: 10.2196/jmir.9465.

[10] Trost Z, Anam M, Seward J, Shum C, Rumble D, Sturgeon J, *et al*. Immersive interactive virtual walking reduces neuropathic pain in spinal cord injury: findings from a preliminary investigation of feasibility and clinical efficacy. Pain. 2022; 163(2): 350-61. doi: 10.1097/j.pain.0000000000002348.

[11] Powell V, Powell W. Therapy-led design of home-based virtual rehabilitation. 2015 IEEE 1st Workshop on Everyday Virtual Reality (WEVR), Arles, France; 2015: 11-4. doi: 10.1109/WEVR.2015.7151688.

[12] Roy AK, Soni Y, Dubey S. Enhancing the effectiveness of motor rehabilitation using Kinect motion sensing technology. 2013 IEEE Global Humanitarian Technology Conference: South Asia Satellite (GHTC-SAS), Trivandrum, India; 2013: 298-304. doi: 10.1109/GHTC-SAS.2013.6629934.

[13] Su WC, Yeh SC, Lee SH, Huang HC. A virtual reality lower-back pain rehabilitation approach: System design and user acceptance analysis. In Stephanidis C, Antona M, Stephanidis C, editors, Universal Access in Human-Computer Interaction: Access to Learning, Health and Well-Being. Proceedings of the 9th International Conference, UAHCI 2015 Held as Part of HCI International 2015. Springer Verlag; 2015: 374-82. doi: 10.1007/978-3-319-20684-4_37.

[14] Kim J, Son J, Ko N, Yoon B. Unsupervised virtual reality-based exercise program improves hip muscle strength and balance control in older adults: a pilot study. Arch Phys Med Rehabil. 2013; 94(5): 937-43. doi: 10.1016/j.apmr.2012.12.010. Epub 2012 Dec 21.

[15] Bryanton C, Bosse J, Brien M, Mclean J, McCormick A, Sveistrup H. Feasibility, motivation, and selective motor control: virtual reality compared to conventional home exercise in children with cerebral palsy. Cyberpsychol Behav. 2006; 9(2): 123-8. doi: 10.1089/cpb.2006.9.123.

[16] Casuso-Holgado MJ, Martín-Valero R, Carazo AF, Medrano-Sanchez EM, Cortes Vega M.D, Montero-Bancalero FJ. Effectiveness of virtual reality on training for balance and gait rehabilitation in people with multiple sclerosis: a systematic review and

meta-analysis. Clin Rehabil. 2018; 32: 1220-34. doi: 10.1177/0269215518768084. Epub 2018 Apr 13.

[17] Iruthayarajah J, McIntyre A, Cotoi A, Macaluso S, Teasell R. The use of virtual reality for balance among individuals with chronic stroke: a systematic review and meta-analysis. Top Stroke Rehabil. 2017; 24(1): 68-79. doi: 10.1080/10749357.2016.1192361. Epub 2016 Jun 16.

[18] Porras DC, Siemonsma P, Inzellberg R, Zeilig G, Plotnik M. Advantages of virtual reality in the rehabilitation of balance and gait: Systematic review. Neurology. 2018; 90(22): 1017-25. doi: 10.1212/WNL.00000000000056 03.Epub 2018 May 2.

[19] Lopes JBP, de Almeida-Carvalho Duarte N, Lazzari RD, Oliveira CS. Virtual reality in the rehabilitation process for individuals with cerebral palsy and Down syndrome: A systematic review. J Bodyw Mov Ther. 2018; 24(4): 479-83. doi: 10.1016/j.jbmt.2018.06.006. Epub 2018 Jun 28.

[20] Howard MC. A meta-analysis and systematic literature review of virtual reality rehabilitation programs. Comput Human Behav Rep. 2017; 70: 317-27. doi: 10.1016/j.chb.2017.01.013.

[21] Peek K, Sanson-Fisher R, Mackenzie L, Carey M. Interventions to aid patient adherence to physiotherapist prescribed self-management strategies: a systematic review. Physiotherapy. 2016; 102(2): 127-35. doi: 10.1016/j.physio.2015.10.003. Epub 2015 Oct 22.

[22] Mujber TS, Szecsi T, Hashmi MSJ. Virtual reality applications in manufacturing process simulation. J Mater Process Technol. 2004; 156: 1834-8. doi:10.1016/j.jmatprotec.2004.04.401.

[23] Zhang G, Qin Y, Liu S, Chen X, Zhang W. Bibliometric analysis of research trends and topic area in traditional Chinese medicine therapy for lymphoma. Pharm Biol. 2024; 62(1): 13-21. doi: 10.1080/13880209.2023.2288697. Epub 2023 Dec 13.

[24] Garrido-Cardenas JA, de Lamo-Sevilla C, Cabezas-Fernandez MT, Manzano-Agugliaro F, Martinerx-Lirola M. Global tuberculosis research and its future prospects. Tuberculosis. 2020; 121: 101917. doi: 10.1016/j.tube.2020.101917. Epub 2020 Feb 23.

[25] Dinic BM, Jevremov, T. Trends in research related to the dark triad: A bibliometric analysis. Curr Psychol. 2021; 40(7): 3206-15. doi: 10.1007/s12144-019-00250-9.

[26] Mongeon, P, Paul-Hus, A. The Journal coverage of web of science and Scopus: A comparative analysis. Scientometrics. 2016: 106(1): 213-28. doi:10.1007/s11192-021-03948-5.

[27] Cobo MJ, Lopez-Herrera AG, Herrera-Viedma E, Herrera F. Science mapping software tools; review, analysis, and cooperative study among tools, J Amer Soc Inform Sci Technol. 2011; 62(7): 1382-402. doi: 10.1002/asi.21525.

[28] Wichaisri S, Sapadan, A. Trends and future future directions in sustainable development. Sustain Develop. 2018; 26(1): 1-17. doi:10.1002/sd.1687.

[29] Aria M, Cuccurullo C. Bibliometrix: An R-tool for comprehensive science mapping analysis. J Inform. 2017; 11(4): 959-75. doi:10.1016/j.joi.2017.08.007.

[30] Salton G, McHill MJ. Introduction to Modern Information Retrieval, McGraw-Hill, Auckland. 1983.

[31] Cons P, Latapy M. Computing communities in large networks using random walks. J Graph Algorithms Appl. 2006; 10(2): 191-218. doi:10.7155/jgaa.00124.

[32] Kamada T, Kawai S. An algorithm for drawing general undirected graphs. Inform Process Letters. 1989; 49 (1112): 7-15.doi:10.1016/0020-0190(89)90102-6.

[33] Leydesdorff L. On the normalization and visualization of author co-citation data: Salton's Cosine versus the Jaccard Index. J Amer Inform Sci Technol. 2008; 59(1): 77-85. doi:10.1002/asi.20732.

[34] Pons P, Latapy M. Computing communities in large networks using random walks. In: Yolum P, Güngör T, Gürgen F, Özturan C. (eds) Computer and Information Sciences - ISCIS 2005. Springer, Berlin, Heidelberg. 2005; 284-93. doi:10.1007/11569596_31.

[35] Kang GJ, Ewing-Nelson SR, Mackey L, Schlitt JT, Marathe A, Abbas KM, *et al*. Semantic network analysis of vaccine sentiment in online social media. Vaccine. 2017; 35(29): 3621-38. doi:10.1016/j.vaccine.2017.05.052.

[36] Lee Y, Lee Y, Seong J, Stanescu A, Hwang CS. A comparison of network clustering algorithms in keyword network analysis: a case study with geography conference presentations. Int J Geospat Environ Res. 2020; 7(3): 1-14. https://dc.uwm.edu/ijger/vol7/iss3/1.

[37] Li Y, Jiang H, Lyu X. Virtual reality as an adjunct to pulmonary rehabilitation of patients with chronic obstructive pulmonary disease: a protocol for systematic review and meta-analysis. BMJ Open. 2023; 13(12): e074688. doi: 10.1136/bmjopen-2023-074688.

[38] Rutkowski S, Bogacz K, Rutkowska A, Szczegielniak J, Casaburi R. Inpatient post-COVID-19 rehabilitation program featuring virtual reality-Preliminary results of randomized controlled trial. Front Public Health. 2023; 11: 1121554. doi: 10.3389/fpubh.2023.1121554. eCollection 2023.

[39] Rutkowski S, Bogacz K, Czech O, Rutkowsha A, Szczegielniak J. Effectiveness of an Inpatient Virtual Reality-Based Pulmonary Rehabilitation Program among COVID-19 Patients on Symptoms of Anxiety, Depression, and Quality of Life: Preliminary Results from a Randomized Controlled Trial. Int J Environ Res Public Health. 2022; 19(24): 16980. doi:10.3390/ijerph192416980.

[40] Cerdan-De-las-heras J, Balbino F, Lokke A, Catalan-Matamoros D, Hilberg O, Bendstrup E. Tele-rehabilitation program in idiopathic pulmonary fibrosis-A single-center randomized trial. Int J Environ Res Public Health. 2021; 18(19): 10016. doi:10.3390/ijerph181910016.

[41] Rutkowski S, Szczegielniak J, Szczepanska-gieracha J. Evaluation of the efficacy of immersive virtual reality therapy as a method-supporting pulmonary rehabilitation: A randomized controlled trial. J Clin Med. 2021; 10(2): 1-12, 352. doi: 10.3390/jcm10020352.

[42] Liu H, Yang X, Wang X, Zhang X, Zhang X, Li Q. Study on adjuvant medication for patients with mild cognitive impairment based on VR technology and health education. Contrast Media Mol Imag. 2021: 1187704. doi:10.1155/2021/1187704.

[43] Xie X, Fan J, Chen H, Zhu L, Wan T, Zhou J, *et al*. Virtual reality technology combined with comprehensive pulmonary rehabilitation on patients with stable chronic obstructive pulmonary disease. J Healthc Eng. 2021: 9987200. doi: 10.1155/2021/9987200.

[44] Jung T, Moorhouse N, Shi X, Amin MF. A virtual reality-supported intervention for pulmonary rehabilitation of patients with chronic obstructive pulmonary disease: Mixed methods study. J Med Internet Res. 2020; 22(7): e14178. doi:10.2196/14178.

[45] Rutkowshi S, Rutknowska A, Kiper P, Jastrzebski D, Racheniuk H, Turolla A, et al. Virtual reality rehabilitation in patients with chronic obstructive pulmonary disease: A randomized controlled trial. Int J Chron Obstruct Pulmon Dis. 2020; 15: 117-24. doi: 10.2147/COPD.S223592.

[46] Alves da Cruz, MM, Ricci-Vitor AL, Bonnini Borges GL, Fernanda da Silva P, Ribeiro F, Marques Vanderlei LC. Acute hemodynamic effects of virtual reality-based therapy in patients of cardiovascular rehabilitation; a cluster randomized crossover trial. Arch Phys Med Rehabil. 2020; 10(14): 642-49. doi: 10.1016/j.apmr.2019.12.006.

[47] Knox L, Dunning M, Davies CA, Bennet RM, Sion TW, Phipps K, et al. Safety, feasibility, and effectiveness of virtual pulmonary rehabilitation in the real world. Int J Chron Obstruct Pulmon Dis. 2019; 12: 775-80. doi: 10.2147/COPD.S193827.

[48] Rutkowski S, Rutkowska A, Jastrzebski D, Racheniuk H, Pawetczyk W, Szczegielniak J. Effect of virtual reality-based rehabilitation on physical fitness in patients with chronic obstructive pulmonary disease. J Hum Kinet. 2019; 69(1): 149-57. doi: 10.2478/hukin-2019-0022.

[49] Wardini R, Dajczman E, Yang N, Baltzan M, Prefontaine D, Stathatos M, et al. Using a virtual game system to innovate pulmonary rehabilitation: Safety, adherence, and enjoyment in severe chronic obstructive pulmonary disease. Can Respir J. 2013; 20(5): 357-61. doi:10.1155/ 2013/563861.

[50] Heradio R, Perez-Morago H, Perez-Morago D, Cabrerizo FJ, Herrera-Viedma E. A bibliometric analysis of 20 years of research on software product lines. Inform Sof Technol. 2016; 72: 1-15. doi: 10.1016/j.infsof.2015.11.004.

[51] Donthu N, Kumar S, Mukherjee D, Pandey N, Lim WM. How to conduct a bibliometric analysis: An overview and guidelines. J Bus Res. 2021; 133(2021): 285-96. doi:10.1016/j.jbusres.2021.04.070.

[52] Sapountzoglou N. A bibliometric analysis of risk management methods in the space sector. J Space Saf Eng. 2023; 10(1): 13-21. doi:10.13140/RG.2.2.36270.84808/1.

[53] Kokol L, Vosner HB, Zavrsnik J. Application of bibliometrics in medicine; a historical analysis. Health Inform Libr J. 2021; 38(2): 125-38. doi: 10.1111/hir.12295.

[54] Pittara M, Matsangidou M, Pattichis CS. Virtual reality for pulmonary rehabilitation: Comprehensive Review. JMIE Rehabil Assist Technol. 2023; 10: e477114. doi:10.2196/47114.

[55] Luukkonen T, Tijssen R, Persson O, Sivertsen G. The measurement of international scientific collaboration. Scientometrics. 1993; 28(1): 15-36. doi:10.1007/BF02016282.

[56] Kobourov SG. Force-directed drawing algorithms. In. Tamassia R (editor). Handbook of graph drawing and visualization, New York: CRC Press; 2013: 383-408.

[57] Waltman L, van Eck NJ. A smart local moving algorithm for large-scale modularity-based community detection. Eur Phys J B. 2013; 86(11): 471. doi:10.1140/epjb/e2013-40829-0.

[58] Wang S, Koopman R. They are clustering articles based on semantic similarity. Scientometrics. 2017; 111(2): 1017-31. doi:10.1007/s11192-017-2298-x.

[59] De Rezende LB, Blackwell P, Pessanha Goncalves M.D. Research focuses, trends, and major findings on project complexity; A bibliometric network analysis of 50 years of project complexity research. Proj Manag J. 2018; 49(1): 42-9. doi:10.1177/875697281804900104.

[60] Zhuang Y, Liu X, Nguyen T, He Q, Hong S. Global remote sensing research trends during 1991-2010; a bibliometric analysis. Scientometrics. 2013; 96(1): 203-19. doi:10.1007/s11192-012-0918-z.

[61] Colombo V, Aliverti A, Sacco M. Virtual reality for COPD rehabilitation: a technological perspective. Pulmonology. 2022; 28(2): 119-33. doi:10.1016/j.pulmoe.2020.11.010.

[62] Patsaki I, Avgeri V, Rigoulia T, Zekis T, Koumantakis GA, Grammatopoulou E. Benefits from incorporating virtual reality in pulmonary rehabilitation of COPD patients: A systematic review and meta-analysis. Adv Respir Med. 2023; 91(4): 324-36. doi:10.3390/arm91040026.

[63] Nederhof AJ. Bibliometric monitoring of research performance in the social sciences and the humanity: A review. Scientometrics.2006; 66(1): 81-100. doi:10.1007/s11192-006-0007-2.

Instructions for Authors

Instructions for Authors

Original article/thesis can be submitted through the on-line system via website https://www.tci-thaijo.org/index.php/bulletinAMS/

General Principles

Journal of Associated Medical Sciences is a scientific journal of the Faculty of Associated Medical Sciences, Chiang Mai University. The articles submitted to the journal that are relevant to any of all aspects of Medical Technology, Radiologic Technology, Occupational Therapy, Physical Therapy, Communication Disorders, and other aspects related to the health sciences are welcome. Before publication, the articles will go through a system of assessment and acceptance by at least three experts who are specialized in the relevant discipline. All manuscripts submitted to Journal of Associated Medical Sciences should not have been previously published or under consideration for publication elsewhere. All publications are protected by the Journal of Associated Medical Sciences' copyright.

Manuscript categories

1. **Review articles** must not exceed 20 journal pages (not more than 5,000 words), including 6 tables/figures, and references (maximum 75, recent and relevant).
2. **Original articles** must not exceed 15 journal pages (not more than 3,500 words) including tables, figures, and 40 references (maximum 40, recent and relevant).
3. **Short communications** including technical reports, notes, and letter to editor must not exceed 5 journal pages (not more than 1,500 words), including 2 tables/figures, and references (maximum 10, recent and relevant).
4. **Register** base on institute of official email address only.

Manuscript files

To submit your manuscripts, you will need the following files:

1. A Title page file with the names of all authors and corresponding authors*
2. Main document file with abstract, keywords, main text and references
3. Figure files
4. Table files
5. Any extra files such as Supplemental files or Author Biographical notes
6. Register base on institute of official email address only.

Manuscript Format

1. **Language**: English, Caribri 10 for text and 7 for all symbols. PLEASE be informed that the Journal only accept the submission of English manuscripts.
2. **Format**: One-side printing, double spacing. Use standard program and fonts and, add page and line number for all pages.
3. **A Title page**: Include article title, names of all authors and co-authors, name of the corresponding author and acknowledgements. Prepare according to following contents;
   - *Title of the article*: Concise and informative. Titles are often used in information-retrieval systems. Avoid abbreviations and formulate where possible.
   - *Author names and affiliation*: Where the family name may be ambiguous (e.g. a double name), please indicate this clearly. Present the authors' affiliation addresses (where the actual work was done) below the names. Indicate all affiliations with superscript number immediately after author's name and in front of appropriate address. Provide the full postal address of each affiliation, including the province, country and, if available, the e-mail address of each author.
   - *Corresponding author*: Clearly indicate who will handle correspondence at all stages of refereeing and publication, also post-publication, ensure that telephone and fax numbers (with postal area code) are provided in addition to the e-mail address and the complete postal address. Contact details must be kept up to date by the corresponding author.
   - *Acknowledgements*: Acknowledgements will be collated in a separate section at the end of the article before the references in the stage of copyediting. Please, therefore, include them on the title page, List here those individuals who provided help during the research (e.g. providing language help, writing assistance or proof reading the article, etc.)
4. **Main article structure**: The manuscripts should be arranged in the following headings: Title, Abstract, Introduction, Materials and Methods, Results, Discussion and Conclusion, and Reference. Prepare according to following contents;
   - *Abstract*: Not exceeding 400 words, abstract must be structured with below headings in separated paragraph:
     - Background,
     - Objectives,
     - Materials and methods,
     - Results,
     - Conclusion, and
     - Keywords (3-5 keywords should be included)
   - *Introduction*: State the objectives of work and provide an adequate background, avoiding a detailed literature survey or a summary of the results.
   - *Materials and Methods*: Provide sufficient detail to allow the work to be reproduced. Methods already published should be indicated by a reference, only relevant modifications should be described. Ensure that each table, graph, or figure is referred in the text. According to the policy of ethical approval, authors must state the ethical approval code and conduct informed consent for human subject research (If any) and for animal research, authors must include a statement or text describing the experimental procedures that affirms all appropriate measures (if any) in this section.

- *Results*: Results should be clear and concise. Present the new results of the study such as tables and figures mentioned in the main body of the article and numbered in the order in which they appear in the text or discussion.
- *Discussion*: This should explore the significance of the results of the work, not repeat them. A combined Results and Discussion section is often appropriate. Avoid extensive citations and discussion of published literature.
- *Conclusion*: The main conclusions of the study may be presented in a short Conclusions section, which may stand alone or form a subsection of a "Discussion" or "Results and Discussion".
- *Conflict of interes*t: All authors must declare any financial and personal relationship with other people or organization that could inappropriately influence (bias) their work. If there is no interest to declare, then please state this: "The authors declare no conflict of interest".
- *Ethic approval*: Ethic clearance for research involving human and animal subjects.
- *References*: Vancouver's style.

5. **Artwork Requirements**
   - Each table, graph and figure should be self-explanatory and should present new information rather than duplicating what is in the text. Prepare one page per each and submit separately as supplementary file(s).
   - Save the figures as high resolution JPEC or TIFF files.

Note: Permission to reprint table(s) and/or figure(s) from other sources must be obtained from the original publishers and authors and submitted with the typescript.

Ensuring a double-blinded peer review

To ensure the integrity of the double-blinded peer-review for submission to this journal, every effort should be made to prevent the identities of the authors and reviewers from being known to each other. The authors of the document have deleted their names from the main text, with "Author" and year used in the references and footnotes, instead of the authors' name, article title, etc. After the journal was accepted, the name of authors and affiliation and the name of the corresponding author must be included into the document and re-submitted in the copyediting stage.

Proof correction

The Editor-in-Chief and production team are in charge of the reprint preparation for online publication. The corresponding author will shortly be informed by email the proof of final reprint paper to approve for publication.

Page charge

No page charge.

References Format

1. References using the Vancouver referencing style (see example below).
2. In-text citation: Indicate references by number(s) in the order of appearance in the text with superscript format. Reference numbers are to be placed immediately after the punctuation (with no spacing). The actual authors can be referred to, but the reference number(s) must always be given. When multiple references are cited at a given place in the text, use a hyphen (with no spacing) to join the first and last numbers that are inclusive. Use commas (with spaces) to separate non-inclusive numbers in a multiple citation e.g. (2-5, 7, 10). Do not use a hyphen if there are no citation numbers in between inclusive statement e.g. (1-2). Use instead (1, 2).
3. References list: number the references (numbers in square brackets) in the list must be in the order in which they are mentioned in the text. In case of references source from non-English language, translate the title to English and retain "in Thai" in the parentheses.
4. Please note that if references are not cited in order the manuscript may be returned for amendment before it is passed on to the Editor for review.

Examples of References list

Multiple Authors: List up to the first 6 authors/editors, and use "et al." for any additional authors.

Journal Articles (print): In case of reference source contains Digital Object Identifier (DOI), retain doi: at the end of reference. Vancouver Style does not use the full journal name, only the commonly-used abbreviation: "Physical Therapy" is cited as "Phys Ther". As an option, if a journal carries continuous pagination throughout a volume (as many medical journals do) the month and/or issue number may be omitted. Allow one space after semi-colon and colon then end each reference with full stop after page number.

[1] Pachori P, Gothalwal R, Gandhi P. Emergence of antibiotic resistance Pseudomonas aeruginosa in intensive care unit; a critical review. Genes Dis. 2019; 6(2): 109-19. doi: 10.1016/j.gendis.2019.04.001.

[2] Hung Kn G, Fong KN. Effects of telerehabilitation in occupational therapy practice: A systematic review. Hong Kong J Occup Ther. 2019; 32(1): 3-21. doi: 10.1177/1569186119849119.

[3] Wijesooriya K, Liyanage NK, Kaluarachchi M, Sawkey D. Part II: Verification of the TrueBeam head shielding model in Varian VirtuaLinac via out-of-field doses. Med Phys. 2019; 46(2): 877-884. doi: 10.1002/mp.13263.

[4] Velayati F, Ayatollahi H, Hemmat M. A systematic review of the effectiveness of telerehabilitation interventions for therapeutic purposes in the elderly. Methods Inf Med. 2020; 59(2-03): 104-9. doi: 10.1055/s-0040-1713398.

[5] Junmee C, Siriwachirachai P, Chompoonimit A, Chanavirut R, Thaweewannakij T, Nualnetr N. Health status of patients with stroke in Ubolratana District, Khon Kaen Province: International Classification of Functioning, Disability and Health-based assessments. Thai J Phys Ther. 2021; 43(1): 45-63 (in Thai).

Journal Articles on the Internet

[1] Siegel PM, Bojti I, Bassler N, Holien J, Flierl U, Wang X, et al. A DARPin targeting activated Mac-1 is a novel diagnostic tool and potential anti-inflammatory agent in myocarditis, sepsis and myocardial infarction. Basic Res Cardiol [Internet]. 2021; 116(1): 1-25. Available from: https://doi.org/10.1007/s00395-021-00849-9.

Journal Articles from an Online Database

[1] Jackson D, Firtko A, Edenborough M. Personal resilience as a strategy for surviving and thriving in the face of workplace adversity: A literature review. J Adv Nurs [serial online]. 2007;60(1):1-9. DOI: 10.1111/j.1365-2648.2007.04412.x.

Book / Chapter in an Edited Book References

PLEASE be informed that references of books and chapter in edited book should not be include in the research article, but others manuscript categories.

[1] Grove SK, Cipher DJ. Statistics for nursing research: A workbook for evidence-based practice. 3rd ed. St. Louis, Missouri: Elsevier; 2019.

[2] Haznadar M, editor. Cancer metabolism: Methods and protocols. New York: Humana Press; 2019. doi: 10.1007/978-1-4939-9027-6.

[3] Perrin DH. The evaluation process in rehabilitation. In: Prentice WE, editor. Rehabilitation techniques in sports medicine. 2nd ed. St Louis, Mo: Mosby Year Book; 1994: 253–276.

E-book

[1] Dehkharghani S, editor. Stroke [e-book]. Brisbane (AU): Exon Publications; 2021 [cited 2021 Jul 31]. Available from: https://www.ncbi.nlm.nih.gov/books/NBK572004/ doi: 10.36255/exonpublications.stroke.2021

[2] Tran K, Mierzwinski-Urban M. Serial X-Ray radiography for the diagnosis of osteomyelitis: A review of diagnostic accuracy, clinical utility, cost-effectiveness, and guidelines [e-book]. Ottawa (ON): Canadian Agency for Drugs and Technologies in Health; 2020 [cited 2021 Jul 31]. Available from: https://www.ncbi.nlm.nih.gov/books/NBK562943/

Dissertation/Thesis

[1] On-Takrai J. Production of monoclonal antibody specific to recombinant gp41 of HIV-1 subtype E [Term paper]. Faculty of Associated Medical Sciences: Chiang Mai University; 2001 [in Thai].

[2] Seale AC. The clinical and molecular epidemiology of streptococcus agalactiae in Kenya: maternal colonization and perinatal outcomes [Dissertation on the Internet]. [Oxford (England)]: University Oxford; 2015 [cited 2015 Jul 28]. Available from: http://ora.ox.ac.uk/objects/uuid:6e7d952a-dc5b-4af0-b0bb-f2ae2184eed0.

.

Conference Proceedings

[1] Lake M, Isherwood J, Clansey. Determining initial knee joint loading during a single limb drop landing: reducing soft tissue errors. Proceedings of 34th International Conference of Biomechanics in Sport; 2016 Jul 18-22; Tsukuba, Japan, 2016. Available from: https://ojs.ub.uni-konstanz.de/cpa/article/view/7126

[2] Ellis MD, Carmona C, Drogos J, Traxel S, Dewald JP. Progressive abduction loading therapy targeting flexion synergy to regain reaching function in chronic stroke: preliminary results from an RCT. Proceedings of the 38th Annual International Conference of the IEEE Engineering in Medicine and Biology Society; 2016: 5837-40. doi: 10.1109/EMBC.2016.7592055.

Organization as Author / Government Document

[1] Australian Government, Department of Health. Physical activity and exercise guidelines for all Australian. 2021 [updated 2021 May 7; cited 2021 Jul 15]. Available from: https://www.health.gov.au/health-topics/physical-activity-and-exercise/physical-activity-and-exercise-guidelines-for-all-australians.

[2] Department of Health. Situation survey on policy and implementation of physical activity promotion in schools for first year 2005. Nonthaburi: Ministry of Public Health; 2005. (in Thai).

[3] Department of Local Administration, Ministry of Interior Affairs. Standard of Sports Promotion. Bangkok. 2015: 7–9. (in Thai).

[4] World Health Organization. WHO guidelines on physical activity and sedentary behaviour. Geneva: World Health Organization; 2020. Licence: CC BY-NC-SA 3.0 IGO.

[5] World Health Organization. The epidemiology and impact of dementia: current state and future trends. 2015 [cited 2021 Mar 8]. Available from: http://www.who.int/mental_health/neurology/dementia/dementia_thematicbrief_epidemiology.pdf.

Journal History

Established in 1968

- 1968-2016 As the Bulletin of Chiang Mai Associated Medical Sciences
  - Vol1, No1 - Vol.49, No3
- 2017, the Journal of Associated Medical Sciences
  - Vol.50, No1 and forward.

Journal Sponsorship Publisher

Faculty of Associated Medical Sciences, Chiang Mai University


JOURNAL OF ASSOCIATED
MEDICAL SCIENCES
JAMS